UNIVERSITÀ DEGLI STUDI DI TRIESTE

UNIVERSITÀ DEGLI STUDI DI TRIESTE

XXXIV CICLO DEL DOTTORATO DI RICERCA IN FISICA

On de Sitter string vacua in the Large Volume Scenario

Settore scientifico-disciplinare: FIS/02

DOTTORANDA
Chiara Crinò

COORDINATORE
Prof. Francesco Longo

SUPERVISORE DI TESI
Prof. Roberto Valandro

ANNO ACCADEMICO 2020/2021

Abstract

Purpose of this thesis is to analyze certain aspects of the presence of de Sitter space in type IIB string compactifications. It focuses, in particular, on the mechanism based on the introduction of an $\overline{D3}$-brane at the tip of a warped throat of the compact space, which under certain conditions allows to stabilize all the moduli at a de Sitter minimum of their scalar potential.

The first part is a review of the background material used in this work. It starts with an introduction to string compactification on a Calabi-Yau three-fold, which is followed by the description of the main techniques that are used to stabilize all the (complex structure and Kähler) moduli arising in such compactification. Then, it presents the problem of finding de Sitter minima in string theory and the main proposals to address it, with a specific focus on the method based on $\overline{D3}$-branes and on the issues related to the $D3$-tadpole cancellation condition, which is one of the main aspects analyzed in the thesis. Finally it reviews several important topics which are important for the construction of explicit models in string theory.

The second part contains my original research work. First, we construct and analyze an explicit model in the frame of the Large Volume Scenario, in which all the moduli can be consistently stabilized in a de Sitter minimum. We also list a set of important requirements that need to be fulfilled in order to have a consistent solution in which all the approximations are under control and we analyze them in the context of the class of models under consideration. After that, we perform a statistical analysis of the distribution of the $D3$-charge for models with several Kähler moduli (up to 12) and we stress the important role of the $D7$-brane configuration known as Whitney brane (already used in the explicit construction mentioned before) in relation to the $D3$-tadpole cancellation condition. Finally, we provide an additional explicit construction in which, with respect to the first one, we add the requirement of having a K3 fibration, a configuration which is more promising from the phenomenological point of view.

Acknowledgements

First, I would like to thank my PhD supervisor, Roberto Valandro, for his full availability during all the PhD and for his expert and continuous support and encouragement.

Working in teams with other scientists from all over the world was one of the most interesting and educational parts of my PhD. I am therefore grateful to the people I have collaborated with, always in a very nice and respectful environment: Fernando Quevedo, Andreas Schachner, Pramod Shukla and Shehu AbdusSalam. Without them, many of the results presented in this work would have not been obtained. A special thank goes in particular to Pramod and Shehu, with whom I collaborated for the final project of the PhD and who very kindly adapted their plans to my PhD deadlines.

Furthermore, I would like to thank my friends and PhD fellows Andrea Sangiovanni and Francesca Gebbia with whom I shared joys and pains of these almost four years of PhD, as well as all the other PhD students and postdocs I met at ICTP and at SISSA, regardless the duration of the time spent together. Their friendship made my stay in Trieste a very pleasant experience.

I am also grateful to my uncle Marcello Crinò, who hosted and accompanied me in Trieste during my first exploratory visits and supported me especially at the beginning.

Last but not least, I thank my parents Francesca and Vincenzo for their encouragement and support in any choice of my life, and my brothers Matteo, Simone and Andrea (and also Giorgia and Sara) for listening numerous times to my attempts to explain the technical issues I was struggling with, despite their life and academic interests do not exactly include string theory...

Contents

Chapter 1

Introduction

This thesis aims to contribute to the current debate on whether it is possible to construct a consistent model with a positive cosmological constant (de Sitter space) in the frame of string theory. Models of this kind would fit very well cosmological observations, but they are so difficult to find that it was recently speculated that it is impossible to have long-living de Sitter (dS) vacua in string theory. On the other side, several mechanisms were proposed over the years that point towards the opposite direction.

Let us start from the beginning. Over the last century, we have assisted to a huge improvement of our understanding of the observable world. The Standard Model (SM), developed in the early 1970s, describes three of the four fundamental interactions consistently unifying, within the framework of quantum field theory (QFT), electromagnetism, as well as the theory of the weak and strong nuclear forces. On the other hand, General Relativity (GR), first introduced by A. Einstein in 1915, profitably deals with the fourth fundamental interaction, that is gravity. Both these theories have successfully passed a large number of experimental tests and consistency checks (just to mention two of the most recent ones, the Higgs boson - the last missing building block of SM - was discovered at LHC in 2012, while the first direct observation of gravitational waves - predicted by GR - was achieved by the LIGO-Virgo collaboration in 2015). However, it is important to notice that up to now, the SM has only been tested in regimes in which gravitational effects can be safely ignored. Similarly, the predictions of GR essentially concern phenomena happening at astronomical scales, where the three interactions described by the SM are negligible.

The problems come when we try to make predictions in regimes in which the four fundamental interactions have a comparable intensity[1], as any trivial attempt to include gravity in the SM in order to get some theory of *Quantum Gravity* (QG)[2], leads to conceptual and mathematical inconsistencies. Signals of the incompleteness of the theory can be found already in the fact that GR breaks down at loci of the space-time with a very large

[1] This is expected to happen at very large energies, around the so-called Planck scale $M_p = 1.22 \times 10^{19} GeV$.

[2] GR is a classical theory, hence it can not be applied at the scales in which quantum effects become relevant.

curvature (space-time singularities), such as the interior of Black Holes or the Big Bang. Moreover, when we try to construct a quantum field theory of gravity, with the interaction mediated by a spin-2 field called the *graviton*, we run into unavoidable divergencies at the ultraviolet energy scales (non-renormalizability), a clear signal that a theory of this kind is only valid up to a certain cut-off scale, while no predictions can be done regarding what happens beyond this scale. In fact, the SM itself (even without including gravity) is just an effective field theory, which can be only applied at small energies, not to mention other reasons that make it not completely satisfactory from the theoretical point of view, such as the large number of free parameters whose values can only be fixed through experiments. It is therefore reasonable to hope that the same new (high energy) physics will complete both the SM and the quantum theory of gravity in a consistent and unified way.

Several proposals have been done over the years. The present thesis takes into consideration one of the most studied and, up to now, successful theories of QG, that is *String Theory* [1][3]. The premise of the theory is simple: instead of considering the elementary particles as points, we describe them as one-dimensional objects, or *strings*, whose (very small) length scale is $l_s = 2\pi\sqrt{\alpha'}$ [4] and which can be either open or closed. Different oscillator modes of a string correspond to different particle or spin states at low energy. The states with minimal energy are massless, while the others have masses $\propto \frac{1}{\sqrt{\alpha'}}$. We will consider the point-particle limit $\alpha' \to 0$, in which all massive states are integrated out and only the massless spectrum remains.

The relativistic quantum theory of one-dimensional objects presents several advantages: one of these is that string theory automatically includes the three interactions described by the SM *and* gravity. Moreover, it is renormalizable (at least at the perturbative level), hence there are no UV divergencies that can not be absorbed by a finite number of counterterms.

However, string theory is far from being complete. We still lack an exact theory of strings, hence we are only able to make computations and predictions within certain perturbative expansions and under certain approximations. Moreover, there is a huge number of solutions of string theory (*string vacua*) and it is very difficult to understand which is the one describing our universe (provided that such a solution actually exists). The problem is, in particular, that we are not able to test the specific features of string theory yet, for the same reason why the SM is in such a good agreement with experiments: at the energies E that we are able to reach with the current technologies, the corrections due to QG are expected to be suppressed by a very small factor $\sim \frac{E}{M_p}$, hence we do not detect them[5]. Nonetheless, string theory is not completely disconnected from observations: a realistic model constructed in this frame, indeed, needs to reproduce the features of the SM in the corresponding limit or at least it can not be in contradiction with any experiment or

[3] See also [2].

[4] α' is the Regge slope.

[5] There are however proposals of experiments and observations that might help to discriminate between different quantum gravity theories or to constrain string theory, in the near future. See e.g. [3] for a recent review.

cosmological observation. This is the premise of the branch of string theory called *String Phenomenology*, whose main purpose is to try to make contact between the formalism of the theory and the observations, constructing models which reproduce all the features of the SM. It will also be the guiding principle of the rest of this introduction, as well as of the whole thesis.

Originally, string theory only described the bosonic fields, being therefore not suitable for a realistic description of our universe. The inclusion of fermions, led to one of the most important predictions of string theory, that is *Supersymmetry*[6], according to which one can associate a fermionic field to any existing bosonic field and vice versa. A field and its so-called superpartner, share the same mass and charge, but differ for the spin (which is integer for the bosonic field and half-integer for the fermionic one). Up to now, experiments didn't show any supersymmetric partner of the known particles, hence we need to assume that, if present, supersymmetry is broken at some energy scale larger than the ones that we can currently reach. From now on, whenever we will mention string theory, we will actually mean its supersymmetric completion, that is *Superstring Theory* [5, 6, 7].

A second important prediction of string theory is the existence of extra dimensions; in particular, superstring theory requires a 10-dimensional (10d) space-time[7]. The idea of studying GR in a space-time with more than three spatial dimensions was first taken into consideration in 1921 by T. Kaluza, who analyzed the case of a 5d space-time. The fact that we do not detect the 5th dimension was justified by the assumption that the variation of the physics observables along the extra dimension is negligible with respect to their variation along the other three directions ('cylinder condition'). Surprisingly the model reproduced, together with the 4d Einstein field equations, also the Maxwell equation for the electromagnetic field. Later on, in 1926, O. Klein considered a quantum version of the theory, showing that the fifth extra dimension is actually compatible with quantum mechanics, provided that it is curled up in a circle with a very small radius, of the order of the Planck length $l_p = \frac{1}{M_p}$. While the Kaluza-Klein (KK) 5d theory turned out to be not suitable for a fully realistic description of our universe, these early results happened to be extremely useful for the interpretation of the string theory prescription of a 10d space-time. The modern view of the KK mechanism is indeed that the full 10d space-time can be actually factorized as

$$\mathcal{M}_{10} = \mathcal{M}_4 \times X_6 \,,$$

where $\mathcal{M}_4$ is the four-dimensional space-time we observe, while X_6 is a *compactified* 6d space whose characteristic length scale is very small. Since we do not directly detect the manifold X_6, we do not know its geometrical features; string theory, indeed, allows for many different choices. A crucial point of this picture, however, is that these features determine the low energy physics that we observe in the 4d space-time. The choice of the geometry of the manifold X_6 is therefore an important topic for string phenomenology.

[6] See [4] for a review and a list of useful references on the topic.

[7] This is actually the simplest version, called *critical* superstring theory. There exist also (more involved) non-critical string theories, allowing for a different number of spatial dimensions, but we will not consider them here.

There are two main strategies that one can follow for the construction of realistic models in string theory (*model building*). The traditional *top-down* approach consists in starting from a 10d superstring theory and explicitly compactifying it to 4 dimensions, obtaining an internal manifold corresponding to a spectrum of massless particles which is as similar as possible to the SM spectrum (the introduction of further ingredients to the theory might then allow to add the remaining needed features). The more modern and somehow complementary *bottom-up* approach [8], which is the one we will follow, takes into account the fact that we know by now that certain features of a string construction are essentially local, that is that they do not depend on the full picture. This is the case, e.g., for the matter content of the SM which, according to certain constructions, can be localized in specific regions of the compact space, without affecting (nor being affected by) other characteristics of the full compactification. The idea is therefore to subdivide the work in different steps: first, one starts from local constructions, in which only certain specific requirements need to be taken into account; after that, one tries to embed them in a consistent global context, whose details can be treated almost independently with respect to the local configuration.

Besides deriving gravity and electromagnetism, the compactification of the original 5d KK theory produced a 4d massless scalar field. The presence of fields of this kind, which correspond to deformations of the internal manifold X_6 and are called *moduli*, turns out to be ubiquitous in string compactifications and it is a problem from the point of view of model building. Generically, indeed, a string compactification produces hundreds of moduli: since they are massless, if they existed we should have already detected them, which is not the case. In order to have a theory which is not in contrast with observations, therefore, we need to introduce additional ingredients which are such that in the new model the moduli turn out to be massive and with a large mass (out of the reach of current experiments). The new ingredients should in particular generate a scalar potential for the moduli, so that they can be fixed at the minimum of this potential (*moduli stabilization*).

We essentially distinguish two classes of moduli: the complex structure moduli correspond to deformations of the complex structure of X_6, while the Kähler moduli parametrize the size of its internal cycles. The issue of stabilizing all the moduli of a given compactification has been a major topic of string phenomenology for several years, but nowadays we have at our disposal well-established techniques that allow, at least in principle, to do the job.

The stabilization of the complex structure moduli can be achieved by turning on non-vanishing background fluxes threading cycles of the internal manifold [9][8]. These fluxes generate a scalar potential allowing, if generic enough, to stabilize all of them. It is important to notice that the fluxes need to be quantized, hence they take discrete values. The theory therefore acquires a large number of new degrees of freedom, as the scalar potential for the moduli depends on this new set of discrete parameters. Different values of the quantized fluxes produce a family of scalar potentials, hence, after minimization, a

[8] See also [10] for a review.

large set of different *string vacua* (the so-called *Landscape*).

As concerns the Kähler moduli stabilization, two main proposals have been developed over the years, the KKLT[9] mechanism [11] and the Large Volume Scenario (LVS) [12, 13], both relying on the presence of certain perturbative and non-perturbative corrections to the scalar potential for the moduli. In both cases (even though for different reasons) it turns out to be possible to separate the procedure of moduli stabilization into two steps, first fixing the complex structure moduli to their minimum and, only after that, stabilizing the Kähler moduli via sub-leading effects. In general, we will assume the complex structure moduli to be already stabilized by the fluxes, while we will consider the stabilization of the Kähler moduli explicitly.

Regardless of the mechanism that we choose to implement in order to stabilize the moduli, the value of the scalar potential at the minimum in which they are fixed turns out to be always negative. A minimum of this kind is said *Anti-de Sitter* (AdS) minimum and corresponds to an universe with a negative vacuum energy. On the other side, cosmological observations are consistent with the idea that we live in a universe with positive vacuum energy, which means that the string vacuum describing our world should be a *de Sitter* (dS) minimum. Again, we need to introduce further ingredients to the theory, in order to get a scalar potential for the moduli which is consistent with the observations, that is it has a minimum with positive energy.

The first proposal of a mechanism for constructing dS string vacua is the one on which we will mainly focus in this work and it traces back to the original paper by KKLT, in 2003 [11]. Since then, it has survived several challenges, so that it can be considered quite robust. However, the debate on its validity and, more generically, on the possibility of having such vacua in the context of string theory, is still open and it was recently revived by the dS Swampland Conjectures [14, 15], claiming that this kind of solutions, obtained in the low energy limit, are actually inconsistent with string theory in the UV.

The KKLT *uplift* mechanism is based on the presence of an $\overline{D3}$-brane at the tip of a highly warped throat of the compact manifold X_6. This particular configuration produces an additional term in the moduli scalar potential, which can now have, under certain conditions, a de Sitter minimum. A new challenge to this mechanism was pointed out in [16, 17], and it is related to the *$D3$-tadpole cancellation condition*. A generic string construction contains several charged objects defined in X_6: since X_6 is a compact manifold, the sum of all the charges must vanish. This requirement turns out to be particularly constraining for a specific kind of charge, the $D3$-charge. Sources of $D3$-charge in the models we will consider here are the background fluxes responsible for the stabilization of the complex structure moduli (positive $D3$-charge), as well as the orientifold planes and the D-branes (negative $D3$-charge).

A consequence of the fact that, in order to have a setup suitable for $\overline{D3}$ uplift, the complex structure of X_6 is locally deformed in a highly warped throat is that the complex structure modulus parametrizing this deformation turns out to be somehow special with

[9] From the names of the authors who proposed it: S. Kachru, R. Kallosh, A.D. Linde and S.P. Trivedi.

respect to the other complex structure moduli (in particular, it is stabilized at a much smaller mass, potentially comparable to the mass of the Kähler moduli). It therefore deserves an explicit analysis, at the same level as the Kähler moduli. By doing this, one realizes that the amount of fluxes that we need to turn on inside the throat (hence the corresponding $D3$-charge) is bounded by below and is typically quite large. This large value has to be compensated by a large negative contribution coming from orientifold planes and D-branes, which is generically difficult to obtain as these sources are strongly constrained by the geometric features of the internal manifold.

Purpose of this thesis is to analyze the $\overline{D3}$ uplift mechanism in the frame of LVS, with a specific focus on this new challenge. We do this by following two main strategies:

1. *Explicit examples.* We construct concrete models, which are simple enough to be explicit but rich enough to include all the ingredients of moduli stabilization and dS uplift in LVS. This allows to point out and to better understand several challenges related to this mechanism, which can be then generalized to more involved configurations.

2. *Statistical analysis.* We focus on a single feature of this kind of constructions, the $D3$-charge, and we study it from a statistical perspective. In particular, we analyze from a quantitative point of view, by means of a scan over a large number of possible models, the actual limits in obtaining large negative $D3$-charge contributions in string compactifications[10].

Organization of the thesis

The thesis can be separated into two main parts. The first one (from Ch. 2 to Ch. 5) contains a review of the topics mentioned in this introduction, that is string compactification, moduli stabilization and the problem of having dS vacua in string theory.

- Chapter 2 contains a brief introduction to type IIB[11] superstring compactifications. We start presenting the 10d theory and we explain how it can be compactified to a 4d space-time, giving rise to a certain number of moduli. Generically, it is convenient to consider compactifications that leave some supersymmetry unbroken. We show that this requirement corresponds to specific features of the compact space X_6, which in particular needs to be a Calabi-Yau (CY) manifold.

  After that we introduce a new symmetry operation (*orientifold involution*), specifying why we need it and deriving the massless spectrum of a theory which is invariant under this symmetry.

  We conclude the chapter by listing a few phenomenological reasons that led to the choice of type IIB string theory with respect to the other possible frameworks.

[10] In this case we extend our analysis also to models that are not suitable for $\overline{D3}$ uplift, but can, at least in principle, support other uplift mechanisms, already proposed in the literature.

[11] There exist, as we will see, five possible 10d superstring theories, which are called type I, type IIA, type IIB, heterotic $SO(32)$ and heterotic $E_8 \times E_8$.

- Chapter 3 is devoted to the theme of moduli stabilization. For the purpose of stabilization of the complex structure moduli we introduce background fluxes and their main features. In particular their presence imposes the definition of a new metric ansatz, that is the *warped metric* (we also describe the standard choice for the new metric, which is the warped deformed conifold). The fluxes determine a scalar potential for the complex structure moduli which can therefore be stabilized to the minimum of this scalar potential. In the description of complex structure moduli stabilization, we take into consideration two complementary limits, the *dilute flux* regime and the *strongly warped* regime, highlighting the differences between the two cases. This distinction will turn out to be important after the introduction of the $\overline{D3}$ uplift mechanism.

  As concerns the Kähler moduli stabilization, we describe both the KKLT and the LVS mechanisms, summarizing the main differences between the two approaches and explaining why we chose to work within the second scenario.

- In Chapter 4 we introduce the main topic of the thesis, that is the presence of de Sitter vacua in type IIB string theory. After a brief reference to the Swampland program (and in particular to those conjectures that are specifically related to dS minima), we present the mechanism based on the introduction of an $\overline{D3}$-brane at the tip of a highly warped throat. We explain how this set-up can be described in a fully supersymmetric way, by means of the introduction of a new field, the *Nilpotent Goldstino* and we apply this mechanism to the Large Volume Scenario. This is a local configuration which, following the bottom-up approach mentioned above, must be embedded in a consistent global compactification: we briefly list the main steps that allow to do this.

  Finally, we introduce the new challenge to this mechanism, as well as other recent issues related to $D3$-tadpoles and we mention other uplifting proposals that have been developed over the years.

- In the last chapter of the first part, Chapter 5, we cover a series of additional relevant topics that one needs to know in order to properly construct and analyze a model in the frame of type IIB compactifications.

  We describe how we set the geometric background, focusing on the class of compact geometries that we take into consideration in the present thesis (CY manifolds constructed as hypersurfaces in toric ambient spaces). We concentrate, in particular, on those geometrical tools that are relevant for the analyses of the second part of the thesis, such as the topology of toric divisors and different orientifold planes configurations. We also introduce the so-called Kähler cone conditions, which need to be imposed in order to have a positive definite metric.

  After that, we illustrate different $D7$-brane configurations that are important for the topic of tadpole cancellation conditions and we give some additional detail regarding the presence of non-perturbative effects (which are needed both for KKLT and LVS moduli stabilization).

Finally, we notice that it might happen that the KKLT/LVS scalar potential does not explicitly depend on all the Kähler moduli, therefore leaving some of them unstabilized. These remaining flat directions of the scalar potential can develop a minimum due to sub-leading corrections: we delineate the main ones in the conclusive part of the chapter, specifying their origin.

The second part of the thesis is dedicated to the original results of my research work.

- Chapter 6 presents the results reported in [18], where we consider a concrete type IIB CY compactification, with 2 Kähler moduli stabilized on a dS minimum in the frame of LVS. This is the simplest possible LVS construction (as this scenario can not be applied to geometries with a single Kähler modulus). The dS minimum is obtained by introducing an $\overline{D3}$-brane at the tip of a warped throat of Klebanov-Strassler (KS) type. Before analyzing the selected explicit example, we provide a more generic study of this class of models, with a specific focus on the constraints that one needs to impose in order to obtain a consistent result (that is a model in which all the approximations are under control), among which the bounds on the $D3$-charge assume a particular relevance. It turns out that finding an explicit consistent model is not easy, as many of these constraints are in tension one with the other. Moreover, as anticipated, the strongest obstructions appear to be related to the need to cancel the total $D3$-charge in a setup which is, at the same time, suitable for $\overline{D3}$ uplift to dS. Nonetheless, we manage to obtain a model in which all the requirements are satisfied, already in the very simple construction that we take into consideration. We also stress that the possibility to cancel the $D3$-tadpole, despite the presence of a large positive contribution coming from the fluxes, is due to the introduction of a specific brane configuration, called Whitney brane, which allows for large negative $D3$-charges.

- Chapter 7 is partially motivated by the results of the previous one and it is based on [19]. The two main results of Ch. 6 are indeed that the strongest obstruction to the construction of consistent models is due to the difficulty in having large negative $D3$-charges and that, nevertheless, such large contributions can be obtained by means of a Whitney brane. It is therefore reasonable to ask which is the largest (in absolute value) $D3$-charge contribution one can get from O-planes and D-branes, as well as to verify in a more quantitative way the claim that Whitney branes should be preferred with respect to other configurations, in order to obtain such large values. In fact these are two of the main topics covered by [19].

  In order to do so, we exhibit a systematic classification of CY orientifolds (hypersurfaces in toric ambient spaces) from holomorphic reflection involutions with up to 12 Kähler moduli. For each model (geometry plus involution), we analyze the orientifold-plane configuration and the corresponding $D3$-charge. Moreover, we take into consideration different possible brane configurations, showing how the above-mentioned Whitney brane generically allows to significantly increase the total negative $D3$-charge contribution with respect to more commonly used setups. We derive

an upper bound for the total (negative) $D3$-charge contribution, which is larger than any bound reported in the literature before. All these data have been collected in a publicly available database.

- Finally, Chapter 8 is again an extension of the work performed in Ch. 6, this time along the path of the construction of concrete models, and it is based on [20]. Having only two Kähler moduli, the CY orientifold presented in Ch. 6, does not allow for the introduction of any other features, which we expect to be present in a realistic model. In Ch. 8, therefore, we present a new explicit model which, besides having all the moduli stabilized in a dS minimum, is defined on a compact manifold which is a K3 fibration, a feature that makes it more interesting from the phenomenological point of view. The introduction of this additional characteristic presents new challenges, at least for models with a few Kähler moduli as the ones we take into consideration in order to have a better control on our analysis. We describe these, before analyzing the selected example.

The thesis is accompanied by four appendices:

- In App. A, we recall the relation between the so-called String and Einstein frames, the latter being the one used along the thesis. Moreover, we list the relevant energy scales of string theory, highlighting the relations between them and their dependence on other parameters, such as the volume of the compact space and the string coupling.

- App. B contains a short introduction to cohomology and homology groups, which are extensively used along the thesis.

- In App. C, we perform the computation of the masses of the moduli through the canonical normalization of their Lagrangian. Moreover we prove that the values of the masses can be equivalently calculated as the eigenvalues of the matrix $K^{I\bar{L}}V_{\bar{L}J}|_{\text{min}}$ (where $K^{I\bar{L}}$ is the inverse Kähler metric, which is introduced in Ch. 6, and $V_{\bar{L}J}$ is the Hessian of the scalar potential for the moduli).

- Finally, in App. D we derive the scalar potential for a generic number of Kähler moduli and the complex structure modulus parametrizing the warped throat. We also show an application of this formula to a simple configuration with more than two Kähler moduli, including some consideration regarding the expected $D3$-charge for this more generic setup.

The thesis is based on the following papers:

[18] *On de Sitter String Vacua from Anti-D3-Branes in the Large Volume Scenario*
C. Crinò, F. Quevedo and R. Valandro
JHEP **03** (2021) 258, arXiv: 2010.15903

[19] *A Database of Calabi-Yau Orientifolds and the Size of D3-Tadpoles*
C. Crinò, F. Quevedo, A. Schachner and R. Valandro
arXiv: 2204.13115

[20] *On K3-fibred LARGE Volume Scenario with de Sitter vacua from $\overline{D3}$ - branes*
S. AbdusSalam, C. Crinò and P. Shukla
arXiv: 2206.12889

Chapter 2

Type IIB compactification on a Calabi-Yau three-fold

The aim of this chapter is to give a review, short but as much self-contained as possible, of type IIB string theory compactified on a Calabi-Yau threefold, both with and without the presence of an orientifold involution. It is organized as follows. In Sec. 2.1 we briefly introduce the ten-dimensional type IIB string theory. In Sec. 2.2, we explain how the 10d manifold can be connected to the observed 4-dimensional space-time; we also present the massless spectrum of the four-dimensional effective field theory. In Sec. 2.3 we add a symmetry operation to the set up, explaining why it is needed, and we describe how the massless spectrum changes in the orientifolded theory. Finally, in Sec. 2.4 we summarize the main reasons that make type IIB string theory an interesting and promising framework. Most of the notions presented here are based on [21]. For general reviews, see also [22, 23, 5].

2.1 Type IIB supergravity in 10d

The earliest version of string theory included only bosonic particles. It was later modified, via the introduction of supersymmetry (SUSY), in order to include also space-time fermions, leading to the so-called superstring theories.

In a superstring theory, one distinguishes between periodic and antiperiodic worldsheet fermions, under transport around the closed string worldsheet. The periodic fermions are said to be in the Ramond (R) sector, while the anti-periodic ones are in the so-called Neveu-Schwarz (NS) sector. Since worldsheet fermions are separated into left- and right-moving modes and the choice of their periodicity can be made separately for the two kinds of fermions, one ends up with four possible sectors, that is with four different kinds of closed superstring: NS-NS, R-R, R-NS and NS-R. In the 10-dimensional (10d) low energy effective theory, the so-called supergravity theory (SUGRA)[1], whose action describes the interactions of the massless states of the superstring, the different sectors give rise to different kinds of fields: bosonic fields come from string states in the NS-NS and R-R sectors, while space-time fermions arise from R-NS and NS-R sectors. From now on, we

[1] Supergravity is the theory of local supersymmetry [24].

will consider only the bosonic fields. Indeed, the couplings of their fermionic partners will be automatically fixed by supersymmetry.

There are five possible 10d superstring theories (I, IIA, IIB, heterotic $SO(32)$ and heterotic $E_8\times E_8$), interconnected by several dualities and corresponding to different weakly coupled limits of an underlying theory of quantum gravity. In this work we will focus only on type IIB superstring theory. A brief motivation of this choice will be given at the end of this chapter.

In type IIB supergravity, the NS-NS sector contains the dilaton ϕ, a 2-form[2] B_2 and the metric G_{MN}. On the other side, the R-R sector contains a scalar C_0, called axion, a 2-form C_2 and a 4-form C_4.

The bosonic effective action is given by [5, 21]:

$$\begin{aligned} S_{IIB}^{(10d)} =& S_{NS} + S_R + S_{CS} = \frac{1}{2\kappa_{10}^2}\int\left(R*\mathbb{I} - \frac{1}{2}d\phi\wedge *d\phi - \frac{1}{2}e^{-\phi}H_3\wedge *H_3\right) \\ &- \frac{1}{4\kappa_{10}^2}\int\left(e^{2\phi}F_1\wedge *F_1 + e^{\phi}\tilde{F}_3\wedge *\tilde{F}_3 + \frac{1}{2}\tilde{F}_5\wedge *\tilde{F}_5\right) \\ &- \frac{1}{4\kappa_{10}^2}\int C_4\wedge H_3\wedge F_3\,, \end{aligned} \tag{2.1}$$

where κ_{10} is the 10d gravitational coupling, defined as $2\kappa_{10}^2 = (2\pi)^7\alpha'^4$ in terms of the string constant α' (see also App. A); R is the Ricci scalar; $*$ denotes the Hodge-$*$ operator ($*\mathbb{I}\equiv d^{10}X\sqrt{-G}$ is the 10-dimensional measure); $F_{p+1} = dC_p$ and $H_3 = dB_2$ are the field strengths for C_p and B_2 respectively and

$$\begin{aligned} \tilde{F}_3 &= F_3 - C_0\wedge H_3 \\ \tilde{F}_5 &= F_5 - \frac{1}{2}H_3\wedge C_2 + \frac{1}{2}B_2\wedge F_3 \end{aligned} \tag{2.2}$$

with $\tilde{F}_5$ satisfying the self-duality condition $\tilde{F}_5 = *\tilde{F}_5$. The first two terms in (2.1) regroup fields in the NS-NS and R-R sector respectively, while S_{CS}, the Chern-Simons action, contains both.

The above action is written in 10d *Einstein frame*[3], which is obtained by a redefinition of the metric tensor via a Weyl transformation as:

$$G_{MN,E} = e^{\frac{\phi-\phi_0}{2}}G_{MN,s} \tag{2.3}$$

where ϕ_0 is the vacuum expectation value (VEV) of the dilaton field and $G_{MN,s}$ is the *string frame* metric. In the following, we will consider $\phi_0 = 0$ for simplicity. With our choice, as we can see from Eq. (2.1), the action for the metric is decoupled from that of the dilaton and both the fields appear with canonical kinetic terms.

2.2 Compactification on a six-dimensional manifold

From a phenomenological point of view, we are only interested in those solutions of the equations of motion that are built on a space-time that can be factorized into an extended

[2] A differential p-form is a tensor of type $[0,p]$ with completely antisymmetric components.
[3] See also Appendix A.

4d space-time (the one we observe) times a compact 6-dimensional manifold, whose length scale is small enough to justify the fact that we do not observe it:

$$\mathcal{M}_{10} = \mathcal{M}_4 \times X_6 \,.$$

A solution of this kind is called a *compactification* of string theory on X_6.

A standard choice for the metric of the compactified 10-dimensional background is the block diagonal one

$$ds^2 = G_{MN}\, dX^M dX^N = g_{\mu\nu}\, dx^\mu dx^\nu + g_{i\bar{\jmath}}\, dy^i d\bar{y}^{\bar{\jmath}} \,, \tag{2.4}$$

where $g_{\mu\nu}$ is the Minkowski metric and $g_{i\bar{\jmath}}$ is the metric of the compact 6-dimensional manifold X_6 (with $y^i, \bar{y}^{\bar{\jmath}}$ complex coordinates on it)[4].

As we will see in the following, even though we do not directly observe the compact space, its geometry has a crucial role in determining the field content of the 4-dimensional effective theory. In order to derive such theory we need to perform the so-called *dimensional reduction*, which is presented in the next section.

2.2.1 Dimensional reduction

In order to understand how dimensional reduction works and which are its effects on the four-dimensional theory, let us briefly review the simple example, analyzed in [23], of a 10-dimensional geometry with only one 'breathing mode', $e^{u(x)}$:

$$ds^2 = G_{MN}\, dX^M dX^N = e^{-6u(x)} g_{\mu\nu}\, dx^\mu dx^\nu + e^{2u(x)} \hat{g}_{mn}\, dy^m dy^n \,.$$

The breathing mode parametrizes the change in size of the internal 6-dimensional space, as a function of the 4-dimensional coordinates x^μ; $\hat{g}_{mn}$ is a reference metric with fixed volume[5] $\int_{X_6} d^6y \sqrt{\hat{g}_6} \equiv \mathcal{V}$.

For simplicity we consider only the 10d Einstein-Hilbert (EH) term of the action (2.1), in string frame:

$$S_{EH}^{(10d)} = \frac{1}{2\kappa_{10}^2} \int d^{10}X \sqrt{-G}\, e^{-2\phi} R_{10} \,,$$

where R_{10} is the 10d Ricci scalar. The purpose of dimensional reduction is to deduce from this action the corresponding 4-dimensional one. In order to do so, we need to distinguish, in particular, the different contributions coming from the 4d metric $g_{\mu\nu}$ (from which we construct the Ricci scalar R_4) and the 6d metric $\hat{g}_{mn}$ (with the Ricci scalar R_6).

Since G_{MN} is block-diagonal, one can write:

$$\begin{aligned} R_{10} &\equiv G^{MN} R_{MN} = g'^{\mu\nu} R_{\mu\nu} + \hat{g}'^{mn} R_{mn} = R'_4 + R'_6 \\ d^{10}X \sqrt{-G} &= d^4x \sqrt{-g'_4}\, d^6y \sqrt{g'_6} \end{aligned} \tag{2.5}$$

[4] *Notation:* the capital letters $M, N = 0, ..., 9$ are used in the 10-dimensional metric; the lower case letters $m, n = 1, ..., 6$ in the 6-dimensional metric expressed in terms of real coordinates; the lower case letters $i, \bar{\jmath} = 1, ..., 3$ in the 6-dimensional metric expressed in terms of complex coordinates and the Greek letters $\mu, \nu = 0, ..., 3$ in the 4-dimensional one. The choice of a complex manifold X_6 is dictated by supersymmetry, as we will see later.

[5] $\hat{g}_6 = \det(\hat{g}_{mn})$.

where $g'^{\mu\nu}$ is the inverse of the metric $g'_{\mu\nu} \equiv e^{-6u(x)} g_{\mu\nu}$, g'_4 is its determinant and R'_4 is the corresponding 4-dimensional Ricci scalar (similar definitions are introduced for g'^{mn}, with $g'_{mn} \equiv e^{2u(x)} \hat{g}_{mn}$, and the corresponding g'_6 and R'_6).

Being interested in the action in terms of R_4, R_6 instead of R'_4, R'_6, we can use the fact that when two d-dimensional metrics are related by a Weyl transformation

$$g'_{MN} = e^{2\omega(x)} g_{MN} \,,$$

as it is the case for both $g_{\mu\nu}, g'_{\mu\nu}$ $(d = 4)$ and g_{mn}, g'_{mn} $(d = 6)$, then their determinants are related by $\sqrt{-g'_d} = \sqrt{-g_d}\, e^{\omega(x) d}$, from which we can also derive the relation between the corresponding Ricci scalars and Laplacians [23].

By putting all this information together, we get the following action:

$$S_{EH}^{(10d)} = \frac{1}{2\kappa_{10}^2} \int d^4x \sqrt{-g_4} \int_{X_6} d^6y \sqrt{\hat{g}_6}\, e^{-2\phi} \left(R_4 + e^{-8u} R_6 + 12\, \partial_\mu u \partial^\mu u \right) \tag{2.6}$$

from which, assuming that the string coupling $g_s \equiv e^{\phi}$ is constant over the internal space, we can read the 4-dimensional EH action:

$$S_{EH}^{(4d)} = \frac{1}{2\kappa_4^2} \int d^4x \sqrt{-g} R_4 \,.$$

Here, $\kappa_4^2 = \sqrt{8\pi G_N}$ is the 4d gravitational coupling, which turns out to be related to the 10d one by:

$$\frac{1}{2\kappa_4^2} = \frac{\mathcal{V}_s}{2\kappa_{10}^2\, g_s^2} = \frac{m_p^2}{2} \,. \tag{2.7}$$

It should be noted (see Eq. (2.6)) that the breathing mode appears now as the kinetic term for a 4d scalar field $12\, \partial_\mu u\, \partial^\mu u$. This is an example of how a geometric deformation of the compact manifold appears as a *massless* scalar in the 4d theory. These scalars are called *moduli* and they are ubiquitous in string compactifications.

2.2.2 Calabi-Yau manifolds

In general, it is convenient to consider compactifications that leave some supersymmetry unbroken. Indeed, they are more stable, simpler to study and more promising for model building (see [22, 6, 25] for a review).

A local supersymmetry transformation can be described in terms of the 10d infinitesimal supersymmetry parameter $\eta_\alpha(X^M)$, which depends on the space-time coordinates X^M and is in the **16** spinorial representation of $SO(1,9)$. Under $SO(1,9) \to SO(1,3) \times SO(6)$, it decomposes as $\mathbf{16} \to (\mathbf{2}, \mathbf{4}) \oplus (\mathbf{2'}, \bar{\mathbf{4}})$, where $\mathbf{2}, \mathbf{2'}$ (one being the complex conjugate of the other) denote the positive- and negative-chirality spinorial representations of $SO(1,3)$; similarly, $\mathbf{4}$ and $\bar{\mathbf{4}}$ are the spinorial representations of $SO(6)$, which is isomorphic to $SU(4)$.

The condition for having some unbroken supersymmetry is that it is possible to choose $\eta_\alpha(X^M)$ such that the variations of the elementary 10d fermionic fields under the corre-

sponding supersymmetry transformation, vanish[6]:

$$\delta\psi_M = 0\,; \tag{2.9a}$$

$$\delta\lambda = 0\,; \tag{2.9b}$$

$$\delta\chi^a = 0\,. \tag{2.9c}$$

Here ψ_M is the gravitino, λ is the spin one-half 'dilatino' and the χ^a's are the gluinos. In this section we work under the simplifying assumption that we are in a vacuum state where there are no fluxes and the dilaton field is constant:

$$H_3 = 0; \qquad \phi = \text{ const}\,. \tag{2.10}$$

Moreover, we focus exclusively on the vanishing of the variation of the gravitino field (2.9a), which allows to determine the properties of the compact manifold X_6 [7]. Under the assumption (2.10), the condition (2.9a) reads $\delta\psi_M \equiv \nabla_M\eta = 0$ (∇_M is the covariant derivative defined on the 10d manifold), which implies that there must exist a well-defined and no-where vanishing 6d spinor field η defined on X_6, satisfying:

$$\nabla_m\eta(y^m) = 0\,. \tag{2.11}$$

Eq. (2.11) says that if one parallel transports η around a loop in X_6, it does not get rotated. A spinor of this kind is called a *Killing spinor*.

The requirement of having a Killing spinor can be equivalently expressed in terms of the holonomy group[8] $\mathrm{Hol}(X_6)$ of X_6. The holonomy group of a manifold which admits the existence of a spinor η satisfying (2.11), indeed, consists of the subset of matrices U of $SO(6)$ that keep η invariant: $U\eta = \eta$. In other words, if we assume η to have positive chirality, and therefore to belong to the $\mathbf{4}$ spinorial representation of $SO(6)$, $\mathrm{Hol}(X_6)$ is the proper subgroup of $SO(6)$ such that the $\mathbf{4}$ is decomposed as $\mathbf{1}\oplus\ldots$ under representations of the holonomy group itself.

The number of singlets in this decomposition gives the number of supersymmetries in 4d. In particular, an $SU(3)$ holonomy corresponds to a string compactification with $\mathcal{N}=1$ supersymmetry, as $\mathbf{4}\to\mathbf{1}\oplus\mathbf{3}$.

[6] To be more precise, we have an unbroken supersymmetry if we can choose η such that the conserved supercharge Q associated to it annihilates the vacuum state $|\Omega\rangle$, that is if

$$\langle\Omega|\{Q,U\}|\Omega\rangle = 0\,, \tag{2.8}$$

for any (fermionic and bosonic) operator U. This condition is automatically satisfied for any bosonic field (for which $\{Q,U\}$ is a fermionic operator, hence its VEV is forced to vanish by the 4d Lorenz symmetry). If instead U is a fermionic operator, the condition (2.8) is equivalent, in the classical limit, to asking that the variation δU of the elementary fermionic fields under the supersymmetry transformation generated by Q, vanishes.

[7] The requirement (2.9b) turns out to be automatically satisfied under our simplifying assumption (2.10), while (2.9c) does not impose additional requirements on the compact space X_6.

[8] The holonomy group is the set of rotations experienced by the spinor for all possible closed loops in X_6. For a generic 6d manifold, the holonomy group is $SO(6)$.

How can we determine whether a manifold satisfies the above requirement, without explicitly computing its metric?

The answer to this question is given by the Calabi's conjecture, proven by Yau, which states that an N-dimensional complex Kähler manifold with vanishing first Chern class admits an $SU(N)$ holonomy metric, therefore providing a way to recognize manifolds that are suitable for compactifications preserving SUSY. A manifold of this kind is called *Calabi-Yau* (CY) *manifold* and, consequently, a compactification on it is called a CY compactification.

Let us analyze the definition in more detail [5]. A Kähler manifold is a complex manifold with a Hermitean metric ($g_{ij} = g_{\bar{i}\bar{j}} = 0$) such that its Kähler form

$$J = i g_{i\bar{j}}\, dz^i \wedge d\bar{z}^{\bar{j}} \tag{2.12}$$

is closed: $dJ = 0$ ($z, \bar{z}$ are the complex coordinates defined on the manifold). The holonomy group of a Kähler manifold is $U(N) \simeq U(1) \times SU(N)$, but it can be further reduced to the desired $SU(N)$ by imposing also Ricci-flatness. According to the CY theorem this is equivalent to requiring a vanishing first Chern class. Finally, the metric of a Kähler manifold can be locally expressed in terms of the so-called Kähler potential $K(z, \bar{z})$, as:

$$K_{i\bar{j}} = \frac{\partial}{\partial z^i} \frac{\partial}{\partial \bar{z}^{\bar{j}}} K(z, \bar{z})\,. \tag{2.13}$$

A CY threefold has a nowhere vanishing holomorphic (3,0)-form

$$\Omega_{3,0} = \Omega_{ijk}\, dz^i \wedge dz^j \wedge dz^k\,, \tag{2.14}$$

which is covariantly constant in the Ricci-flat metric: $\bar{\partial}\Omega_{3,0} = 0$.

The choice of the complex structure and of the Kähler form defines the metric of the CY uniquely. The metric moduli can then be defined by considering deformations of J (said Kähler moduli) and Ω (complex structure moduli). The Kähler form is closed but not exact, hence it is cohomologically non-trivial[9] and it can be expanded in a basis of the cohomology group $H^{1,1}(X_6)$, consisting of the harmonic $(1,1)$-forms $\{\omega_a\}_{a=1,\dots,h^{1,1}}$ [10]:

$$J = t^a(x)\, \omega_a\,. \tag{2.15}$$

The $h^{1,1}$ real parameters $t^a(x)$ are known as Kähler moduli and they parametrize the size of the internal 2-cycles of the CY. Notice that the 'breathing mode' of the example in the previous section is one of the Kähler moduli of the CY.

Similarly, deformations of the complex structure are defined by a 3-form $\delta\Omega$ in the cohomology group $H^{1,2}(X_6)$; this can be expanded in a basis $\{\chi_A\}_{A=1,\dots,h^{1,2}}$ of $H^{1,2}(X_6)$, leading to the definition of $h^{1,2}$ complex parameters $Z^A(x)$, called complex structure moduli, controlling the size of 3-cycles in the internal space. These correspond to the metric deformations δg_{ij}, according to the relation:

$$\delta g_{ij} = \frac{i}{||\Omega||^2} Z^A(x)\, (\chi_A)_{i\bar{j}\bar{k}}\, \Omega^{\bar{j}\bar{k}}{}_j \tag{2.16}$$

[9] See App. B for a short review of cohomology and homology groups.

[10] A_p is a harmonic p - form if it is such that $dA_p = d(*A_p) = 0$, where d is the exterior derivative defined in App. B and $*$ is the Hodge-$*$ operator.

where $||\Omega||^2 = \frac{1}{3!}\Omega_{ijk}\bar{\Omega}^{ijk}$.

The metric moduli of a CY are then $h^{1,1}$ Kähler moduli (real) and $h^{1,2}$ complex structure moduli (complex). Moreover, one can see that the only non-trivial Hodge numbers of a CY three-fold are[11] $h^{1,1}$ and $h^{1,2}$. It is also useful to introduce the Euler number of the CY that is:

$$\chi(X_6) \equiv \sum_{i,j=0}^{3} (-1)^{i+j} h^{i,j} = 2(h^{1,1} - h^{1,2}) \,. \tag{2.17}$$

2.2.3 Moduli for type IIB compactification on a CY

In this section we present the low energy 4d spectrum of type IIB string theory compactified on a CY.

As mentioned before, any string compactification produces massless scalars called moduli, corresponding to deformations of the internal manifold. In particular, any compactification on a CY three-fold contains the $h^{1,1}$ Kähler and the $h^{1,2}$ complex structure moduli introduced in the previous section. These are not the only 4d fields arising from compactification: other ones appear after expanding in terms of harmonic forms all the 10d fields included in the effective action (2.1):

$$\begin{aligned} &B_2 = B_2(x) + b^a(x)\omega_a, \quad C_2 = C_2(x) + c^a(x)\omega_a; \quad a = 1, ..., h^{1,1} \\ &C_4 = D_2^a \wedge \omega_a + V^A(x) \wedge \alpha_A - U_A(x) \wedge \beta^A + \theta_a(x)\tilde{\omega}^a; \quad A = 0, ..., h^{1,2} \,. \end{aligned} \tag{2.18}$$

Here, the dependence on the space-time coordinates is highlighted in the 4d fields in order to distinguish them from the 10d ones. In the above expansions, (α_A, β^A) form a basis of harmonic 3-forms for $H^3(X_6)$, while $\{\tilde{\omega}^a\}_{a=1,...,h^{1,1}}$ is a basis of $H^{2,2}(X_6)$. Notice that the self-duality condition of $\tilde{F}_5$ eliminates half of the degrees of freedom in C_4. With a proper choice of basis (see [21]), one can leave the scalars θ_a and the 1-forms V^A. Finally, the dilaton and the axion give rise to two more scalars in the 4d theory: ϕ, C_0.

All these fields can be grouped into multiplets of the 4d $\mathcal{N} = 2$ supersymmetry.

2.3 Calabi-Yau orientifolds

Compactifications with $\mathcal{N} = 2$ supersymmetry do not allow for fermions in chiral representations of gauge groups, therefore they can not lead to realistic models. However, $\mathcal{N} = 2$ supersymmetry can be broken to the more promising $\mathcal{N} = 1$ by appropriately introducing branes and/or orientifold planes.

The D-branes wrap submanifolds of the space time on which an open string can end. A Dp-brane, in particular, is an object with p space dimensions, charged under C_{p+1} via the electric coupling:

$$S_{CS} = T_p \int_{\Sigma_{p+1}} C_{p+1} \tag{2.19}$$

with $T_p = (2\pi)^{-p}(\alpha')^{-\frac{p+1}{2}}$. In type IIB string theory, only branes with p odd appear.

[11] For the other Hodge numbers we have: $h^{0,0} = h^{0,3} = 1$, while $h^{0,1} = h^{0,2} = 0$. All the other values can be derived from these, using the symmetries (B.5) and (B.6).

The orientifold planes (O-planes) are non-dynamical extended objects placed at the fixed point loci of an involution of the spacetime. As for the Dp-branes, an Op-plane has p space dimensions. The main reason why we are interested in them is that since X_6 is a compact space, the sum of all the charges defined inside it must vanish. Therefore, any theory containing D-branes must also include sources with negative charge: the O-planes are the best understood sources of this kind.

Let us focus on the extra-dimensions, that live on a (compact) CY three-fold X_6. Depending on the transformation properties of the holomorphic $(3,0)$-form Ω, two different symmetry operations are possible:

$$\begin{aligned} \mathcal{O}_{(1)} &= (-1)^{F_L}\Omega_{ws}\,\sigma^*; \quad \sigma^*\Omega = -\Omega \\ \mathcal{O}_{(2)} &= \Omega_{ws}\,\sigma^*; \quad \sigma^*\Omega = \Omega\,. \end{aligned} \tag{2.20}$$

Here, F_L is the space-time fermion number in the left-moving sector, while Ω_{ws} reverses the worldsheet orientation, by exchanging left- and right- moving modes. σ is the geometric involution ($\sigma^2 = 1$) that can act non-trivially on Ω (as specified in the equation), leaving the metric and complex structure (and hence J) invariant; its action on forms (pull-back) is indicated with σ^*. In this work we will only consider the involution $\mathcal{O}_{(1)}$ (therefore dropping the subscript from now on).

What kind of O-planes are allowed by type IIB string theory with the selected involution?

- Since σ is an internal symmetry, all the allowed Op-planes need to be space-time filling ($p \geq 3$).
- Being a holomorphic involution, σ only allows for even-dimensional (including the time direction) orientifold planes ($p = 2n+1;\ n = 1, ..., 4$).
- Since it is always possible to choose locally $\Omega \propto dz^1 \wedge dz^2 \wedge dz^3$, our choice $\sigma^*\Omega = -\Omega$ implies that either one or three complex coordinates are inverted by σ.

We can therefore conclude that the only orientifold planes allowed in type IIB string theory orientifolded by $\mathcal{O}$ are $O3$- and $O7$-planes.

Our purpose is to 'orientifold' the theory, which means that we will mod it out by $\mathcal{O}$. In order to understand how this affects the massless spectrum of the theory, we should first notice that the holomorphic involution σ splits each cohomology group $H^{(p,q)}$ into two eigenspaces under its action:

$$H^{(p,q)} = H^{(p,q)}_+ \oplus H^{(p,q)}_-$$

where $H^{(p,q)}_+$ contains all the (p,q)-forms that are even under σ^*, while $H^{(p,q)}_-$ is the odd eigenspace of σ^*. From the properties of σ^* one can deduce the following rules for the corresponding Hodge numbers [21]:

$$\begin{gathered} h^{1,1}_\pm = h^{2,2}_\pm; \quad h^{2,1}_\pm = h^{1,2}_\pm; \quad h^{3,0}_+ = h^{0,3}_+ = 0; \quad h^{3,0}_- = h^{0,3}_- = 1; \\ h^{0,0}_+ = h^{3,3}_+ = 1; \quad h^{0,0}_- = h^{3,3}_- = 0\,. \end{gathered} \tag{2.21}$$

Moreover, the projection $\mathcal{O}$ acts on the fields according to the following rules:

1. $(-1)^{F_L}$ only acts on the RR sector, changing the sign to C_0, C_2 and C_4
2. Ω_{ws} only acts on B_2, C_0 and C_4, changing their sign.
3. The action of σ^* is deduced from the previous rules, imposing that each field is invariant under the whole projection $\mathcal{O}$. In particular, it turns out that it acts non-trivially only on B_2 and C_2. Moreover we recall that σ^* is such that:

$$\sigma^* J = J; \quad \sigma^* \Omega = -\Omega \,. \tag{2.22}$$

With all this information it is now straightforward to derive the massless spectrum of the orientifolded theory, by restricting the expansions (2.15), (2.16), (2.18) to the terms that are invariant under σ^*. As an example, the expansion of the Kähler form J can now contain only even modes under σ, therefore becoming

$$J = t^i(x)\,\omega_i; \quad i = 1, \dots, h^{1,1}_+$$

(where $\{\omega_i\}_{i=1,\dots,h^{1,1}_+}$ is a basis for $H^{1,1}_+$), while only the $h^{1,2}_-$ odd modes will be kept in the expansion for Ω.

In conclusion the 4d massless spectrum of the orientifolded theory is given by the following fields[12], appropriately combined in order to have proper Kähler coordinates on the moduli space:

- The dilaton ϕ and the axion C_0, combined in the axio-dilaton

$$S = e^{-\phi} - iC_0 \,. \tag{2.23}$$

- $h^{1,1}_+$ complex scalars $T_i(x)$, called Kähler moduli, obtained by reorganizing the $h^{1,1}_+$ scalars $t^i(x)$, coming from the Kähler form J, and the $h^{1,1}_+$ θ_i, coming from the RR C_4:

$$T_i = \frac{3}{4}\tau_i + \frac{3i}{2}\theta_i - \frac{3}{4(S+\bar{S})} k_{iJK} G^J (G-\bar{G})^K \,, \tag{2.24}$$

  where $G^I = c^I - iSb^I$ $(I = 1, \dots, h^{1,1}_-)$ is a combination of $b^I(x)$ and $c^I(x)$, the $2h^{1,1}_-$ complex scalars coming from B_2 and C_2. Furthermore, the $\tau_i = \frac{1}{2} k_{ijk}\, t^j(x)\, t^k(x)$ are the volumes of the 4-cycles corresponding to the 2-cycle moduli t_i and $k_{ijk} = \int_Y \omega_i \wedge \omega_j \wedge \omega_k$ are the intersection numbers of the CY manifold.

- $h^{1,2}_-$ complex structure moduli $Z^\alpha(x)$.
- $h^{1,2}_+$ massless vectors $V^\kappa(x)$, coming from C_4.

The theory also contains moduli coming from the open string sector. With a few exceptions (see Sec. 4.5), in this work we will not take them into consideration. In the following, we will consider only cases with $h^{1,1}_- = 0$, therefore the complex scalars G^I will not be included in the analysis and Eq. (2.24), will simply read (after having re-absorbed the constant terms in τ_i and θ_i): $T_i = \tau_i + i\theta_i$.

[12] They reside in chiral multiplets of the $\mathcal{N} = 1$ supersymmetry.

The Kähler potential for the CY manifold in terms of the moduli reads[13]:

$$\kappa_4^2 K = K_{cs}(Z,\bar{Z}) + K_K(S,\bar{S},T,\bar{T}) \tag{2.25}$$

with

$$K_{cs} = -\ln\left[-i\int \Omega(Z)\wedge\bar{\Omega}(\bar{Z})\right]; \quad K_K = -\ln\left[S+\bar{S}\right] - 2\ln\left[\mathcal{V}(T,\bar{T})\right] . \tag{2.26}$$

Here $\mathcal{V}$ is the volume of the compact space (in Einstein frame and in units of the string length $l_s = 2\pi\sqrt{\alpha'}$), defined as:

$$\mathcal{V} = \int_{X_6} J\wedge J\wedge J = \frac{1}{3!}\,k_{ijk}\,t^i(x)t^j(x)t^k(x)\,. \tag{2.27}$$

Due to the form (2.25), the metric of the moduli space is block diagonal and correspondingly the moduli space has the form

$$\mathcal{M} = \mathcal{M}_{cs}^{h_-^{1,2}} \times \mathcal{M}_K^{h_+^{1,1}+1}\,, \tag{2.28}$$

where each factor is a Kähler manifold.

2.4 Why IIB?

In this section we summarize the main reasons that make type IIB string theory particularly promising from a phenomenological point of view and that, therefore, led to the choice of this framework for the present research work. Most of the topics mentioned here will be developed in more detail in the next chapters.

- *Moduli stabilization:* As explained before, string compactifications produce a lot of moduli. Since they are not observed in experiments, one needs to add further ingredients to the compactification, in order to give them large enough masses. This is, in general, a difficult task. In type IIB string theory, nevertheless, there are several well-known and well-studied mechanisms that, at least in principle, allow to stabilize all the moduli with large masses. In particular, as we will see in the next chapter, the dilaton and all the complex structure moduli can be stabilized at leading order by turning on worldvolume fluxes [10, 9], while sub-leading corrections allow to stabilize the Kähler moduli [11, 12].

- *Calabi-Yau manifold:* The fluxes that we turn on in order to stabilize the complex structure moduli and the dilaton, have a non-vanishing back-reaction on the geometry of the compact space, so that in general the new manifold is not a CY anymore. While, e.g., in type IIA string theory, even a small amount of fluxes usually affects dramatically the geometry, the back-reaction of the fluxes on type IIB is less severe.

[13] Along this work we will explicitly write the dependence on the gravitational coupling κ_4 (or equivalently the reduced Planck mass $m_p = \kappa_4^{-1}$) whenever it is useful to understand the dimensions of a given quantity ($[mass]^2$ for the Kähler potential), e.g. when we introduce a new element. We will omit it elsewhere.

In particular, for a large class of models in this framework, the new metric will only differ from the original one by a factor, keeping the same topology of the original one (conformal CY) [9].

- *Phenomenology:* Type IIB string models appear to be particularly promising from the point of view of string phenomenology and model building. First of all, due to the presence of the quantized fluxes (that stabilize the complex structure moduli and the dilaton), the theory has a high degree of discrete tunability of physical parameters, so that, at least in principle, they can be set to be of the order of the measured ones. Moreover, constructions of this type allow for a rich set of explicit D-brane configurations, useful for model building (see e.g. [26, 27, 28, 29, 30]) and naturally admit $D3$ and anti-$D3$ branes, which are necessary to develop promising models for inflation and present-day cosmic acceleration [11, 31]. Finally, they naturally contain strongly warped throats of Klebanov-Strassler type, that allow to generate large scale hierarchies [9].

Chapter 3

Moduli Stabilization

As mentioned in the previous chapter, a realistic string model cannot admit as many massless fields as the moduli, given that we do not observe them in experiments. We need therefore to add new ingredients and to find a mechanism such that in the new theory they all have a non-vanishing mass, which is large enough to justify the fact that we did not detect them. The procedure of giving a mass to the moduli, hence fixing them at a stable minimum of their scalar potential, is called *moduli stabilization*. In this chapter we will face the problem of stabilizing all the (hundreds of) moduli arising in type IIB string compactifications.

In general, after supersymmetry is broken, there should be nothing that protects the scalars to become massive, therefore one would expect quantum corrections to easily stabilize all of them. The issues come in the form of the so-called Dine-Seiberg problem [32], that can be summarized as follows: a stable minimum for the scalar potential of the moduli, can only be obtained via the competition of (perturbative and non perturbative) corrections at different orders of approximation. This means that at least some of the higher order corrections have a magnitude comparable with the first order ones, hence we are not in the weakly coupled regime and all higher order corrections might be relevant. This is usually encapsulated by the statement that "when corrections can be computed, they are not important, and when they are important, they cannot be computed" [33].

As we will see in the next section, flux compactification in type IIB string theory provides a natural way out for this problem, given that it includes a large number of parameters, such as the integer fluxes, which are not associated with the continuous VEV of any field and therefore can be tuned in order to get weakly coupled solutions. This possibility was already considered in the original paper [32].

Moreover, it should be noted that, as in any effective field theory, even if we don't have full computational control we can still trust the results of a computation as long as the couplings are small enough. In particular if we assume at the beginning that the two string expansion parameters are small and obtain weak couplings at the end of the computation, we will then be able to trust the approximation [18].

The starting point for moduli stabilization in string theory is given by the fact that in $\mathcal{N} = 1$ supergravity, knowing the Kähler potential K and the superpotential W (which we

will introduce in the next section) determines the scalar potential for the moduli[1]:

$$V = e^{\frac{K}{m_p^2}} \left(K^{I\bar{J}} D_I W \overline{D_J W} - 3\frac{|W|^2}{m_p^2} \right) \tag{3.1}$$

where $K_{\bar{I}J} \equiv \partial_{\bar{I}}\partial_J K$ is the Kähler metric ($K^{I\bar{J}}$ is its inverse, transposed) and $D_I W = \partial_I W + (\partial_I K)W$ is the Kähler covariant derivative of the superpotential. It should be noticed that the potential (3.1) only includes the so-called *F-term*. In addition to this, one should also consider the D-term[2] potential, generated by charged matter fields. With a few exceptions (see e.g. Sec. 4.5) we will not consider the presence of such fields. The purpose of the next sections is to explicitly compute the above scalar potential for certain situations and to find a minimum for all the corresponding moduli.

3.1 Complex structure moduli stabilization

In this section we review flux compactification in type IIB string theory, which leads to the stabilization of all the complex structure moduli and the dilaton. This was first studied by S. B. Giddings, S. Kachru and J. Polchinski (GKP) in [9], where they also highlighted the relationship between flux compactifications and large hierarchies of physical scales.

First of all, in Sec. 3.1.1 we introduce the background fluxes and their main features, starting from the need of a new metric ansatz. In Sec. 3.1.2 we present the moduli stabilization procedure. Finally, in Sec. 3.1.3 we describe in more detail the standard choice for the new warped metric, that is the warped deformed conifold.

3.1.1 Fluxes

In type IIB string theory, one can turn on non-trivial background RR and NSNS harmonic three-form fluxes H_3 and F_3 in the Calabi-Yau. From what was said in Sec. 2.3, it is easy to see that in the presence of an orientifold involution, both H_3 and F_3 need to be odd under the action of σ, given that they are defined as $H_3 = dB_2$, $F_3 = dC_2$ and that the exterior derivative commutes with σ^*. As a consequence they can be expressed in terms of elements of $H^{(3)}_-(Y)$. In particular, it is convenient to combine them into the complex three-form[3]

$$G_3 = F_3 + iSH_3 \,, \tag{3.2}$$

where S is the axio-dilaton defined in the previous chapter.

The presence of fluxes imposes a modification of the metric ansatz (2.4) to the warped one [34]:

$$ds^2 = e^{2A(y)} g_{\mu\nu}(x) dx^\mu dx^\nu + e^{-2A(y)} \tilde{g}_{i\bar{j}}(y) dy^i d\bar{y}^{\bar{j}} \,. \tag{3.3}$$

[1] *Notation*: the capital letters $I, \bar{J}$, are used when the indices run over all the moduli; the lower case letters $i, \bar{\jmath}$ when they run only over the complex structure moduli and the dilaton; the Greek letters $\alpha, \bar{\beta}$ when they run only over the Kähler moduli.

[2] The terminology comes from supersymmetry.

[3] Not to be confused with the scalar fields G^I defined in Sec. 2.3.

In particular, we are interested in backgrounds maintaining the four-dimensional Poincaré symmetry. This implies that G_3 has non-vanishing components only along compact directions, and that the self-dual five-form $\tilde{F}_5$ can be written in the form [9]:

$$\tilde{F}_5 = (1+*)d\alpha(y) \wedge dx^0 \wedge dx^1 \wedge dx^2 \wedge dx^3$$

where $\alpha(y)$ is a scalar function defined on the compact space. In (3.3), $e^{2A(y)} \equiv h^{-1/2}(y)$ [9], where $h(y)$ is the *warp factor*, which satisfies a Poisson-like equation sourced by 3-form fluxes and localized objects, like D-branes and O-planes: in regions in which it is large, points that would be close in the unwarped metric are instead far away one from the other, therefore it acts as a redshift factor for objects localized in such regions.

The fluxes are discrete degrees of freedom. Indeed, the extension to p-forms of the Dirac quantization condition [35, 36], establishes that they must be integrally quantized, that is the integrals of the fluxes over arbitrary closed 3-cycles Σ must be integer:

$$\frac{1}{(2\pi)^2\alpha'}\int_\Sigma F_3 \in \mathbb{Z}; \quad \frac{1}{(2\pi)^2\alpha'}\int_\Sigma H_3 \in \mathbb{Z}\,. \tag{3.4}$$

Tracing the ten-dimensional Einstein's equations it is possible to derive important information on the allowed flux/brane configurations. Indeed, one gets [23]

$$\nabla^2 e^{4A} = \left[e^{8A}\frac{|G_3|^2}{2\,\mathrm{Re}\,S} + e^{-4A}\left(|\partial\alpha|^2 + |\partial e^{4A}|^2\right)\right] + 2\kappa_{10}^2\, e^{2A}\mathcal{J}_{loc}\,, \tag{3.5}$$

where ∇^2 is the Laplacian on X_6 and $\mathcal{J}_{loc} \equiv \frac{1}{4}(T^m_m - T^\mu_\mu)^{loc}$ is the contribution coming from possible local sources (T_{MN} is the stress-energy tensor). Since

$$\int_{X_6} \nabla^2 e^{4A} = 0$$

and the terms inside the squared brackets are positive definite, one deduces the following:

- In the absence of localized sources ($\mathcal{J}_{loc} = 0$) the fluxes must vanish ($G_3 = 0, \alpha =$ const and constant warp factor).
- In presence of non-vanishing fluxes ($G_3 \neq 0$), one must impose $\mathcal{J}_{loc} < 0$, which is obtained by introducing objects with negative charge, such as the orientifold planes.

Another important constraint is the *tadpole cancellation condition* given by the integrated Bianchi identities for $\tilde{F}_5$

$$\frac{1}{(2\pi)^4\alpha'^2}\int_{X_6} H_3 \wedge F_3 + Q_3^{loc} = 0\,, \tag{3.6}$$

according to which the total $D3$ charge from the supergravity background and the local sources must vanish.

Combining (3.5) and (the non integrated form of) (3.6), one obtains:

$$\nabla^2\left(e^{4A} - \alpha\right) = \frac{e^{8A}}{24\,\mathrm{Re}\,S}|iG_3 - *_6 G_3|^2 + e^{-4A}|\partial(e^{4A} - \alpha)|^2 + 2\kappa_{10}^2\, e^{2A}(\mathcal{J}_{loc} - T_3\rho_3^{loc}) \tag{3.7}$$

where $*_6$ is the 6-dimensional Hodge star operator, ρ_3^{loc} is the $D3$-brane density charge ($Q_3^{loc} = \int_{X_6} \rho_3^{loc}$) and T_3 is the tension associated to the local source of $D3$ charge[4].

As we can see by integrating it, Eq. (3.7) is solved by an imaginary self-dual (ISD) three-form flux

$$*_6 G_3 = iG_3 \,, \tag{3.8}$$

a warp factor $e^{4A(y)} = \alpha(y)$ and local sources satisfying

$$\mathcal{J}_{loc} = T_3 \, \rho_3^{loc}. \tag{3.9}$$

It should be noted that (3.9) implies that only $D3$-branes, $O3$-planes and $D7$-branes are allowed in this kind of configuration.

At tree-level in the four-dimensional low energy theory, non-vanishing fluxes generate the superpotential, first derived by Gukov, Vafa and Witten (GVW) in [37]:

$$W_{GVW} = \int_{X_6} \Omega \wedge G_3 \tag{3.10}$$

which is such that the F-term equations obtained from it reproduce the ISD condition (3.8). It is important to notice that W_{GVW} only depends on the dilaton and the complex structure moduli.

3.1.2 Complex structure moduli stabilization

Let us now study how the presence of 3-form fluxes allows to stabilize all the complex structure moduli and the dilaton.

First of all, let us compute the SUGRA scalar potential (3.1) for a model described by the Kähler potential (2.25) and the Gukov-Vafa-Witten superpotential (3.10), generated by the fluxes. Regarding this, it is crucial to notice that (2.25) depends on all the moduli, while (3.10) depends only on the dilaton and the complex structure moduli. Moreover, the Kähler potential is such that[5] $K^{\alpha\bar{\beta}}\partial_\alpha K \partial_\beta K = 3$. This is the so-called *no-scale* structure [38, 39], thanks to which the scalar potential simplifies to

$$V = e^K \left(K^{i\bar{\jmath}} D_i W \, \overline{D_j W} \right) \,, \tag{3.11}$$

where we also used the fact that $K^{\alpha\bar{\jmath}} = K^{i\bar{\beta}} = 0$.

The scalar potential (3.11) is positive definite and it has a minimum at

$$D_i W = 0 \tag{3.12}$$

with vanishing vacuum energy. Such minimum is non-supersymmetric due to the fact that $D_\alpha W \neq 0$ (because $\partial_\alpha K \neq 0$)[6]. Moreover, the equations (3.12) only involve the complex structure moduli and the dilaton, therefore solving them means fixing all those moduli. In particular, (3.11) also tells us that once we fix the moduli at their minimum, the scalar potential vanishes; the Kähler moduli are then flat directions.

[4] See the beginning of Sec. 2.3.

[5] For the notation used for the indices, see footnote 1 of this chapter.

[6] A minimum is supersymmetric if it solves $D_I W = 0, \ \forall I$.

The masses (squared) of the moduli at the minimum of the scalar potential are given by the eigenvalues of the matrix[7] $M_k^i = K^{i\bar{j}}\partial_{\bar{j}}\partial_k V$. In particular for the complex structure moduli we get [13]:

$$m_{cs}^2 \sim \frac{g_s^4 N^2 m_p^2}{\mathcal{V}_s^2} \sim \frac{M_s^2}{\mathcal{V}_s} \tag{3.13}$$

where $N \sim \mathcal{O}\left(\sqrt{\frac{\chi}{24}}\right)$ is a measure of the typical number of flux quanta and the volume is expressed in the string frame.

It should be noted that, though the above result generically ensures the presence of a minimum of the scalar potential for the complex structure moduli and the dilaton, the explicit analysis of such scalar potential and the solution of the equations (3.12) can be very difficult, due to the fact that typically we have to deal with CY geometries with a few Kähler moduli but many ($\mathcal{O}(100)$) complex structure moduli. Nonetheless there is the possibility that for a subset of all the CY geometries, additional symmetries of the complex structure moduli space allow to reduce the effective number of complex structure moduli, as was studied, for example in [40, 41, 42].

3.1.3 The conifold and the KS solution

Let us consider the so-called *conifold*, which is a cone whose base is the coset space $T^{11} = \frac{SU(2)\times SU(2)}{U(1)}$ that has the topology of $S^2 \times S^3$. It is described by the following equation in $\mathbb{C}^4$:

$$\sum_{n=1}^{4} z_n^2 = 0 \tag{3.14}$$

that is singular at $z_1 = ... = z_4 = 0$.

One can place integral and fractional $D3$-branes on top of the singularity. From a geometric point of view, a fractional D-brane can be described as a brane wrapped over a cycle shrunk to zero volume. In particular, in our framework, the fractional $D3$-branes are given by $D5$-branes wrapped on the S^2 of the base of the conifold, which, at the singularity, collapses to zero volume.

By placing N $D3$-branes and M fractional $D3$-branes at a conifold point, one ends up with a theory with gauge group $SU(N+M) \times SU(N)$. The supergravity dual of the theory includes M units of the 3-form flux and N units of the 5-form flux:

$$\int_{S^3} F_3 = M; \quad \int_{T^{11}} F_5 = N\,.$$

This theory is not conformal: the relative gauge coupling runs logarithmically at all scales and we observe a flow in which the size of the gauge group is repeatedly reduced by M units (Seiberg duality cascade), as was studied by I.R. Klebanov and M.J. Strassler (KS) in [34]. If nothing happened to stop this flow, one would end up with a warped singular conifold. Nonetheless, it was shown that at a certain point, in the IR, non-perturbative effects become relevant and resolve the singularity [43, 34].

[7] See also App. C.

The fact that from the supergravity side the conifold can be replaced by a deformed conifold is actually an assumption, but it is supported by several arguments. The main one is that the field theory analysis shows that the spacetime geometry is indeed modified in the IR and the deformed conifold is compatible with the deformed moduli space that one gets in that frame [34].

A deformed conifold is obtained by blowing-up, to a finite volume, the S^3 of the base of the cone (while leaving the S^2 with zero volume). Its equation in $\mathbb{C}^4$ is:

$$\sum_{n=1}^{4} z_n^2 = \Sigma\,. \tag{3.15}$$

The introduction of Σ, which controls the size of the (blown-up) S^3, removes the singularity, as the point $\{z_i\}_{i=1,\dots,4} = 0$ does not belong to the space anymore. On the other side, far from the (former) singular point Σ is negligible and the metric of the deformed conifold is well approximated by that of the singular one.

The warped metric of the deformed conifold (*KS throat*) can be written, in terms of an appropriate basis of 1-forms on the compact space [44], in the diagonal form:

$$\begin{aligned} ds_6^2 =& \frac{1}{2}|\Sigma|^{2/3}\mathcal{K}(y)\left[\frac{1}{3\,\mathcal{K}^3(y)}\left[dy^2+(g^5)^2\right]+\cosh^2\left(\frac{y}{2}\right)\left[(g^3)^2+(g^4)^2\right]\right.\\ &\left.+\sinh^2\left(\frac{y}{2}\right)\left[(g^1)^2+(g^2)^2\right]\right] \end{aligned} \tag{3.16}$$

where all the moduli dependence is in the Σ factor and

$$\mathcal{K}(y) = \frac{(\sinh(2y)-2y)^{1/3}}{2^{1/3}\sinh y}.$$

To better understand this metric, it is useful to notice that if we set $y = 0$, we obtain the metric of the S^3:

$$d\Omega_3^2 = \frac{1}{2}|\Sigma|^{2/3}\left(\frac{2}{3}\right)^{1/3}\left[\frac{(g^5)^2}{2}+(g^3)^2+(g^4)^2\right]$$

where we used that $\mathcal{K}(0) \approx \left(\frac{2}{3}\right)^{1/3}$.

On the other side, given that $\sinh^2\left(\frac{y}{2}\right) \underset{y\to 0}{\approx} \frac{y^2}{4}$, we can see that the two shrinking directions have the metric of an S^2 fibred over the S^3:

$$\frac{1}{8}|\Sigma|^{2/3}\left(\frac{2}{3}\right)^{1/3} y^2\left[(g^1)^2+(g^2)^2\right] \xrightarrow[y\to 0]{} 0\,.$$

The KS solution describes a non-compact smooth manifold; nonetheless this result can be extended to the compact context [9] by considering warped manifolds such as (3.3) in which the local geometry of the warped throat is close to that of the KS throat. To be clearer, let us consider again the ansatz (3.3) which, after a few simple manipulations, can be written as [45] (see also [46]):

$$ds^2 = \left(c+\frac{e^{-4A(y)}}{\mathcal{V}^{2/3}}\right)^{-1/2} g_{\mu\nu}dx^\mu dx^\nu + \left(c+\frac{e^{-4A(y)}}{\mathcal{V}^{2/3}}\right)^{1/2} ds^2_{CY_0}\,. \tag{3.17}$$

Notice that, with abuse of notation, we are redefining $e^{-4A(y)} \to c + \frac{e^{-4A(y)}}{\mathcal{V}^{2/3}}$. Here, $ds^2_{CY_0}$ is the metric of an unit-volume CY ($ds^2_{CY} = \mathcal{V}\, ds^2_{CY_0}$) and c is a constant. From this form, some properties of the metric become more evident: in particular, at large volume $\mathcal{V}^{2/3} \gg e^{-4A(y)}$, the metric becomes the standard unwarped one (2.4), while the highly warped limit, in which the metric of the internal manifold can be approximated by the KS solution, corresponds to $\mathcal{V}^{2/3} \ll e^{-4A(y)}$.

Assuming that we are in a background in which the dilaton is constant, the warp factor can be obtained by solving the Einstein equations, together with the IIB equations satisfied by the 3-form fluxes and it reads [17]:

$$e^{-4A(y)} = \alpha\, \frac{2^{2/3}}{|\Sigma|^{4/3}} \int_y^\infty dx\, \frac{x \coth x - 1}{\sinh^2 x} \left(\sinh(2x) - 2x\right)^{1/3} \tag{3.18}$$

where $\alpha \propto (\alpha' g_s M)^2$ is a normalization factor. The above expression satisfies [34]

$$e^{-4A(y)} \underset{y\to 0}{\longrightarrow} a_0 \,,$$

from which it is manifest that there is no singularity at the tip of the deformed conifold.

An important feature of this result is that given that the integral in (3.18) converges, we have

$$a_0 \underset{y=0}{\sim} \alpha \,. \tag{3.19}$$

Therefore, since in this limit the 10-dimensional metric reads

$$ds^2 \underset{y\to 0}{\longrightarrow} a_0^{-1/2} g_{\mu\nu}(x)\, dx^\mu dx^\nu + a_0^{1/2} \left[\frac{1}{2} dy^2 + d\Omega_3^2 + \frac{1}{8}|\Sigma|^{2/3} \left(\frac{2}{3}\right)^{1/3} y^2 \left[(g^1)^2 + (g^2)^2\right]\right] ,$$

the radius-squared of the S^3 at $y = 0$ is:

$$R^2_{S^3} \sim a_0^{1/2} \sim \alpha' g_s M \,. \tag{3.20}$$

In other words, if the 't Hooft coupling $g_s M$ is large, the radius of the S^3 is large as well (compared to the string scale) and the curvatures are small, so that we can trust the SUGRA approximation.

The global setup of interest for us is a deformed conifold glued to a compact CY space. We will call Z the relevant complex structure modulus for this configuration, that is the one controlling the size of the S^3 at the tip of the conifold[8]. With this notation, the singular point corresponds to $Z = 0$. In terms of this modulus, the warp factor (3.18) reads [17]:

$$e^{-4A(y)} \sim 2^{2/3} \frac{g_s M^2}{(\mathcal{V}_w |Z|^2)^{2/3}}\, \mathcal{I}(y) \tag{3.21}$$

[8] Z is therefore related to the deformation parameter Σ introduced in (3.15). However, the former has the dimensions of [length]^3, while Z is dimensionless. The relation between the two was derived in [17] as:

$$\Sigma \to (\alpha')^{3/2} \sqrt{g_s^{3/2} \mathcal{V}_w}\, Z \,.$$

where $\mathcal{V}_w$ is the warped volume of the CY in units of α':

$$\mathcal{V}_w = \frac{1}{g_s^{3/2}(\alpha')^3}\int d^6y\, e^{-4A}\sqrt{\tilde{g}} \sim \mathcal{V}$$

and $\mathcal{I}(y)$ is the integral which appears in (3.18).

Assuming for definiteness that the conifold is centered at $y = 0$ and that it is glued to the CY at a distance $y \simeq \Lambda_0$, we can distinguish three main regions [47]:

1. $y \geq \Lambda_0$: the transition region between the conifold and the bulk.
2. $(g_s M\alpha')^{1/2} \leq y \leq \Lambda_0$: a deformed conifold with an approximately constant warp factor $e^{-4A(y)} \sim c$. In this region, the back-reaction of the fluxes on the geometry is negligible. This regime, which is called the *dilute flux regime* corresponds to the limit $\mathcal{V}^{2/3} \gg e^{-4A(y)}$ in (3.17) or, equivalently, to $\mathcal{V}_w|Z|^2 \gg 1$ in terms of the conifold complex structure modulus (see (3.21)).
3. $y \ll (g_s M\alpha')^{1/2}$: near the tip of the conifold the back-reaction of fluxes is not negligible anymore and we are in the strongly warped limit, described by the KS solution.

In the following we will consider the stabilization of the conifold complex structure modulus both in the dilute flux and in the strongly warped limit, highlighting the main differences.

The dilute flux regime

In the deformed conifold, there are two relevant 3-cycles: following the notation of [9], we will call A the 3-cycle vanishing at the singularity ($Z \to 0$) and B the 3-cycle dual to A. The presence of the second 3-cycle is ensured by the fact that we are in a compact space. The Kähler potential can be written in terms of the periods Π_α as [17]:

$$K_{df} = -\log\left(-i\int_X \bar{\Omega}\wedge\Omega\right) = -\log\left(-i\,\bar{\Pi}\,\eta\,\Pi\right) \tag{3.22}$$

where η is the symplectic pairing:

$$\eta = \begin{pmatrix} 0 & \mathbb{I} \\ -\mathbb{I} & 0 \end{pmatrix}. \tag{3.23}$$

The periods we are interested in are [48]:

$$\Pi_A = \int_A \Omega = \Sigma \qquad \Pi_B = \int_B \Omega = \frac{\Sigma}{2\pi i}\left(\log\frac{\Lambda_0^3}{\Sigma} + 1\right) + C + \mathcal{O}(\Sigma)$$

where C depends on the details of the compactification manifold but is constant with respect to Σ and Λ_0 is the cutoff corresponding to the transition between the highly warped region and the rest of the compact Calabi-Yau manifold. Substituting these expressions in (3.22) we obtain:

$$K_{df} = -\log\left(-\frac{|\Sigma|^2}{2\pi}\log\frac{\Lambda_0^6}{|\Sigma|^2} + A + \mathcal{O}(\Sigma)\right) \tag{3.24}$$

with $A > 0$ a real constant, from which we can derive the Kähler metric for the conifold complex structure modulus:

$$K_{\Sigma\bar{\Sigma}} = \frac{\partial^2 K_{df}}{\partial\bar{\Sigma}\,\partial\Sigma} \approx \frac{1}{2\pi A}\log\frac{\Lambda_0^6}{|\Sigma|^2}\,. \tag{3.25}$$

Let us turn on M units of F_3 on the A-cycle and $-K$ units of H_3 on the B-cycle:

$$\frac{1}{2\pi\alpha'}\int_A F_3 = 2\pi M\,; \quad \frac{1}{2\pi\alpha'}\int_B H_3 = -2\pi K\,. \tag{3.26}$$

The $D3$-charge associated to these fluxes is

$$\frac{1}{2\kappa_{10}^2 T_3}\int_{X_6} H_3\wedge F_3 = MK \tag{3.27}$$

and they generate the superpotential (3.10), which in this case reads [17]:

$$W = W_{cs} + (2\pi)^2\alpha'\left(M\int_B\Omega + iKS\int_A\Omega\right) \approx W_{cs} + \frac{M}{2\pi i}\Sigma\left(\log\frac{\Lambda_0^3}{\Sigma}+1\right) + iKS\,\Sigma \tag{3.28}$$

where W_{cs} is a constant depending on the other complex structure moduli, that we consider to be stabilized at higher energies.

We can therefore conclude that the scalar potential for the conifold complex structure modulus, which we now write in terms of the (dimensionless) variable Z, is:

$$V_Z \approx m_p^4\frac{g_s}{\mathcal{V}^2\log\frac{\Lambda_0^3}{|Z|}}\left|\frac{M}{2\pi i}\log\frac{\Lambda_0^3}{Z} + i\frac{K}{g_s}\right|^2 \tag{3.29}$$

where the cutoff Λ_0 was consistently redefined so that now it is dimensionless; we assumed the axio-dilaton to be stabilized at $S_0 = \frac{1}{g_s}$ and the factor $\frac{g_s}{\mathcal{V}^2}$ comes from $e^{K(\mathcal{V},S,Z)}$. After writing Z as $Z = \zeta e^{i\sigma}$, it is straightforward to see that V_{cs} is stabilized at:

$$\zeta_0 = \Lambda_0^3\, e^{-\frac{2\pi K}{g_s M}}; \quad \sigma_0 = 0. \tag{3.30}$$

An important consequence of the introduction of the fluxes in the compact space is that, deforming the manifold to a warped one, they produce a large and finite hierarchy of physical scales in the 4d theory [9]. This allows, in particular, to give an explanation to the origin of the observed small ratio M_{weak}/M_p . In a warped space-time, indeed, a single invariant energy scale can give rise to several 4-dimensional scales whose magnitude is determined by the (position-depending) gravitational redshift in the transverse space. Hence, the hierarchy of energy scales depends on the warp factor and it is fixed once the complex structure moduli in terms of which the last is defined are stabilized. Since the hierarchy of energy scales was estimated in [9] to be

$$e^{A_{min}} \sim \zeta^{1/3} \sim e^{-\frac{2\pi K}{3g_s M}}\,,$$

we can observe from (3.30) that if we choose the fluxes such that $\frac{K}{g_s M} \ll 1$, ζ turns out to be exponentially small and the same is true for the hierarchy itself.

It should be noted that the mass square of the conifold complex structure modulus Z can be estimated as [17]:

$$m_Z^2 \sim \frac{m_p^2}{\mathcal{V}^2|Z|^2} \sim \frac{M_s^2}{\mathcal{V}|Z|^2} \,. \tag{3.31}$$

Since it is smaller than the string scale in the limit $\mathcal{V}|Z|^2 \gg 1$ we are considering, we conclude that the supergravity approximation is trustworthy. Moreover, by comparing (3.31) with (3.13) we can see that the conifold modulus is heavier with respect to the other complex structure moduli, hence in this regime we can consistently stabilize all these moduli at the same stage. We will see that this is not the case in the strongly warped regime.

As a final remark, it is worth to mention that the large number of possible discrete flux choices makes a statistical analysis of the possible vacua very interesting. From this kind of analysis [49, 50, 51] we know that there is an exponentially large number of solutions and that the regions close to conifold singularities in the moduli space act as attractors, where many solutions concentrate.

The strongly warped regime

When we approach the conifold singularity, the dilute flux regime cannot be trusted anymore. Indeed, it is exactly the fact that the backreaction of the fluxes is not negligible that generates a warped compactification. In this section we analyze how the complex structure moduli stabilization changes when we are in a strongly warped region. From (3.21) it is clear that a strongly warped limit corresponds to $\mathcal{V}_w|Z|^2 \ll 1$ (that is essentially the opposite limit with respect to the one considered in the previous section).

Since the warp factor can be written as

$$e^{-4A} \sim c + e^{-4A_0} \,,$$

assuming that the only region of the CY manifold with a non-constant warp factor is the throat, we can derive the Kähler potential as a perturbation of the one found for the dilute flux regime [52, 17]:

$$K_{KS} \approx K_{df} + \frac{c'\xi'|Z|^{2/3}}{\mathcal{V}^{2/3}} + ... \tag{3.32}$$

where $\xi' = 9g_sM^2$ and $c' \simeq 1.18$ as computed in [52]. The omitted terms, indicated by "...", are of higher order in $\frac{\xi'|Z|^{2/3}}{\mathcal{V}^{2/3}}$.

The additional term due to the strong warping produces an extra term in the Kähler metric, which is dominant with respect to the original one in the regime of interest:

$$K_{Z\bar{Z}} \approx c \log\frac{\Lambda_0^3}{|Z|} + \frac{c'g_sM^2}{\mathcal{V}^{2/3}|Z|^{4/3}} \approx \frac{c'g_sM^2}{\mathcal{V}^{2/3}|Z|^{4/3}} \,. \tag{3.33}$$

It can be proven that, even if the new term in the Kähler potential introduces non-diagonal elements between Kähler and complex structure moduli in the Kähler metric, a modified no-scale condition can still be recovered as:

$$K^{I\bar{J}}\partial_I K \partial_{\bar{J}} K = 3; \quad I, J \in \{T, Z\} \tag{3.34}$$

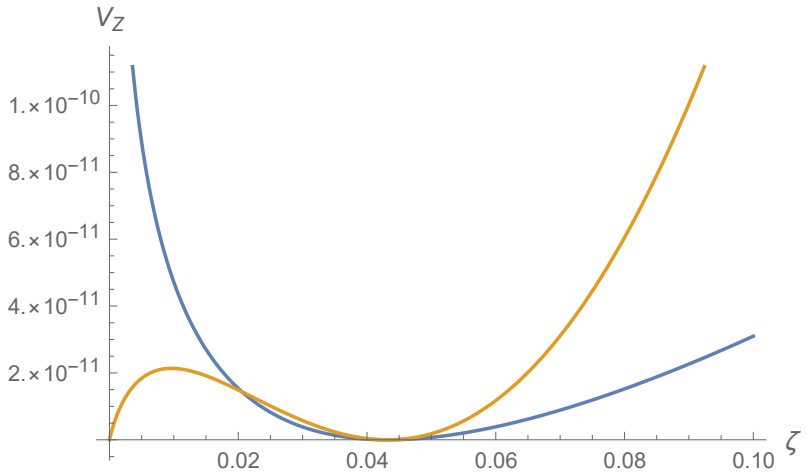

Figure 3.1: Scalar potential for the complex structure moduli in the dilute flux regime (3.29) (blue) and the warped regime (3.35) (orange), with the choice of values: $M = 20$; $K = 1$; $g_s = 0.1$; $\mathcal{V} = 10^5$; $\sigma = 0$. The latter shows an additional minimum at $\zeta = 0$ corresponding to a Klebanov-Tseytlin throat.

and the mixed terms ($\propto K^{I\bar{\alpha}}$) are subleading in the scalar potential. Hence, considering also that the superpotential is the same as in the dilute flux regime, we obtain the new scalar potential

$$V_Z \approx m_p^4 \frac{|Z|^{4/3}}{c' M^2 \mathcal{V}^{4/3}} \left| \frac{M}{2\pi i} \log \frac{\Lambda_0^3}{Z} + i \frac{K}{g_s} \right|^2 , \tag{3.35}$$

which is again stabilized to a Minkowski minimum in the same way as the one in the dilute flux regime (3.30).

Nonetheless, two important differences are worth to be noted [16, 17]. First, the scalar mass is now:

$$m_Z^2 \sim \frac{(\mathcal{V}_w |Z|^2)^{1/3}}{g_s M^2} \frac{m_p^2}{\mathcal{V}_w} \sim \frac{(\mathcal{V}_w |Z|^2)^{1/3}}{g_s^{3/2} M^2} M_s^2 . \tag{3.36}$$

It is still smaller than the string scale, but it is also exponentially smaller than the masses of the other complex structure moduli (3.13). Therefore one has to be more careful when assuming it to be stabilized before the Kähler moduli. Secondly, when we move away from the minimum, the functional behavior of the scalar potential is different in the two limits (see Fig. 3.1). This will have important consequences in presence of a dS uplift.

3.2 Kähler moduli stabilization

As we saw at the end of the previous section, an appropriate choice of fluxes allows to stabilize the complex structure moduli and the dilaton at the classical level. In this section, we freeze them to their VEVs and we only consider the unstabilized Kähler moduli (with the exception of the conifold modulus in the strongly warped regime, which we will treat explicitly). In the end we will see that this choice is consistent by computing the masses

of the Kähler moduli and comparing them to the ones of the complex structure moduli (3.13).

We denote the tree-level superpotential (evaluated at the fixed values of the moduli) as W_0, which, if not specified differently, will be restricted to be real, for simplicity. Moreover, the flux choice is assumed to be such that the string coupling $\frac{1}{S_0} = g_s$ is small, so that all string loop corrections are suppressed. In order to stabilize the Kähler moduli, we need to introduce quantum corrections to the Kähler potential and the superpotential.

The leading order perturbative correction to the Kähler potential comes from an $\mathcal{O}(\alpha'^3)$ term in the type IIB effective action [53]. The corrected Kähler potential reads[9]:

$$K_{S,K} = -\ln[(S+\bar{S})] - 2\ln\left[\mathcal{V} + \xi\left(\frac{S+\bar{S}}{2}\right)^{3/2}\right], \tag{3.37}$$

where

$$\xi = -\frac{\zeta(3)\chi(X_6)}{4(2\pi)^3} \tag{3.38}$$

($\zeta(3) \sim 1.202$ and $\chi(X)$ is the Euler characteristic of the internal manifold).

On the other side, due to the symmetries of the four-dimensional effective field theory, Kähler moduli dependent perturbative corrections are not allowed in the superpotential [9], which therefore can only acquire non-perturbative corrections. The two most studied ways to generate corrections to the superpotential rely either on the introduction of Euclidean $D3$-branes ($E3$-instantons) [54] or on the addition of stacks of N coincident $D7$- branes [55]. Under some conditions on the wrapped divisors, the low-energy theory corresponding to the second case is a pure $\mathcal{N} = 1$ supersymmetric YM gauge theory, which undergoes gaugino condensation. We will give some additional detail about non-perturbative corrections in Ch. 5. Both sources produce a similar correction to the superpotential:

$$W_{np} = A\, e^{-aT} \tag{3.39}$$

where A depends on the complex structure of the CY manifold (therefore it is constant at this stage), T is the Kähler modulus controlling the size of the wrapped 4-cycle (its real part τ is the volume of the 4-cycle itself) and the value of a depends on the source we are considering[10]: for $E3$-instantons $a = 2\pi$, while for gaugino condensation it depends on the condensing group (for $SO(8)$, $a = \frac{\pi}{3}$). There is also the possibility that the $E3$ wraps the divisor n times and therefore $a = 2\pi n$ [56], but we will not consider this case in detail.

3.2.1 KKLT

One of the most famous mechanisms for the stabilization of the Kähler moduli is due to S. Kachru, R. Kallosh, A. Linde and S.P. Trivedi (KKLT) [11], who considered only

[9] Since the α' correction depends on the dilaton, in principle one can not consider it to be stabilized together with the complex structure moduli (that is before the introduction of the new term). Even though in the large volume limit the scalar potential turns out to be the same that is found considering $S = \frac{1}{g_s}$, we report here the complete Kähler potential for both the dilaton and the Kähler moduli, which is the one to be considered in order to derive the exact scalar potential.

[10] See also Sec. 5.4.

non-perturbative quantum corrections to the superpotential W and assumed that the α' corrections to the Kähler potential are negligible due to the largeness of the volume of the CY (the expansion in α' is essentially an expansion in $\frac{1}{\mathcal{V}}$). In this section we will review this mechanism both in the unwarped and in the strongly warped regimes.

The unwarped regime

Following the original paper [11] let us consider, for simplicity, the case of a single Kähler modulus $T = \tau + i\theta$ (with the volume of the CY given by $\mathcal{V} = \left(\frac{T+\bar{T}}{2}\right)^{3/2}$): the qualitative results, indeed, don't change in presence of several Kähler moduli. The Kähler potential and the superpotential for the Kähler moduli are:

$$K = -3\ln(T+\bar{T}); \qquad W = W_0 + Ae^{-aT} \tag{3.40}$$

from which we can derive the scalar potential (3.1):

$$V_{KKLT} = e^K \left(K^{T\bar{T}} D_T W \overline{D_T W} - 3|W|^2\right) = \frac{aA^2 e^{-2a\tau}}{2\tau^2} - \frac{aAe^{-a\tau}W_0}{2\tau^2} + \frac{a^2A^2e^{-2a\tau}}{6\tau}. \tag{3.41}$$

Its (supersymmetric) minimum is obtained by solving

$$D_T W = 0\,,$$

which results in $\theta = \frac{\pi}{a}$ and

$$e^{-a\tau} = \frac{3W_0}{A(3+2a\tau)}\,. \tag{3.42}$$

By substituting this result in (3.41) we can observe that the scalar potential is negative at the minimum, which means that the solution is an Anti-de Sitter (AdS) vacuum:

$$V_{AdS} = (-3e^K|W|^2)_{min} = -\frac{3a^2W_0^2}{2\tau_{min}(3+2a\tau_{min})^2}\,. \tag{3.43}$$

This is generic: as we will see, adding perturbative corrections to the Kähler potential as well as including a larger number of Kähler moduli doesn't change the fact that the scalar potential is stabilized at negative vacuum energy.

It is crucial to notice that, in order to be consistent, the KKLT mechanism requires that the fluxes are tuned in a way that $W_0 \ll 1$. Indeed it relies on the assumption that any multi-instanton contribution to W_{np} can be neglected, that is only single-instanton corrections are relevant. This is true if $a\tau \gg 1$ which implies $W_0 \ll 1$ as we can easily see by rewriting Eq. (3.42) as:

$$W_0 = Ae^{-a\tau_{min}}\left(1 + \frac{2}{3}a\tau_{min}\right)\,. \tag{3.44}$$

The requirement of having $W_0 \ll 1$ is highly non-generic. Nonetheless, given the large number of possible flux choices, it is expected to be possible to fulfill.

The masses of the two scalar fields are [57]:

$$m_\theta^2 = \frac{W_0^2 a^3}{3+2a\tau_{min}} m_p^2; \quad m_\tau^2 = \frac{W_0^2 a^2(2+a\tau)(1+2a\tau)}{\tau(3+2a\tau)^2} m_p^2 \tag{3.45}$$

which, as expected, are parametrically lighter than the ones of the complex structure moduli (3.13) due to the smallness of W_0.

The strongly warped regime

Near the conifold singularity, we need to consider the modified Kähler potential (3.32) while the non-perturbative contribution is now added to (3.28):

$$W = W_{cs} + W_{KS} + W^{(T)} = W_{cs} + \frac{M}{2\pi i} Z \left(\log \frac{\Lambda_0^3}{Z} + 1 \right) + iKSZ + Ae^{-aT} \, .$$

If we assume that the conifold complex structure modulus is stabilized at larger energies by $\partial_Z W_{KS} = 0$ at the same value Z_0 (3.30) as before, the superpotential simplifies further:

$$W = W_{cs} + \frac{M}{2\pi i} \Lambda_0^3 \, e^{-\frac{2\pi K}{g_s M}} + Ae^{-aT} \, .$$

In this case, the resulting scalar potential is the same that we found in the unwarped regime (3.41), with the only difference that we know explicitly the dependence of W_0 on the conifold modulus, hence the minimum is again supersymmetric and AdS. Moreover the masses for Z (3.36) and T (3.45) are the ones that we computed before, from which we can conclude that the above assumption is consistent, provided that

$$\frac{m_\tau^2}{m_Z^2} \approx (M^3 |Z_0|)^{4/3} \ll 1 \, ,$$

where we used $W_0 \approx M|Z_0|$.

3.3 The Large Volume Scenario (LVS)

Despite its relevance in string phenomenology and a large number of applications studied over the years, the KKLT mechanism shows some weaknesses. One of these is that it is a highly model-dependent mechanism, given, for example, its requirement of having the dilaton and complex structure moduli stabilized by a choice of fluxes that guarantees a small value for the superpotential W_0 [11].

An analysis of the model-independent features of type IIB string compactifications, was instead developed in [12], where it was shown that a generic non-supersymmetric AdS minimum arises at exponentially large volume, as a consequence of the competition between the non-perturbative correction (3.39) to the superpotential (already included in KKLT) and the leading perturbative correction to the Kähler potential[12] (3.37).

For the sake of clarity we write again the Kähler potential and superpotential in the most generic case:

$$K = -\ln \left[-i \int \Omega \wedge \bar{\Omega} \right] - \ln[S + \bar{S}] - 2 \ln \left[\mathcal{V} + \xi \left(\frac{S + \bar{S}}{2} \right)^{3/2} \right] \, ; \qquad (3.46)$$

[11] Recently, the authors of [58] developed a method for the construction of flux vacua with exponentially small W_0 in type IIB flux compactifications with weak string coupling and large complex structure. This work was then extended in [59, 60], where a method for finding flux vacua with $W_0 \ll 1$ *and* a warped throat region is introduced (as we will see in the next chapter, this setup is crucial for one of the most studied uplift mechanisms, based on the introduction of $\overline{D3}$-branes at the tip of a warped throat).

[12] Other possible contributions at $\mathcal{O}(\alpha'^3)$ where considered in [13], where it was shown that their main effect is to change the factor in ξ.

$$W = \int \Omega \wedge G_3 + \sum_{i=1}^{n} A_i e^{-a_i T_i} \tag{3.47}$$

where we are assuming that a generic number of divisors $1 \leq n \leq h^{1,1}$ supports non-perturbative contributions. As in KKLT, we consider the complex structure moduli and the dilaton to be stabilized in a first, separate step at $D_i W = D_S W = 0$ (in the end we will verify that the two sectors are indeed decoupled). However, as we already noticed in the footnote 9, the α' correction to the Kähler potential depends on the dilaton S; hence, in order to get the correct expressions for the elements of the inverse Kähler metric we need to compute it including both the dilaton and the Kähler moduli. We will fix the dilaton to its stabilized value only after this computation. This is consistent with the generic decomposition (2.28) of the moduli space.

Following [61] (with a slightly different notation), we find the first derivatives of the Kähler potential:

$$\partial_S K = -\frac{1}{2s}\left(1 + \frac{3\hat{\xi}}{\mathcal{V}+\hat{\xi}}\right) = \partial_{\bar{S}} K; \qquad \partial_{T_i} K = -\frac{t^i}{2(\mathcal{V}+\hat{\xi})} = \partial_{\bar{T}_i} K$$

where $s = \frac{S+\bar{S}}{2} = \frac{1}{g_s}$ and $\hat{\xi} = \xi s^{3/2}$. The second expression, in particular, is obtained considering the implicit dependence of the volume of the compact space on the Kähler moduli $\{T_i\}$ [13]:

$$\mathcal{V} = \frac{1}{6} k_{ijk}\, t^i t^j t^k = \frac{1}{3} t^i \tau_i = \frac{1}{6} t^i (T_i + \bar{T}_i) \tag{3.48}$$

where we used the fact that

$$\frac{T_i + \bar{T}_i}{2} = \tau_i = \partial_{t_i} \mathcal{V} = \frac{1}{2} k_{ijk}\, t^j t^k.$$

The last term of Eq. (3.48) still contains an implicit dependence on T_i via t_i, which can be taken in consideration by observing that

$$t^i = k^{ij} k_j \,,$$

where we used the shorthand notation of [61]: $k^{ij} = (k_{ijk} t^k)^{-1}$ and $k_i = k_{ijk} t^j t^k$. From these considerations we conclude that

$$\frac{\partial \mathcal{V}}{\partial T_i} = \frac{1}{4} t^i \,.$$

We now have all the tools to compute the elements of the Kähler metric:

$$K_{\bar{S}S} = \frac{1}{4s^2}\left(1 - \frac{3\hat{\xi}}{2(\mathcal{V}+\hat{\xi})} + \frac{9\hat{\xi}^2}{2(\mathcal{V}+\hat{\xi})^2}\right); \quad K_{\bar{S}T_i} = \frac{3 t^i \hat{\xi}}{8s(\mathcal{V}+\hat{\xi})^2} = K_{\bar{T}_i S} \,;$$

$$K_{\bar{T}_i T_j} = \frac{t^i t^j}{8(\mathcal{V}+\hat{\xi})^2} - \frac{k^{ij}}{4(\mathcal{V}+\hat{\xi})}$$

[13] See also App. D.

and of its (transposed) inverse:

$$K^{S\bar{S}} = \frac{2s^2(2\mathcal{V}-\hat{\xi})}{(\mathcal{V}-2\hat{\xi})}; \qquad K^{T_i\bar{S}} = -\frac{6s\hat{\xi}\tau_i}{\mathcal{V}-2\hat{\xi}};$$

$$K^{T_i\bar{T}_j} = \frac{8(\mathcal{V}+\hat{\xi})}{(2\mathcal{V}-\hat{\xi})}\tau_i\tau_j - 4(\mathcal{V}+\hat{\xi})k_{ijk}t^k + \frac{18\hat{\xi}^2}{(\mathcal{V}-2\hat{\xi})(2\mathcal{V}-\hat{\xi})}\tau_i\tau_j\,.$$

Hence the SUGRA scalar potential (3.1), after having imposed $D_iW = D_SW = 0$ is [62]:

$$\begin{aligned} V = e^K \Big[K^{T_i\bar{T}_j}\left(a_iA_ia_j\bar{A}_je^{-(a_iT_i+a_j\bar{T}_j)}\right) + K^{T_i\bar{T}_j}\left(a_iA_ie^{-a_iT_i}\bar{W}\partial_{\bar{T}_j}K\right. \\ \left. +a_j\bar{A}_je^{-a_j\bar{T}_j}W\partial_{T_i}K\right) + 3\hat{\xi}\frac{4\hat{\xi}^2+14\hat{\xi}\mathcal{V}+\mathcal{V}^2}{2(\mathcal{V}-2\hat{\xi})(\mathcal{V}+\hat{\xi})^2}|W|^2\Big] = V_{np1}+V_{np2}+V_{\alpha'}\,, \end{aligned} \tag{3.49}$$

where the last term comes from the fact that the α' corrections to the Kähler potential break the no-scale structure.

The KKLT minimum is obviously included in this generic argument, as we can reproduce it (if the fluxes are tuned such that $W_0 \ll 1$), by imposing the supersymmetric conditions $D_{T_i}W = 0$.

The above potential is expected to generically have a minimum at large volume if at least one of the 4-cycles is relatively small. Indeed the last term in (3.49) scales as $V_{\alpha'} \sim \frac{1}{\mathcal{V}^3}$ at large volume and it might compete with the non-perturbative contribution coming from a not-so-large 4-cycle (while all the other contributions are exponentially suppressed). Let us therefore consider the limit in the moduli space in which $\mathcal{V} \to \infty$ and $\tau_i \to \infty$ for all 4-cycles except one, that we will call τ_s. We also assume that τ_s supports non-perturbative effects and the volume of the compact space is well-defined, that is it never becomes negative in the considered limit. The three components of the scalar potential can be written as:

$$V_{np1} = e^{K_{cs}}\frac{2a_s^2A_s^2e^{-2a_s\tau_s}(-k_{ssi}t^i)}{s\mathcal{V}} + \mathcal{O}(\frac{1}{\mathcal{V}^2})\,,$$

$$V_{np2} = e^{K_{cs}}\frac{2a_sA_s^2e^{-2a_s\tau_s}\tau_s + 2a_sA_sW_0e^{-a_s\tau_s}\tau_s\cos(a_s\theta_s)}{s\mathcal{V}^2} + \mathcal{O}\left(\frac{1}{\mathcal{V}^3}\right)\,,$$

$$V_{\alpha'} = e^{K_{cs}}\frac{3A_s^2e^{-2a_s\tau_s}\hat{\xi} + 3W_0^2\hat{\xi} + 12A_se^{-a_s\tau_s}W_0\hat{\xi}\cos(a_s\theta_s)}{4s\mathcal{V}^3} + \mathcal{O}\left(\frac{1}{\mathcal{V}^4}\right)\,,$$

where $e^{K_{cs}}$ depends on the (stabilized) complex structure moduli (K_{cs} is the corresponding Kähler potential, as defined in (2.26)) and for simplicity we considered both A_s and W_0 to be real and positive. Despite the minus sign, V_{np1} is always positive as a consequence of the fact that the Kähler metric is positive definite. V_{np2} will instead turn out to be negative once we stabilize the axion θ_s. Finally, $V_{\alpha'}$ is positive, provided that $h^{2,1} > h^{1,1}$ for the CY space under consideration, so that the Euler characteristic appearing in ξ (3.38) is always negative (hence ξ is positive). On the other side, while the large volume trend does not change when $h^{2,1} < h^{1,1}$, the small volume behavior is more model-dependent and difficult to define, given the possible competition between a positive and a negative term.

More precisely [62], when we consider the large volume limit $\mathcal{V} \to \infty$ with all but n cycles going to infinity, the scalar potential admits a set of AdS non-supersymmetric minima at $\mathcal{V} \sim e^{a_j \tau_j}$; $(\forall j = 1, ..., n)$ *if and only if*:

1. $h^{2,1} > h^{1,1}$ $(\chi(X) < 0)$;

2. each τ_j is a local blow-up mode resolving a point-like singularity.

Moreover, if $h^{1,1} > n+1$, after the LVS stabilization process there are still $h^{1,1} - n - 1$ flat directions left.

Putting together all these results and keeping only the leading terms in the volume, we get:

$$V_{LVS} = g_s e^{K_{cs}} \left[\frac{2a_s^2 A_s^2 e^{-2a_s\tau_s}(-k_{ssi}t^i)}{\mathcal{V}} + \frac{2a_s\tau_s A_s W_0 e^{-a_s\tau_s}\cos(a\theta_s)}{\mathcal{V}^2} + \frac{3W_0^2\hat{\xi}}{4\mathcal{V}^3} \right] + \mathcal{O}\left(\frac{1}{\mathcal{V}^4}\right) \tag{3.50}$$

from which it is now clear that the axion θ_s is stabilized at $\theta_0 = \frac{\pi}{a_s}$ so that the corresponding term in the potential is negative.

Let us consider the generic behavior of (3.50). In the decompactification limit

$$\mathcal{V} \to \infty \text{ with } a_s\tau_s \propto \ln(\mathcal{V})\,,$$

the leading term is $V_{np2} \sim -\frac{\ln\mathcal{V}}{\mathcal{V}^3}$ therefore the scalar potential approaches zero from below. On the other hand, when the volume is small (though still large with respect to the string length, so that we can trust the supergravity approximation), one of the 2 positive terms dominates, from which it follows that this scalar potential develops a local AdS minimum. Moreover, we can argue that the minimum appears when the negative term V_{np2} begins to dominate. This happens when $\tau_s \sim \ln\mathcal{V}$ is large, therefore we expect the minimum to be at (exponentially) large values of the volume of the CY. Finally, it can be shown that $D_{T_s}W \neq 0$, which means that the LVS minimum is non-supersymmetric. In general one would expect non-perturbative instabilities to arise for non-supersymmetric minima. Nonetheless, as was proven in [63], as long as the Effective Field Theory is valid the AdS LVS vacua are stable.

To make this argument more concrete, let us briefly consider the minimal case of a CY compactification with $h^{1,1} = 2$ and a volume

$$\mathcal{V} = \kappa_b\tau_b^{3/2} - \kappa_s\tau_s^{3/2}\,, \tag{3.51}$$

where κ_b, κ_s are constants depending on the intersection numbers on X_6 and $\tau_b \gg \tau_s$. In the following we will re-scale the modulus τ_b so that $\kappa_b = 1$ and we will only keep κ_s as a parameter. This model will be extensively used along this work and analyzed in great detail in Chapter 6.

The scalar potential (3.50) in this case reads:

$$V_{LVS} = \frac{4g_s A_s^2 a_s^2\sqrt{\tau_s}e^{-2a_s\tau_s}}{3\kappa_s\mathcal{V}} + \frac{2g_s A_s a_s W_0\tau_s e^{-a_s\tau_s}}{\mathcal{V}^2}\cos(a_s\theta_s) + \frac{3W_0^2\xi}{4g_s^{1/2}\mathcal{V}^3} \tag{3.52}$$

where we absorbed the factor $e^{K_{cs}}$ in the definition of A_s and W_0. V_{LVS} has a non-supersymmetric minimum at

$$\partial_{\theta_s} V_{LVS} = 0 \Rightarrow \theta_s = \frac{\pi}{a_s}\,, \tag{3.53a}$$

$$\partial_{\tau_s} V_{LVS} = 0 \Rightarrow \tau_b^{3/2} = \frac{3W_0\kappa_s\sqrt{\tau_s}e^{a_s\tau_s}}{a_s A_s}\frac{(a_s\tau_s-1)}{(4a_s\tau_s-1)} \simeq \frac{3W_0\kappa_s\sqrt{\tau_s}e^{a_s\tau_s}}{4a_s A_s}\,, \tag{3.53b}$$

$$\partial_{\tau_b} V_{LVS} = 0 \Rightarrow \tau_s^{3/2} = \frac{\xi}{16a_s\tau_s\kappa_s g_s^{3/2}}\frac{(4a_s\tau_s-1)^2}{(a_s\tau_s-1)} \simeq \frac{\xi}{g_s^{3/2}\kappa_s}\,, \tag{3.53c}$$

where the right hand terms correspond to the limit $a_s\tau_s \gg 1$. As expected, this is an Anti-de Sitter vacuum:

$$V_{min} = -\frac{6g_s W_0^2\kappa_s\tau_s^{3/2}(a_s\tau_s-1)}{\tau_b^{9/2}(4a_s\tau_s-1)^2} \simeq -\frac{3g_s W_0^2\kappa_s\sqrt{\tau_s}}{8a_s\tau_b^{9/2}}\,. \tag{3.54}$$

The masses of the normalized moduli (obtained as usual as the eigenvalues of $K^{T_i\bar{T}_j}\partial_{T_i}\partial_{\bar{T}_j}V$) are [57]:

$$m_\Theta^2 = 0; \quad m_\theta^2 = \frac{16g_s W_0^2 a_s^2\tau_s^2(a_s\tau_s-1)}{\tau_b^3(4a_s\tau_s-1)}m_p^2\,, \tag{3.55}$$

$$m_\Phi^2 = \frac{108g_s W_0^2 a_s\kappa_s\tau_s^{5/2}\,(a_s\tau_s-1)\left(5-11a_s\tau_s+12a_s^2\tau_s^2\right)}{\tau_b^{9/2}\,(4a_s\tau_s-1)^2\,(1+3a_s\tau_s-6a_s^2\tau_s^2+8a_s^3\tau_s^3)}m_p^2\,, \tag{3.56}$$

$$m_\phi^2 = \frac{8g_s W_0^2\,(a_s\tau_s-1)\left(1+3a_s\tau_s-6a_s^2\tau_s^2+8a_s^3\tau_s^3\right)}{\tau_b^3\,(4a_s\tau_s-1)^2}m_p^2\,, \tag{3.57}$$

where θ, Θ are related to the axions $\theta_{s,b}$ and ϕ, Φ to the moduli $\tau_{s,b}$. It should be noted that only m_ϕ^2 (which corresponds to the mass of the volume modulus) is hierarchically lighter than the masses of the complex structure moduli. However, the 2-steps procedure is still consistent due to the specific form of the LVS scalar potential, as highlighted in the next subsection.

The situation analyzed above can be generalized to the case in which there are more than one small cycles, while the overall volume remains exponentially large. Indeed, as was argued in [13] via qualitative and geometric considerations, it is reasonable to expect a generic case (though not the only possible one) to be characterized by one single large Kähler modulus and $h^{1,1}-1$ moduli that tend to be stabilized at small values. This is the so-called *Swiss-cheese* picture of the CY, whose volume reads:

$$\mathcal{V} = \tau_b^{3/2} - \sum_{i=1}^{h^{1,1}-1}\tau_{s,i}^{3/2}\,. \tag{3.58}$$

Obviously, the larger is the volume, the more it is insensitive to the size of the small cycles. Algorithms for finding Swiss cheese manifolds among all the complete intersection and toric hypersurface CY three-folds, were developed, e.g. in [64, 65]. With these configurations, if all the small cycles appear in the non-perturbative superpotential, one expects to be

able to find a LVS minimum for all the Kähler moduli. If instead a given Kähler modulus does not support non-perturbative effects, at least the corresponding axion will remain unstabilized (giving no contribution to the scalar potential); the overall volume modulus will be fixed anyway.

As a final remark we mention that in presence of less trivial forms of the volume of the CY, like for example fibrations, where not all the moduli can be stabilized with the procedure described above, there is still the possibility to include additional terms to the scalar potential in order to fix also the remaining moduli. This is the case, for example of string loop corrections, that are sub-leading terms in the expansion over g_s (see also Sec. 5.5) [62].

3.4 Why LVS?

The LVS minimum shows many interesting features, some of which were only heuristically argued in the original paper, but were then confirmed by several explicit examples in the subsequent ones. As a conclusion to this chapter, we review, by comparison with the KKLT scenario, the main reasons that make the Large Volume Scenario promising from the string phenomenology point of view and that therefore justify our choice of working in this framework. Most of the arguments listed below, are related to the fact that the Large Volume Scenario is, by construction, more generic than the KKLT mechanism.

- *α' corrections and small superpotential.* While KKLT is based on the assumption that all the α' corrections can be neglected, it should be noticed that the models in which this is actually true are highly non-generic in type IIB [13]. Indeed, if we write the Kähler potential and superpotential as

$$K = K_0 + J\,,$$

$$W = W_0 + \Omega\,,$$

where J is the leading perturbative correction to K and Ω is the leading non-perturbative correction to W, the corresponding scalar potential can be expanded in powers of J and Ω as:

$$V = V_0 + V_J + V_\Omega + ...$$

where

$$V_0 \sim W_0^2; \quad V_J \sim J W_0^2; \quad V_\Omega \sim \Omega^2 + W_0\Omega\,.$$

From this, it is clear that whenever the tree-level potential has a flat direction ($V_0 =$ const), the structure of the scalar potential is determined by its corrections. This is precisely what happens here, where the complex structure moduli and the dilaton are stabilized by fluxes at $V_0 = 0$, but all the Kähler moduli are left unfixed at tree level. In particular the only cases in which we expect the non-perturbative correction V_Ω to dominate over the perturbative one are when $W_0 = 0$ (hence $V_J = 0$) or when $W_0 \sim \Omega$ (which requires $W_0 \ll 1$). The last case is the one considered by the KKLT scenario but it is obviously very unnatural. As was shown in [13], in particular, the

range of values of the stabilized Kähler moduli for which the perturbative corrections can be safely neglected is rather limited even in the case of $W_0 \ll 1$, while for generic values of W_0 it is impossible to consistently neglect such corrections.

In addition to this, a statistical analysis of the flux vacua that can be obtained in type IIB string theory, shows that among the exponentially many possibilities the values of $e^{K_{cs}}|W_0|^2$ are uniformly distributed inside a range which is fixed by the tadpole cancellation condition (so that $W_0 \lesssim 100$) [51, 49]; therefore the set of solutions with small superpotential is very limited.

On the other side, the Large Volume Scenario does not require a small W_0, therefore the only needed fine-tuning is the one ensuring that the string coupling g_s is small enough, so that we have the string perturbative expansion under control.

- *Decoupling of the dilaton and the complex structure moduli.* Both KKLT and LVS rely on the assumption that one can safely separate the moduli stabilization procedure in two steps: first, all the complex structure moduli and the dilaton are stabilized, considering only tree-level quantities; then quantum corrections stabilize the Kähler moduli without affecting the previously fixed ones. This assumption is justified in KKLT, provided that the masses of the complex structure moduli and the dilaton are always fixed at much larger values than the masses of the Kähler moduli. However, as it was observed in [66], in some cases the presence of quantum corrections can destabilize some of the previously stabilized moduli. The possible destabilizing effect of KKLT can also be argued by observing that the scalar potential for the complex structure moduli and the dilaton[14]

$$V_{cs,S} \simeq \frac{K^{i\bar{j}} D_i W D_{\bar{j}} \bar{W}}{\mathcal{V}^2}$$

is positive definite and it vanishes at the minimum. Hence, whenever we move away from the minimum in the complex structure/dilaton moduli space we introduce a positive $\sim \mathcal{O}\left(\frac{1}{\mathcal{V}^2}\right)$ contribution to the total scalar potential. Nonetheless, when the Kähler moduli are stabilized in a KKLT minimum, the corresponding term in the scalar potential is negative and scales in the same way as $V_{cs,S}$:

$$V_{min}^{KKLT} = -\frac{3e^{K_{cs}}|W|^2}{\mathcal{V}^2} \, .$$

As a consequence we don't know a priori whether the whole scalar potential will increase (the minimum is still there) or decrease (destabilization) when moving away from the tree-level minimum ($D_i W = 0$) [13].

On the other side, the LVS does not present such issue: the Kähler moduli are stabilized at $V_{min}^{LVS} \sim -\frac{1}{\mathcal{V}^3}$, hence the positive definite contribution $V_{cs,S}$ is always dominant and the shift of a complex structure modulus from its tree-level minimum can only produce an increase in the value of the total scalar potential. This means

[14] As usual the indices $i, \bar{j}$ indicate that we are summing over the dilaton and complex structure moduli only.

that if the Kähler moduli are stabilized in LVS, all the other moduli are in a minimum as well and we don't need to check this feature model by model.

- *Exponentially large volume.* The fact that the volume of the compact space is expected to be stabilized at exponentially large values has two convenient consequences. First, in LVS the fundamental string scale is hierarchically smaller than the 4d Planck scale, given that the two scales are related by[15] [13]

$$M_s = \frac{g_s^{1/4}}{(4\pi\mathcal{V})^{1/2}} m_p \,,$$

where $\mathcal{V}$ is in Einstein frame. Moreover, the presence of a naturally small expansion parameter $\left(\frac{1}{\mathcal{V}}\right)$ ensures that the α' expansion (which is basically an expansion in powers of $\frac{1}{\mathcal{V}}$) is under control and higher order perturbative corrections can be safely neglected.

- *Gravitino mass.* The supergravity theory contains a spin-$\frac{3}{2}$ fermion, called the gravitino, which is the supersymmetric partner of the graviton. When supersymmetry is spontaneously broken, the gravitino acquires a mass

$$m_{3/2} = e^{K/2}|W|$$

via the analogue of the Higgs effect in supergravity, called super-Higgs effect. Hence the mass of the gravitino defines the scale of supersymmetry breaking.

In KKLT, the gravitino mass depends linearly on W_0, therefore it is a statistical variable [13]. On the other side, the gravitino mass for LVS appears to be independent of the flux choice, which is encoded by W_0. Indeed, by analyzing Eq. (3.50), we can see that the volume of the compact space at the minimum is given by [12]

$$\mathcal{V} \sim \frac{W_0}{A_s} f(a_s, X_6) + (\text{subleading corrections}) \,, \tag{3.59}$$

where $f(a_s, X_6)$ does not depend on any of the fluxes. The gravitino mass $m_{3/2}$ is therefore given by:

$$m_{3/2} \sim \frac{1}{\sqrt{2s}\mathcal{V}}|W| \sim \frac{A_s}{\sqrt{2s} f(a_s, X_6)}.$$

As an aside, from Eq. (3.59) we can also notice that in LVS the volume increases as W_0 increases so that larger values of W_0 are actually favored, while the opposite behavior is observed in KKLT (see Eq. (3.44)): as the volume increases, W_0 decreases.

- *SUSY breaking.* While the KKLT mechanism stabilizes the moduli in a supersymmetric minimum, leaving the possible uplifting effect as the only susy breaking source, the LVS minimum is non-supersymmetric. There are therefore many sources of susy breaking: already the fluxes break supersymmetry by stabilizing the complex structure moduli and the dilaton in a minimum with $W_0 \neq 0$ and $D_{T_i} W \neq 0$ (even after

[15] See also App. A.

having stabilized the Kähler moduli). Moreover there are the non-perturbative effects and, finally, the uplift mechanism, whose contribution to the soft terms is usually negligible [13]. This fact renders KKLT much more vulnerable to possible tachyonic contributions (coming for example from anomaly mediation) [45], especially in presence of an uplifting mechanism.

- *dS vacua and tadpole constraints.* In the next chapter we will describe in detail how one can obtain a dS minimum in the frame of LVS, via the introduction of a $\overline{D3}$-brane. This mechanism (which was originally applied to KKLT moduli stabilization) has recently had to face several new challenges, essentially related to the need to combine the presence of a de Sitter vacuum with the tadpole cancellation conditions and the control over the perturbative expansions (see Sec. 4.4). As we will see, the exponentially large volume makes the LVS set up stronger than KKLT with respect to these new criticisms [67].

Chapter 4

De Sitter vacua in type IIB string theory

In [68], the implications of the presence of a non-constant warp factor in $D = 10$ supergravity theories with some residual supersymmetry (which, as we mentioned in Sec. 2.2.2 are preferable for several reasons) were analyzed, deriving very restrictive Einstein equations for Minkowski and de Sitter space-times. In particular, in type IIB supergravities of this kind, de Sitter solutions are not an option and Minkowski spaces are subject to severe constraints. In [69], Maldacena and Nuñez proved an important no-go theorem, according to which a large class of supergravity theories described by the standard Einstein-Hilbert action does not admit any non-singular warped compactification on a Minkowski or de Sitter space-time[1]. A refined version of these no-go theorems, keeping into account a larger class of theories was given in [71].

These are just a few important examples that point out the generic difficulty that we face in constructing de Sitter spaces in string theory. Furthermore, the debate on the topic has been recently revived by the proposal of a *de Sitter Swampland conjecture* [14], which speculates that dS vacua are not consistent with quantum gravity. We will shortly review this conjecture and some of its later refinements in the next subsection. As a matter of fact, the two well established procedures allowing to stabilize all the moduli of a given CY compactification, the KKLT and LVS mechanisms analyzed in the previous section, can only lead to Anti-de Sitter vacua. As a general conclusion we can say that if we consider only the lowest order terms in the 10-dimensional supergravity action, without further ingredients, it is not possible to stabilize all the moduli in a minimum with positive energy.

On the other side, cosmological observations led, already in [72, 73] (see also [74]) to the conclusion that the present universe is accelerating. In particular, according to the astrophysical and cosmological data, the equation of state of dark energy is $w = -1.03 \pm 0.03$ [75], which would be consistent with a positive cosmological constant ($w = -1$), though very small ($\Lambda = (2.846 \pm 0.076) \times 10^{-122} M_p^2$ [75]), and therefore with the presence

[1] Already in 1984, G. Gibbons et al. had proven that two-derivative supergravity with only positive tension objects does not admit solutions [70].

of a de Sitter vacuum[2]. This motivated the increasing interest in finding dS minima in string theory. Not only we would like to show the existence of these vacua (which, as we will review here, we claim to be allowed in presence of additional extended sources like O-planes and D-branes); it would also be interesting to understand why we live in a de Sitter minimum instead of one of the many stable and supersymmetric AdS vacua more easily provided by string theory (see e.g. [77]).

In this chapter, after a brief introduction to the de Sitter swampland conjectures, we focus on one of the most studied methods, again due to KKLT, to obtain dS vacua in type IIB string compactifications. This method is based on the introduction of an anti-$D3$ brane ($\overline{D3}$) at the tip of a warped throat in the internal manifold (Sec. 4.1). After having presented it, we review its supersymmetric description in terms of a nilpotent goldstino (Sec. 4.2) and its embedding in a global theory (Sec. 4.3). In Sec. 4.4 we discuss some challenges that this mechanism has to face, essentially based on the difficulty in satisfying the tadpole cancellation condition (3.6). Finally, in Sec. 4.5 we mention a selection of other proposals for the construction of dS vacua in string theory and we briefly present one of them, based on the introduction of a T-brane.

The Swampland Program

As we saw in the last chapter, moduli stabilization allows to produce a huge number (see e.g. [78]) of possible string vacua, corresponding to consistent low energy effective field theories (EFT) that can be completed to string theory in the ultraviolet. It is therefore reasonable to ask whether *any* consistent EFT can be actually coupled to gravity in a consistent way, that is whether it arises from some string theory compactification. If this was true, one could simply look for phenomenologically interesting EFTs, assuming that they can be completed in the UV, leading to string theory. However, the answer to this question, as was argued in [79], is no: besides the large *Landscape* of string vacua there is an even larger set of EFTs (which are said to belong to the *Swampland*) that appear to be consistent in the low energy limit, but show inconsistencies when one tries to complete them into quantum gravity in the ultraviolet.

The idea beneath the so-called *Swampland Program* is to look for generic criteria allowing to determine whether a given EFT belongs to the Landscape or to the Swampland, without having to introduce any UV feature. These criteria are generically based on the analysis of known realizations of string theory as well as on general properties of quantum gravity; until now none of them could be rigorously proved from a microscopic physics perspective (even though some of them are much more substantiated than others) so that scientists refer to them as *Swampland conjectures*.

A recent extensive review of the Swampland program can be found in [80]. Here we focus on the so-called *de Sitter Swampland conjecture*, which is of more interest for the purposes of this work. First proposed in [14], it presents itself in the form of a bound on

[2]There are some alternative proposals, like quintessence models [76], but we will not consider them in this work.

the scalar potential $V(\phi)$ of a theory consistently coupled to gravity:

$$|\nabla V| \geq \frac{c}{m_p} V \,, \tag{4.1}$$

where $c \sim \mathcal{O}(1) > 0$ is a constant and ∇ includes the derivatives with respect to all the scalar fields in the theory. Eq. (4.1) clearly forbids any de Sitter stationary point ($\nabla V = 0;\ V > 0$), and severely constrains slow-roll inflationary models [81, 82], especially if considered together with other Swampland constraints. An intense debate followed the original conjecture, leading on one side to the proposition of several possible counterexamples (see e.g. [83, 84, 85]) and on the other to the suggestion of possible refinements [86, 87].

A refined dS Swampland conjecture evading the previously proposed counterexamples, was developed in [15] stating that the scalar potential $V(\phi)$ of a low energy effective field theory describing any consistent quantum gravity, must satisfy either (4.1) or

$$min(\nabla_i \nabla_j V) \leq -\frac{c'}{m_p^2} V \,, \tag{4.2}$$

where $c' \sim \mathcal{O}(1) > 0$ is again a constant and the left-hand side is the minimum eigenvalue of the Hessian in an orthonormal frame. In the same paper it was also shown how this refined conjecture can be derived starting from the more studied Distance Swampland conjecture [88]. A more recent research line in the frame of the Swampland program, indeed, aims to highlight the fact that the various conjectures are actually interrelated and can often be derived one from the other.

A further update that is worth to be mentioned is the so-called *Trans-Planckian Censorship Conjecture* (TCC), according to which sufficiently short-living de Sitter vacua might be allowed due to quantum instabilities [89]. It should be noticed, though, that, as pointed out in the same paper, the most famous uplifting proposals (among which there is the one we will consider here) are not short-living, therefore they are still ruled out by this conjecture.

4.1 De Sitter vacua from $\overline{D3}$-branes

The idea of adding anti-$D3$-branes at the tip of a warped throat in order to obtain a minimum with positive energy was first proposed in the original KKLT paper [11].

Warped throats, as discussed in the previous chapters, are common in type IIB compactifications, as a consequence of the presence of non-vanishing three-form fluxes. Since $\overline{D3}$-branes explicitly break supersymmetry, one might wonder whether the effective field theory is still under control: placing the $\overline{D3}$-branes inside a Klebanov-Strassler geometry has the advantage that the amount of supersymmetry breaking is controlled by the warp factor so that it can be taken to be small enough.

Generically, D-branes back-react with the geometry in which they are introduced. For the case under consideration, we know that while the typical size of the throat is $R \simeq \sqrt{g_s M}$, the amount of back-reaction for n anti-branes is expected to extend over a region

of size $r \simeq \sqrt{g_s n}$ [90]. Therefore, as long as the number of anti-branes is much smaller than the number of quantized 3-form fluxes $n \ll M$, we can safely neglect their back-reaction and treat the $\overline{D3}$ as probes inside the KS geometry. In particular, we will consider the case of a single $\overline{D3}$, since it appears to be the most convenient one in terms of the stability of the solution [91]. Moreover, such configuration does not show the singular behavior observed in [92, 93] for a larger number of branes.

Other observations to be kept into account are:

- Since an $\overline{D3}$ carries a negative $D3$-charge, in order to include it we will assume that the fluxes do not saturate the tadpole cancellation condition (3.6), which otherwise would be violated by the brane itself.
- It is natural to expect the $\overline{D3}$ to be exactly at the tip of the throat, being this its configuration of minimum energy.
- Unlike what one might expect, the introduction of the $\overline{D3}$ does not imply the presence of additional moduli, since its position is fixed by fluxes with the flux/brane annihilation mechanism described in [90].

The bosonic action of a $D3$ ($\overline{D3}$)-brane in the linear approximation can be written as the sum of the Dirac-Born-Infeld-Nambu-Goto action S_{DBI} and the Wess-Zumino term S_{WZ} in the background super-space [94]:

$$S^q = S_{DBI} + q\, S_{WZ} = -T_3 \int d^4x \sqrt{-g_{\mu\nu} - \mathcal{F}_{\mu\nu}} + q\, T_3 \int C\, e^{\mathcal{F}} \,,$$

where $T_3 = \frac{1}{(2\pi)^3 \alpha'^2}$ is the tension of the $D3$-brane, $g_{\mu\nu}$ is the metric, $\mathcal{F} = dA - B_2$ is the 2-form field strength, $C = \sum_{\text{r even}} C_r$ is the formal sum of RR forms in the superspace and $q = \pm 1$ depending on whether we are considering a $D3$- or an $\overline{D3}$-brane. The difference in q is due to the fact that the $\overline{D3}$ has the same tension but an opposite five-form charge with respect to the $D3$. As was highlighted in [31] for a brane fixed at a given position (or slowly moving in a given background), at leading order in the low energy limit, $|S_{DBI}| \simeq |S_{WZ}|$, due to the competition between the electrostatic interaction from the five-form background and the gravitational attraction. Hence, the resulting $D3$-brane action vanishes at any fixed position ($S_{D3} = 0$), while for the $\overline{D3}$ we have:

$$S_{\overline{D3}} = -2T_3 \int d^4x \sqrt{-\det(g_{\mu\nu})} \,. \tag{4.3}$$

An analogous doubling/cancellation feature was derived also in presence of Volkov-Akulov fermions living on the brane and it was proven to be exact, under certain orientifold conditions. This feature is analyzed in [95] for a flat background and in [94] for a curved GKP background.

The action (4.3) corresponds to a positive term in the scalar potential, with a magnitude depending on the position $y_{\overline{D3}}$ of the brane in the compact space. For a warped background,

it reads [45]:

$$\delta V = -2T_3 \int d^4x\sqrt{-g_4} = \\ = \frac{2}{(2\pi)^3\alpha'^2}\frac{\mathcal{V}^{2/3}}{e^{-4A(y_{\overline{D3}})}+\mathcal{V}^{2/3}} \sim \begin{cases} \frac{e^{4A(y_{\overline{D3}})}}{\mathcal{V}^{4/3}}m_p^4; & e^{-4A(y_{\overline{D3}})} \gg \mathcal{V}^{2/3} \\ \\ \frac{1}{\mathcal{V}^2}m_p^4; & \mathcal{V}^{2/3} \gg e^{-4A(y_{\overline{D3}})} \end{cases} \tag{4.4}$$

where we used the notation of (3.17) for the warp factor and the relation between the string scale and the 4d Planck scale (A.9). Moreover, we distinguished between the strongly warped region of the compact space and the rest of the manifold in which we assume the warping to be negligible. The idea behind the introduction of the $\overline{D3}$ is therefore that this positive term, opportunely tuned, can compensate the negative vacuum energy of the KKLT minimum, producing a dS vacuum. The presence of the warp factor, indeed, allows to control (by tuning the fluxes) the magnitude of this additional term in order to obtain a small cosmological constant, as desired[3]. In particular, it can be seen that if the new minimum is close to the Minkowski (vanishing vacuum energy) one, the shape of the new potential doesn't change significantly with respect to the original one. This is reassuring, given that it means that a large volume remains large even after the uplifting and all the approximations are still expected to be trustworthy.

The introduction of $\overline{D3}$-branes, as well as other proposals to get de Sitter minima, are often called *uplifting* proposals. This terminology should not mislead the reader: we are not just adding a positive term to the already stabilized potential. On the contrary, we consider the full potential, with the additional term, and we stabilize it finding that the new minimum has indeed a positive energy.

The de Sitter minimum is always metastable, given that the scalar potential always vanishes in the decompactification limit ($\mathcal{V} \to 0$). Nonetheless, as was argued in [11], the lifetime of the dS minimum obtained with $\overline{D3}$-branes is expected to be very large in Planck time, while much shorter than the Poincaré recurrence time, as it is needed (see e.g. [96]).

In the following we will focus on an $\overline{D3}$ placed on top of an orientifold 3-plane at the tip of a warped throat, since, as we will see, this allows to conveniently describe the setup in a fully supersymmetric way, in terms of a nilpotent goldstino.

4.2 $\overline{D3}$ uplift and the Nilpotent Goldstino

In [97], a refined version of the O'KKLT model [98], consisting in the introduction of a Volkov-Akulov (VA) nilpotent goldstino superfield X [99, 100] in the KKLT framework, is shown to provide an uplifting of AdS vacua to de Sitter in a manifestly supersymmetric EFT. Furthermore, the uplifting term turns out to be the same as in the standard KKLT (both in the warped and unwarped backgrounds), therefore giving a supergravity description to the low energy physics of $\overline{D3}$-branes. A relation between $D3$-brane actions,

[3] In addition to this, it is important to be able to tune the additional term to small values, otherwise it might generate a runaway in the scalar potential.

constrained superfields and non-linear realization of supersymmetry had already been analyzed in [101].

A chiral superfield is a field X in the superspace (an extension of the ordinary space-time where the supersymmetry is manifest) such that $\bar{D}_{\dot{\alpha}} X = 0$ ($\bar{D}_{\dot{\alpha}} = \bar{\partial}_{\dot{\alpha}} + i\theta^{\beta}\sigma^{\mu}{}_{\beta\dot{\alpha}}\partial_{\mu}$ is a covariant derivative). Its components are given by [45]:

$$X = X_0(y) + \sqrt{2}\psi(y)\theta + F(y)\theta\bar{\theta}\,, \tag{4.5}$$

where we are following the usual notation for chiral superfields (see e.g. [4]) according to which the coordinates of the superspace are $(y^{\mu}, \theta_{\alpha}, \bar{\theta}_{\dot{\alpha}})$, with $\theta_{\alpha}, \bar{\theta}_{\dot{\alpha}}$ anti-commuting Grassmann coordinates and $y^{\mu} \equiv x^{\mu} + i\theta\sigma^{\mu}\bar{\theta}$ (σ^{μ} are the Pauli matrices). In this notation, each component of the superfield is an ordinary field. In particular, ψ is a goldstino fermion, $X_0(y)$ is its supersymmetric scalar partner and $F(y)$ is an auxiliary scalar field. In this sense we can define a superfield as a *multiplet* of fields.

An unconstrained goldstino multiplet (4.5) is a key ingredient for several inflationary models in string theory, but its presence entails issues related to its stabilization. For this reason the authors of [97] proposed to replace it with a *Nilpotent Goldstino*, that is a goldstino multiplet that satisfies the nilpotency condition:

$$X^2 = 0\,. \tag{4.6}$$

Indeed, they noticed that in this case the effect on inflation is analogous, but without the above-mentioned potential instabilities. In terms of the ordinary fields the nilpotency condition (4.6) corresponds to the following constraint:

$$X_0 = \frac{\psi\psi}{2F}$$

which means that the only propagating field is the goldstino ψ. As a consequence, when computing the scalar potential, we have to impose $\langle X \rangle = 0$, as expected for Lorentz symmetric vacuum configurations (where the fermions have vanishing vacuum expectation values).

A new manifestly supersymmetric uplifting mechanism, as mentioned before, arises by including X in the supergravity description of KKLT [45]:

$$W = W_{KKLT} + \eta X\,,$$
$$K = K_{KKLT} + \beta\frac{\bar{X}X}{(T+\bar{T})^{\kappa}}\,,$$

where η depends on the tension T_3 of the brane and on the geometry of the background, β is a constant and the Kähler modulus dependence of the $\bar{X}X$ term is chosen in order to make it modular invariant (assuming that X transforms as a modular form with weight κ)[4]. W_{KKLT} and K_{KKLT} are defined in (3.40). In principle also linear terms in X are

[4] A modular transformation acts on the Kähler moduli as:

$$T \to \frac{aT - ib}{ict + d}; \quad \text{with } ad - bc = 1.$$

The fact that X transforms as a modular form with weight κ means that, under modular transformations, $X(T) \to (icT + d)^{\kappa}X(T)$. Hence $\bar{X}X/(T+\bar{T})^{\kappa}$ is invariant under modular transformations.

allowed in the Kähler potential, but provided that their coefficients are constant, they do not contribute to the scalar potential, therefore we will not consider them. It should be noticed that in order to get the correct result, one has to compute the scalar potential as usual and to impose $\langle X \rangle = 0$ only after that. Since

$$\left. \frac{\partial^2 K}{\partial T \partial X} \right|_{\langle X \rangle = 0} = 0 \,,$$

the Kähler metric is diagonal (or block diagonal in the immediate generalization to more than one Kähler moduli), hence the scalar potential is simply given by the original KKLT (3.41) one plus a positive term

$$V = V_{KKLT} + \frac{|\eta|^2}{\beta (T + \bar{T})^{3-\kappa}} \,,$$

where we also used $D_X W = \eta$. Recalling that $\mathcal{V} \propto (T + \bar{T})^{3/2}$ and comparing this result with Eq. (4.4), it is immediate to see that if $\kappa = 0$ the additional term captures the low energy physics of an $\overline{D3}$ in a flat background, while if $\kappa = 1$ it describes the same $\overline{D3}$ in warped compactifications.

The relation between the emergence of a nilpotent superfield in $D = 4$ supergravity and the $\overline{D3}$ uplift was analyzed in more detail in [95] (for a flat background) and in [94] (for a curved GKP background preserving $\mathcal{N} = 1$ supersymmetry). Remarkably, the main results do not depend on the chosen background.

As we mentioned before, the description of the $\overline{D3}$ in terms of the action (4.3) (and therefore the possibility of reproducing its low energy physics in a supersymmetric way through the nilpotent goldstino) is exact, provided that certain orientifold conditions are fulfilled. The simplest of these orientifold configurations corresponds to a single $\overline{D3}$ sitting on top of an $O3$-plane. In this case, indeed, all the scalars are projected out and only the 16 components worldvolume fermion remains, which is consistent with the fact that the scalar component of the nilpotent goldstino is not a propagating field. The absence of worldvolume scalars means that the brane is stuck on top of the $O3$-plane (it has no orientifold image), which eliminates any risk of potential tachyons. On the other side, the remaining worldvolume fermions are responsible for the fact that the $\overline{D3}$ action is different from zero and coincides with the Volkov-Akulov (VA) action[5]. We underline that the above-mentioned orientifold conditions can be fulfilled also in a more general way, with similar results. We will not consider this possibility.

It is important to notice that the location of the orientifold planes is determined by the analysis of the fixed points locus under the geometric part of an orientifold action, hence it cannot be controlled by a mere choice of free parameters [102]. As a consequence not all warped throats can host orientifold planes at their bottom. Nonetheless, as it was observed in [103], already the standard deformed conifold singularity admits such configuration, if one chooses the proper involution.

[5] For a $D3$-brane on top of an $O3$-plane, instead, all the fields are projected out, which is consistent to the fact that the resulting action vanishes.

The important points of this section can be summarized as follows. An $\overline{D3}$-brane spontaneously breaks supersymmetry. Under certain orientifold conditions, the only remaining degree of freedom is a Volkov-Akulov goldstino, which emerges on the world-volume of the $\overline{D3}$ and has no bosonic superpartner. In supergravity the VA goldstino is described by a nilpotent chiral superfield X, which is characterized by the fact that the supersymmetric partner X_0 of the goldstino ψ is not a fundamental field, but a combination of the other ones.

The setup for the rest of this work will be a warped background with fluxes (as sources of the warping), whose $D3$-charge is canceled by orientifold planes. In particular, we will consider the cases in which the fixed point locus of the orientifold involution includes $O3$-planes at the tip of a warped throat and we will place a single $\overline{D3}$ on top of these.

Nilpotent goldstino in LVS

The effect of the introduction of a nilpotent goldstino in the LVS frame is analogous to the KKLT case. Following [45], let us consider again the simplest LVS example, with only two Kähler moduli. As usual, we assume that all the complex structure moduli and the dilaton are stabilized, considering only the goldstino and the Kähler moduli. The supergravity theory is defined by:

$$K = K_{LVS} + \frac{\beta_0}{\mathcal{V}^{2/3}}\left(1 - \beta_1 \frac{\xi s^{3/2}}{\mathcal{V}}\right) X\bar{X} \,,$$
$$W = W_{LVS} + \eta X \,,$$

with K_{LVS} and W_{LVS} defined in Sec. 3.3. The coefficient η can be expressed in terms of the complex structure modulus of the throat as $\eta = \frac{Z^{2/3} i S}{M}\sqrt{\frac{c''}{\pi}}$ [48] with $c'' = \frac{2^{1/3}}{\mathcal{I}(0)} \approx 1.75$ (considering $y_{\overline{D3}} = 0$, that is the $\overline{D3}$ placed at the tip of the throat) [16]. The only difference with respect to the KKLT case is that, given that we included α' corrections in K_{LVS}, we are also taking into account the fact that the coefficient for the $X\bar{X}$ term might get an α' correction as well: however, as we can see from the next result, this correction will turn out to be negligible in the scalar potential, once we consider the large volume limit.

It is then straightforward to derive the new scalar potential, which is given by:

$$V = V_{LVS} + \frac{|\eta|^2}{2\beta_0 s \mathcal{V}^{4/3}}\left(1 - \frac{s^{3/2}\xi}{\mathcal{V}}(1-\beta_1)\right) \tag{4.7}$$

where V_{LVS} is defined in Eq. (3.52). For future reference it useful to make explicit the dependence of the (leading order) uplifting term on the conifold modulus, which is:

$$V_{up} = \frac{c''}{2\pi g_s M^2}\frac{|Z|^{4/3}}{\mathcal{V}^{4/3}} \,. \tag{4.8}$$

Analyzing the derivatives of (4.7) we find that Eqs. (3.53a), (3.53b) remain unchanged (because the new term does not depend neither on θ_s nor on τ_s), while Eq. (3.53c) becomes

$$\tau_s^{3/2} = \frac{(4a\tau_s - 1)^2}{16 a \kappa_s \tau_s (a\tau_s - 1)}\left(\frac{\xi}{g_s^{3/2}} + \frac{8\,|\eta|^2\,\mathcal{V}^{5/3}}{27\,W_0^2\,\beta_0}\right) \,,$$

where we neglected the α' correction in (4.7). Therefore the scalar potential at the minimum now reads:

$$V_{min} = -\frac{6W_0^2 g_s \kappa_s \tau_s^{3/2}(a\tau_s - 1)}{(4a\tau_s - 1)^2 \mathcal{V}^3} + \frac{5\, g_s \eta^2}{18\, \beta_0\, \mathcal{V}^{4/3}}\,,$$

which can be set to be positive by opportunely choosing the values of η and β_0.

4.3 Deformed conifold with $O3$-planes and global embedding

It is important to notice that the introduction of the nilpotent goldstino is a local feature, which needs to be consistently embedded in a global compact space in order to get a valid model. One way to do this is to start with a Calabi-Yau threefold supporting an involution with $O3$-planes and try to deform the complex structure of the orientifolded manifold around the $O3$-planes in order to obtain a local conifold, with vanishing tadpoles [103]. In this way, one could aim to find, among existing phenomenologically interesting models, cases in which a goldstino sector (and therefore an uplift to dS) can be easily introduced. This section is devoted to a review of this strategy.

4.3.1 The geometric action and the conifold

First of all it is useful to understand, following [103], how the geometric action of an involution acts on the coordinates of the conifold. We will consider two different coordinates systems, each of which allows to highlight some interesting features.

As was said in Sec. 2.3, an involution allowing for $O3$-planes must be such that its geometric part acts on the holomorphic three-form Ω as

$$\sigma^*\Omega = -\Omega\,,$$

where for the deformed conifold[6]

$$\sum_{i=1}^{4} z_i^2 = 4\epsilon^2, \tag{4.9}$$

in the patch $z_4 \neq 0$, we have

$$\Omega = \frac{dz_1 \wedge dz_2 \wedge dz_3}{z_4}\,.$$

For an $O3$-plane, therefore, σ simply flips the three local coordinates:

$$\sigma : (z_1, z_2, z_3, z_4) \to (-z_1, -z_2, -z_3, z_4). \tag{4.10}$$

As it is well known, the deformed conifold can also be parametrized, in terms of the new coordinates $\{x, y, z, w\} = \{\frac{z_1+iz_4}{2}, -\frac{z_1-iz_4}{2}, \frac{z_3+iz_2}{2}, \frac{z_3-iz_2}{2}\}$ as:

$$zw = xy + \epsilon^2\,. \tag{4.11}$$

With this choice, the action (4.10) reads:

$$\sigma : (x, y, z, w) \to (y, x, -z, -w)$$

[6] The numerical factor in the deformation parameter is introduced for future convenience.

whose fixed point locus is given by: $(x, y, z, w) = (\lambda, \lambda, 0, 0)$, with $\lambda \in \mathbb{C}$. We can easily see that it corresponds to the origin in the singular case ($\epsilon = 0$) and to a double fixed point $(\pm i\epsilon, \pm i\epsilon, 0, 0)$ in the deformed one. We can interpret this by saying that a deformed conifold supports two $O3$-planes at the poles of the blown-up three-sphere at its bottom and that these $O3$ collapse on top of each other in the singular limit. In addition to this, in [103], it was also argued that the two $O3$-planes are both of the same type (that is they share the sign of their $D3$-charge and tension). The simplest goldstino configuration requires, in particular, two negative-charge $O3$-planes, also called $O3^-$ [7] [102], hence we will focus on this case.

4.3.2 The embedding

Let us finally come to the problem of embedding the local orientifolded conifold in a global setup. As already mentioned, the idea is to start with a certain geometry, equipped with an involution with the right features and try to deform it in order to create the local configuration needed for the inclusion of a nilpotent goldstino (or equivalently of an $\overline{D3}$). This strategy [103] will be explicitly applied to a concrete construction in Chapter 6. Here, we only list and comment the main steps of the procedure:

1. *Choice of the model.* A model is given, for our present purposes, by a Calabi-Yau threefold and an involution acting on it. We will consider only Calabi-Yau hypersurfaces in toric varieties [105, 106] and only involutions defined as the inversion of one of the toric coordinates describing the manifold:

$$z_i \to -z_i.$$

   This ensures, for a favorable[8] geometry, $h^{1,1}_- = 0$ [9]. In particular, an eligible geometry is such that it admits an involution whose fixed points locus includes at least two $O3$-planes. Notice that a model is described by the equation of the CY hypersurface, modified in order to be invariant under the selected involution. A generic $O3$-plane is therefore given by:

$$\begin{cases} \text{eq}_{\text{CY}} = 0 \\ x_i = x_j = x_k = 0 \end{cases} . \tag{4.12}$$

2. *Deformation.* By analyzing the equation of the CY, we need to understand whether it is possible to deform it so that at least two of the zeroes in (4.12) come together in a certain limit (the singular limit). From (4.12) we can observe that it is generically impossible to do it if the two orientifold planes are originally placed in different fixed

[7] More precisely an Op^- is an Op-plane such that stacks of Dp-branes on top of it have orthogonal gauge groups, while for an Op^+ their gauge group is symplectic (see footnote 6 of [104]).

[8] A *favorable geometry* is characterized by the fact that the Kähler moduli on the ambient toric variety $\mathcal{A}$ descend to Kähler moduli on the Calabi-Yau hypersurface X_3, defined on $\mathcal{A}$. If X_3 is favorable, than $h^{1,1}(X_3) \cong \dim(\text{Pic}(\mathcal{A}))$ [107].

[9] See [108] for a discussion about why one might instead prefer (more involved) models with $h^{1,1}_- \neq 0$, obtained, e.g., via certain exchange involutions $x_i \leftrightarrow x_j$.

points loci in the ambient space[10]. We will therefore select only involutions such that the second equation in (4.12) has more than one zero.

3. *Conifold.* From the previous steps we obtained a model with at least two $O3$-planes which can be brought on top of each other via an appropriate deformation of the complex structure of the Calabi Yau. However, what we need is that the two O-planes sit at the tip of a (deformed) conifold, therefore we have to check whether the deformation introduced before actually led to a local conifold geometry. In other words, the equation of the CY in the neighborhood of the fixed point locus has to be written as a sum of squares, like in (4.9). In general this feature turns out to be automatically true.

4. *Consistency checks.* Finally we need to verify that the action of the involution on the conifold is the expected one (4.10) and that it is possible to satisfy the $D3$-charge tadpole cancellation condition (3.6).

4.4 Conifold destabilization and other tadpole-related issues

As we mentioned, the choice of using as uplifting mechanism a single $\overline{D3}$-brane on top of an $O3$-plane, frees the construction from many issues, mainly related to the presence of tachyonic destabilizations and singularities due to the interaction between different branes at the tip of the warped throat (see e.g. [92, 109, 93, 110, 111]).

Nonetheless, as was highlighted by I. Bena et. al in [16] (see also [17]), one needs to carefully pay attention to the stability of the obtained configuration also in presence of a single $\overline{D3}$. The argument can be summarized as follows: in a strongly warped compactification, as the one we need in order to recover a small cosmological constant, the conifold modulus plays a special role with respect to the other complex structure moduli, therefore it has to be treated separately. This is confirmed by the analysis of Sec. 3.1.3, where we showed that the scalar potential away from the minimum changes significantly with respect to the unwarped case (see Fig. 3.1) and that the mass of the conifold modulus (3.36) can be much lighter than the one of the other complex structure moduli. Moreover, the contribution to the scalar potential coming from the warped throat (3.35) has the same dependence on $\frac{\zeta^{4/3}}{\mathcal{V}^{4/3}}$ as the uplifting term (4.8), so that under certain conditions the presence of the second one might cause a destabilization of the minimum for ζ, leading to a runaway behavior.

To be more precise let us consider the sum of the scalar potential for the conifold modulus (3.35) with the contribution coming from the presence of an $\overline{D3}$ at the tip of the warped throat (4.8):

$$V_{Z+up} = \frac{|Z|^{4/3}}{c' M^2 \mathcal{V}^{4/3}} \left| \frac{M}{2\pi i} \log \frac{\Lambda_0^3}{Z} + i \frac{K}{g_s} \right|^2 + \frac{c''}{\pi g_s M^2} \frac{|Z|^{4/3}}{\mathcal{V}^{4/3}} \,. \tag{4.13}$$

By analyzing the derivatives, it is easy to see that (4.13) has two stationary points:

$$\zeta_0 = e^{-\frac{2\pi K}{g_s M} - \frac{3}{4} \pm \sqrt{\frac{9}{16} - \frac{4\pi}{g_s M^2} c' c''}} ; \quad \sigma_0 = 0 \tag{4.14}$$

[10] See also Fig. 5.2 in the next chapter.

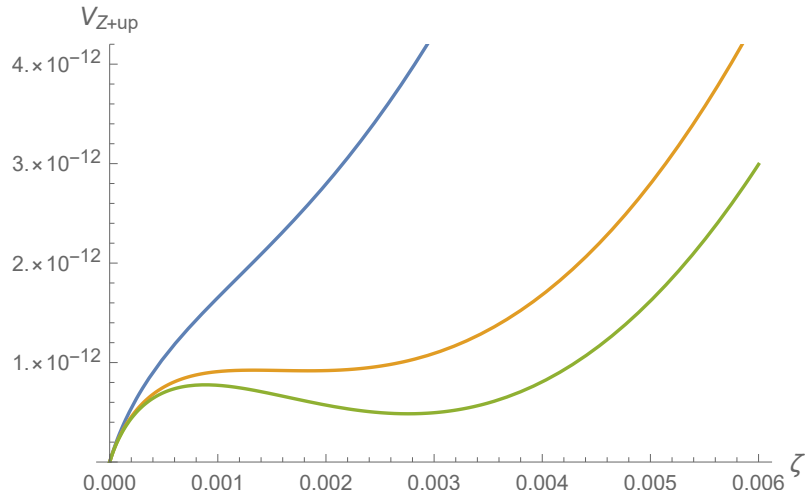

Figure 4.1: Scalar potential V_{Z+up} computed at $\mathcal{V} = 10^5$, $\sigma = 0$ and $g_s = 0.1$, for different choices of the fluxes (but keeping $\frac{M}{K} = 11$, so that the position of the possible minimum is always the same). Under our choice of g_s, the constraint (4.15) reads: $M \gtrsim 21.5$. In particular the blue curve shows a runaway ($M = 11$) and the green one a stable minimum ($M = 33$). The orange curve ($M = 22$) is at the boundary between the two possible behaviors.

where the case with a positive sign corresponds to a local minimum, while the other one is a local maximum. Although the numeric amount of this correction with respect to the standard solution (3.30) is usually negligible in explicit constructions, the presence of a square root in (4.14) imposes a lower bound on $g_s M^2$, which has to be taken into account in order to avoid a runaway behavior[11] (Fig. 4.1):

$$g_s M^2 \geq \frac{64\pi}{9} c' c'' \approx 46.1 \,. \tag{4.15}$$

Given that the string coupling needs to be small (so that the string perturbative expansion is under control), this means that the number of fluxes we need to turn on cannot be too small. Hence, one has to look for configurations with a large enough negative $D3$-charge, so that it is possible to compensate a potentially large positive contribution to the $D3$-tadpole cancellation condition. While this is certainly something to keep into account when looking for explicit constructions, we stress here that the situation is not as dramatic as depicted in [16]: we will show indeed that it is possible to consistently satisfy this requirement already in the frame of perturbative Type IIB string theory.

The problem of balancing the presence of a strongly warped throat with a de Sitter minimum and the tadpole cancellation condition has recently achieved a lot of attention in the field of string compactification, appearing as a non-trivial challenge for the realization of consistent de Sitter models. It is therefore worth to mention, in the remainder of

[11] This constraint was significantly relaxed, after a more accurate computation of the scalar potential for the modulus Z in the recent paper [112]. We will take into account this new update in Ch. 8.

this section, some of these challenges to give an idea of the prolific debate that has been developing in the latest years. Here, we will consider the so-called Singular-bulk Problem [113] and the Tadpole Problem [114, 115].

Before entering the topic it is useful to have in mind a more explicit form of the tadpole cancellation condition (3.6) for the configurations we will consider in this work, that is:

$$N_{D3} + N_{flux} = |Q_{D3}^{D7} + Q_{D3}^{Op}| \tag{4.16}$$

where we separated the positive (N_{D3}, N_{flux}) and the negative (Q_{D3}^{D7}, Q_{D3}^{Op}) contributions. Here N_{flux} is the contribution coming from background fluxes: given that the fluxes necessary to stabilize only the conifold modulus contribute with (3.27) and that we consider $N_{D3} = 0$, we will need to ensure that the total negative charge, coming from $D7$-branes and orientifold planes, *exceeds* this value, that is: $|Q_{D3}^{D7} + Q_{D3}^{Op}| > MK$.

The *Singular-bulk Problem* configures itself as a consequence of the constraint (4.15): the required largeness of the positive $D3$-charge coming from the fluxes provokes a too strong variation of the warp factor (due to the back-reaction of the fluxes themselves) in a generic KKLT model, producing a singularity over a large region of the original CY. Differently from other divergences in string theory, this singularity appears to be pathological and unacceptable. However, the term *generic* in the previous sentence is crucial as some non-generic configurations as well as some extension or variation with respect to KKLT, are expected to escape the singular-bulk problem. In particular, the condition to be satisfied in order to avoid the singularity is estimated to be:

$$\frac{\tau_\Sigma}{\mathcal{V}^{2/3}} \lesssim \frac{1}{g_s M^2} \ll 1$$

where τ_Σ is the volume (in Einstein frame) of the 4-cycle supporting non-perturbative effects. Assuming that we are in a CY with only one small cycle and with all the moduli stabilized in a de Sitter minimum (which requires $V_{AdS} \sim V_{up}$), we can estimate the volume τ_Σ as

$$\tau_\Sigma \sim \frac{16\pi K}{9\, a_s g_s M}\,,$$

which, introduced in the previous relation, leads to:

$$\frac{MK}{\mathcal{V}^{2/3}} \lesssim \frac{9\, a_s}{16\pi} \sim 1\,. \tag{4.17}$$

It is interesting to notice that the Large Volume Scenario is expected to satisfy this constraint more easily than KKLT, due to the large hierarchy between the volume of the compact space and that of the 4-cycle supporting non-perturbative effects.

However, in [116, 67] it was noticed that before leading to the formation of singular regions in the CY, a strong warping might imply that some curvature correction, which one usually neglects, becomes large. This would not mean that the theory is inconsistent by itself but that the effective theory one is using is not trustworthy in this case (while the exact one is not known at all). To estimate this effect the authors of [67] consider, as an example, a correction to the 4d Einstein-Hilbert action arising from the interplay between

the 10d R_{10}^4 term and a varying warp factor, which produces an additional term in the scalar potential[12]:

$$\delta V = \frac{15\xi MKW_0^2}{4\sqrt{g_s}\mathcal{V}^{11/3}}\mathcal{C}\,,$$

where $\mathcal{C}$ depends on the complex structure and, being unknown, is generically considered as an order one constant. Given the possibly large value of MK, this term might be relevant, despite the large power of $\mathcal{V}$ in the denominator, and, depending on the sign of $\mathcal{C}$ it risks to spoil the minimum. Imposing instead that it is much smaller than the value of the scalar potential at the AdS minimum (3.54) and using the expression (3.53c) for τ_s at the minimum, one obtains a stronger constraint with respect to (4.17) :

$$\frac{10\,a_s\xi^{2/3}\mathcal{C}}{\kappa_s^{2/3}g_s}\frac{MK}{\mathcal{V}^{2/3}} \ll 1\,, \tag{4.18}$$

where we have again considered only one small 4-cycle, for simplicity.

The *Tadpole Problem* is instead related to the complex structure moduli stabilization. In particular, the authors of [114] conjectured, on the basis of analytic examples and extended scans over the possible geometries, that the number of fluxes needed to stabilize an increasing number of moduli, increases so fast that they cannot be stabilized within tadpole constraints. In the type IIB language the conjecture states that the 3-form fluxes needed to stabilize the $h^{2,1}$ complex structure moduli of a smooth CY compactification, when $h^{2,1}$ is large, contribute to the total $D3$-charge according to the bound[13]:

$$-Q_{D3}^{(2,1)} > \alpha\, h^{2,1}; \quad \alpha > \frac{2}{3}\,. \tag{4.19}$$

On the other side, the negative contribution due to possible negative-charged sources ($O3/O7$-planes and $D7$-branes) is generically bounded from above so that it might be difficult to stabilize all the moduli and simultaneously cancel all the tadpoles, especially in presence of additional constraints like the ones imposed by an uplift mechanism. However, it is worth to be mentioned that a more optimistic vision is proposed in [67] where it is observed that a crucial assumption for the bound (4.19) is the smoothness of the CY manifold, while singular geometries can sidestep it. It is then possible to rephrase the conjecture saying that all vacua in the landscape at large number of complex structure moduli have singular internal geometries.

Finally, we mention that, again in [67] a new lower bound, called *The LVS parametric tadpole constraint*, was proposed for the $D3$-charge contribution coming from $O3/O7$-planes and $D7$-branes in the Large Volume Scenario, in order to get a controlled uplift term from $\overline{D3}$. The conclusion of the authors was, essentially, that the tadpole constraint appears to be difficult, but generically not impossible to satisfy.

[12] The difference in the numerical factor with respect to [67] is due to a difference in the definition of ξ with respect to the convention adopted here.

[13] With respect to [114] we compute the $D3$-charge in the perturbative type IIB double cover set up, hence $Q_{D3} = -\frac{\chi(Y_4)}{12}$, with a difference of a factor of 2 which consequently modifies the lower bound of α.

4.5 Other uplifting proposals

The anti-brane uplift is certainly one of the most famous and studied mechanisms for the construction of de Sitter vacua in string theory, but it is far from being the only one. A plethora of alternative methods have been proposed over the years, differing in the properties of the considered CY manifold as well as on the initial assumptions and on the ingredients introduced in the compactification. Following the classification proposed in [117] for top-down compact constructions, we can find attempts to develop dS models both in critical and non-critical ($D > D_c = 10$) string theory[14]. Moreover, besides being categorized by the branch of superstring theory in which they are defined (e.g. type IIB), the (geometric) critical constructions can be divided into classical, aiming to find a dS vacuum at tree level in 10d supergravity, and quantum solutions. KKLT and LVS belong to this last class of models, being based, as we said, on the introduction of perturbative and non-perturbative quantum corrections. Other proposals include, without any pretence of completeness, dS vacua coming from: hidden sector matter interactions [119]; AdS/CFT dual pairs [120]; LVS with dilaton-dependent non-perturbative effects and $\overline{D3}$ [121]; spontaneous supersymmetry breaking dynamics of strongly coupled gauge theory sectors on $D3$-branes [122]; complex structure F-terms [123, 124]; D-terms [125, 126, 127] and T-branes [128].

In the following, we briefly review the mechanism based on T-branes, which will be mentioned in Ch. 7 of this thesis.

T-branes

T-branes constitute a very generic way to obtain a de Sitter minimum in type IIB compactifications, through the interplay between background and gauge fluxes. The name refers to the eight-dimensional description of the mechanism. Here we present it from the (more intuitive) 4d point of view and we briefly go to the higher-dimensional interpretation towards the end of this section.

$D7$-branes are a typical ingredient of type IIB compactifications, especially in presence of an orientifold involution. Their positive charge, indeed, allows to cancel, as required, the negative $D7$-charge coming from the $O7$-planes produced by the involution. In the next chapter we will review some details about possible $D7$-branes configurations, their effects and their charges. Here it is sufficient to know that $D7$-branes wrapping a divisor D, support a non-vanishing worldvolume gauge flux $\mathcal{F}$, inducing a $U(1)$ charge q_{Di} on the i-th Kähler modulus and a moduli-dependent Fayet-Iliopulos (FI) term ξ_D:

$$q_{Di} = \frac{1}{(2\pi)^2\alpha'^2}\int_D \hat{D}_i \wedge \mathcal{F}; \qquad \frac{\xi_D}{m_p^2} = \frac{e^{-\phi/2}}{4\pi\mathcal{V}}\frac{1}{(2\pi)^2\alpha'^2}\int_D \mathcal{F}\wedge J = \frac{1}{2\pi}\sum_i \frac{q_{Di}}{2}\frac{t_i}{\mathcal{V}} \tag{4.20}$$

where $\hat{D}$ indicates the Poincaré dual[15] of the divisor D, ϕ is the dilaton ($e^{\langle\phi\rangle} = g_s$) and $J = \sum_i t_i \hat{D}_i$ is the usual Kähler form, which can be expressed as a combination of the

[14] In non-critical string theory the additional terms in the effective action, due to $D > D_c$, act as an uplift term (see e.g. [118]).

[15] See Eq. (5.10).

volumes of the 2-cycles t_i; the dilaton-dependence in the last passage of ξ_D is included in the definition of the t_i's. Moreover, the flux yields $U(1)$-charged $D7$ matter fields φ_i, with charge $q_{\varphi_j} = \pm 2$, belonging to the open string sector. These elements give rise to the D-term potential [129]

$$V_D = \frac{\pi}{\tau_D}\left(\sum_j q_{\varphi_j}\frac{|\varphi_j|^2}{s} - \xi_D\right)^2 \tag{4.21}$$

and the vanishing D-term condition (to be imposed in order to minimize the potential) turns out to fix the open string modes φ_i in terms of the Kähler moduli, which instead remain as flat directions [128]. Substituting the VEV of the φ_i into their F-term scalar potential results in a moduli-dependent positive definite term which can be used to obtain a Minkowski/dS minimum

$$V_{up} = \frac{c_{up}}{\mathcal{V}^{8/3}} m_p^4\,, \tag{4.22}$$

where c_{up} is an $\mathcal{O}(1)$ constant depending on the triple intersection numbers of the CY threefold and the gauge flux quanta. This means, in particular, that (4.22) cannot be tuned too much unlike the uplifting term obtained by the $\overline{D3}$-brane.

It is important to notice that this mechanism cannot be used in KKLT where the fact that the AdS minimum is supersymmetric ($D_T W = 0$), combined with the requirement of having a non-vanishing and gauge-invariant non-perturbative superpotential even in presence of chiral matter (see also Sec. 5.4), forbids the presence of a non-zero matter-dependent F-term like (4.22). It is instead applicable to LVS (non-supersymmetric vacuum), where the tuning in order to obtain a vanishing/small cosmological constant is operated on the original AdS minimum (and in particular on the background fluxes through W_0 and g_s) rather than on the uplifting term.

A deeper understanding of this 4d uplifting mechanism, including the check of certain consistency conditions, requires an analysis from a higher-dimensional point of view. The result of this analysis [128] is that the supersymmetric configuration corresponding, in the 4d EFT, to the mechanism described above, is a T-brane solution of the 8-dimensional equations of motion for the theory living on the $D7$-brane world-volume. A T-brane, first introduced in [130], is a bound state of $D7$-branes which is realized when the presence of non-vanishing gauge fluxes prevents the scalar field Φ (describing the deformation of the $D7$-brane) to commute with its conjugate. In this case, the field Φ is described by an upper triangular form, hence the name T-brane.

Chapter 5

Constructing an explicit model

In the previous sections we addressed some important features that a realistic string theory is expected to fulfill: string compactification (Sec. 2.2) is needed to justify the fact that we only observe a four-dimensional space-time; moduli stabilization (Ch. 3) allows to get rid of the hundreds of unobserved massless fields that arise from string compactification and mechanisms such as the one described in Ch. 4 provide a way to obtain a positive cosmological constant. However, many other features need to be taken into account in order to construct an explicit model.

Prerequisites to construct explicit global models

Since the analysis of concrete models will characterize a large part of the rest of this work, it is important, and it is the purpose of this chapter, to review some specific arguments that will be useful to understand these constructions.

- *Geometry*: First of all, one has to set the geometric background, that is to choose a Calabi-Yau manifold with appropriate features. Most of the needed geometric data for all the CY threefolds which are hypersurfaces in toric varieties (the case we will consider here) with Hodge numbers $h^{1,1} \leq 6$, are conveniently stored in the Ross Altman Toric CY Database [106]. A description of the database, with a theoretical introduction to the data included there, is provided in [107, 65]. A recent update also included several new data relative to orientifold CY three-folds obtained via exchange involutions [108]. Sec. 5.1 is devoted to a brief presentation of Calabi-Yau three-folds in toric varieties, with a focus on the topics that will be relevant for our constructions, including the determination of the topology of the divisors (Sec. 5.1.1) and the effects of an orientifold involution on the geometric data (Sec. 5.1.2).

- *Kähler cone conditions*: A set of relations constrains the volumes of the 2-cycles associated to the Kähler moduli, in order to have a well-defined theory. As we will see, they come from the requirement that all the effective curves have a positive volume. These relations are known as Kähler cone conditions (KCC) and we present them in Sec. 5.2.

- *D-branes*: The presence of orientifold planes at the fixed point set of the involution imposes the introduction of $D7$-branes in order to cancel the tadpole. As reviewed in Sec. 5.3, there are several possible configurations, contributing with a different amount of charge and having many important roles in the realization of quasi-realistic models. The $D3$-charge contribution of these objects is one of the major topics of Sec. 5.3, even though other generic features are described as well.

- *Non-perturbative effects:* As we mentioned in the previous chapters, non-perturbative effects have a crucial role in the process of moduli stabilization. However, in presence of certain configurations, one needs to explicitly check whether such non-perturbative contributions can actually be generated (Sec. 5.4).

- *Loop corrections to the scalar potential*: Finally, for a theory with several Kähler moduli, some additional effect might be needed in order to stabilize all the moduli. One possibility is to also include sub-leading terms coming from loop corrections, which might be relevant also for phenomenological reasons (e.g. for the construction of inflationary models). Sec. 5.5 is dedicated to the description of the main known corrections of this kind.

5.1 Calabi Yau threefolds as hypersurfaces in toric varieties

A toric variety $\mathcal{A}$ of dimension n (the case of interest will be $n = 4$) is an algebraic variety containing a n-torus $\mathbb{T} = (\mathbb{C}^*)^n$ as a dense open subset such that the natural action of the torus on itself extends to an action of $\mathbb{T}$ on $\mathcal{A}$ [131]. When $\mathcal{A}$ is a Gorenstein toric Fano variety[1], an anti-canonical divisor inside $\mathcal{A}$ defines a co-dimension one subvariety $X_3 \subset \mathcal{A}$ which is a CY manifold. Moreover, as we review in what follows, several relevant quantities can be computed via combinatoral and linear algebra involving a pair of dual reflexive lattice polytopes.

We define a n-dimensional polytope Δ with vertices w_i on the lattice $M_{\mathbb{R}} \simeq \mathbb{Z}^n \subset \mathbb{R}^n$ and containing only the origin as an interior point. People often refer to Δ as the *Newton polytope*. Its polar dual lattice polytope Δ°, with vertices v_i, is defined as:

$$\Delta^\circ = \{v \in N_{\mathbb{R}} \simeq \mathbb{Z}^n \subset \mathbb{R}^n \, : \langle v, w\rangle \geq -1, \, \forall w \in \Delta\} \tag{5.1}$$

and it is such that $(\Delta^\circ)^\circ = \Delta$. The polytope Δ (as well as Δ°) is said to be *reflexive* if also its polar dual Δ° is a lattice polytope containing only the origin as an interior point. A complete classification of all 473 800 766 reflexive polytopes in 4d was operated by M. Kreuzer and H. Skarke in [105, 132], using the software `PALP` [133]. The crucial point is that there is a one-to-one correspondence (up to birational equivalence) between reflexive polytopes and a Gorenstein toric Fano variety.

From a given triangulation[2] of the dual polytope Δ°, we can construct the normal fan Σ over the faces of Δ° (see Fig. 5.1): its rays are generated by (a subset of) the lattice points

[1] A Gorenstein toric Fano variety is a variety whose anti-canonical divisor is an ample Cartier divisor.

[2] A triangulation is a partition of the polytope into n-dimensional cones (generated by n rays) such that their union equals the polytope itself.

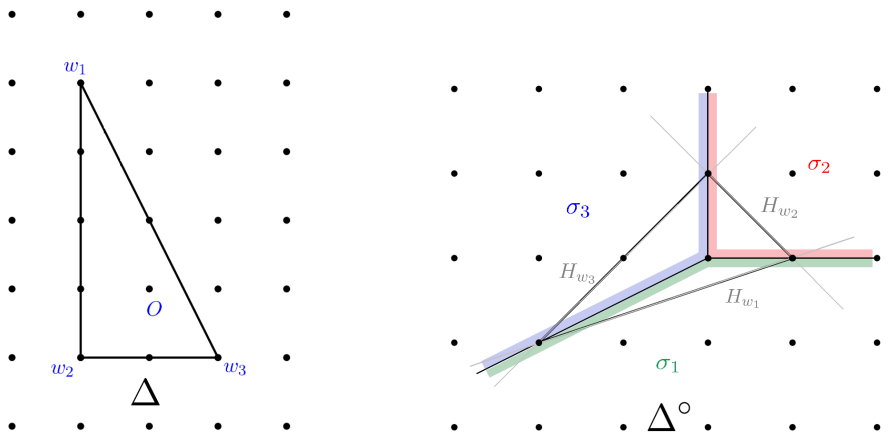

Figure 5.1: Construction of the fan Σ from a pair of reflexive polytopes on a 2d ($n = 2$) lattice. Starting from the lattice points of Δ (it is sufficient to consider only the vertices w_i) we can define the supporting hyperplanes $H_w = \{v \in N_{\mathbb{R}} : \langle v, w\rangle = -1,\ \forall w \in \Delta\}$. Hence the $(n-1)$-dimensional faces of Δ° are given by $F = \Delta^\circ \cap H_w$. The rays that pass from the origin through the points in F define a set of rational cones σ_i. In particular the figure shows three 2d rational cones generated by the rays passing through the vertices of the dual polytope. A set of n-dimensional cones constructed in this way, with all their intersections, is called the fan Σ of Δ°. Different choices for the rays generating the fan (so that they also include lattice points different from the vertices v_i) correspond to different triangulations [107].

of the polytope $\{\nu_i\}$ and each of them is in one-to-one correspondence with a homogeneous coordinate x_i,

$$\nu_i \leftrightarrow x_i\ , \tag{5.2}$$

in the toric ambient space (or, more precisely, with the toric divisor defined as the zero locus $D_i : x_i = 0$). The choice of the set $\{\nu_i\}$ corresponds to the choice of the triangulation.

The Batyrev formula provides a way to derive the defining equation for a CY manifold X_3 which is a hypersurface in $\mathcal{A}$, starting from the reflexive polytopes [134]:

$$P_{CY}(x_1, ..., x_n) = \sum_{w \in \Delta \cap M_{\mathbb{R}}} a_w \prod_i x_i^{\langle \nu_i, w\rangle + 1} = 0\ , \tag{5.3}$$

where the w's are lattice points of Δ and the a_w's are parameters depending on the complex structure of the CY. Hence, each lattice point in Δ produces a monomial of the CY equation. Moreover, from the polytopes it is possible to derive the Hodge numbers of the corresponding CY hypersurfaces [134, 127]:

$$h^{1,1}(X_3) = l(\Delta^\circ) - 5 - \sum_{\Theta^{\circ[3]}} l^*(\Theta^{\circ[3]}) + \sum_{\Theta^{\circ[2]}, \Theta^{[1]}} l^*(\Theta^{\circ[2]}) \cdot l^*(\Theta^{[1]})\ , \tag{5.4}$$

$$h^{2,1}(X_3) = l(\Delta) - 5 - \sum_{\Theta^{[3]}} l^*(\Theta^{[3]}) + \sum_{\Theta^{[2]}, \Theta^{\circ[1]}} l^*(\Theta^{[2]}) \cdot l^*(\Theta^{\circ[1]})\ , \tag{5.5}$$

where $l(\Delta)$ is the number of lattice points of the polytope Δ, $\Theta^{[k]}$ is a k-dimensional face of the same polytope and $l^*(\Theta^{[k]})$ is the number of interior lattice points of $\Theta^{[k]}$ (analog definitions are valid for the dual polytope). From these formulas it is evident the correspondence between reflexive polytopes and mirror CY hypersurfaces as the exchange of the roles of Δ and Δ° is equivalent to the exchange $h^{1,1} \leftrightarrow h^{1,2}$ in the CY.

It should be noticed that different polytopes can give rise to the same pair of Hodge numbers ($h^{1,1}$, $h^{2,1}$) of the CY, which corresponds to the fact that the same CY hypersurface can be embedded in different ambient spaces. Indeed the 473 800 766 reflexive polyhedra classified in [105] were found to correspond to 30 108 distinct pairs of Hodge numbers. However, not even this number corresponds to the number of possible CY hypersurfaces. Indeed, while the Hodge numbers depend only on the polytope, other characteristics of the CY change with the triangulation so that a given polytope can give rise to more than one distinct CY geometry.

The toric variety $\mathcal{A}$ can be described also as a generalization of a weighted projective space. Following [135], let us consider only *maximal* (that is 4-dimensional) polytopes, which can be represented in terms of the 4d weighted projective space $\mathbb{CP}^4_{q_1\,q_2\,q_3\,q_4\,q_5}$. This means in particular that we can associate each of the five homogeneous coordinates x_i on $\mathcal{A}$ to a positive integer q_i determining the equivalence relation:

$$(x_1, x_2, x_3, x_4, x_5) \sim (\lambda^{q_1} x_1, \lambda^{q_2} x_2, \lambda^{q_3} x_3, \lambda^{q_4} x_4, \lambda^{q_5} x_5)\,, \quad \text{with } \lambda \in \mathbb{C}^*\,. \tag{5.6}$$

This property can be represented by the following scheme:

$$\begin{array}{|ccccc|} \hline x_1 & x_2 & x_3 & x_4 & x_5 \\ \hline q_1 & q_2 & q_3 & q_4 & q_5 \\ \hline \end{array} \tag{5.7}$$

A hypersurface on a toric space defined as above is a CY, that is it has a vanishing first Chern class, if the degree of the defining equation is $\sum_{i=1}^5 q_i$. We know that any toric CY three-fold which is not a quintic ($q_i = 1, \forall i$) is defined in a non-smooth ambient space, therefore if this is the case we need to resolve the possible singularities that intersect the CY itself. This can be done by adding new lines of weights (hence new homogeneous coordinates) obtaining, in the end, a $k \times (k+5)$ *weights matrix* where each line represents a different equivalence relation for the homogeneous coordinates. In terms of the reflexive polytopes this corresponds to taking as additional generators of the fan Σ also the rays passing from the origin through (some of the) points of Δ° which are not vertices (see again Fig. 5.1). The weights matrix can be derived from the reflexive polytopes using the fact that the q_i^j's ($i = 1, ..., k$, $j = 1, ..., k+5$) need to satisfy the equations [107]:

$$\sum_i q_i^j \nu_i = 0\,, \tag{5.8}$$

where the ν_i's are defined around Eq. (5.2). Again, the sum of the weights of each line corresponds to the degree of the CY equation: a method to find such equation, alternative to (5.3), is therefore to sum all the possible monomials with the given degrees. Usually there are several possible resolutions, corresponding to different weights matrices, and, in terms of the original polytopes, to different triangulations. In any case, for 4d polytopes

it is always possible to choose a triangulation such that the corresponding CY three-fold is smooth. This is true, in particular, for the so-called Fine, Regular, Star Triangulations (FRSTs), that are such that all points of Δ° not interior to facets appear as vertices of a simplex (*fine*), the origin is a vertex of each full-dimensional simplex (*star*) and the corresponding toric variety is actually a projective space (*regular*).

Finally, toric varieties can be represented also as supersymmetric moduli spaces of a gauged linear sigma model (GLSM) whose charges correspond to the weights defined above, which is why often people refer to the weights matrix as the GLSM matrix [136].

Toric Divisors

The zero locus $x_i = 0$ of each coordinate in the ambient space can be associated to a *toric divisor class* $[D_i]$ [3]. In some cases the divisor $x_i = 0$ can split into several components, when intersected with the CY. However, we will consider only *favorable* geometries which are characterized precisely by the fact that this splitting does not happen, so that $H_4(X_3)$ is completely described by the toric divisors of the ambient space, by:

$$D_i : \; x_i = P_{CY} = 0 \, .$$

This justifies the fact that, as we mentioned before, the grades of the equation of the CY are obtained by summing the weights of each line of the GLSM matrix. In terms of the toric divisor classes the CY hypersurface is defined as:

$$X_3 = \sum_i D_i \, . \tag{5.9}$$

An important duality, called *Poincaré duality* relates the toric divisor classes (and in general any non-trivial p-cycle $\in H_p(X_3, \mathbb{R})$) to the cohomology group[4] $H^p(X_3, \mathbb{R})$. Here, we state it only in the form that will be useful for our purposes but it can be easily generalized. Given a divisor D_i there exists a unique cohomology class $[\hat{D}_i]$ (where $\hat{D}_i$ is a 2-form) such that:

$$\int_{D_i} \rho_{d-2} = \int_{X_3} \rho_{d-2} \wedge \hat{D}_i \, , \quad \forall \rho_{d-2} \text{ (d-2)-dimensional forms} \tag{5.10}$$

with $d = \dim X_3$. The 2-form $\hat{D}_i$ is called the Poincaré dual of the divisor D_i. In other words the Poincaré duality establishes an isomorphism between the space of toric divisor classes $H_4(X_3, \mathbb{R})$ and the space of 2-forms $H^2(X_3, \mathbb{R})$, which has the structure of a vector space. This allows, for example, to describe the toric ambient space and (in the case of favorable geometries) the CY hypersurfaces in terms of a basis of generators $\{\hat{D}_i\}$. An important consequence of this property, which is manifest in (5.10) and will be extensively used in the next chapters, is that integrals over p-cycles can be expressed in terms of

[3] In the following we will mostly omit the square brackets, identifying the equivalence class with its representative D_i.

[4] The cohomology group $H^p(X, \mathbb{R})$ is the group of *closed* p-forms (A_p such that $dA_p = 0$) defined up to an *exact* p-form $A_p = dB_{p-1}$, where d indicates the exterior derivative. See also App. B.

integrals over the whole CY space. Moreover, we can define the isomorphism $H_p \cong H_{d-p}$ which means that a generic p-cycle and a generic $(d-p)$-cycle intersect each other at a finite number of points.

The toric divisors need to satisfy the relation [107]

$$\sum_i \nu_i \cdot D_i = 0\,, \tag{5.11}$$

with ν_i defined around Eq. (5.2). By comparing this relation with (5.8), we can notice a correspondence between the columns of the weights matrix and the toric divisor classes, which turns out to be very useful in explicit computations.

Intersections and SR-ideal

Also the intersections among divisors descend from the properties of the original pair of reflexive polytopes, as follows. Two divisors intersect each other if and only if the corresponding rays of the fan Σ share a common cone. In particular, in the ambient space $\mathcal{A}$, four divisors intersect in a point if the rays span a cone in Σ: the resulting intersection number is $\frac{1}{V}$, where V is the volume of the cone. Assuming that the geometry is favorable, a similar relation can be obtained for the intersection of three divisors in the CY hypersurface. If we look at divisors intersections from this point of view, we can easily deduce that the intersection numbers depend on the choice of the triangulation (that is on the way in which the dual polytope is subdivided into cones).

On the other side, the coordinates x_i's of divisors D_i's coming from rays that do not belong to the same cone can never vanish simultaneously. The set of toric divisors with this feature is called the *Stanley-Reisner* (SR) ideal. Introducing the notation of intersection among divisors as the product between the divisor classes

$$[D_i \cap D_j] = [D_i] \cdot [D_j] = \int_S \hat{D}_i \cdot \hat{D}_j\,,$$

we define the SR-ideal as the set generated by the elements $R_I = [D_{i_1}] \cdot \ldots \cdot [D_{i_k}]$ with $R_I = 0$, where for each element it is sufficient to consider only the minimal set of divisors such that the corresponding rays do not belong all to the same cone.

Given a basis of divisors, it is often convenient to present the non-vanishing intersection numbers in the form of an *intersection polynomial*:

$$I_3 = \sum_{i,j,k=1}^{h^{1,1}} k_{ijk} D_i\, D_j\, D_k\,,$$

where $k_{ijk} = \int_{X_3} \hat{D}_i \wedge \hat{D}_j \wedge \hat{D}_k$.

Chern classes

The Chern classes are topological invariants associated with n-dimensional vector bundles on smooth manifolds. The total Chern class of a vector bundle V is given by

$$c(V) = \sum_{i=0}^{n} c_i(V)\,, \tag{5.12}$$

with $c_0 = 1$. In the special case in which V is a line bundle, the above summation is truncated to: $c(V) = 1 + c_1(V)$. Moreover, according to the splitting principle, we can always write the Chern class of a given vector bundle in terms of the product of Chern classes of line bundles.

The application of these concepts to our case is straightforward if we recall that a Gorenstein toric Fano variety is defined through k toric divisors (that is k line bundles $\mathcal{O}(D)$) for which the first Chern class reads [137]

$$c_1(\mathcal{O}(D)) = -c_1(\mathcal{N}_{D|X_3}) = -[\hat{D}]\,, \tag{5.13}$$

where $\mathcal{N}_{D|X_3}$ is the normal bundle of D. In particular, for the divisors of the CY we have $c_1(D) = -\iota_D^* D$, where ι_D^* indicates the pull-back on the divisor D. Therefore the Chern class of $\mathcal{A}$ is given by:

$$c(\mathcal{A}) = \prod_{i=1}^{k}[1 + c_1(\mathcal{O}(D_i))] = \prod_i (1 - \hat{D}_i) \tag{5.14}$$

from which we can derive each of the four $c_i(\mathcal{A})$. A completely analogous formula is true for a (favorable) CY geometry embedded in $\mathcal{A}$.

Finally, the Euler characteristic (2.17) can be also defined as the integral of the top Chern class, hence for a CY hypersurface we have:

$$\chi(X_3) = \int_{X_3} c_3(X_3)\,. \tag{5.15}$$

The Wall's theorem

As we mentioned at the beginning of this section, while certain features of a CY three-fold descend directly from the two reflexive polytopes, others depend on the choice of the triangulation so that the same pair of polytopes, associated to different triangulations, can give rise to different geometries. However, it is also true that different triangulations can produce the same Calabi-Yau. The Wall's theorem [138] allows precisely to understand when two three-folds are equivalent as real manifolds. When related specifically to Calabi-Yau threefolds, it can be enunciated as follows:

The homotopy types[5] *of complex compact CY 3-folds are classified by the Hodge numbers, the intersection numbers and the second Chern class.*

In other words two different triangulations correspond to the same CY geometry if they share the same Hodge numbers, intersection numbers and second Chern class.

5.1.1 Topology of divisors

Several properties of the toric divisors depend on their topology, which is mainly defined by their Hodge numbers. The Hodge numbers of a divisor can be expressed either in the

[5] Two continuous functions are said to be of the same homotopy type if one of them can be continuously deformed into the other.

form of the so-called *Hodge diamond*

$$\begin{array}{ccccc} & & h^{2,2} & & \\ & h^{2,1} & & h^{1,2} & \\ h^{2,0} & & h^{1,1} & & h^{0,2} \\ & h^{1,0} & & h^{0,1} & \\ & & h^{0,0} & & \end{array} \quad , \tag{5.16}$$

or with the more compact notation (which also takes into account the fact that the Hodge diamond is symmetric):

$$h^{\bullet} = \{h^{0,0},\, h^{0,1},\, h^{0,2},\, h^{1,1}\} \, . \tag{5.17}$$

For $h^{1,1}(X_3) < 5$ the Hodge numbers of the divisors can be computed via the package `CohomCalg` [139, 140]. However, for larger values of $h^{1,1}(X_3)$ the algorithm usually fails, hence they need to be computed with a different method.

The Hodge numbers $h^{0,p}(D_i)$ depend only on the location of the lattice points v in the polytope Δ°. In particular (see the previous section for the notation) [134, 141][6]:

- If $v =$ vertex of Δ°, D_i is an irreducible divisor on X_3. Moreover $h^{0,1} = 0$, $h^{0,2} = l^*(\Theta^{[3]})$.
- If $v \in \Theta^{\circ[1]}$, D_i is irreducible. Moreover, $h^{0,1} = l^*(\Theta^{[2]})$; $h^{0,2} = 0$.
- If $v \in \Theta^{\circ[2]}$, D_i is generically reducible. Moreover, $h^{0,1} = h^{0,2} = 0$. However we will consider only favorable geometries, for which all toric divisors are irreducible, hence we will never encounter this kind of lattice points.
- If $v \in \Theta^{\circ[3]}$, the toric divisor on $\mathcal{A}$ does not intersect the Calabi-Yau, hence there is no D_i associated to it. Again, this never occurs in favorable geometries.

The remaining Hodge numbers can be derived from the Euler characteristic and the holomorphic Euler characteristic[7] of the divisor [137]:

$$\chi(D_i) = 2h^{0,0} - 4h^{0,1} + 2h^{0,2} + h^{1,1} = \int_{D_i} c_2(D_i) \, , \tag{5.18}$$

$$\chi_h(D_i) = h^{0,0} - h^{0,1} + h^{0,2} = \frac{1}{12} \int_{D_i} 2\, c_1^2(D_i) + c_2(X_3) \, , \tag{5.19}$$

obtaining:

$$h^{0,0} = \chi_h(D_i) + h^{0,1} - h^{0,2}; \quad h^{1,1} = \chi(D_i) - 2\chi_h(D_i) + 2h^{0,1} \, . \tag{5.20}$$

The values of the Hodge numbers provide a way to classify different divisors on the basis of their topology. We distinguish in particular [142, 143]:

[6] See also [127].

[7] The holomorphic Euler characteristic is defined as $\chi_h(D) = \sum_i (-1)^1 h^{i,0}(D)$.

- *Completely rigid divisors*: $h^{0,0}=1$; $h^{0,1}=h^{0,2}=0$; $h^{1,1}\neq 0$ [8].

  Among these, the so-called shrinkable del Pezzo divisors, which are presented below, play an important role in string phenomenology.

- *'Wilson' divisors:* $h^{0,0}=1$; $h^{0,2}=0$; $h^{0,1}$, $h^{1,1}\neq 0$.

- *Deformation divisors:* $h^{0,1}=0$; $h^{0,2}\neq 0$.

  Besides the K3, which is described in more detail in the following, other deformation divisors that are often encountered in toric Calabi-Yau hypersurfaces are:

$$SD_1:\ h^\bullet=\{1,0,1,21\};\quad SD_2:\ h^\bullet=\{1,0,2,30\}\,.$$

  People refer to them as special deformation divisors.

Let us consider in more detail the (completely) rigid divisors and the K3 divisors, which will be relevant in the upcoming chapters.

Completely rigid divisors

Among completely rigid divisors, we distinguish:

- Del Pezzo surfaces: dP_n $(n=0,...,8)$;
- Rigid but not del Pezzo divisors: NdP_n $(n\geq 9)$.

A *del Pezzo* divisor is obtained by blowing up $\mathbb{CP}^2$'s at n generic points. dP_0 coincides with the $\mathbb{CP}^2$ itself. The Hodge numbers of a dP are $h^\bullet=\{1,0,0,n+1\}$ and its Euler characteristic is $\chi(dP_n)=n+3$ (while $\chi_h(dP_n)=1$). Furthermore, a necessary condition for a given D_s to be a dP is:

$$D_s^3=k_{sss}=9-n>0;\quad D_iD_s^2\leq 0\,\forall i\neq s\,. \tag{5.21}$$

A dP surface can be either *shrinkable* ('diagonal') or *non-shrinkable* (non-diagonal). In the first case the divisor is arbitrarily contractible to a point and it is always possible to find a basis of divisors such that $D_{dP}^3\neq 0$ and $D_{dP}D_iD_j=0$ for any other $i,j=1,...,h^{1,1}$ (this is the reason why it is often called 'diagonal'). The diagonality condition can be expressed in terms of the triple intersection numbers as [144]:

$$ddP:\ k_{ssi}k_{ssj}=k_{sss}k_{sij},\quad \text{if } k_{ssi}\neq 0 \text{ for some } i\,. \tag{5.22}$$

As a consequence, recalling that the volume of the CY is given by $\mathcal{V}=\frac{1}{6}k_{ijk}t^it^jt^k$ and that the volumes of the divisors can be obtained from $\mathcal{V}$ as $\tau_i=\frac{\partial\mathcal{V}}{\partial t^i}$, we find:

$$\tau_{ddP}=\frac{1}{2k_{sss}}(k_{ssi}t_i)^2\,. \tag{5.23}$$

[8] To be precise, a *rigid* divisor is a divisor with $h^{0,2}=0$. From the phenomenological point of view it is useful to further classify rigid divisors in completely rigid divisors, with $h^{0,1}=0$ (indicating that the surface do not contain non-contractible 1-cycles), and 'Wilson' divisors, with $h^{0,1}\neq 0$. It should be noticed, in particular, that only completely rigid divisors support non perturbative effects like the ones described in Sec. 5.4.

On the other side, a non-shrinkable dP divisor is such that the property (5.22) is not satisfied, so that it cannot be contracted to a point. Instead of the resolution of singular points, it can be seen as the resolution of line-like singularities [27].

In [145] it was conjectured that the CY three-folds arising from the 4d reflexive polytopes listed in the Kreuzer-Skarke database do not exhibit a 'diagonal' (that is satisfying Eq. (5.22)) dP_n for $1 \leq n \leq 5$. The conjecture was verified for $1 \leq h^{1,1}(X_3) \leq 5$. Regarding this, it should be noticed that looking only at the Hodge numbers it is impossible to distinguish between a dP_1 and the Hirzebruch surface $\mathbb{F}_0 = \mathbb{CP}^1 \times \mathbb{CP}^1$. In particular, already at $h^{1,1} \leq 5$ it is possible to find CY 3-folds with a 'diagonal' divisor of the second kind. In order to discriminate between these two cases for a given divisor D_s, we can consider the intersection numbers:

$$\int_{X_3} \hat{D}_s^2 \hat{D}_i = m, \quad \int_{X_3} \hat{D}_s \hat{D}_i^2 = n; \quad s \neq i \tag{5.24}$$

and apply the following criteria [145]:

1. A sufficient condition for D_s to be a dP_1 is that there exist some divisors D_i for which at least one between m and n is odd.

2. If all the m are even ($m = 2k$) and it is impossible to find a solution for one of the two conditions:

$$2k = p^2 - q^2 \quad \text{for some } p, q \in \mathbb{Z}, \quad k \in \mathbb{Z}^* \tag{5.25}$$

$$\exists k_1, k_2 \in 2\,\mathbb{Z}^* : \quad \frac{k_2}{k_1} = \left(\frac{p}{q}\right)^2, \quad \text{for some } p, q \in \mathbb{Q} \tag{5.26}$$

   then D_s cannot be a dP_1 (hence we assume that it is a $\mathbb{CP}^1 \times \mathbb{CP}^1$).

However, we will usually don't need to distinguish between the two cases, since for our purposes, they both show the same behavior.

Finally, a *rigid-but-not del Pezzo* divisor has the same Hodge numbers as the dP_n, but with $n \geq 9$. As we can deduce from the first relation in (5.21), it is characterized by $D_s^3 < 0$. Similarly to the non-diagonal dP's, it is not contractible to a point.

The reasons why we are particularly interested in dP divisors (especially the shrinkable ones) are that, besides several applications in model building (see e.g. [28]), they have a crucial role in the generation of non-perturbative effects (see also Sec. 5.4), which is even more important in the context of the Large Volume Scenario, where the fact that the rigid divisor is shrinkable allows to write the volume of the CY in the Swiss cheese form (3.58).

K3 divisors

A K3 surface is a compact $2d$ Calabi-Yau manifold, with Hodge numbers and Euler characteristic given by:

$$h^\bullet = \{1, 0, 1, 20\}\,; \qquad \chi(K3) = 12\,\chi_h(K3) = 24\,. \tag{5.27}$$

Its first Chern class is zero. Since for a divisor D in a CY one has $c_1(D) = -\iota^* D$ (see Eq. (5.13) and the comment below), then

$$\int_{X_3} \hat{D}^2_{K3} \hat{D} = 0, \quad \forall D \in H^{1,1}(X_3) \tag{5.28}$$

and in particular

$$\int_{X_3} \hat{D}^3_{K3} = 0\,. \tag{5.29}$$

It should be noticed that a divisor with the Hodge numbers of a K3 is not necessarily a K3. In order to see this, let us consider a divisor S whose topology is defined by (5.27). Eq. (5.19) now reads:

$$\chi_h(S) = 2 = \frac{1}{12}\int_S 2\,c_1^2(S) + c_2(X_3) = \frac{1}{12}\left(\chi(S) + \int_S c_1^2(S)\right)\,, \tag{5.30}$$

where the last term comes from the definition (5.18) of the Euler characteristic in which the second Chern class is computed via the adjunction formula:

$$c_2(S) = c_1^2(S) + c_2(X_3)\,. \tag{5.31}$$

Substituting the value $\chi(S) = 24$ we find that S satisfies the relation[9]:

$$\int_S c_1^2(S) = 0\,. \tag{5.32}$$

This is a necessary but not sufficient condition for S to be a K3. An example of a space satisfying Eq. (5.32) but with $c_1(S) \neq 0$ will be presented in Sec. 7.5.1. In conclusion, we will identify with a K3 any divisor which has the Hodge numbers (5.27) *and* satisfies the fibration condition (5.28).

The reason why we are interested in K3-fibrations is that they are particularly promising for phenomenological and cosmological applications, especially in the frame of LVS [27]. Indeed, the volume of a K3-fibred CY containing at least one rigid divisor can be expressed in the form:

$$\mathcal{V} = \sqrt{\tau_1}\tau_2 - \tau_s^{3/2}$$

(where we have restricted to the case $h^{1,1} = 3$, for simplicity), which is a generalization of the usual 'Swiss-cheese' volume. In this case the volume is controlled by two large cycles instead of one. This allows, for example, to stabilize two of the three moduli in LVS, as usual, leaving a flat direction which can be fixed in a second moment (via the introduction of subleading corrections) to a much smaller mass. For this reason, this 'light' modulus might play the role of an inflaton field (see e.g. [146]).

5.1.2 Orientifold involution and O-planes

Up to now, we didn't consider any symmetry operation of the kind presented in Sec. 2.3. Let us therefore review how the presence of an orientifold involution with geometric action

$$x_i \to -x_i \tag{5.33}$$

modifies certain aspects of the geometry with respect to what was said above.

[9] Notice that it coincides with Eq. (5.29), given that $\int_S c_1(S) = -\int_S S$.

Hodge numbers and Calabi-Yau equation

First, as already explained in Sec. 2.3, it splits each cohomology group (hence the corresponding Hodge numbers) into an even and an odd eigenspaces, whose Hodge numbers can be easily determined. Indeed, invariance under the inversion of a coordinate rules out all odd divisors: $h_-^{1,1} = 0$ (hence $h_+^{1,1} = h^{1,1}$). The remaining $h_\pm^{1,2}$ [10] can be computed by means of the Lefschetz fixed point theorem, according to which

$$\sum_i (-1)^i (b_+^i(X_3) - b_-^i(X_3)) = \chi(O_\sigma)\,, \tag{5.34}$$

where $b_\pm^i(X_3)$ are the even and odd Betti numbers, related to the Hodge numbers by[11]:

$$b_\pm^i = \sum_{p+q=i} h_\pm^{p,q}(X_3)\,; \tag{5.35}$$

$\chi(O_\sigma)$ is the sum of the Euler characteristics of all the divisors wrapped by orientifold planes:

$$\chi(O_\sigma) = \sum_i \chi(O7_i) + \sum_k \chi(O3_k); \quad (\chi(O3_k) = 1)\,. \tag{5.36}$$

In our case, Eq. (5.34) becomes (see also Eq. (2.21)):

$$2\,(2 + h^{1,1} + h_-^{1,2} - h_+^{1,2}) = \chi(O_\sigma)\,, \tag{5.37}$$

which can be solved for $h_\pm^{1,2}$, recalling also that $h^{1,2} = h_+^{1,2} + h_-^{1,2}$.

In addition to this, the equation of the CY (5.3) must be modified so that it only includes terms that are invariant under the involution. In particular all the monomials containing an odd power of x_i are ruled out by the involution.

Orientifold planes

We already know that the involution (5.33) produces a certain number of orientifold planes. These can be easily recovered by carefully scrutinizing all the equivalence relations encoded in the weights matrix in order to understand which coordinates need to be set to zero in order to obtain an invariant locus. Here we list all the cases that can arise from this study. Each of them is characterized by a set of vanishing coordinates, under which the equation of the CY (assuming that it has been modified in order to be invariant under the involution) may or may not vanish[12].

- $x_i = 0$.
  - $P_{CY}|_{x_i=0} = 0$: $O9$-plane. This never happens for the involutions we are considering ($\sigma^*\Omega = -\Omega$), as already noticed in Sec. 2.3.

[10] $h_-^{1,2}$ gives the number of complex structure deformations of the equation of the CY invariant under the chosen involution, while $h_+^{1,2}$ gives the number of abelian bulk vectors.

[11] See also App. B.

[12] When we write $P_{CY}|_{(x_{i_1}=\ldots=x_{i_n}=0)} = 0$, we mean that the equation vanishes for any value of the other (non-zero) coordinates.

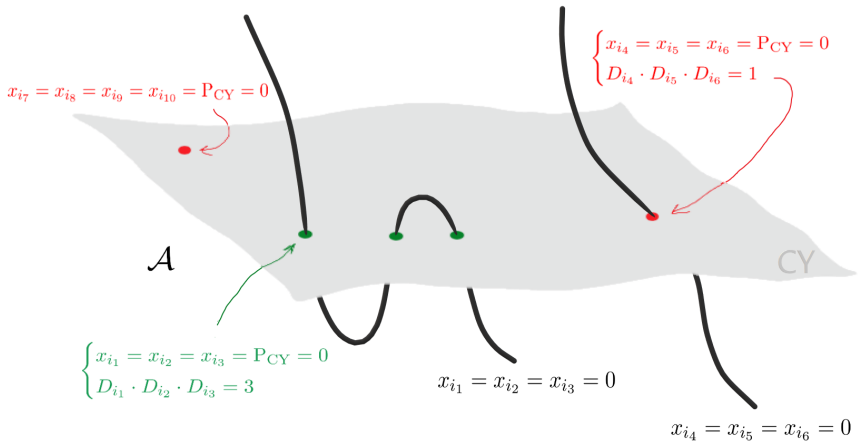

Figure 5.2: An illustrative representation of different kinds of $O3$-planes in a CY orientifold. The locus $x_i = x_j = x_k = 0$ is a curve in the ambient space, intersecting the CY hypersurface in n points (with $n = k_{ijk}$). If $n > 1$, it is generically possible to deform the three-fold so that two points belonging to the same fixed curve (green in the figure) come on top of each other, as needed for $\overline{D3}$ uplift: in this case, we say that there are n *'collapsable'* $O3$-planes. We do not expect, instead, to be able to find a deformation bringing together points (red in the figure) belonging to different curves or, even more, points given by $x_i = x_j = x_k = x_l = P_{CY} = 0$, corresponding to isolated points of the ambient space located on the CY.

  - $P_{CY}|_{x_i=0} \neq 0$: $O7$-plane.

- $x_i = x_j = 0$ ($x_i\, x_j \notin SR$).
  - $P_{CY}|_{(x_i=x_j=0)} = 0$: $O7$-plane. We will exclude all examples presenting this configuration, since they are expected to be singular. Indeed, this feature implies that the (invariant) equation of the CY factorizes in:

$$x_i^{n_i} P_i + x_j^{n_j} P_j = 0 \tag{5.38}$$

    where P_i and P_j are polynomials depending on all the coordinates. The fact that this factorization only happens *after* the involution indicates that the number of toric divisors is increased by the involution (now there is the new divisor $x_i = x_j = 0$), which is a signal of singularity. In particular we notice that (5.38), when $n_i = n_j = 1$, is the equation of a conifold, which is singular in $x_i = P_i = x_j = P_j = 0$.
  - $P_{CY}|_{(x_i=x_j=0)} \neq 0$: $O5$-planes. Similarly to $O9$-planes, these configurations are forbidden by the involution under consideration.

- $x_i = x_j = x_k = 0$ (if allowed by the SR-ideal).
  - $P_{CY}|_{(x_i=x_j=x_k=0)} = 0$: $O5$-planes (again forbidden).

  - $P_{CY}|_{(x_i=x_j=x_k=0)} \neq 0$: $O3$-planes. The number of planes coming from the same curve $x_i = x_j = x_k = 0$ in the ambient space is given by the intersection numbers of the CY: $D_i \cdot D_j \cdot D_k = k_{ijk}$. If $k_{ijk} > 1$, it is generically possible to deform the complex structure of the three-fold so that the planes come on top of each other. In this case, we say that there are k_{ijk} '*collapsable*' $O3$-planes (see Fig. 5.2).

- $x_i = x_j = x_k = x_l = 0$ (if allowed by the SR-ideal).

  - $P_{CY}|_{(x_i=x_j=x_k=x_l=0)} = 0$: $O3$-plane. We are not particularly interested in these configurations, when trying to realize the scenario of Ch. 4. Indeed, they correspond to isolated points on the CY (see again Fig. 5.2), hence, it is generically impossible to deform the manifold so that they end up to collapse on top of another $O3$-plane as we need in order to introduce the $\overline{D3}$ uplifting term.
  - $P_{CY}|_{(x_i=x_j=x_k=x_l=0)} \neq 0$. For this case, as well as for the more generic case $x_{i_1} = ... = x_{i_n} = 0$ with $n > 4$, generically there are no solutions.

Each O-plane carries RR-charges of different degrees. The total RR charge of a seven-dimensional orientifold plane wrapping the divisor D_{O7} is formally expressed by the 'Mukai' charge vector, which is the vector Γ_{O7} appearing in the action [28]:

$$S_{O7} = \int_{\mathbb{R}^{1,3}\times X_3} C \wedge \Gamma_{O7} \tag{5.39}$$

with $C = \sum_p C_p$. Its expansion on a CY is given by:

$$\Gamma_{O7} = -8[D_{O7}] + [D_{O7}] \wedge \frac{c_2(D_{O7})}{6} \,. \tag{5.40}$$

We can notice that Γ_{O7} is the sum, in this order, of a two-form and a six-form. Introducing (5.40) in the action (5.39), we deduce that these terms encode, respectively, the $D7$-charge and the $D3$-charge of the $O7$-plane. The $D7$-charge will be canceled by a suitable choice of the D-brane configuration (see Sec. 5.3), hence we will only need to worry about the $D3$-charge contribution, which is given by (minus) the integral over the CY of the six-form term:

$$Q_{D3}^{O7} = -\int_{X_3} \Gamma_{O7}|_{6-form} = -\frac{\chi(D_{O7})}{6} \,. \tag{5.41}$$

The $O3$-planes, instead, carry only $D3$-charge, with a contribution, for each of them, of:

$$Q_{D3}^{O3} = -\frac{1}{2} \,. \tag{5.42}$$

5.2 Kähler cone conditions

In order to have a positive definite metric we need to impose that the integral of J over all the effective curves $\mathcal{C}$ is positive:

$$\int_{\mathcal{C}} \hat{J} > 0 \,. \tag{5.43}$$

This requirement is the analog of the one of having a positive volume of the divisors $\left(\int_S J \wedge J > 0\right)$ and of the CY $\left(\int_X J \wedge J \wedge J > 0\right)$. The conditions (5.43) define a cone, said *Kähler cone* and constrain the (Poicaré dual) of the CY to lie within it.

The effective curves $\mathcal{C}$ form a cone as well, which is known as Mori cone and is generated by the set of curves $[\mathcal{C}^i]$. A way to specify these curves is through the *Mori cone matrix*, parametrizing their intersections with the toric divisor classes:

$$M^i_j = [\mathcal{C}^i] \cdot [D_j] = \int_{[\mathcal{C}^i]} \hat{D}_j \,. \tag{5.44}$$

The Kähler cone conditions (5.43) (KCC) correspond to a set of constraints on the volumes of the 2-cycles t_i, which can be derived, once the matrix (5.44) is given[13], as follows:

$$\int_{[\mathcal{C}^i]} \hat{J} \geq 0 \Leftrightarrow [\mathcal{C}^i] \cdot \sum_j t^j [\hat{D}_j] = \sum_j M^i_j \, t^j \geq 0 \,. \tag{5.45}$$

We stress that the procedure outlined above allows to define the Kähler cone only for the ambient space $\mathcal{A}$. This is due to the fact that, at least in principle, not all the effective curves of $\mathcal{A}$ lie in the Mori cone of X. As a consequence the Kähler cone of the ambient space is expected to be smaller than the one of the CY, which means, on the other side, that taking the KCC for the ambient space is a sufficient condition. For this reason we will not worry too much about this issue, but we mention that some attempt to find a better approximation for the CY Kähler cone was done, for example, in [28], taking advantage of the explicit knowledge of the properties (and in particular of the Mori cones) of certain curves. In [144], instead, the Kähler cones are estimated by comparing them with the (smaller) ambient Kähler cone and the larger intersection Kähler cone (obtained from the Mori cone given by the intersection of all the Mori cones of the ambient varieties which are connected via 'irrelevant' flop transitions): notice that in the non-generic case in which the two cones coincide, this method provides the exact CY Kähler cone.

Finally, it is important to notice that when different triangulations lead to the same Calabi-Yau geometry, the full Kähler cone will be given by the union of the Kähler cones of the individual *phases*. Indeed, in this case the Kähler form J is allowed to stay in the Kähler cone of either representation.

5.3 D-branes and Tadpole Cancellation conditions

The presence of a set of orientifold planes, due to the involution, makes the addition of $D7$-branes essential in order to cancel the total $D7$-charge. In particular, as we will better see in Sec. 5.3.1, for each $O7$-plane in the equivalence class $[D_{O7}]$ we need to add $D7$-branes in the equivalence class

$$[D_{D7}] = 8[D_{O7}] \,. \tag{5.46}$$

[13] In the examples analyzed in the subsequent chapters, we will extract the Mori cone matrix from the Ross Altman database [106].

Besides the ones needed for $\overline{D3}$ uplift (whose configuration is chosen so that they do not contribute to the $D3$-charge), we will not include any $D3/\overline{D3}$-brane, hence this section is dedicated to the study of $D7$-branes.

Let us consider a CY geometry described by the equation $\xi^2 = h(u_1, ..., u_n)$ (where h is a homogeneous polynomial) in the coordinates $\{u_1, ..., u_n, \xi\}$ equipped with the involution $\xi \to -\xi$, so that there is (at least) an $O7^-$-plane[14] wrapping the divisor $D_{O7} : \{\xi = 0\}$. The most generic form for the equation describing the world-volume of a $D7$-brane on top of the $O7^-$-plane can be obtained by studying the IIB theory as the weak coupling limit of an F-theory and it turns out to be [104]:

$$\Sigma_{D7} : \ \eta^2(u_1, ..., u_n) - \xi^2 \chi(u_1, ..., u_n) = 0 \,, \tag{5.47}$$

where η and χ are two homogeneous polynomials, invariant under the involution, whose degrees are determined by the degrees of the CY equation. Moreover, $\xi \in \mathcal{O}(D_{O7})$, $\eta \in \mathcal{O}(4D_{O7})$ and $\chi \in \mathcal{O}(6D_{O7})$. For generic polynomials the locus is connected, hence it corresponds to a single orientifold invariant $D7$-brane. Analyzing the equation (5.47), we notice that Σ_{D7} has double point intersections with the $O7$-plane ($\xi = 0$), which can be interpreted by saying that it locally looks like a brane-image brane pair:

$$(\sqrt{\chi}\,\xi + \eta)\,(\sqrt{\chi}\,\xi - \eta) = 0 \,. \tag{5.48}$$

This feature is true also at the global level only if χ assumes the non generic form $\chi = \psi^2$: in this case Σ_{D7} splits in two separate branes (one the image of the other), each wrapping a divisor in the cohomology class $4[D_{O7}]$. Furthermore, in confirmation with what said above, it can be proven [104] that single $D7$-$O7$ intersections would violate Dirac quantization, which justifies the fact that Eq. (5.47) is the most general allowed configuration for a $D7$ on top of an $O7^-$, even without taking into account F-theory.

Let us analyze some other features of the world-volume described by equation (5.47). It is straightforward to see that the double points intersections at $\eta = \xi = 0$ are actually double points singularities. Moreover there is a pinch point singularity at $\xi = \eta = \chi = 0$. Around the singular points the divisor turns out to be isomorphic to the so-called Whitney umbrella, which is defined as: $x^2 = zy^2$, with $x, y, z \in \mathbb{C}^3$ (see Fig. 5.3). For this reason a brane of this kind is usually called *Whitney brane* [147].

Different brane configurations can be obtained when η and χ are not generic (we already mentioned the case in which $\chi = \psi^2$). The simplest possibility, which characterizes branes wrapping a rigid divisor[15], is:

$$\eta = \alpha\,\xi^4; \ \chi = \beta\,\xi^6 \quad \Rightarrow \quad \Sigma_{D7} : \ \xi^8 = 0 \,. \tag{5.49}$$

It corresponds to four $D7$-branes (and four image-branes) placed on top of the $O7$-plane, realizing a $SO(8)$ gauge group.

[14] An $O7^+$, having positive $D7$-charge, would be incompatible with tadpole cancellation.

[15] A rigid divisor D_ξ has $h^{0,1}(D_\xi) = 0$. This means that the equation of a generic representative of the divisor class ($\xi = 0$) cannot be deformed in any way. The class $8[D_\xi]$, therefore, can only be represented by the equation $\xi^8 = 0$.

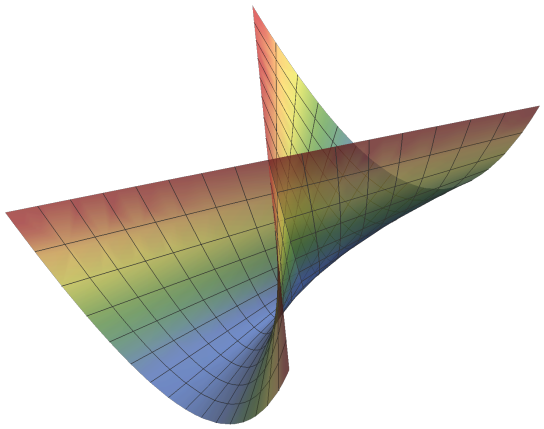

Figure 5.3: Projection of the Whitney umbrella to $\mathbb{R}^3$, where we can easily recognize the 'pinched-point' singularity.

Generalizing a bit, it is possible that the polynomials factorize in:

$$\eta = u_i^m \tilde{\eta};\ \chi = u_i^{2m}\tilde{\chi} \quad \Rightarrow \quad \Sigma_{D7}:\ u_i^{2m}\left(\tilde{\eta}^2 - \xi^2\tilde{\chi}\right)\ . \tag{5.50}$$

In this case we have a $Sp(2m)$ stack of m $D7$ (plus their images) along u_i and a Whitney brane of lower degree in the homology class $8[D_{O7}] - 2m[D_i]$.

World-volume flux

As we mentioned in Sec. 4.5, a $D7$-brane wrapping the divisor D_{D7} supports a non-trivial gauge flux F living on its world-volume and generating 4d chiral modes. In general we are not allowed to set it to zero because of the need to cancel the Freed-Witten (FW) anomaly [148], which requires, in particular, that [26]:

$$(2\pi\alpha')F + \frac{1}{2}c_1(D_{D7}) \in H^2(X_3, \mathbb{Z})\ . \tag{5.51}$$

In order to satisfy this constraint, it is sufficient to choose:

$$(2\pi\alpha')F = \sum_{i=1}^{h^{1,1}} n_i\, \iota^*_{D_{D7}}\hat{D}_i - \frac{1}{2}c_1(D_{D7}); \quad n_i \in \mathbb{Z} \tag{5.52}$$

where the sum runs over the elements of a basis of divisors. The form $\frac{1}{2}c_1(D_{D7})$ is relevant only when D_{D7} is a *non-spin* divisor (if D_{D7} is spin, that form is integral). For the cases of our interest the only situation in which we will not have to worry about FW anomaly is when D_{D7} is a K3, due to the fact that $c_1(K3) = 0$.

In order to have a gauge invariant object we combine F with (the pull-back $\iota^*_{D_{D7}}$ of) the background B-field B_2:

$$\mathcal{F} = (2\pi\alpha')F - \iota^*_{D_{D7}}B_2\ . \tag{5.53}$$

It is possible to set $\mathcal{F} = 0$ by a choice of B_2. This will become important later. In presence of multiple stacks of branes, setting $\mathcal{F}$ to zero on all of them is not a trivial task since B_2 is a global quantity (hence it must be the same for all the branes).

Finally, it is worth to mention that there is another kind of Freed-Witten anomaly to be taken into account; in order to prevent it we need to impose [127]:

$$\iota^*_{D_{D7}} H_3 = 0; \quad H_3 = dB_2 \,. \tag{5.54}$$

This requirement is automatically satisfied when the worldvolume of the divisor wrapped by the D7-brane does not contain closed 3-forms (that is it has $h^{1,0}(D) = 0$, hence $H_3 = 0$).

5.3.1 *D*-branes charges

*D*7-branes supporting a holomorphic gauge bundle carry RR *D*7-, *D*5- and *D*3- charges. As for the orientifold planes we can introduce the 'Mukai' charge vector for a *D*7-brane. that is the $\Gamma_{\mathcal{E}}$ appearing in the Chern-Simons action of the *D*7 [28]:

$$S_{CS} = \int_{\mathbb{R}^{1,3}\times X_3} C \wedge e^{-B} \wedge \Gamma_{\mathcal{E}} \,, \tag{5.55}$$

where again $C = \sum_p C_p$. Expanding it on a CY we find, for a single *D*7-brane:

$$\Gamma_{D7}(D_{D7}, \mathcal{F}) = [D_{D7}] + [D_{D7}] \wedge \mathcal{F} + \frac{1}{2}[D_{D7}] \wedge \left(\mathcal{F} \wedge \mathcal{F} + \frac{c_2(D_{D7})}{24} \right) \tag{5.56}$$

which is the sum of a 2-form, a 4-form and a 6-form. Introducing this result in (5.55) we deduce that these terms encode, respectively, the *D*7-charge, the *D*5-charge and the *D*3-charge carried by the brane. Comparing the *D*7-charge in the above expansion with the one in (5.40) we can now easily understand why *D*7-tadpole cancellation requires (5.46). Moreover, since we are considering only invariant configurations[16], it appears obvious from (5.56) that the total *D*5-charge is automatically canceled. The only non-trivial term coming from (5.56) is therefore the *D*3-charge contribution:

$$Q^{D7}_{D3} = -\int_{X_3} \Gamma_{\mathcal{E}}|_{6-form} = -\frac{\chi(D_{D7})}{24} - \frac{1}{2}\int_{D_{D7}} \mathcal{F} \wedge \mathcal{F} \,. \tag{5.57}$$

Having a singular world-volume, the Whitney brane deserves more care. An useful (smooth) representation of a Whitney brane wrapping the divisor $D_W = 8D_{O7}$ consists in considering it as the result of the recombination of a brane-image brane system, in which each brane wraps a divisor $4D_{O7}$. This is motivated by the local form of Σ_{D7} (5.48) as well as by the fact that the charge is conserved under brane recombination. Applying Eq. (5.57) to this system we obtain therefore:

$$Q^W_{D3} = 2Q^{D7}_{D3}(4D_{O7}) = -\frac{\chi(4D_{O7})}{12} - 4\int_{X_3} D_{O7} \wedge \mathcal{F} \wedge \mathcal{F} \,, \tag{5.58}$$

[16] Each brane equipped with the gauge flux $\mathcal{F}$ is associated to an image brane wrapping the same divisor class and carrying a flux $-\mathcal{F}$.

where $\mathcal{F}$ is the flux supported by one of the branes in the brane-image brane pair. However, there are subtleties that need to be taken into account. First, contrary to what one might expect, the recombination process can induce an integral flux [104]. Indeed, it is well known that the $D3$-charge contribution of a brane includes a geometric and a flux charge. Hence, there exists the possibility that the geometric charge is modified during the recombination process and that this change is compensated by the appearance of a new flux, so that the total charge is conserved. When this happens, the equation (5.47) is forced to take the form:

$$\Sigma_{D7}: \ \eta^2 = \xi^2(\psi^2 - \rho\tau) \tag{5.59}$$

where $\psi \in \mathcal{O}(3D_{O7})$, $\rho \in \mathcal{O}(3D_{O7} - 2F + 2B_2)$ and $\tau \in \mathcal{O}(3D_{O7} + 2F - 2B_2)$ (F is an integer form). Not all flux configurations (encoded in the line bundles for ρ and τ) are allowed: if one of the last two line bundles has no holomorphic sections, indeed, the corresponding polynomial is forced to vanish and the equation splits into the brane-image brane system:

$$(\eta + \xi\psi)(\eta - \xi\psi) = 0\,. \tag{5.60}$$

In order to avoid this, we need to choose, if possible, a B-field and a flux F such that the two divisor classes $[3D_{O7} - 2F + 2B_2]$ and $[3D_{O7} + 2F - 2B_2]$ are positive definite, which happens if:

$$-\frac{3D_{O7}}{2} \leq F - B_2 \leq \frac{3D_{O7}}{2}\,. \tag{5.61}$$

Furthermore, as it is clear already from Eq. (5.58) the value of the $D3$-charge depends also on $\mathcal{F}$. Recalling that we need a large negative $D3$-charge in order to compensate possibly large contributions coming from the background fluxes, it is useful to select, among the flux choices allowed by (5.61) the one that minimizes this contribution. A very simple way to make this choice can be found once one explicitly separates the flux and geometric charges of the brane:

$$Q^W_{D3,\text{geom}} = -\frac{1}{3}\int_{X_3} D_{D7} \wedge (43D_{D7} \wedge D_{D7} + c_2(X_3)) = -\frac{\chi(4D_{D7})}{12} - 9\int_{X_3} D^3_{D7} \tag{5.62}$$

$$Q^W_{D3,\text{flux}} = \int_{X_3} D_{D7} \wedge (3D_{D7} - 2F + 2B_2) \wedge (3D_{D7} + 2F - 2B_2) \tag{5.63}$$

(consistently, the sum of the two terms gives (5.58)). Indeed, it is now clear that while the geometric contribution is negative, the flux charge is positive. As a consequence the largest (negative) possible $D3$-charge is given by the (5.62) alone, provided that it is possible to choose the flux so that the pull-back of at least one of the two corresponding line bundles on the brane vanishes, so that $Q^W_{D3,\text{flux}} = 0$.

Comparing (5.57) (at $\mathcal{F} = 0$) with (5.62), we understand one of the main advantages of using a single invariant brane rather than several stacks: indeed the $D3$-charge of the Whitney brane can assume much larger (negative) values, leaving more room for the introduction of background fluxes needed for complex structure moduli stabilization (see Sec. 4.4). In addition, this configuration prevents the generation of dangerous chiral modes at the intersection with (fluxless) branes wrapping rigid divisors, which would

obstruct the presence of non-perturbative effects, essential for Kähler moduli stabilization (see also Sec. 5.4). Finally, it automatically has a vanishing D-term (as we can see looking Eq. (4.21), which allows to avoid possible issues related to having a hidden brane wrapping a large cycle (which is usually the case for divisors admitting also a Whitney brane). Indeed, it can be shown [147] that a non-vanishing D-term would imply a FI term proportional to the volume of the wrapped cycle, which, as a consequence of the vanishing D-term condition, would be forced to shrink to zero, thus ruining the large volume limit.

Phenomenology

The main purpose of the present work is to analyze the presence of de Sitter minima in string theory, focusing on the challenge of stabilizing all the moduli in a way that satisfies all the many consistency requirements, among which the tadpole cancellation condition assumes a prominent role. Nonetheless it is worth to notice that besides being essential in satisfying this condition, $D7$-branes are crucial for several model building applications, especially in relation to the fact that they are a key ingredient to gain chirality in string compactifications (see e.g. [26, 146]). Chiral matter, indeed, is obtained at the intersection between $D7$-branes supporting a non-vanishing gauge flux. In particular, interesting phenomenological features characterize configurations based on the presence of $D3$- and $D7$-branes at del Pezzo singularities as studied, e.g., in [149, 150, 28, 29], the last two with a specific focus on the topic of consistently embedding such local configurations in global setups.

5.4 Non-perturbative effects

Non-perturbative effects, as mentioned in Sec. 3.2, are generated by specific brane configurations. However, in a model including multiple non-perturbative effects or, more generically, several branes stacks, some additional constraint is usually needed in order to ensure that W_{np} is actually non-zero. This section is dedicated to an overview of these issues.

First of all, let us briefly review the three possible effects of our interest:

- *Gaugino condensation* [55]: A stack of $D7$-branes is placed on top of a divisor wrapped by an $O7$-plane (so that the $D7$-charge is canceled). The $D7$-branes support a condensing gauge theory, thus producing the usual non-perturbative term (3.39), with $a = \frac{6\pi}{b_0}$ (b_0 is the coefficient of the one-loop beta function). In perturbative string theory, $SO(8)$ (corresponding to four branes and four image branes wrapping a rigid divisor - see Sec. 5.3) is the only condensing gauge group on a $D7$-brane stack with no (chiral and non-chiral) matter [18]. In this case, $a = \frac{\pi}{3}$.

- $O(1)$ *instanton* [54]: A $D3$-brane wraps a (rigid) four-cycle D in the compact space. Since such brane appears as point-like in the non-compact space-time, it is usually called euclidean $D3$-brane, or $E3$-instanton. The classical action for this configuration is [127]:

$$S_{E3} = 2\pi \cdot \mathrm{rk}(E3) \cdot \tau_D \,, \tag{5.64}$$

where τ_D is, as usual, the volume of the four-cycle wrapped by the $E3$. From this, it follows $a = 2\pi$ in (3.39).

In order to generate a non-perturbative effect, the $E3$-instanton has to be invariant under the involution, otherwise it would be projected out. If $h^{1,1}_{-} = 0$, this implies that the gauge flux on the brane is forced to vanish: $\mathcal{F}_{E3} = 0$. However, the brane usually wraps a non-spin divisor, hence F needs to be non-zero in order to cancel the FW anomaly. As a consequence $W_{np}^{E3} \neq 0$ only if it is possible to choose a B-field which cancels this contribution.

- *Rank two instanton* [56] (see also [127]): When it is impossible to select a proper B-field for the rank one $E3$ to be invariant, there is still the possibility of introducing a rank-two $E3$-instanton. In this case, the $E3$-instanton, wrapping an invariant divisor, is equipped with a rank two vector bundle (instead of a line bundle): $\mathcal{E} = \mathcal{L}_1 \oplus \mathcal{L}_2$, where $\mathcal{L}_{1,2}$ are two line bundles. Then, in order to have an invariant configuration, we do not need to impose the vanishing of the gauge fluxes, but only $\mathcal{L}_2 = \mathcal{L}_1^{-1}$, corresponding to two $D3$-branes, one the image of the other. It should be noticed that, again from (5.64) the coefficient in the exponential of W_{np} is now $a = 4\pi$. This implies that whenever a rank-one instanton is allowed, it will dominate, therefore one will need to take into account rank-two instantons only when the first ones are forbidden.

The above configurations do not always generate a non-perturbative superpotential. More precisely, there is the possibility that, under certain conditions, W_{np} is forced to vanish. Here, following mainly [127, 147], we will focus on $E3$-instantons (both rank one and two), but similar considerations apply also to gaugino condensation[17].

In [54], E. Witten developed a criterion, based on F-theory, allowing to understand whether a given $E3$-brane may generate a non-vanishing W_{np}. However, a similar criterion can be formulated also in type IIB, stating that a suitable $E3$-brane cannot have more than two fermionic neutral zero modes [147]. This justifies some of the assumptions considered up to now. In the absence of intersections with other D-brane stacks, indeed, there are three classes of neutral zero modes. The first class includes the so-called *universal zero-modes*, which are model-independent; they correspond to the four fermionic superpartners of the real scalars parametrizing the motion of the $E3$-brane in the 4d space-time. Imposing that the $E3$-brane is invariant under the orientifold involution projects out two of these modes. The other two classes come from the possible moduli of the wrapped divisor (corresponding to scalar fields in the world-volume field theory) and from the Wilson line moduli. However, the firsts are counted by $h^{0,2}(D)$ and the latter are present only if $h^{0,1} \neq 0$. Hence, if the $E3$ wraps a completely rigid divisor ($h^{0,1} = h^{0,2} = 0$) as we required, these modes are absent[18].

Let us now consider the case in which the $E3$ intersects other $D7$-branes. In this case

[17] In particular the form of (5.66) coming from gaugino condensation is different [151], but the qualitative conclusions remain the same.

[18] If this sufficient condition is not satisfied, there might still be the possibility to soak up some of the zero modes, but a more involved configuration is needed (see e.g. [152]).

the strings stretched between the two stacks give rise to fermionic zero modes in the bi-fundamental representation with respect to the gauge groups living on the $E3$ and/or on the $D7$. The number of chiral states can be evaluated by means of the *chiral index*:

$$I_{D7-E3} = \int_{D7\cap E3} (\mathcal{F}_{D7} - \mathcal{F}_{E3}) \tag{5.65}$$

which counts the difference between the chiral states in the fundamental representation and the ones in the anti-fundamental representation. Notice that according to this formula the intersection of branes with trivial fluxes do not generate chiral modes. Moreover, even for non-zero fluxes, one can try to arrange them so that $I_{D7-E3} = 0$.

If $I_{D7-E3} \neq 0$ [19], the chiral modes induce charged chiral superfields Φ in the path integral for the superpotential:

$$W \sim \prod_i \Phi_i e^{-S_{inst}} \tag{5.66}$$

so that it is different from zero only if the Φ_i can be stabilized to a non-vanishing VEV (this requirement might be avoided considering more involved configurations, such as $h^{1,1}_{-} \neq 0$). Notice that, though it is a strong assumption, this might be possible *if* the intersecting branes belong to the hidden sector. The visible sector is instead constrained by the Standard Model (or by its supersymmetric extension, the MSSM), so that one should always require that the instanton does not intersect the $D7$-branes supporting the visible sector [151]. As a final remark, we mention that there are some situations in which (5.66) is automatically zero, regardless the VEVs of the matter fields Φ_i [127]. Indeed the superpotential comes from the action:

$$A \sim \int d\eta_1 ... d\eta_n \, e^{-S_{inst}} \tag{5.67}$$

where the η_i are n fermions and the effective instantonic action S_{inst} contains gauge invariant terms of the form: $S_{inst} \supset \sum_{i,j=1}^{n} g_{ij}\, \eta_i \phi\, \eta_j$ (g_{ij} is the coupling constant and the ϕ_i are the scalar fields living on the brane). Since the η_i are, as it is well known, Grassmann variables, if n is odd the integral (5.67) vanishes automatically. However, all the brane configurations that we usually consider in order to cancel the $D7$-charge are such that n is even.

5.5 Sub-leading corrections to the scalar potential

The Large Volume Scenario generically allows to stabilize few Kähler moduli[20], that is (some of) the small cycles and the total volume. The results of Sec. 3.3 can be easily generalized to the case of more than one 'diagonal' small cycle, which therefore are stabilized as well. In order to fix any other modulus, instead, one generically needs to include sub-leading corrections to the scalar potential. Since the CY space is compact, with a volume fixed in a previous step, the expectation is that the sub-leading corrections will not spoil the minimum. Moreover a promising candidate for a string theory inflationary model,

[19] Sometimes this might be even a desired feature, as in [127] .

[20] As we have seen in Sec. 5.4, conditions for generating non perturbative effects in W are very constraining.

called fibre inflation [153, 137, 146], is based precisely on the presence of one (or more) hierarchically lighter modulus which is stabilized at subleading order by the interplay of these perturbative corrections.

The known perturbative corrections (sub-leading with respect to the ones that we use in LVS) come from the exchange of closed strings winding non-contractible cycles, the exchange of Kaluza-Klein modes between non-intersecting D-branes/O-planes (g_s expansion) or higher derivatives terms (α' expansion). The explicit form of these corrections is only conjectured; however, over the years it has passed several low energy tests, hence it is considered to be robust enough.

Winding loop corrections

Whenever the model contains two intersecting divisors D_i and D_j ($D_i \cap D_j \neq 0$), wrapped by O-planes or D-branes, such that the intersection locus admits non-contractible one-cycles (that is $h^{1,0}(D_i \cup D_j) \neq 0$), there is an exchange of closed strings winding the non-contractible cycles. This produces a correction to the Kähler potential (recall that the superpotential cannot achieve any perturbative correction), which was exactly computed for the simple case of toroidal orientifolds [154]. The generalization to Calabi-Yau manifolds was conjectured in [155] (see also [137]) to be:

$$\delta K^W_{g_s} \sim \sum_i \frac{\mathcal{C}_i^W}{\mathcal{V}\, t_i^{\cap}} \,. \tag{5.68}$$

Here, the $\mathcal{C}_i^W$ are unknown functions of the (stabilized) complex structure moduli, hence at this stage we can consider them as unknown constants. The $t_i^{\cap}$ are the two-cycles where the branes/planes intersect:

$$t_i^{\cap} = \int_{X_3} J \wedge D_i \wedge D_j \,. \tag{5.69}$$

The correction $\delta K^W_{g_s}$ contributes to the scalar potential with

$$\delta V^W_{g_s} = -g_s \frac{W_0^2}{\mathcal{V}^2} \delta K^W_{g_s} = -g_s \frac{W_0^2}{\mathcal{V}^3} \sum_i \frac{\mathcal{C}_i^W}{t_i^{\cap}} \,, \tag{5.70}$$

where we are assuming $e^{K_{cs}} = 1$.

Kaluza-Klein corrections

Kaluza-Klein (KK) corrections are due to the exchange of KK modes between stacks of non-intersecting D-branes and/or O-planes. The (conjectured) term in the Kähler potential is, in this case [155, 137]:

$$\delta K^{KK}_{g_s} = g_s \sum_i \frac{\mathcal{C}_i^{KK} t_i^{\perp}}{\mathcal{V}} \,, \tag{5.71}$$

where the $\mathcal{C}_i^{KK}$ are again unknown constants, whose value depends on the stabilized complex structure moduli. The $t_i^{\perp}$ are, instead, the two-cycles transverse to the branes/planes, therefore they parametrize the distance between them.

In [156], the following statement, called *extended no-scale structure*, was proven (for a CY three-fold in a type IIB $\mathcal{N}=1$ SUGRA theory): given the Kähler potential $K = K_{tree} + \delta K$ and the superpotential $W = W_0$ (both in Einstein frame), if and only if the loop correction δK is a homogeneous function of degree $n=-2$ in the 2-cycles volumes, than at the leading order $\delta V_{g_s} = 0$.

From (5.71) it is clear that $\delta K_{g_s}^{KK}$ satisfies the hypothesis of the theorem (recall that $\mathcal{V} \sim t^3$), hence the exchange of KK modes contribute to the scalar potential at the next-to-the-leading order, with:

$$\delta V_{g_s}^{KK} = \frac{g_s^3}{2}\frac{W_0^2}{\mathcal{V}^2}\sum_{i,j}\mathcal{C}_i^{KK}\mathcal{C}_j^{KK}K_{ij}^0 \tag{5.72}$$

where K_{ij}^0 is the tree-level Kähler metric, derived from $K_0 = -2\ln\mathcal{V}$ and the indices $\{i,\,j\}$ run only over the cycles contributing to the summation in (5.71).

α'^3F^4 correction

This correction comes from the α' expansion. As we know, the first order α' contribution to the $10d$ type IIB action is at order $(\alpha')^3$. In particular, we already encountered the α'^3F^2 correction, which is the one ensuring the LVS Kähler moduli stabilization.

The subsequent term, which is of order α'^3F^4, was computed instead in [157] and it contributes to the scalar potential with

$$\delta V_{F^4} = -\frac{g_s^2}{4}\frac{\lambda\, W_0^4}{g_s^{3/2}\,\mathcal{V}^4}\sum_{i=1}^{h^{1,1}}\Pi_i t_i\,, \tag{5.73}$$

where the $\Pi_i = \int_{X_3} c_2\wedge\hat{D}_i \sim 10-100$ [21] are topological numbers, while λ is an unknown combinatorial factor expected to scale as $|\lambda| \sim \frac{\xi}{g_s^{3/2}\chi(X_3)} \sim 10^{-3}$. The sign of λ derives from the explicit 4d reduction of the 10d action at the considered order, which is not completely known. However, it was observed that only $\lambda < 1$ would produce a minimum for the scalar potential, hence usually people work under this assumption.

As was pointed out in [67], in order to be sure that this correction (depending on the potentially large W_0^4) is actually subleading, one should impose that it is much smaller than the value of the potential at the AdS minimum (3.54). This realizes in the constraint

$$\frac{4W_0^2 a_s}{3\kappa_s^{2/3}\xi^{1/3}\mathcal{V}^{2/3}}\mathcal{C} \ll 1\,, \tag{5.74}$$

where we have also used the expression for τ_s at the minimum (3.53c); $\mathcal{C}$ is an order one constant coming from the combination of the parameter λ and the topological numbers Π_i.

[21] In the following, we will refer to these topological invariants also as *2nd Chern numbers*.

Chapter 6

An explicit example of $\overline{D3}$ uplift in the Large Volume Scenario

This chapter is based on the paper [18] in which we studied a concrete realization of the $\overline{D3}$ uplifting mechanism analyzed in the previous sections[1].

The main motivation for this work is that the construction of consistent explicit models involves several non-trivial ingredients, like fluxes, throats, non-perturbative effects and branes. While each of these is allowed within type IIB string theory, putting all of them together in a single model where all the approximations are under control is very challenging and deserves an accurate analysis by means, as a start, of the simplest explicit construction admitting all of them.

In the first part, we analyze the general features of moduli stabilization for type IIB orientifold compactifications on CY threefolds with two Kähler moduli ($h^{1,1} = 2$) and a Klebanov-Strassler throat. In particular, we consider the three-moduli potential describing the conifold complex structure modulus Z and the two Kähler moduli. This turns out to be unnecessary, as the results do not deviate too much from the case in which the warped factor is assumed to be fixed.

Basing on these generic results, in the second part we construct an explicit model in which the uplift is obtained by introducing an $\overline{D3}$ on top of an $O3$ at the tip of a warped throat and all the moduli are stabilized in a dS vacuum. This turns out to be a not so easy task, given the large number of consistency requirements[2], often in tension one with the other, that we need to take into account. The example that is discussed here, satisfies all these conditions.

We dedicate particular attention to the bound discovered in [16] and reviewed here, in Sec. 4.4, according to which the flux number M along the throat must be such that $g_s M^2 \gtrsim 46.1$, in order to avoid a runaway in the scalar potential. However, we stress that this requirement turns out to be weaker than the one that we need to impose in order to

[1] Previous concrete examples of de Sitter uplift in type IIB orientifold compactifications have been obtained by means of different sources of uplift, such as T-branes, α'-corrections or D-term generated racetrack potential [28, 29, 41, 103, 158, 124, 135, 127], see also Sec. 4.5. For previous proposals to obtain dS space in string theory, see for instance [159, 118, 160, 161].

[2] See [162] for a classical analysis of consistency constraints in a different context.

have control over the Klebanov-Strassler approximation, that is $g_s|M| \gg 1$ [3].

The bound on M, as we already mentioned, corresponds to a lower bound in the D3-charge contribution MK coming from the fluxes along the throat. This means that a large negative charge (coming from O-planes and D-branes) is needed in order to satisfy the tadpole cancellation condition. This might be, in principle, a serious issue in type IIB compactifications. Nonetheless, we noticed that already the perturbative regime admits objects with large negative D3-charge, the Whitney brane, which might allow to cancel a large positive contribution coming from the fluxes.

6.1 The de Sitter LVS minima of the scalar potential

6.1.1 The scalar potential

We consider the minimal case of a CY threefold X_3 with $h^{1,1} = 2$ and a Swiss cheese form of the volume (3.51), because it is the simplest possible realization of antibrane uplift in LVS.

In this section we derive the scalar potential for the complex structure modulus Z and the Kähler moduli, in presence of a warped throat. The $\overline{D3}$ uplift term is obtained in the SUGRA theory, through the introduction of a nilpotent goldstino X, as explained in Sec. 4.2. The axio-dilaton is fixed ($S = \frac{1}{g_s}$) as well as all the complex structure moduli, except for the one parametrizing the throat.

In order to derive the scalar potential, let us start, as always, with the Kähler potential and the superpotential describing the supergravity theory. The Kähler potential is given by[4]:

$$K = -2\ln\left[\mathcal{V} + \frac{\xi}{g_s^{3/2}}\right] + \frac{c'\xi'|Z|^{\frac{2}{3}}}{\mathcal{V}^{2/3}} + \frac{X\bar{X}}{\mathcal{V}^{2/3}}\,, \tag{6.1}$$

where, as usual, $\xi = -\frac{\chi(X_3)\zeta(3)}{4(2\pi)^3}$, $c' \simeq 1.18$ and $\xi' = 9g_sM^2$. The effective superpotential is instead:

$$W = W_0 + A_s e^{-a_s T_s} - \frac{M}{2\pi i} Z(\log Z - 1) + i\frac{KZ}{g_s} + \frac{i|Z|^{\frac{2}{3}}}{g_s M}\sqrt{\frac{c''}{\pi}}X\,, \tag{6.2}$$

where W_0 is the vev of the tree-level superpotential for the complex structure moduli (but Z) and $c'' \simeq 1.75$. Moreover, since the model has two Kähler moduli and, for LVS to be consistent we expect $\tau_b \gg \tau_s$, we are considering only one non-perturbative effect.

Recalling that the goldstino is decoupled with respect to the other moduli (due to the fact that in the vacuum $\langle X\rangle = 0$), and using the approximation $\mathcal{V} \gg 1$, we obtain the

[3] The bound on M may be improved by making g_s larger (still within the limits of the perturbative regime). However, at the LVS minimum, g_s is related to the volume of the Calabi-Yau that for larger g_s tends to be not so large, eventually violating the supergravity approximation.

[4] Notice that in principle we should include in the Kähler potential also the axio-dilaton S, as we did in Sec. 3.3. However, in the large volume limit the result is the same, hence here we will consider it to be fixed at its stabilized value.

sugra scalar potential:

$$\begin{aligned} V_{\rm tot} =& \frac{8a_s^2A_s^2g_s\sqrt{\tau_s}e^{-2a_s\tau_s}}{3\kappa_s\mathcal{V}} + \frac{4a_sA_sg_s\tau_se^{-a_s\tau_s}}{\mathcal{V}^2}\left[W_0\cos(a_s\theta_s+\varphi)+\zeta\frac{M}{2\pi}\sin(a_s\theta_s+\sigma)\right] \\ &+\frac{3\xi}{2\sqrt{g_s}\mathcal{V}^3}\left[W_0^2-16\zeta^2\left(\frac{M}{2\pi}\log\zeta+\frac{K}{g_s}\right)^2+\frac{M^2\zeta^2}{\pi^2}\left(\frac{1}{4}+\frac{2\pi K}{Mg_s}-4\sigma^2+\log\zeta\right)\right. \\ &\left.+2\frac{M}{\pi}W_0\zeta\sigma\cos(\sigma-\varphi)+W_0\zeta\sin(\sigma-\varphi)\left(\frac{M}{\pi}+2\frac{M}{\pi}\log\zeta+\frac{4K}{g_s}\right)\right] \\ &+\frac{\zeta^{4/3}}{c'M^2\mathcal{V}^{4/3}}\left[\frac{c'c''}{\pi g_s}+\frac{M^2\sigma^2}{4\pi^2}+\left(\frac{M}{2\pi}\log\zeta+\frac{K}{g_s}\right)^2\right], \end{aligned} \tag{6.3}$$

where $Z\equiv\zeta e^{i\sigma}$ and, with abuse of notation, we have replaced $W_0\to W_0e^{i\varphi}$, so that now W_0 is real and positive and φ is the phase (not to be confused with the dilaton ϕ) of the complex W_0 appearing in (6.2).

6.1.2 De Sitter minima of the potential

The potential (6.3), is quite difficult to analyze explicitly. However some simple considerations allow to considerably simplify it, by means of some reasonable approximation. First of all, we recall that the strongly warped regime, in which we are working, is characterized by $\zeta\ll 1$. Hence Eq. (6.3) contains at least two small parameters[5], $\frac{1}{\mathcal{V}}$ (we are in the LVS regime $\mathcal{V}\gg 1$) and ζ, which we would like to relate one to the other. This can be easily done, by noticing that, as in the standard LVS, a small cosmological constant is obtained when the uplifting term (reported in the last line of (6.3) and of order $V_{\rm up}\sim\frac{\zeta^{4/3}}{\mathcal{V}^{4/3}}$) compensates the AdS energy at the minimum $V_{AdS}\sim\frac{W_0^2}{\mathcal{V}^3}$. We conclude that we need to work in the approximation:

$$\zeta^{4/3}\sim\frac{W_0^2}{\mathcal{V}^{5/3}} \tag{6.4}$$

which, for $\mathcal{V}\gg 1$, is also consistent with the requirement $\zeta\ll 1$. Under this assumption, the scalar potential (6.3) simply becomes[6]:

$$\begin{aligned} V_{\rm tot}\simeq& \frac{8a_s^2A_s^2g_s\sqrt{\tau_s}e^{-2a_s\tau_s}}{3\kappa_s\mathcal{V}}+\frac{4a_sA_sg_s\tau_se^{-a_s\tau_s}W_0}{\mathcal{V}^2}\cos(a_s\theta_s+\varphi) \\ &+\frac{3\xi}{2\sqrt{g_s}\mathcal{V}^3}W_0^2+\frac{\zeta^{4/3}}{c'M^2\mathcal{V}^{4/3}}\left[\frac{c'c''}{\pi g_s}+\frac{M^2\sigma^2}{4\pi^2}+\left(\frac{M}{2\pi}\log\zeta+\frac{K}{g_s}\right)^2\right]. \end{aligned} \tag{6.5}$$

Let us now analyze the new potential. To start with, we notice that the first derivatives of $V_{\rm tot}$ with respect to θ_s and σ vanish for $\theta_{s_0}=\frac{\pi-\varphi}{a_s}$ and $\sigma_0=0$ and that

$$\frac{\partial^2V_{\rm tot}}{\partial x_i\partial y_j}|_{\sigma_0,\theta_{s_0}}=0\,,$$

[5] Though small enough to admit a consistent perturbative expansion, the string coupling g_s is usually larger than $\frac{1}{\mathcal{V}}$ and ζ.

[6] With respect to the expressions in Sec. 3.3 we have absorbed a factor of 2 in the complex structure term of the scalar potential: $\frac{e^{K_{cs}}}{2}\to e^{K_{cs}}$ (with $e^{K_{cs}}$ itself included in the definition of W_0 and A_s).

where $x_i = \{\theta_s, \sigma\}$ and $y_i = \{\tau_s, \tau_b, \zeta\}$. Hence, we can conclude that these moduli are decoupled from ζ, τ_b, τ_s and that they can be stabilized at θ_{s_0} and σ_0 [7].

Fixing $\theta_s = \theta_{s_0}$ and $\sigma = \sigma_0$ in $V_{\rm tot}$ we get:

$$\begin{aligned} V &= \frac{8a_s^2 A_s^2 g_s \sqrt{\tau_s} e^{-2a_s\tau_s}}{3\kappa_s \mathcal{V}} - \frac{4a_s A_s g_s \tau_s W_0 e^{-a_s\tau_s}}{\mathcal{V}^2} + \frac{3W_0^2 \xi}{2\sqrt{g_s}\mathcal{V}^3} \\ &+ \frac{\zeta^{4/3}}{c' M^2 \mathcal{V}^{4/3}} \left[\frac{c'c''}{\pi g_s} + \left(\frac{M}{2\pi} \log\zeta + \frac{K}{g_s} \right)^2 \right] , \end{aligned}$$

where the usual LVS (plus an uplift) structure is now manifest.

From the analysis of the derivatives of (6.6) and considering $\mathcal{V} \simeq \tau_b^{3/2}$, we derive the values of the remaining moduli at the minimum:

$$\partial_\zeta V = 0 \Leftrightarrow \zeta = e^{-\frac{2\pi K}{g_s M} - \frac{3}{4} + \sqrt{\frac{9}{16} - \frac{4\pi}{g_s M^2} c'c''}} , \tag{6.6a}$$

$$\partial_{\tau_s} V = 0 \Leftrightarrow \tau_b^{3/2} = \frac{3e^{a_s\tau_s} W_0 \kappa_s \sqrt{\tau_s}}{a_s A_s} \frac{(1 - a_s\tau_s)}{(1 - 4a_s\tau_s)} , \tag{6.6b}$$

$$\partial_{\tau_b} V = 0 \Leftrightarrow \tau_s^{3/2} \frac{16 a_s\tau_s (a_s\tau_s - 1)}{(1 - 4a_s\tau_s)^2} = \frac{\xi}{g_s^{3/2}\kappa_s} + \frac{8\, q_0 \zeta^{4/3}\, \tau_b^{5/2}}{27 g_s \kappa_s W_0^2} , \tag{6.6c}$$

where

$$q_0 \equiv \frac{3}{8\pi^2 c'} \left(\frac{3}{4} - \sqrt{\frac{9}{16} - \frac{4\pi c'c''}{g_s M^2}} \right) \tag{6.7}$$

and the relations (6.6a) and (6.6b) were used in (6.6c).

The fact that $a_s\tau_s \gg 1$ (which is also needed in order to have a large volume, as it is clear from (6.6b)) allows to further approximate the equations (6.6a)-(6.6c):

$$\zeta = e^{-\frac{2\pi K}{g_s M} - \frac{3}{4} + \sqrt{\frac{9}{16} - \frac{4\pi}{g_s M^2} c'c''}} , \tag{6.8a}$$

$$\tau_b^{3/2} \simeq \frac{3W_0 \kappa_s \sqrt{\tau_s}}{4a_s A_s} e^{a_s\tau_s} , \tag{6.8b}$$

$$\tau_s^{3/2} \simeq \frac{\xi}{g_s^{3/2}\kappa_s} + \frac{8\rho\, \tau_b^{5/2}}{27 g_s \kappa_s W_0^2} , \tag{6.8c}$$

where we have also defined $\rho \equiv q_0 \zeta^{4/3}$. For later convenience, it is useful to notice that ρ depends only on the background fluxes M, K and g_s (once we substitute ζ with the expression (6.8a)):

$$\rho \equiv q_o' e^{-\frac{8\pi K}{3 g_s M}} \quad \text{with} \quad q_0' \equiv q_0 e^{-\frac{32\pi^2 c'}{9} q_0} . \tag{6.9}$$

In particular, q_0' does not depend on the flux number K.

[7] In the end we will check that they actually correspond to a minimum, by analyzing the second derivatives $\frac{\partial^2 V_{tot}}{\partial x_i \partial x_j}|_{\sigma_0, \theta_{s_0}}$.

The expression (6.8a) obtained for ζ at the minimum is consistent with the results of [16, 17, 162], according to which ζ is shifted with respect to the KS vacuum (3.30), due to the introduction of the uplifting term. However, as we already observed in Sec. 4.4, the shift is numerically irrelevant, as it scales ζ at worst by a factor close to 1, hence the only important reason why one should include this correction is that it imposes the additional constraint (4.15) [16]. On the other side, we observe that the equations (6.6b)-(6.6c) agree with the ones derived in [45], where the value of ζ was assumed to be fixed at higher scales at the KS solution (3.30). We can therefore conclude that even if the mass of the modulus Z is small, its stabilization is still decoupled from the stabilization of the Kähler moduli.

Finally, the potential at the minimum is:

$$V_{min} = \frac{5q_0\zeta^{4/3}}{9\tau_b^2} - \frac{12W_0^2 g_s\kappa_s\tau_s^{3/2}}{\tau_b^{9/2}}\frac{(a_s\tau_s-1)}{(1-4a_s\tau_s)^2} \simeq \frac{5\rho}{9\tau_b^2} - \frac{3W_0^2 g_s\kappa_s\tau_s^{1/2}}{4a_s\,\tau_b^{9/2}}\,, \tag{6.10}$$

where the second term is obtained in the limit $a_s\tau_s \gg 1$. As expected, in the limit (6.4) under consideration the vacuum is approximately Minkowski: depending on the exact value of ρ, it can be AdS, Minkowski or dS.

6.2 Moduli masses

The masses for the moduli at the minimum are computed, as usual, by looking at the eigenvalues of the matrix $M = K^{-1}\partial^2 V$, where $\partial^2 V$ is the Hessian of the scalar potential and K^{-1} is the inverse of the Kähler metric of the scalar fields space. The characteristic polynomial of the 3×3 matrix relative to the three moduli τ_b, τ_s, ζ is a third degree polynomial of the form $-\lambda^3+b\lambda^2+c\lambda+d=0$, where at the leading order of our approximation (in particular $a_s\tau_s \gg 1$) we have:

$$b = tr(M) \simeq A+B, \quad c = -\frac{1}{2}\left(tr(M)^2 - tr(M^2)\right) \simeq -AB, \quad d = det(M) \simeq ABC \tag{6.11}$$

with:

$$A \equiv \frac{\zeta^{2/3}}{6\pi^2 c'^2 g_s M^2\tau_b}\sqrt{\frac{9}{16} - \frac{4\pi c' c''}{g_s M^2}} \ll 1\,, \tag{6.12}$$

$$B \equiv \frac{2g_s W_0^2 a_s^2\tau_s^2}{\tau_b^3} \ll 1\,, \tag{6.13}$$

$$C \equiv \frac{5}{3\tau_b^2}\left(\frac{9}{4}\frac{27 g_s W_0^2\kappa_s\tau_s^{1/2}}{20\,a_s\tau_b^{5/2}} - \rho\right) \ll 1\,. \tag{6.14}$$

From these expressions, we notice that $b \gg c \gg d$ and, in particular, $C \ll A, B$, which implies $\frac{d}{bc} \ll 1$. The cubic equation can therefore be solved perturbatively and the result is:

$$m_1^2 \simeq b = A+B\,, \qquad m_2^2 \simeq -\frac{c}{b} = \frac{A\,B}{A+B}\,, \qquad m_3^2 \simeq -\frac{d}{c} = C\,. \tag{6.15}$$

We conclude this section with two important observations regarding this result:

- In the limit $B \gg A$, which is realized by typical values of the parameters, $m_1^2 \simeq B = m_{\tau_s}^2$ (cfr. Eq. (3.57) in the limit $a_s\tau_s \gg 1$). In the same limit, $m_2^2 \simeq A$.
- m_3^2 is much smaller than the other two masses and, remarkably, it is not necessarily positive. The requirement of having positive masses, therefore, constrains the possible values of the parameters when we look for a concrete realization of this model.

6.2.1 Bounds on the warp factor

When we keep the parameters $\{W_0, A_s, \kappa_s, a_s, g_s\}$ fixed, the value of ρ depends on the choice of the fluxes M, K. The following argument shows in particular, that once the other parameters have been fixed, one can obtain a de Sitter minimum only for a limited range of values of ρ.

Solving the equation $V_{\rm min} = 0$ (with V_{min} defined in (6.10)), we can find the expression for ρ at a Minkowski vacuum:

$$\rho_{\rm low} \simeq \frac{27 g_s W_0^2 \kappa_s \tau_s^{1/2}}{20\, a_s \tau_b^{5/2}}\,, \tag{6.16}$$

where τ_s and τ_b are functions of the parameters $\{W_0, A_s, \kappa_s, a_s, g_s\}$, determined by solving the equations (6.6a)-(6.6c). This means that a de Sitter minimum is characterized by $\rho > \rho_{\rm low}$: the larger is ρ, the larger is the value of the scalar potential at the minimum.

However, we can increase the value of ρ only as far as m_3^2 in (6.15) is positive, that is up to an upper value $\rho_{\rm up}$ above which a solution of (6.6a)-(6.6c) is not a minimum of the scalar potential anymore. The value of ρ corresponding to $m_3^2 = 0$ is:

$$\rho_{\rm up} \simeq \frac{9}{4}\,\frac{27 g_s W_0^2 \kappa_s \tau_s^{1/2}}{20\, a_s \tau_b^{5/2}}\,. \tag{6.17}$$

We conclude that the order of magnitude of admissible ρ, hence of the warp factor, is fixed by the other parameters $\{W_0, A_s, \kappa_s, a_s, g_s\}$. In particular, on a dS minimum we find

$$\rho \simeq \alpha\,\frac{27 g_s W_0^2 \kappa_s \tau_s^{1/2}}{20\, a_s \tau_b^{5/2}}\,, \tag{6.18}$$

where α is a number in $]1, \frac{9}{4}[$.

Using this fact, we can rewrite the equation (6.8c) as

$$\tau_s^{3/2} \simeq \frac{\xi}{g_s^{3/2}\kappa_s} + \frac{2\alpha\,\tau_s^{1/2}}{5 a_s}\,. \tag{6.19}$$

Solving the cubic equation in $\tau_s^{1/2}$ we realize that τ_s is shifted with respect to the LVS minimum ($\tau_s \simeq \frac{\xi^{2/3}}{g_s \kappa_s^{2/3}}$) by the small quantity $\delta\tau_s = \frac{4\alpha}{15 a_s} \lesssim 1$. This small shift affects the exponentially large τ_b by a factor of $\mathcal{O}(1)$, hence the uplift term in the potential modifies the relations determining the AdS LVS minimum only at subleading order.

6.3 Consistency conditions and limits on the $\overline{D3}$ tadpole

The equations (6.6a)-(6.6c) are valid only in certain regions of the moduli space (τ_b, τ_s, ζ) and of the parameter space $(W_0, g_s, a_s, A_s, M, K, \chi(X))$, inside which all the approximations that we are considering can be trusted. In this section we collect and summarize the requirements that define these regions of validity, specifying the ones that are automatically satisfied in the cases of interest for us.

Among these constraints the ones regarding the tadpole, as we said several times, have a particular relevance. More specifically, in section 6.3.2 we analyze what is the minimal value of MK that is allowed. We will see that this number is typically large, even larger than what expected by the no-runaway condition of [16, 17].

6.3.1 Constraints

- Since we aim at a de Sitter vacuum, the potential at the minimum must be positive and with a very small vacuum energy:

$$V_{min} \gtrsim 0 \,. \tag{6.20}$$

  This produces the lower bound on ρ, discussed in the previous section.

- The minimum of the scalar potential should be found in a regime where one keeps control over the EFT. This translates into different constraints.

  First, the minimum should be located in a region with a large volume, so that the α' expansion is trustworthy[8]:

$$\mathcal{V}_E \gg \frac{\xi}{g_s^{3/2}} \gg 1 \quad \Longleftrightarrow \quad \tau_b \gg \tau_s \,. \tag{6.21}$$

  Having a large volume is also an advantage in terms of the stability of the (metastable) vacuum, whose probability to decay towards the 10d decompactification vacuum ($\mathcal{V} \to \infty$) was estimated in $P_{dec}/P_{dS} = e^{-\mathcal{V}^2}$ [63]. However, the volume cannot be arbitrarily large due to the fact that all the relevant energy scales would become too small with respect to phenomenological expectations (see App. A for the dependence of these scales on $\mathcal{V}$) [163].

  Secondly, multi-instanton effects can be consistently neglected in the non-perturbative corrections only if $a_s \tau_s \gg 1$. In addition to this, the supergravity approximation requires each 4-cycle to be stabilized with a large volume, that is[9]:

$$\tau_s \gg 1 \,. \tag{6.22}$$

[8] The authors of [13] pointed out that the large volume constraint should be actually imposed on the string frame volume ($\mathcal{V}_s = \mathcal{V}_E g_s^{3/2}$) instead of the Einstein frame one, in which we are working.

[9] Notice that a similar requirement can be imposed also to the volumes of the two-cycles t_i (expressed in units of the string length $l_s = 2\pi\sqrt{\alpha'}$ and in Einstein frame), which have to be much larger than the string scale: $|t_i| \gg \frac{1}{g_s^{1/2}(2\pi)^2}$, $\forall i = 1, ..., h^{1,1}$ [61]. This will be useful in Ch. 8, where the analysis of the scalar potential is performed in terms of the t^i instead of the τ_i.

The two conditions are essentially equivalent in our case, in which $a_s \gtrsim 1$.

Finally, a weak string coupling $g_s \ll 1$ is required in order to ensure that string loop corrections like the ones presented in Sec. 5.5 are actually sub-leading, which means that the perturbative string expansion is under control. In the minima of the potential this condition automatically ensures that both (6.21) and (6.22) are satisfied.

- The Kähler moduli need to be stabilized inside the Kähler cone (Sec. 5.2).

  Since for the class of models we are considering the Kähler cone conditions simply read $\tau_b > \tau_s$, this requirement is automatically satisfied in the region defined by (6.21).

- The low-energy SUGRA provides a valid 4d description only if the following hierarchy holds [61]:

$$M_p \gg 2\pi M_s \gtrsim M_{\rm KK}^{(i)} \gg m_{\rm moduli}\,, m_{3/2}\,. \tag{6.23}$$

  The mass scales are defined in App. A [10], where we also point out that the fact that we are in a large volume region implies that $M_p \gg 2\pi M_s \gtrsim M_{\rm KK}^{(i)}$ is automatically satisfied.

  The requirement $M_{KK}^{bulk} \gg m_{3/2}$ imposes instead an additional constraint [61, 165], in the form[11]:

$$\sqrt{\frac{g_s}{2\pi}} W_0 \ll \mathcal{V}^{1/3}\,, \tag{6.24}$$

  which puts an upper bound on W_0.

- Our uplifting mechanism relies on the presence of a highly warped throat, i.e.

$$\mathcal{V}^{2/3}\rho \ll 1\,, \tag{6.25}$$

  with $\rho = q_0\,\zeta^{4/3}$, evaluated at the minimum of the potential.

  Moreover we need to take into account the fact that in the large volume limit, the massive string states of the $\overline{D3}$-brane at the tip of the throat are redshifted to lower masses by the factor $\Omega = \mathcal{V}^{1/6}\rho^{1/4}$ and could be lighter than $m_{3/2} \sim \frac{1}{\mathcal{V}}$, invalidating the use of a low-energy effective field theory that neglect these states. In order to avoid this, we need to require [45, 164]:

$$M_s^w \sim 2\pi\,\Omega\,M_s \sim \frac{g_s^{1/4}\pi^{1/2}\rho^{1/4}}{\mathcal{V}^{1/3}} \gg m_{3/2}\,,$$

  hence

$$\rho^{1/4}\mathcal{V}^{2/3} \gg \frac{g_s^{1/4}W_0}{\sqrt{2\pi}} \sim 1 \tag{6.26}$$

  in Einstein frame.

[10] Notice that our definition for M_s differs of a factor of 2π with respect to the one of [61] and [164].

[11] We are, as usual, neglecting the factor $e^{K_{cs}}$. Moreover, our W_0 is rescaled by a factor of $\sqrt{4\pi}$ with respect to what is found in [61].

These two conditions are always satisfied at the dS minima of the potential. This is clear from using the equations (6.8a)-(6.8c) and taking the expression (6.18) of ρ at the minimum.

- The KS solution for the warped metric is trustworthy only if the size of the S^3 at the tip of the conifold stays larger than the string length (see also Sec. 3.1.3). From the warped KS metric, the radius of the S^3 reads [17]: $R^2_{S^3} \sim \alpha' g_s |M|$, which means that the gravitational KS solution is trustworthy only in the limit

$$g_s |M| \gg 1 \,. \tag{6.27}$$

  For fixed (small) g_s, this puts a lower bound on the flux M, which appears in the warp factor. Furthermore if M is large, K is expected to be large as well. Indeed, in order to generate a ρ in the (small) range individuated by (6.18), we need the exponent in (6.9) to be not too small. The conclusion of this argument is that the flux contribution to the $D3$-charge may be very large and hence difficult to cancel.

- In order to avoid runaways in the moduli space [16, 17] we need:

$$g_s M^2 \gtrsim 46.1$$

  (see also Sec. 4.4). As we will see better in the following, however, this constraint is typically weaker than (6.27), so that fluxes satisfying that condition are not expected to show any runaway.

- Finally, as pointed out in [48, 113], the Z field in the KS solution is assumed to be fixed to its supersymmetric value, hence it is not a modulus. As a consequence we can consistently consider an off-shell Z-dependence of the warp factor only if the stabilized value of Z does not deviate much from the flux stabilized value (3.30). For the models under consideration this condition is always fulfilled as ζ in (6.6a) differs from the KS value (3.30) by a factor of order one (as it can be checked in our explicit model in Sec. 6.4).

6.3.2 Bounds on the flux $D3$-charge

The constraints of the previous section can be summarized as follows. To be consistent with all the approximations, the parameters of a model showing a de Sitter minimum, that is satisfying (6.6a)-(6.6c) and (6.18), must fulfill the following three conditions:

(1) $g_s \ll 1$ such that $\mathcal{V} \gtrsim 10^4$;

(2) $\sqrt{\frac{g_s}{2\pi}} W_0 \ll \mathcal{V}^{1/3}$ (we will take $\mathcal{O}(10)$ as limiting ratio);

(3) $g_s |M| \gg 1$ (we will take $g_s |M| \gtrsim 5$ [12]).

[12] We assume that this is enough for the analysis of [90] on the $\overline{D3}$ stability to hold. In particular, with this constraint one always finds $M > 15$ in the perturbative regime.

These conditions, as we will show, put a *large* lower bound for the flux $D3$-charge (see also [59]). Even if we claim that the situation is not as bad as suggested in [16], it is important to stress that the uplift mechanism we are considering needs to be taken carefully, at least if we want to use the KS approximation. A large positive $D3$-charge, indeed, is typically difficult to cancel in perturbative type IIB string theory, where the negative contribution to the $D3$-charge is only due to the orientifold properties of the compact space and to the D-brane configuration.

From condition (3) we notice that larger values of g_s (though still satisfying condition (1)) are preferable in order to minimize the flux $D3$-charge. However, for a fixed volume $\mathcal{V}$, the maximal value of g_s strongly depends on the Euler characteristic $\chi(X_3)$ of the CY threefold, on the parameter κ_s and on a_s, as we can observe substituting $\tau_s \sim \frac{\xi^{2/3}}{g_s \kappa_s^{2/3}}$ (see Eq. (6.19)) into (6.8b):

$$\mathcal{V} \sim \frac{3W_0 \kappa_s^{2/3} \xi^{1/3}}{4 a_s A_s \sqrt{g_s}} e^{a_s \xi^{2/3}/g_s \kappa_s^{2/3}} \,. \tag{6.28}$$

From (6.28) we notice that the value of g_s can be increased also by making W_0 larger. However, condition (2) constrains the possible choices of W_0.

Once the values of the parameters $\{\chi, \kappa_s, a_s, g_s, W_0\}$ are fixed, in order to minimize the $D3$-charge MK, one has to take M close to the bound defined by condition (3). Since the warp factor ρ, defined in (6.9), can only vary in the small range corresponding to $1 \leq \alpha < \frac{9}{4}$ (see Eq. (6.18)), for a fixed M, K can take only few values. In practice, we will typically select the maximum g_s admitted by condition (1); then we will choose the lowest M compatible with (3), while we will fix K to the smallest value allowing ρ to be inside the prescribed range.

There is a caveat: a model with a_s and $\chi(X_3)$ large or κ_s small, might produce a very large $\mathcal{V}$ even if g_s is fixed at the largest value compatible with perturbation theory. This is only apparently good: indeed, even neglecting the possible phenomenological issues mentioned in the previous section, a very large volume corresponds to a very small ρ (see equation (6.18)), which is in turn characterized by a large ratio $\frac{K}{g_s M}$ (see equation (6.8a)). This implies a large K, even for a not so big $g_s M$, which eventually leads to a large $D3$-charge MK.

In general, we noticed that the values of the parameters that minimize the tadpole MK are typically at the boundary of our consistency conditions. In order to strengthen these considerations, we made a rough scan over models with fixed $\chi(X_3)$, a_s and κ_s, by varying the parameters g_s, W_0, K, M (and keeping $A_s = 1$) and selecting the cases that minimize the $D3$-charge MK, though satisfying conditions (1)-(3). Our strategy can be summarized by the following steps:

1. We select a geometry X_3 (with Euler characteristic $\chi(X_3)$). This essentially fixes also κ_s (determined by the intersection numbers) and a_s. The reason why a_s is fixed is that typically there are only few possible non-perturbative divisors and the choice of the involution determines whether a given divisor will support gaugino condensation (if it is wrapped by an $O7$-plane) or $E3$-instantons.

While we leave a complete scan over the CY's parameters $\chi(X_3), a_s, \kappa_s$ for a future work, we report here the results obtained for a few different values of these parameters, in order to have an idea of the generic behavior of these models.

2. We scan over values of $W_0 \in [1, 30]$ (with step 1) and $g_s \in [0.01, 0.33]$ (with step 0.001).

3. Having fixed W_0 and g_s, we compute the lower ρ_{low} (6.16) and upper ρ_{up} (6.17) bounds for the warped factor ρ, ensuring that condition (2) is satisfied.

4. Scanning over integer values of M and K, we select the ones that are such that $\rho \in [\rho_{\text{low}}, \rho_{\text{up}}]$, where ρ is defined in (6.9), and condition (3) is fulfilled. Among these, we choose the couple with the minimum value of MK.

The following tabular contains the results for the case in which the non-perturbative superpotential is generated by gaugino condensation ($a_s = \frac{\pi}{3}$)[13]. For each given MK we report also the values of g_s and W_0 producing it[14].

$(MK)_{\{g_s,W_0\}}$		$-\chi(X)$				
		50	100	150	200	250
κ_s	$\frac{\sqrt{2}}{9} \simeq 0.16$	$260_{\{0.077,13\}}$	$230_{\{0.11,5\}}$	$175_{\{0.144,5\}}$	$145_{\{0.174,5\}}$	$125_{\{0.202,5\}}$
	$\frac{\sqrt{2}}{3\sqrt{3}} \simeq 0.27$	$360_{\{0.056,12\}}$	$320_{\{0.079,4\}}$	$245_{\{0.103,5\}}$	$200_{\{0.126,5\}}$	$175_{\{0.144,5\}}$
	$\frac{\sqrt{2}}{3} \simeq 0.47$	$504_{\{0.04,7\}}$	$316_{\{0.064,9\}}$	$340_{\{0.074,4\}}$	$280_{\{0.09,4\}}$	$240_{\{0.105,4\}}$

From this tabular we can deduce a general trend, according to which larger values of $|\chi(X_3)|$ and smaller values of κ_s are expected to provide smaller values of $(MK)_{\text{low}}$. Indeed these values allow for larger g_s at fixed volume.

The analogous analysis performed at $a_s = 2\pi$ is reported in the following table:

$(MK)_{\{g_s,W_0\}}$		$-\chi(X)$				
		50	100	150	200	250
κ_s	$\frac{\sqrt{2}}{9} \simeq 0.16$	$119_{\{0.301,7\}}$	$208_{\{0.323,1\}}$	$288_{\{0.331,2\}}$	$368_{\{0.321,1\}}$	$432_{\{0.332,2\}}$
	$\frac{\sqrt{2}}{3\sqrt{3}} \simeq 0.27$	$132_{\{0.237,8\}}$	$128_{\{0.313,2\}}$	$176_{\{0.333,11\}}$	$240_{\{0.318,1\}}$	$288_{\{0.318,1\}}$
	$\frac{\sqrt{2}}{3} \simeq 0.47$	$140_{\{0.183,11\}}$	$90_{\{0.292,12\}}$	$112_{\{0.316,3\}}$	$144_{\{0.33,4\}}$	$176_{\{0.333,5\}}$

From this results we notice that for $\chi(X_3) \gtrsim 150$ and/or $\kappa_s \lesssim 0.2$, the caveat introduced above applies, that is the volume is too large to allow for a small tadpole MK. We conclude, therefore, that despite what one might naively expect, having a non-perturbative effect generated by an $E3$-instanton is not necessarily to be preferred in order to get a small positive $D3$-charge.

[13] With respect to [18], here we made a different choice of the values of $\chi(X_3)$ and κ_s, which takes into account the actual range of possible values of the Euler characteristics for geometries with $h^{1,1} = 2$ (according to the Ross Altman's database [106]) and the possible values of κ_s. In particular, for a dP_n we have $\kappa_s = \frac{\sqrt{2}}{3\sqrt{9-n}}$. We thank Pramod Shukla for useful discussions on this point.

[14] We stress that the same tadpole might be obtained by different choices of these parameters. Since here we are mainly interested in the amount of the $D3$-charge, we simply report the values of g_s and W_0 corresponding to the first appearance of $(MK)_{\text{min}}$ in our scan.

We finally observe that the values we obtain are smaller than the recent lower bound $MK \gtrsim 500$ found in [16]. In that case, indeed, a very small warp factor was required for KKLT to preserve the stability of the vacua after the uplift. In the LVS vacua analyzed in this paper, instead, the stability has been taken into account by considering ρ as in (6.18). Hence, we claim that for LVS the bound is a bit smaller: we typically find $MK \gtrsim 100$.

6.4 An explicit model with $\overline{D3}$-branes uplift

In this section, we present an explicit model. We choose a CY threefold that is a hypersurface in a toric variety, and an orientifold involution with $O3$-planes that collapse to each other by taking the conifold limit. This, as we explained in the previous chapters, reproduces a situation with a warped throat modeled on a deformed conifold and represents the simplest possible realization of uplift via a nilpotent goldstino [102].

We will show that this model admits a dS minimum that satisfies the conditions (1)-(3) of section 6.3.2.

6.4.1 Geometric setup

We consider the toric ambient space characterized by the following weights and SR-ideal[15]:

	z	u_1	u_2	v	w	ξ	$D_{\rm H}$
$\mathbb{C}^*_1$	0	1	1	2	3	7	14
$\mathbb{C}^*_2$	1	0	0	0	1	2	4

, $\qquad\qquad \mathrm{SR} = \{z\,w,\, u_1\,u_2\,v\}\,. \qquad (6.29)$

This space contains, as we explained, a hypersurface which is a CY threefold X_3. It is defined by an equation whose degrees are reported in the last column of the GLSM matrix in (6.29) and it corresponds to the geometry obtained from (any of the two triangulations of) the polytope ID#39 of the database [107]. The Hodge numbers are $h^{1,1} = 2$ and $h^{1,2} = 132$, while the Euler characteristic is $\chi(X) = -260$.

As concerns the topology of the divisors (which we analyzed via `CohomCalg`), D_z is a diagonal dP_0 (hence it can support non-perturbative effects), while D_{u_1} and D_{u_2} have the Hodge numbers of a K3 but they are not K3s, since they have $\int_{X_3} D^2_{u_{1,2}} D_{z,w} = 1$ and $\int_{X_3} D^2_{u_{1,2}} D_\xi = 2$ (see Sec. 5.1.1). The remaining ones are deformation divisors with Hodge diamonds:

$$D_v:\begin{array}{ccccc} & & 1 & & \\ & 0 & & 0 & \\ 3 & & 40 & & 3 \\ & 0 & & 0 & \\ & & 1 & & \end{array}\;;\qquad D_w:\begin{array}{ccccc} & & 1 & & \\ & 0 & & 0 & \\ 6 & & 61 & & 6 \\ & 0 & & 0 & \\ & & 1 & & \end{array}\;;\qquad D_\xi:\begin{array}{ccccc} & & 1 & & \\ & 0 & & 0 & \\ 31 & & 206 & & 31 \\ & 0 & & 0 & \\ & & 1 & & \end{array}\;. \qquad (6.30)$$

[15] We present the SR ideal in its most generic form. The coordinate ξ, indeed, can be equivalently placed in the first or in the second element of the ideal. The two cases correspond to two triangulations producing the same ambient space. For the description of the toric variety and of the corresponding CY hypersurface, in terms of the weights matrix see Sec. 5.1.

An integral basis of $H^2(X,\mathbb{Z})$ is composed by the divisor classes D_z (with representative $\{z=0\}$) and D_u (with representative $\{a_1u_1+a_2u_2=0\}$ for arbitrary $a_1,a_2\in\mathbb{C}$), where we are using the same symbol for the 4-cycles and the Poincaré dual 2-forms. In terms of this basis, the intersection form of the Calabi-Yau reads:

$$I_3 = 9D_z^3 - 3D_z^2D_u + D_zD_u^2 \tag{6.31}$$

and the second Chern class is:

$$c_2(X) = 66D_u^2 - 8D_z^2\,. \tag{6.32}$$

For our purposes, however, it will be useful to consider as a basis of $H_4(X)$ also the non-integral[16] basis $\{D_w, D_z\}$, in which the intersection polynomial takes the simple form:

$$I_3 = 9D_w^3 + 9D_z^3\,. \tag{6.33}$$

The volume of the CY can be computed starting from the Kähler form J, expanded on this last basis:

$$J = t_wD_w + t_zD_z\,, \tag{6.34}$$

which allows to express the volumes of the divisors D_w and D_z as:

$$\tau_w = \frac{1}{2}\int_{D_w} J^2 = \frac{9}{2}t_w^2\,, \qquad\qquad \tau_z = \frac{1}{2}\int_{D_z} J^2 = \frac{9}{2}t_z^2\,. \tag{6.35}$$

The volume $\mathcal{V}$ takes therefore the Swiss cheese form (3.51):

$$\mathcal{V} = \frac{1}{6}\int_X J^3 = \frac{3}{2}\left(t_w^3+t_z^3\right) = \frac{\sqrt{2}}{9}\left(\tau_w^{3/2}-\tau_z^{3/2}\right)\,. \tag{6.36}$$

We then identify $\tau_b = \frac{1}{3}\left(\frac{2}{3}\right)^{1/3}\tau_w$, $\tau_s=\tau_z$ and $\kappa_s=\frac{\sqrt{2}}{9}$ and we notice that, as expected, the del Pezzo divisor appears as the 'small' cycle in the volume, that is the one which will support non-perturbative effects.

6.4.2 Involution

We consider the involution[17]

$$\sigma: \qquad w\mapsto -w\,. \tag{6.37}$$

The CY equation (computed from the polytope data using (5.3)) must be restricted to be invariant under this involution, that is only monomials with even powers of w can appear.

[16] A non-integral basis generates the integral divisors by rational linear combinations.

[17] Notice that from the point of view of tadpole cancellation, the most advantageous choice would be the involution of the coordinate with the largest weights, that is ξ. From the corresponding Hodge diamond in (6.30), indeed, we can deduce that this is the divisor with the largest Euler characteristic, from which the $D3$-charge contributions of both the $O7$-planes and the D-branes depend. However, we generically observe (and confirm in this explicit model) that the coordinate with largest weights never contains $O3$-planes that come on top of each other after an appropriate complex structure deformation.

In particular, reabsorbing the linear term in ξ by a redefinition of ξ itself, the defining equation turns out to be:

$$\begin{aligned}\xi^2 &= w^4\left[v+P_2(u)\right]-2b\,w^2z^2\left[v^4+v^3Q_2(u)+v^2Q_4(u)+v\,Q_6(u)+Q_8(u)\right]\\ &\quad +c\,z^4\left[v^7+v^6R_2(u)+v^5R_4(u)+v^4R_6(u)+v^3R_8(u)\right.\\ &\quad \left.+v^2R_{10}(u)+vR_{12}(u)+R_{14}(u)\right]\,,\end{aligned}\tag{6.38}$$

where $P_n(u)$, $Q_n(u)$, $R_n(u)$ are polynomials of degree n in the coordinates u_1, u_2 and $b, c \in \mathbb{C}$.

The fixed point locus under the involution (6.37) is made up of two codimension-1 loci at $w=0$ and $z=0$ and two isolated fixed points at the intersection $\xi = u_1 = u_2 = 0$, corresponding (see Sec. 5.1.2) to two $O7$-planes in the classes $[D_{O7_1}] = D_w$ and $[D_{O7_2}] = D_z$, and two $O3$-planes ($D_\xi D_{u_1} D_{u_2} = 2$).

In order to obtain the Euler characteristic of the divisors of the CY (which for this simple case we can also compute with `CohomCalg`), we can use Eq. (5.18), deriving $c_2(D)$ from the adjunction formula (5.31). In particular, the Euler characteristics of the O7-planes divisors are given by:

$$\chi(O7_1) = \chi(D_w) = \int_{X_3} c_2(X_3) + c_1(D)^2 = 75\,; \tag{6.39}$$

$$\chi(O7_2) = \chi(D_z) = 3\,. \tag{6.40}$$

Using this information, we can calculate the values of $h^{1,2}_\pm$, by means of the Lefschetz fixed point theorem (5.34), where now $\chi(O_\sigma) = \chi(O7_1)+\chi(O7_2)+2\chi(O3) = 75+3+2\cdot 1 = 80$. We find (see Eq. (5.37)):

$$80 = 4+2h^{1,1}+2(h^{1,2}_- - h^{1,2}_+) = 4+4+2(h^{1,2}_- - h^{1,2}_+) \quad\Longleftrightarrow\quad h^{1,2}_- - h^{1,2}_+ = 36\,.$$

Recalling also that $h^{1,2} = h^{1,2}_+ + h^{1,2}_- = 132$, we conclude that $h^{1,2}_+ = 48$ and $h^{1,2}_- = 84$.

6.4.3 $D7$-brane setup

Let us now consider a $D7$-brane setup canceling the $D7$-charge of the orientifold planes and maximizing the (negative) contribution of the $D3$-charge.

The $O7_2$ plane wraps a rigid divisor; hence its charge is canceled by four $D7$-branes (plus their orientifold images) wrapping D_z. By taking

$$B = \frac{D_z}{2}\,, \tag{6.41}$$

one can choose a quantized flux such that $\mathcal{F} = 0$ on the $D7$-branes wrapping D_z. This gives rise to a $SO(8)$ pure super Yang-Mills, supporting gaugino condensation (the zero flux prevents from breaking the gauge group to a subgroup with chiral spectrum, see Sec. 5.4).

As concerns the $D7$-charge of the $O7_1$, we choose to work with a Whitney brane (Sec. 5.3), wrapping the locus $\eta^2_{12,4} - w^2\chi_{18,6} = 0$ (the subscripts indicate the degrees of the polynomials η, χ with respect to the $\mathbb{C}^*$ toric actions in (6.29)) in the homology class $8[D_w]$.

6.4.4 $D3$-tadpole

We now compute the contribution to the $D3$-tadpole of the various objects. The charge of the orientifold planes was introduced in Sec. 5.1.2. In our case:

- The two $O3$-planes give a total charge

$$Q_{D3}^{O3} = 2 \times \left(-\frac{1}{2}\right) = -1\,. \tag{6.42}$$

- The $O7$-planes contribute with:

$$Q_{D3}^{O7_1} = -\frac{\chi(D_w)}{6} = -\frac{75}{6} = -\frac{25}{2}\,, \tag{6.43}$$

$$Q_{D3}^{O7_2} = -\frac{\chi(D_z)}{6} = -\frac{3}{6} = -\frac{1}{2}\,. \tag{6.44}$$

The four $D7$-branes (plus their images) on top of the $O7_2$ divisor have instead a charge (see (5.57), recalling that we have chosen $\mathcal{F} = 0$):

$$Q_{D3}^{D7_2} = -(4+4) \times \frac{\chi(D_z)}{24} = -\frac{\chi(D_z)}{3} = -1\,. \tag{6.45}$$

Finally, let us consider the $D3$-charge of the Whitney brane, recalling that it can be seen as the result of a brane recombination (conserving the total $D3$-charge) between a $D7$-brane at $\eta_{12,4} - w\,\psi_{9,3} = 0$ and its image $D7$-brane at $\eta_{12,4} + w\,\psi_{9,3} = 0$, each wrapping a divisor in the class $D_P = 4D_w$. Since this class is even, the gauge flux F is even. Moreover, the fact that zw is in the SR-ideal ensures that the pull-back of $B = \frac{D_z}{2}$ on D_P vanishes. The flux on one $D7$-brane is then $\mathcal{F} = n\,\iota^* D_u$ ($n \in \mathbb{Z}$), while on its image is $\mathcal{F}' = -n\,\iota^* D_u$. Hence, the $D3$-charge of the Whitney brane is equal to the sum of the $D3$-charges of the two $D7$-branes (see Eq. (5.58)), that is

$$Q_{D3}^{D7_W} = -\frac{\chi(D_P)}{12} - \int_X n^2 D_P \wedge D_u \wedge D_u = -\frac{840}{12} - 4n^2 D_w D_u^2 = -70 - 4n^2\,, \tag{6.46}$$

where we used $\chi(D_P) = \chi(4D_w) = \int_{X_3} (c_2(4D_w) + 16 D_w^2)\, 4D_w = 840$. The range in which n can vary is given by the condition that the Whitney brane is not forced to split into brane/image-brane (5.61), which in our case reads

$$-\frac{3}{2} D_w \leq n D_u \leq \frac{3}{2} D_w \qquad \text{i.e.} \qquad |n| \leq 4\,, \tag{6.47}$$

so that, by choosing the biggest value $n = \pm 4$, we obtain:

$$Q_{D3}^{D7_W} = -70 - 4 \times 16 = -134\,. \tag{6.48}$$

In conclusion, the total $D3$-charge of the $O3/O7/D7$ setup is

$$Q_{D3}^{\mathrm{O3/O7/D7}} = -1 - \frac{25}{2} - \frac{1}{2} - 1 - 134 = -149\,, \tag{6.49}$$

which is quite a big number. We will see that it is large enough to compensate the contribution from the fluxes in the throat and it still leaves space to have bulk fluxes that stabilize the remaining complex structure moduli.

6.4.5 Warped throat with $O3$-planes

Up to now, we have presented a model admitting an involution with two 'collapsable'[18] $O3$-planes. This corresponds to the first step in the procedure of embedding the orientifolded conifold in a global setup, presented in Sec. 4.3.2. In this section, following the subsequent steps enunciated in Sec. 4.3.2, we prove that for the model under analysis there is a corner in the complex structure moduli space, where a long throat is generated and that there is a pair of $O3$-planes at the tip of this throat. This will ensure the correct setup for placing an $\overline{D3}$-brane on top of one of the two $O3$-planes, giving an explicit realization of the construction in [102].

Deformation. Let us start considering the locus of the $O3$-planes, whose equation is obtained by plugging $\xi = u_1 = u_2 = 0$ inside the (invariant) equation (6.38) of the CY three-fold:

$$w^4 v - 2b\, w^2 z^2 v^4 + c\, z^4 v^7 = 0\,. \tag{6.50}$$

This equation is defined in the one-dimensional ambient space with weights system:

	z	v	w
$\mathbb{C}^*_1$	0	2	3
$\mathbb{C}^*_2$	1	0	1

(6.51)

First, we notice that if $z = 0$ in this locus, then also w is forced to vanish. However, the two coordinates cannot vanish simultaneously ($zw \in SR$) hence we conclude that z can never vanish in the $O3$-planes locus (6.50). We can therefore fix $z = 1$ (with a suitable choice of the parameter λ_2 of the second equivalence relation in (6.29)), going to the one dimensional ambient space:

	v	w
$\mathbb{C}^*$	2	3

(6.52)

In addition to this, $u_1 u_2\, v \in SR$, hence $v \neq 0$. Fixing also $v = 1$ (by means of the other $\mathbb{C}^*$-action), we are left with the ambient space $\mathbb{C}/\mathbb{Z}_2$ ($\mathbb{Z}_2$: $w \mapsto -w$) and the equation

$$w^4 - 2b\, w^2 + c = 0\,. \tag{6.53}$$

This equation is solved by $w^2 = \gamma_i$, with γ_i the zeroes of the quadratic equation (the solutions $w = \pm\sqrt{\gamma_i}$ are identified by the $\mathbb{Z}_2$ orbifold action). The two solutions correspond to the two $O3$-planes, which come on top of each other when the discriminant of the quadratic equation is zero, that is:

$$b^2 - c = 0\,. \tag{6.54}$$

This situation can be described through the redefinition:

$$c \equiv b^2 + \delta\,. \tag{6.55}$$

[18] See the caption of Fig. 5.2 for the meaning of 'collapsable' $O3$-planes in this context.

When $\delta = 0$ the two $O3$-planes go on top of each other at the point $w^2 - bz^2 = 0$. When δ is small they are very close to each other. This concludes the step (2) of Sec. 4.3.2: we showed that the CY can be deformed so that the two $O3$-planes come on top of each other in the limit $\delta \to 0$.

Conifold. As a next step we need to check that in the same limit $\delta \to 0$ a conifold singularity is generated on the CY three-fold at the point (where the two $O3$-planes coincide) $\xi = u_1 = u_2 = w^2 - bz^2 = 0$. Let us consider a small neighborhood of the points, given by $\xi = u_1 = u_2 = (w^2 - bz^2)^2 + \delta = 0$. Here, v and z still do not vanish, hence we can fix them to 1. In this local patch, the equation (6.38) becomes (in an ambient space $\mathbb{C}^4/\mathbb{Z}_2$):

$$-\xi^2 + \sum_{i,j=1,2} a_{ij} u_i u_j + (w^2 - b)^2 + ... = \delta \,, \tag{6.56}$$

where '...' are monomials that vanish faster than the quadratic ones at $\xi = u_1 = u_2 = w^2 - b = 0$ (we keep δ small). Diagonalizing the quadratic form a_{ij} we can rewrite the above equation as

$$-\xi^2 + u_1^2 + u_2^2 + (w^2 - b)^2 + ... = \delta \,, \tag{6.57}$$

where it is clear that it describes a deformed conifold singularity (see Eq. (4.9)) with δ controlling the size of the S^3 at the tip of the throat. Notice that at first sight one might think that $\delta \to 0$ corresponds to two conifold singularities at $w = \pm\sqrt{b}$. However, as pointed out before, they are identified by the orbifold action[19].

Consistency checks. Finally let us come to the consistency checks. First, we need to verify that the involution is acting on the conifold as expected (Eq. (4.10)), which can be done by carefully inspecting the gauge fixing $v = z = 1$. Looking at (6.51), indeed, one observes that the choice $z = 1$ corresponds to fixing the parameter of the second $\mathbb{C}^*$-action to $\lambda_2 = \frac{1}{z}$. On the other side, imposing $v = 1$ fixes λ_1 *up to a sign* (the corresponding equivalence relation is indeed $v \sim \lambda_1^2 v$). In other words, the gauge fixing leaves an unfixed subgroup generated by:

$$\{\lambda_1, \lambda_2\} \mapsto \{-\lambda_1, \lambda_2\} \,.$$

Thus, by taking $\lambda_1 = -1$, we obtain the desired action in the local patch we are considering:

$$\{\xi, u_1, u_2, w^2 - b\} \mapsto \{-\xi, -u_1, -u_2, w^2 - b\} \,. \tag{6.58}$$

In the end, as concerns the $D3$-charge, we can see that this configuration allows, at least in principle, to cancel the $D3$-tadpole as required. As we can see from the previous section, indeed, the $D3$-charge of the system of 2 $O3$-planes, 2 $O7$-planes and $D7$-tadpole canceling $D7$-branes is integer (see Eq. (6.49)). Hence, we can choose to put a $D3$-brane at the $O3$-plane sit at one pole of the S^3 and an $\overline{D3}$-brane at the $O3$-plane at the opposite pole [103] as anticipated in Sec. 4.3. In this way, the two branes do not contribute to the total $D3$-charge and at the same time, since they are stuck at the $O3$-planes, there is no

[19] Note also that the conifold point is far apart from the orbifold singularity of the ambient space, that anyway never belongs to the CY three-fold.

perturbative decay channel between them (provided that the complex structure moduli are fixed such that the S^3 has a finite size).

6.4.6 Moduli stabilization

In this section we use the results of Sec. 6.1.2 to stabilize the Kähler moduli and the conifold complex structure modulus of the model under analysis. We take the parameter ξ in the Kähler potential (2.25) as given by $\xi \equiv -\frac{\chi(X)\zeta(3)}{4(2\pi)^3}$, that is without including the correction of [166]. This correction, due to the effect of the orientifold background (in particular the $O7$-planes and the $D7$-branes) on the α'^3 correction can be defined by means of a shift in the Euler characteristic of the model:

$$\chi(X_3) \to \chi(X_3) + 2\int_{X_3} D^3_{O7}\,, \tag{6.59}$$

where for our example $D^3_{O7} = D^3_{O7_1} + D^3_{O7_2} = 18$. Including this effect would mean to perform the computation with Euler characteristic $\chi(X_3) = -224$ instead of $\chi(X_3) = -260$. However, we checked that the results do not change sensibly from those obtained when we add the correction[20].

As observed in Eq. (6.36), $\kappa_s = \frac{\sqrt{2}}{9}$, as we expect for a dP_0. Moreover, since the rigid divisor D_z is wrapped by an $O7$-plane, the non-perturbative superpotential is generated by gaugino condensation on the corresponding $SO(8)$ $D7$-brane stack, hence $a_s = \frac{\pi}{3}$.

Applying the methods of the numerical analysis of Sec. 6.3.2, we find that the only allowed values of the $D3$-charge for the flux inside the throat are $MK = \{88, 92, 125\}$. We choose therefore the values of the parameters W_0, g_s, M, K producing a model with $MK = 88$, i.e.

$$W_0 = 23; \qquad g_s = 0.23; \qquad M = 22; \qquad K = 4\,. \tag{6.60}$$

Notice that $g_s M = 5.02$ [21], in agreement with the requirement (3) of Sec. 6.3.2.

Under this choice, the moduli are stabilized at:

$$\tau_s = 7.6; \qquad \tau_b = 704; \qquad \zeta = 0.005$$

hence the volume is large as needed. In particular, in Einstein frame, it reads $\mathcal{V} \simeq \tau_b^{3/2} = 18698 \gg 1$ (in string frame this corresponds to $\mathcal{V}_s = 2036$) as needed. These values correspond to a de Sitter minimum with $V_{min} \simeq 10^{-12}\, m_p$.

Notice that the value of the scalar potential at the minimum can be decreased (without breaking the other constraints) by fine-tuning W_0: the finer the tuning, the smaller the potential at the minimum.

The masses of the moduli are computed by means of canonical normalization (see App. C):

$$m_1^2 = 3.7 \times 10^{-5} m_p^2\,, \qquad m_3^2 = 1.6 \times 10^{-11} m_p^2\,, \qquad m_2^2 = 2.9 \times 10^{-9} m_p^2\,,$$

[20] This can also be argued by looking at the first table of Sec. 6.3.2, where we can see that while increasing the (absolute value of) the Euler characteristic is an advantage for the sake of the tadpole cancellation conditions, already with $-\chi(X_3) = 200$ we get $(MK)_{\min} < 149$.

[21] $g_s M^2 = 110 \gg 46.1$, hence, as anticipated, the SUGRA requirement is more constraining than the no-runaway one.

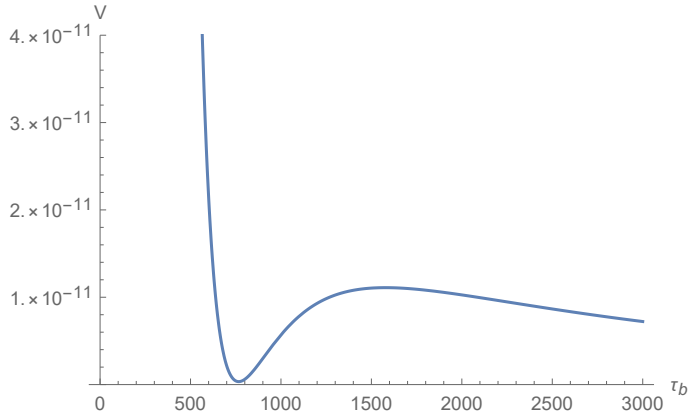

Figure 6.1: The total scalar potential (in units of m_p) along its weakest direction ($\tau_s = \tau_s^{min}$).

where m_1 and m_3 are approximately the masses of the moduli τ_s and τ_b at the LVS minimum. Notice that they also match with the estimations done in Sec. 6.2.

The other relevant scales are:

$$2\pi\, M_s = 9\times10^{-3} m_p \simeq 3.6 M_{KK}^{bulk}, \quad M_{KK}^{bulk} = 2.5\times10^{-3} m_p \simeq 6 m_{3/2}, \quad m_{3/2} = 4.3\times10^{-4} m_p,$$

hence they respect the required hierarchy. We also checked explicitly that, as predicted in Sec. 6.3.1, all the remaining consistency conditions are fulfilled.

In order to have a qualitative idea of the potential, we consider in more detail the two-moduli scalar potential obtained by fixing all the moduli but τ_s, τ_b at their vacuum value[22]. Beside the minimum, we find a second stationary point at

$$(\tau_s, \tau_b) = (8.2, 1123)$$

that turns out to be a saddle point with $V_{\text{saddle}} = 1.8\times10^{-12}\, m_p$. The global maximum of V is, instead, on the boundary of the Kähler cone ($\tau_b = \tau_s = \tau_s^{min}$), where $V_{max} = 0.06\, m_p$.

If we furthermore fix τ_s at its vev, the resulting one modulus potential, plotted in Fig. 6.1, has a maximum at $\tau_b = 1433 \equiv \tau_b^{max}$, with $V_{\tau_b^{max}} = 1.2\times10^{-11}\, m_p$. This gives an estimate of the barrier for tunneling from the minimum to the decompactification limit $\tau_b, \tau_s \to \infty$ (the considered direction is indeed the one along which we observe the smallest barrier between these two regions of the potential). As discussed in [63], the decay rate in LVS can then be estimated to be of order $\Gamma \sim e^{-\mathcal{V}^3} \sim e^{-10^{12}}$ in Planck units which, similarly to the KKLT case, implies a very stable vacuum with a lifetime smaller than the recurrence time (see also Sec. 4.1).

The 2-moduli scalar potential is plotted in Fig. 6.2, where all the significant points and the 1-modulus direction are highlighted.

[22] The 3-moduli analysis, including ζ, gives analogous results, as expected.

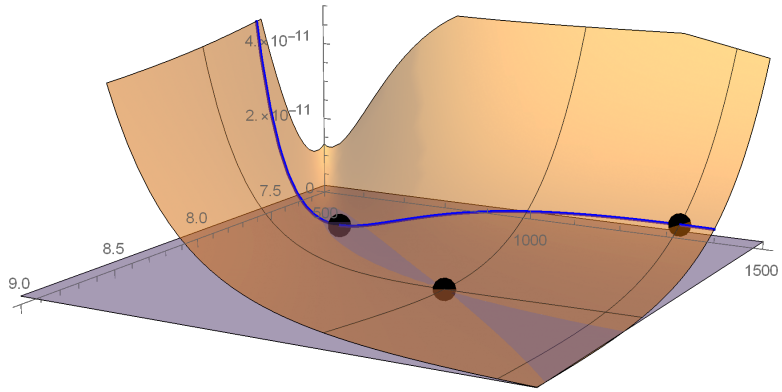

Figure 6.2: Total scalar potential as a function of τ_s and τ_b. The black dots correspond to the de Sitter minimum, the saddle point and the maximum along the 1-modulus direction (the blue curve) analyzed in the text. The grey plan at $V = V_{saddle}$ highlights the unstable direction for the saddle point.

6.5 Conclusions

In this chapter we have studied the moduli scalar potential for a type IIB compactification in the LVS regime, with a dS minimum realized by the introduction of an $\overline{D3}$-brane at the tip of a warped throat. Assuming all the complex structure moduli (except the one parametrizing the throat) and the dilaton to be fixed by fluxes as in GKP, we focussed on the scalar potential for the conifold complex structure modulus and the Kähler moduli.

The uplift term in the scalar potential is controlled by the warp factor ρ. We have seen that de Sitter minima exist only for a limited range of values of ρ, for which the minimum is mildly shifted with respect to the LVS one. Too small values, indeed, correspond to AdS vacua, while if we increase the warp factor (and hence the uplift term) from the value corresponding to a Minkowski minimum, the potential soon develops unstable directions.

The fact that the warp factor can only take values inside a small range, strongly constraints the value of the ratio $\frac{M}{K}$ between the 3-form fluxes along the throat (recall that $\rho \sim e^{-\frac{8\pi K}{3g_s M}}$). In addition to this, the requirement of the validity of the KS approximation, i.e. $g_s|M| \gg 1$, imposes a lower bound on M and, as a consequence of the fixed ratio, on K. This means that the D3-charge generated from the fluxes in the throat is bounded from below, with a typically large bound.

The reason why the presence of this bound must be carefully taken in consideration is that in type IIB compactifications the total flux contribution to the $D3$-charge (coming both from the fluxes MK inside the throat and from the bulk fluxes necessary to stabilize the other complex structure moduli), must be canceled by localized sources ($D7$-branes and $O3/O7$-planes, having a negative $D3$-charge). However, having a large negative $D3$-charge, necessary to compensate the lower bound on MK, is challenging even if it is possible.

In Sec. 6.3.2 we have estimated the lower bound on MK as one varies the parameters of the effective field theory, concluding that it is minimal at the boundary of the region in which the approximations used to obtain the minimum can be trusted.

Furthermore, in Sec. 6.4, we have constructed an explicit example in perturbative type IIB string theory, where a warped throat supporting $O3$-planes is realized. This allows to describe the degrees of freedom of the $\overline{D3}$-brane responsible for the uplift to dS by means of the introduction of a single nilpotent chiral superfield. With this example we have shown how one can generate a relatively large negative $D3$-charge by a proper $D7$-brane background (including in particular a 'Whitney' brane), also in perturbative type IIB string theory. However, the tadpole cancellation conditions impose to take a not-so-large value of g_sM, i.e. $g_sM \sim 5$ that is bigger than 1 but not so large. Moreover also the string coupling should be taken small but not-so-small, i.e. $g_s \sim 0.23$. Of course one may decrease the string coupling (improving string perturbation theory), but if the flux contribution is kept fixed, this leads to a smaller g_sM, therefore worsening the KS supergravity approximation[23]. The possibility of obtaining large negative contributions to the $D3$-charge in perturbative type IIB string theory will be analyzed in a more detailed and systematic way in the next chapter.

In summary we conclude that we were able to provide a concrete model in which all the moduli are stabilized at a de Sitter minimum (obtained by the introduction of an $\overline{D3}$-brane), satisfying all consistency conditions while also having small expansion parameters. We did this within a class of models which are simple enough to be explicit but rich enough to include all the ingredients of moduli stabilization, considering this as a small, but useful step towards a more systematic realization of de Sitter vacua in string compactifications. As expected, this was not a simple task, but having been able to find a vacuum in a regime in which the expansion parameters are small is encouraging. We are confident that with more elaborate compactifications, including chiral matter, de Sitter solutions with small expansion parameters are achievable. We leave a systematic search for the future.

After our paper [18] came out, some interesting developments where proposed in [116][24] and [67]. The first presents a detailed analysis of several possible (curvature, warping and g_s) corrections that may arise in the LVS scalar potential considered in this chapter (that is with $h^{1,1} = 2$ and a conifold modulus). Two of these corrections are potentially problematic for the model analyzed here, in the sense that they do not appear to be parametrically suppressed. In fact, the claim of the paper is that it is generically impossible to neglect all these corrections at the same time. Some of these results are resumed in [67], where the two 'problematic' corrections lead to two additional constraints, reported here in Eq. (4.18) and Eq. (5.74), which therefore are not satisfied by the explicit model analyzed in Sec. 6.4. Nonetheless, we stress that these constraints always depend on complex structure-dependent parameters. Since the value and the sign of these parameters are unknown, they are generically taken to be $\mathcal{O}(1)$ constants. However, nothing forbids them to take different values which, in an explicit model, may be such that the corresponding correction is numerically suppressed or different corrections cancel each other. We will come back to

[23] Our results were later confirmed in [167], where some additional consistency checks are performed. Furthermore, the authors of [167] analyze the same explicit model under the hypothesis (complementary to ours) of a 'weakly-but-still-warped' throat supporting the $\overline{D3}$ uplifting mechanism presented here, finding similar constraints on the tadpole ($MK \sim \mathcal{O}(100)$).

[24] See also [168].

this in Ch. 8.

Possible extensions of this work may go along at least two main directions. First, it would be interesting to analyze certain issues highlighted in our simple construction, in a more systematic way, taking in consideration a larger set of models in the context of type IIB compactifications. The work presented in the next chapter goes in this direction as concerns the size of $D3$-tadpoles in CY orientifolds with $h^{1,1} \leq 12$.

Secondly, one would like to construct more involved explicit examples, with a larger number of Kähler moduli ($h^{1,1} > 2$) and the introduction of additional phenomenologically interesting features, such as chirality and/or some inflationary mechanism. On one side this is expected to add new technical and physical challenges due to the introduction of several new elements; on the other hand, some of the current obstructions may turn out to be absent. Going along this direction, in Ch. 8, we explore the possibility of constructing an explicit example including, besides the elements presented in this chapter, also a K3-fibration. This simple modification already produces new challenges that we describe before analyzing a concrete setup. Furthermore, in App. D we compute the total scalar potential for a generic number $h^{1,1}$ of Kähler moduli plus the conifold complex structure modulus Z, following the strategy presented in [61] (where Z and the uplift term were absent). As an application, we consider in Sec. D.4 the simple case in which all the Kähler moduli but one appear diagonally in the volume of the CY, which is the most immediate generalization of the model analyzed in this chapter. We also provide some estimation of the trend of the flux contribution to the tadpole (MK) as $h^{1,1}$ increases.

Chapter 7

A Database of Calabi-Yau Orientifolds and the Size of D3-tadpoles

This chapter is based on [19] in which we constructed Calabi-Yau orientifolds from holomorphic reflection involutions of toric CY hypersurfaces with $h^{1,1} \leq 7$ (with partial results up to $h^{1,1} = 12$)

As highlighted in the previous chapter, having models admitting orientifold configurations with a large negative $D3$-charge is highly desirable, given the potentially large contribution of the background fluxes in the KS throat. One of the purposes of [19] is therefore to explore the possibility of having such large negative charges, by comparing in particular the contribution of local (like $SO(8)$ stacks) and non-local (Whitney) brane configurations. In addition, we generate a database of CY orientifolds from reflection involutions that, besides allowing to determining the size of the $D3$-tadpole, may have further future applications. The full data can be found in the GitHub repository at: `https://github.com/AndreasSchachner/CY_Orientifold_database`, together with a `jupyter` notebook providing instructions on how to read the data and work with them.

7.1 General setup

Previously in this thesis we have presented the theoretical tools needed for the analyses of this chapter. The CY geometries collected in the database are constructed, starting from the 4d reflexive polytopes listed in [105], as hypersurfaces in toric ambient varieties, as described in Sec. 5.1. In particular, since `CohomCalg` usually fails at $h^{1,1} > 5$, we compute the Hodge numbers of each divisor starting from the properties of the original polytopes, as reviewed in Sec. 5.1.1[1].

[1] The results turn out to be largely consistent with the data provided in [108].

For each CY threefold, we analyze the reflection involution of each toric coordinate

$$\sigma_k : z_k \to -z_k \,,$$

which, we recall, corresponds to $h^{1,1}_{-} = 0$ for a favorable geometry and allows only for $O3$- and $O7$-planes. Under such involution, the cohomology groups $H^{p,q}(X_3)$ split into even and odd subspaces, whose dimensions can be computed by means of the Lefschetz fixed point theorem, see Sec. 5.1.2.

A CY geometry defined as a hypersurface on a toric variety obtained by a FRST[2], which is the only case we consider here, is always smooth. However, the presence of an involution, can force some unwanted singularity, given that, as reviewed in Sec. 5.1.2, it imposes a deformation of the equation defining the CY (all its monomials that are not invariant under the involution itself, need to be removed). Since we want to work with smooth spaces, we need to individuate (and discard) such singularities which in particular might be due either to the fact that the invariant hypersurface is now forced to touch singularities of the ambient space or to the fact that the new invariant defining equation describes a singular hypersurface (i.e. there are points such that $P_{\text{invCY}} = \nabla P_{\text{invCY}}(X_0) = 0$).

A first criterion comes from the Hodge numbers of the orientifold CY: we consider a signal of potential singularity the fact that the computation of $h^{1,2}_{\pm}(X_3)$ leads to non-integer values, hence we discard the models in which this happens. Furthermore, in order to detect more subtle singularities, we consider again the underlying polytopes. In terms of these, the invariant CY equation for the involution $z_k \to -z_k$ is given by the usual Batyrev formula (5.3), where now the points w belong to the polytope Δ_k (instead of Δ) with:

$$\Delta_k = \{w \in \Delta \,:\, \langle w, \nu_k \rangle + 1 \in 2\mathbb{N}\} \,. \tag{7.1}$$

We argue that the properties of Δ_k are in one-to-one correspondence with the features of the CY hypersurface invariant under the involution of z_k, which is obtained from triangulations of the dual polytope Δ_k° . We decide, in particular, to consider only models for which the polytope Δ_k is reflexive and its dual Δ_k° is favorable, claiming that they are smooth. We checked in several models that the excluded CY's are actually singular.

Finally, it is important to notice that string theory is well defined also on singular spaces. For this reason we collected in the database also the data of the singular models that we are excluding here, having decided to limit our analysis to smooth geometries where the usual formulas for the topological invariants can be applied.

The negative $D7$-charge from the $O7$-planes is canceled by appropriate $D7$-branes configurations. We analyzed in Sec. 5.3 the different possibilities, depending on the form of the equation defining the locus of the brane. One of our purposes here, will be to highlight the advantages (from the point of view of the $D3$-tadpole cancellation) of considering, when possible, Whitney branes instead of localized stacks of $D7$-branes.

[2]The definition of a Fine, Regular, Star Triangulation (FRST) was given in the discussion below Eq. (5.8).

7.2 The $D3$-tadpole

In this section we make some estimations of the $D3$-charge contributions that we expect to observe from different configurations. We start recalling our notation for the $D3$-tadpole cancellation condition:

$$N_{\rm D3} + N_{\rm D3'} + N_{\rm flux} = -Q_{\rm D3}\,, \qquad \text{with } Q_{\rm D3} = Q^{\rm tot}_{\rm D7} + Q^{\rm tot}_{Op}\,,$$

where:

$$Q^{\rm tot}_{\rm D7} = \sum_i (Q^i_{\rm D7} + Q^i_{\rm D7'})\,, \quad Q^{\rm tot}_{Op} = \sum_k Q^k_{\rm O3} + \sum_l Q^l_{\rm O7} \tag{7.2}$$

(the pedex $D3'$ and $D7'$ refer to the image branes).

The $D3$-charge from a single $O7$-plane was defined in (5.41). In a setup with several $O7$-planes we will therefore have a total contribution:

$$-Q^{\rm tot}_{\rm O7} = \sum_i \frac{\chi(D_i)}{6} = \frac{\chi(O_\sigma) - N_{\rm O3}}{6} = \frac{h^{1,1}(X_3) + h^{1,2}_-(X_3) - h^{1,2}_+(X_3) + 2}{3} - \frac{N_{\rm O3}}{6}\,, \tag{7.3}$$

where $N_{\rm O3}$ is the number of $O3$-planes (we recall that each $O3$-plane simply contributes with $-\frac{1}{2}$) and we used (5.36) and (5.37) for $\chi(O_\sigma)$. We notice, therefore, that models with many Kähler and/or many complex structure moduli provide a larger[3] charge $|Q^{\rm tot}_{\rm O7}|$.

Let us now consider the $D7$-branes, whose $D3$-charges are computed in Sec. 5.3.1. Considering only local configurations, the brane setup maximizing the $D3$-charge from $O7/D7$ corresponds to a SO(8) stack of four branes (plus their four images) on top of each $O7$-plane wrapping a divisor D_i. In the absence of gauge fluxes ($\mathcal{F} = 0$), we can again estimate the total $D3$-charge contribution by means of (5.37):

$$-Q^{\rm tot}_{\rm SO(8)} = \sum_i \frac{(4+4)\,\chi(D_i)}{24} = 2\frac{h^{1,1}(X) + h^{1,2}_-(X) - h^{1,2}_+(X) + 2}{3} - \frac{N_{O3}}{3}\,. \tag{7.4}$$

Eqs. (7.3) and (7.4), allow to estimate the maximum $D3$-charge that we can obtain when we cancel the $D7$-charge of the $O7$-planes with SO(8) $D7$-branes stacks:

$$-Q_{D3} = -\frac{N_{O3}}{2} - Q^{\rm tot}_{O7} - Q^{\rm tot}_{\rm SO(8)} = 2 + h^{1,1} + h^{1,2}_- - h^{1,2}_+ \leq 2 + h^{1,1} + h^{1,2}\,, \tag{7.5}$$

where we used the fact that $h^{1,2}_- - h^{1,2}_+ \leq h^{1,2}$. This upper bound was also found in [169, 114, 67, 104]. Using for the Hodge numbers the maximum values that we can find in the Kreuzer-Skarke database, that is $(h^{1,1}, h^{1,2}) = (11, 491)$, we find:

$$-Q_{D3} \leq 504\,. \tag{7.6}$$

[3] In the following we will always (unless specified differently) refer to the absolute value of the $D3$-charge coming from O-planes/D-branes. We will therefore aim for configurations that *maximize* this contribution.

As we will see in the following, the introduction of a Whitney brane (when allowed) significantly enhances the bound (7.6). In order to compute the corresponding charge, we will use the equation for the geometric $D3$-charge (5.62). As explained in Sec. 5.3.1, one should, in principle, consider also the flux contribution (5.63), unless it is possible to define the integer flux form F such that $Q^W_{D3,\text{flux}}$ vanishes (a non-generic feature that needs to be checked model by model). However, one can always choose F such that $Q^W_{D3,\text{flux}} \ll Q^W_{D3,\text{geom}}$. We will assume to be in this situation, which justifies our choice to neglect $Q^W_{D3,\text{flux}}$. A similar argument applies to the case of $SO(8)$ stacks, analyzed before: in principle one should explicitly check whether it is possible to choose the B-field such that $\mathcal{F} = 0$ for all divisors wrapped by $O7$-planes, but if we assume that the (possibly non vanishing) flux is tuned so that it minimizes its contribution to Q_{D3} we find that our results are a good approximation of the exact ones.

$D3$-tadpole in F-theory

Before going on with the analysis of the database, it is useful to connect the results we are finding in perturbative type IIB orientifold compactifications with the F-theory language [170]. In particular we stress that the large $D3$-charges that are usually mentioned in the literature as coming from F-theory backgrounds (and typically corresponding to smooth fourfolds with no gauge group or matter), can actually be reached in type IIB, by canceling the $D7$-tadpole by means of Whitney branes.

In F-theory, the $D3$-tadpole cancellation condition takes the form[4]:

$$\frac{1}{2}\int_{Y_4} G_4 \wedge G_4 + N_{D3} = \frac{\chi(Y_4)}{24} = -\frac{Q_{D3}}{2}\,, \tag{7.7}$$

where $\chi(Y_4) = 6\left(8 + h^{1,1}(Y_4) + h^{1,3}(Y_4) - h^{1,2}(Y_4)\right)$ is the Euler characteristic of the CY fourfold Y_4, representing the F-theory compactification manifold[5].

The fourfold Y_4 is an *elliptic fibration*[6] over a base space that is the quotient of X_3 by the orientifold involution σ: $\mathcal{B}_3 = X_3/\sigma$. The cases in which the involution σ is such that the $D7$-tadpole can be canceled by Whitney branes, correspond to smooth CY fourfolds in F-theory. On the other side, splitting the Whitney branes in type IIB produces a non-trivial gauge group G, which corresponds to a deformation of the fourfold generating codimension-3 (for abelian G) or codimension-2 (for non-abelian G) singularities. In particular, the case of a SO(8) gauge group, obtained by placing the $D7$-branes on an $O7$-plane wrapping a

[4] Notice that we are working in the perturbative type IIB double cover setup, in which $Q_{D3} = -\frac{\chi(Y_4)}{12}$.

[5] $\chi(Y_4)$ is computed as follows. Recalling that the Euler characteristic is defined as

$$\chi(Y_4) = \sum_{p,q=0,4} (-1)^{p+q} h^{p,q}(Y_4)$$

and applying the properties (B.5) and (B.6) (with $h^{0,0} = 1$ and $h^{0,1} = h^{0,2} = 0$), we find: $\chi(Y_4) = 4 + 2h^{1,1} - 4h^{1,2} + 2h^{1,3} + h^{2,2}$. Furthermore, we can write $h^{2,2}$ in terms of the other Hodge numbers, using the relation [171, 172] $h^{2,2} = 44 + 4h^{1,1} - 2h^{1,2} + 4h^{1,3}$, from which we obtain the result presented in the text.

[6] A manifold $\mathcal{M}$ is a fibration over the *base* $\mathcal{B}$ with *fiber* F if there exists a continuous map $\pi : \mathcal{M} \mapsto \mathcal{B}$, such that $\pi^{-1}(b) = F$, $\forall b \in \mathcal{B}$. An elliptic fibration is a fibration whose fiber is an elliptic curve.

$h^{1,1}$	2	3	4	5	6	7	total
polytopes	36	244	1197	4990	17 101	50 376	73 944
fav. polytopes	36	243	1185	4897	16 608	48 221	71 190
fav. FRSTs	48	525	5330	56 714	584 281	5 990 333	6 637 231
involutions	184	3035	39 653	495 854	5 777 640	65 625 277	71 941 643
smooth invol.	138	1975	22 933	230 886	2 081 080	17 875 122	20 212 134
only $O7$	49	598	3896	25 391	177 468	1 336 960	1 544 362
≥ 2 collaps. $O3$	71	1089	15 497	164 634	1 480 968	12 596 558	14 258 817

Table 7.1: Number of CY orientifolds obtained in our scan for $h^{1,1} \leq 7$. The distinction between involutions and smooth involutions is explained in the main text. In the last two lines, we count the number of models containing only $O7$-planes and the ones with two or more $O3$-planes coming from the same fixed curve in the ambient space. The last ones are possibly suitable for $\overline{D3}$ uplift to dS, while both classes of models admit T-brane uplift.

rigid divisor, corresponds to a so-called non-Higgsable cluster in the F-theory fourfold [173, 174], i.e. to a non-deformable D_4 singularity. While Eq. (7.7) is valid also when the fourfold is singular, provided that one uses the resolved fourfold [104, 175, 176], in this case the geometric contribution to the tadpole decreases, as a consequence of the fact that we are deforming a smooth manifold to a singular one (with some gauge group and matter). This is precisely what happens in type IIB, where splitting the Whitney brane produces a lower $D3$-charge [104].

7.3 Orientifold database

In this section we generate a database of Calabi-Yau orientifolds, making a large use of the `CYTools` package [177], which allows to construct FRSTs from polytopes at arbitrary $h^{1,1}$. Starting from these data, we have implemented an algorithm to construct CY orientifolds obtained via reflection involutions. The algorithm is generic; however the computation and analysis of all the triangulations of a given polytope Δ° becomes more and more expensive (from the computational point of view) as $h^{1,1}$ increases. For this reason we have collected in the database two sets of data. On one side, we have computed *all* FRSTs of *all* favorable polytopes at $h^{1,1} \leq 7$, constructing the orientifold configuration associated to the involution of each toric coordinate. On the other side, for $8 \leq h^{1,1} \leq 12$ we have generated up to 20 *random* FRSTs of up to 20 favorable polytopes for each combination of Hodge numbers $(h^{1,1}, h^{1,2})$, again deriving the orientifold data obtained by reflecting each toric coordinate.

$h^{1,1}$	7	8	9	10	11	12	total
fav. polytopes	1219	1498	1587	1555	1623	1807	8980
fav. FRSTs	4560	6897	9968	12 189	15 748	15 430	64 792
involutions	49 326	81 911	128 403	169 775	235 216	245 989	910 620
smooth invol.	6491	9102	13 041	15 713	21 892	24 154	90 393
only $O7$	1769	2608	3493	3543	4330	4772	20 515
≥ 2 collaps. $O3$	3168	4084	5865	6692	9978	9507	39 294

Table 7.2: Number of random FRSTs for random favorable polytopes between $7 \leq h^{1,1} \leq 12$. We selected up to 20 polytopes for each combination of Hodge numbers $(h^{1,1}, h^{1,2})$ available in the KS database.

The algorithm determining the fixed points set of each involution $\sigma_k : z_k \mapsto -z_k$ of a given Calabi-Yau geometry is based on the following steps (see also Sec. 5.1.2):

1. We select from the equation of the Calabi-Yau (5.3) the monomials that are invariant under σ_k, therefore deforming the original equation to an equation which is symmetric under the involution.

2. Considering the action of σ_k and $\sigma_k \cdot \lambda_i$ (where the λ_i's are the parameters of the $\mathbb{C}_i^*$ toric equivalence relations) we determine the fixed point loci of the toric ambient space under the involution (keeping only those which are allowed by the SR ideal).

3. We study the invariant equation of the CY at each fixed point locus. All the possibilities that one can get are listed in Sec. 5.1.2 and they can be summarized as follows: if the invariant equation vanishes at the fixed point locus, then a co-dimension n locus corresponds to an Om-plane with $m = 3 + 2(4 - n)$; if it does not vanish, the same locus corresponds to an Om-plane with $m = 3 + 2(3 - n)$.

4. We count the number of $O3$-planes (which is relevant for the computation of the tadpole as well as in order to individuate examples that are suitable for $\overline{D3}$-brane uplift) by means of the intersection numbers. In particular, if the $O3$-plane is given by a co-dimension 3 locus (with a non-vanishing CY equation) we use the intersection numbers of the Calabi-Yau, while if it is defined by a co-dimension 4 locus (with vanishing CY equation) we consider the intersection tensor of the ambient space, obtained from `CYTools`.

Consistently with the expectations due to our choice of the involution, we don't find any $O5/O9$-planes in our scan (see Sec. 2.3).

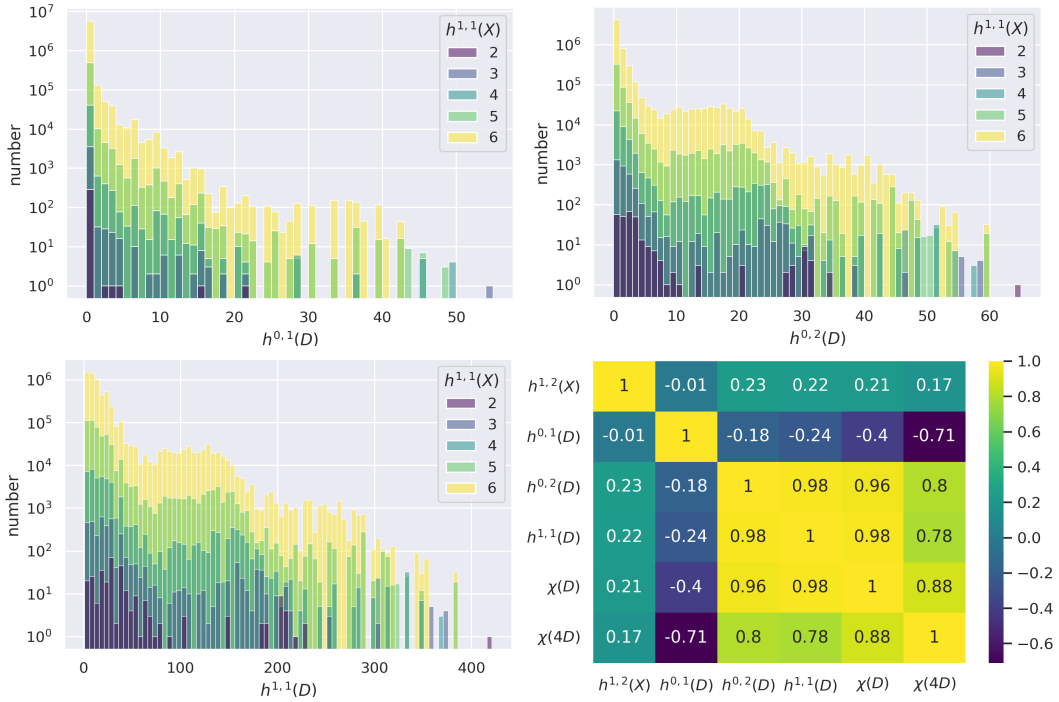

Figure 7.1: Histogram plots for the Hodge numbers $h^{0,1}(D)$, $h^{0,2}(D)$ and $h^{1,1}(D)$ for all divisors at $h^{1,1} \leq 6$. The last figure shows the correlation between the different Hodge numbers and the Euler characteristics of the divisors. We included in it also $\chi(4D)$, which we know to be relevant for the computation of the $D3$-charge contribution of Whitney branes.

A similar algorithm to determine the O-plane configurations up to $h^{1,1} = 6$ and considering exchange involutions ($\sigma : x_i \leftrightarrow x_j$), was introduced in [108]. For the same values of $h^{1,1}$, therefore, we provide a complementary analysis based on reflection involutions, while, in addition to this, we produce additional statistics up to $h^{1,1} = 12$. Furthermore, as we mentioned, we present a systematic study of $D7$-tadpole cancellation via Whitney branes, as opposed to the more commonly studied SO(8) stacks of $D7$-branes.

A summary of the data collected in our scan is provided in Tab. 7.1 ($h^{1,1} \leq 7$) and in Tab. 7.2 ($7 \leq h^{1,1} \leq 12$ [7]). Here, the line 'involutions' includes only *independent* involutions. When scanning over the models, indeed, the inversion of coordinates with the same weights gives rise to equivalent involutions (up to coordinate redefinition), whose inclusion would be redundant. Moreover, since the involution might force some singularity in the invariant CY (see Sec. 7.1), it is useful to distinguish the involutions that do not present any of these pathologies, which we refer to as *smooth involutions*.

The full database can be found at this GitHub repository. It contains 71 941 643 orientifolds therefore extending the previous orientifold databases of 2 004 513 CICY orientifolds [169] and 28 463 divisor exchange involutions of [108]. Notice, however, that our number,

[7] Even though we have computed the full data for $h^{1,1} = 7$, in the analysis we will use only a subset of them (for computational reasons), that is the ones reported in Tab. 7.2.

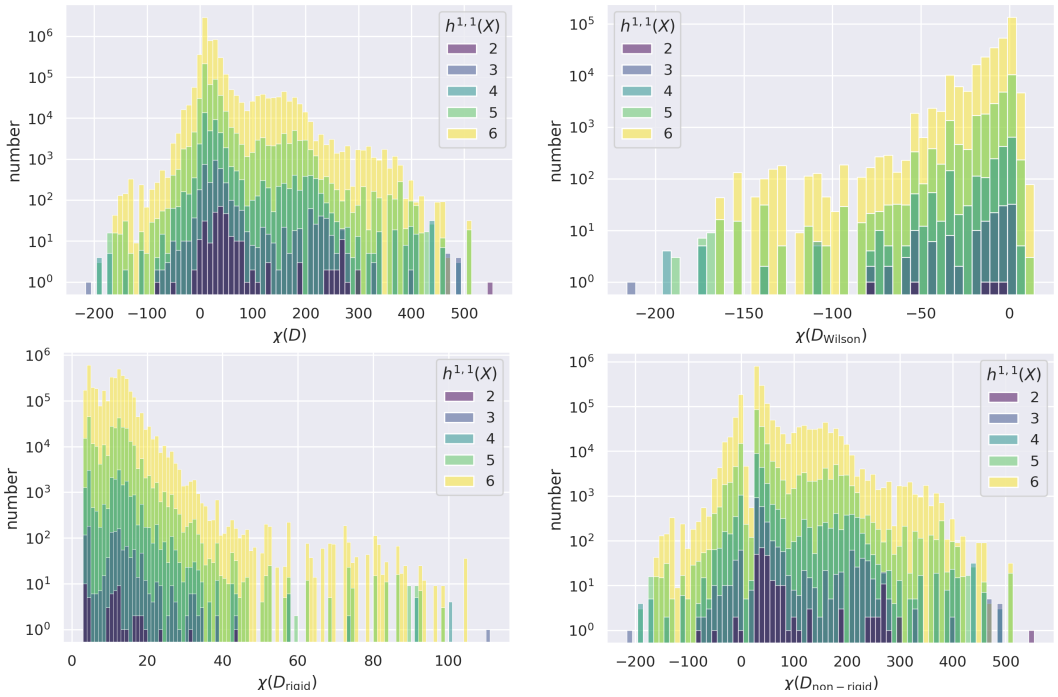

Figure 7.2: Histogram plots for the Euler characteristic of different kinds of divisors. In the left figure of the first row we collect the cumulative data relative to all the divisors, regardless their Hodge numbers. On the right, we show the distribution of χ for the Wilson divisors. In the second row we compare the distribution of Euler numbers between completely rigid (left) and non-rigid (right) divisors. Notice that, with abuse of notation, here we are calling 'non-rigid' any divisor which is not completely rigid, therefore including in this set also the Wilson divisors ($h^{0,2} = 0$).

as well as the one of [108], refers to triangulations and different triangulations may correspond to the same favorable Calabi-Yau geometry (in [108], e.g. the number of proper involutions in distinct geometries reduces to 5 660). The CICY orientifolds in [169] are instead computed at the level of distinct geometries.

7.4 Hodge and Euler numbers of toric divisors for models with $h^{1,1} \leq 6$

In this section we investigate the topology of the individual toric divisors that we find in the models (with $h^{1,1} \leq 6$) collected in the database.

An overview of the divisor topologies for each $h^{1,1}$ (including the available data up to $h^{1,1} = 12$) is given in Tab. 7.3. The first part contains the distribution of the del Pezzo divisors, where we also count how many of them are diagonal. Notice in particular that our analysis allows us to extend the conjecture proposed in [145] about the presence of diagonal dP_n divisors with $1 \leq n \leq 5$ (see Sec. 5.1.1) to all FRSTs with $h^{1,1} = 6, 7$. In the second part of the table we summarize, instead, the different topologies of divisors that we

encountered in the scan: the reason why we distinguish between deformation divisors with $h^{0,2} = 1$ and $h^{0,2} > 1$ will be clear in Sec. 7.5.

In Fig. 7.1, we show the distribution of the various Hodge numbers of divisors, omitting the data for $h^{0,0}$ (which is always equal to 1 in a compact connected Kähler manifold). In the same figure, we present also the correlation plot between the various Hodge numbers, from which we can deduce additional interesting features. The correlation between $\chi(D)$ and the Hodge numbers of D is clear from Eq. (5.18): it decreases as $h^{0,1}(D)$ increases (negative correlation), while it increases as $h^{1,2}(D)$ and/or $h^{1,1}(D)$ increases (strong positive correlation). We observe no significant correlation between $h^{1,1}(X)$ and the other variables reported in the correlation plot, which is why we didn't include it. We notice instead an interesting anti-correlation between $h^{0,1}(D)$ and $h^{0,2}(D), h^{1,1}(D)$, which in turn are strongly correlated between themselves. Looking again at Eq. (5.18), we conclude therefore that larger $h^{1,1}(D)$ implies larger $h^{0,2}$ and smaller $h^{0,1}(D)$, hence larger $\chi(D)$ (which is what we observe also in the correlation between $\chi(D)$ and the other Hodge numbers). Finally, we notice a correlation of $\chi(D)$ and $\chi(4D)$ with $h^{1,2}(X)$ which will be confirmed by the subsequent analysis.

Fig. 7.2 reports the distribution of the Euler characteristic for different divisor topologies. As it is clear from the expressions for the $D3$-charges (5.41), (5.57) and (5.58), a large (in absolute value) contribution is obtained when the Euler characteristic of the corresponding divisor is large. From the results of the database we find the maximal value

$$\chi(D)_{\text{max}} = 549\,, \tag{7.8}$$

which is obtained for a deformation divisor. In general, indeed, deformation divisors provide the largest contributions to the charge, while the maximum value for (completely) rigid divisors turns out to be $\chi(D_{\text{rigid}})_{\text{max}} = 111$. This feature is easily understood by looking again at (5.18) and recalling that while both completely rigid and deformation divisors have $h^{0,1} = 0$ (which eliminates the negative term in $\chi(D)$), deformation divisors, unlike the rigid ones, have $h^{0,2} \neq 0$, which increases the value of the Euler characteristic. Finally, we notice that the divisors with negative Euler characteristic are always Wilson divisors ($h^{0,1}(D) > 0$ and $h^{0,2}(D) = 0$), out of which 44.67% are Exact-Wilson divisors ($h^{0,1}(D) = 1$).

$h^{1,1}$		2	3	4	5	6	7	8	9	10	11	12
dP_n (ddP_n)	dP_0 (ddP_0)	10 (*)	117 (*)	1 282 (*)	15 346 (*)	172 469 (*)	526 (*)	656 (*)	1 135 (*)	1 049 (*)	1 424 (*)	2 086 (*)
	dP_1 (ddP_1)	5 (3)	159 (47)	2 677 (726)	39 355 (8 880)	514 099 (93 000)	4 994 (59)	8 743 (34)	15 007 (61)	20 346 (35)	28 962 (87)	31 671 (49)
	dP_2 (ddP_2)	0 (0)	6 (0)	438 (0)	10 926 (0)	184 992 (0)	2 822 (0)	6 060 (0)	10 176 (0)	15 104(0)	22 350 (0)	23 178 (0)
	dP_3 (ddP_3)	0 (0)	6 (0)	359 (0)	9 211 (0)	166 494 (0)	2 182 (0)	4 375 (0)	7 004 (0)	10 850 (0)	15 618 (0)	17 495 (0)
	dP_4 (ddP_4)	0 (0)	2 (0)	78 (0)	2 227 (0)	50 821 (0)	1 119 (0)	2 196 (0)	3 894 (0)	5 851 (0)	8 533 (0)	8 613 (0)
	dP_5 (ddP_5)	0 (0)	15 (0)	524 (0)	9 482 (0)	144 966 (0)	1 499 (0)	2 487 (0)	3 808 (0)	5 612 (0)	7 689 (0)	8 226 (0)
	dP_6 (ddP_6)	3 (3)	37 (31)	418 (201)	5 714 (1 214)	81 636 (4 719)	959 (0)	1 611 (0)	2 492 (0)	3 412 (0)	5 569 (20)	5 839 (0)
	dP_7 (ddP_7)	6 (6)	134 (92)	2 060 (939)	26 032 (6 158)	302 879 (38 692)	1 841 (23)	2 686 (12)	4 063 (21)	4 822 (9)	6 735 (0)	6 933 (12)
	dP_8 (ddP_8)	7 (7)	134 (83)	1 806 (584)	22 442 (3 458)	269 626 (24 109)	1 722 (41)	2 356 (82)	3 283 (91)	4 149 (67)	4 872 (21)	4 654 (66)
divisor topologies	rigid	52	1 164	20 339	297 112	3 840 467	34 423	58 138	94 621	126 190	178 320	187 751
	$h^{0,2} = 1$	50	924	8 931	86 418	798 972	6 065	8 431	10 555	12 941	15 501	15 550
	$h^{0,2} > 1$	181	1 444	11 486	101 911	910 903	7 689	12 121	18 008	22 478	29 611	27 825
	Wilson	5	143	1 884	24 985	292 468	1 983	4 074	6 400	9 037	12 788	15 754

Table 7.3: Top: Distribution of dP_n and diagonal ddP_n divisors. For $\mathrm{dP}_0 = \mathbb{P}^2$ we write (*) because it always appears diagonally. For $h^{1,1} \geq 7$, as usual, the data are obtained from random runs. Bottom: Classification of the topologies of toric divisors encountered in the scan.

7.5 $D3$-charge in the database and non-local $D7$-tadpole cancellation

Let us now use our database to compute the $D3$-charge of different $O7/D7$ configurations. To begin with, we consider only the contribution from O-planes, which is summarized, for each value of $h^{1,1}$, in the plots of Fig. 7.3. Notice that the lower diagonal line corresponds to models with $h^{1,2}_{+}(X_3) = 0$, which is in complete agreement with Eq. (7.3), according to which non-vanishing values of $h^{1,2}_{+}(X_3)$ decrease the (absolute value of the) $D3$-charge and for $h^{1,2}_{+} = 0$, $Q_{D3} \sim -\dfrac{h^{1,2}_{-}}{3}$. A similar behavior was also argued from the correlation between the Euler characteristic $\chi(D)$ and $h^{1,2}(X_3)$ in Fig. 7.1. We find the maximal contribution coming from O-planes for the model $(h^{1,1}, h^{1,2}_{-}, h^{1,2}_{+}) = (11, 491, 0)$, for which:

$$Q^{Op}_{\rm min} = -168\,. \tag{7.9}$$

As concerns $D7$-branes, since we want to maximize the D3-charge contribution, we need to study the topology of each divisor which is wrapped by an orientifold plane in order to determine whether it is possible to cancel its $D7$-tadpole by means of a Whitney brane. If this is not possible, we compensate the $D7$-charge with the usual SO(8) stacks of $D7$-branes. To be more specific:

- If the $O7$-plane wraps a completely rigid divisor, the generic equation of the Whitney brane is forced to split in two stacks of $(4+4)$ $D7$-branes, supporting a SO(8) gauge group (see (5.49)). The same is true for a Wilson divisor.
- If the $O7$-plane wraps a divisor with $h^{0,2}(D) > 1$, it is always possible to cancel the $D7$-tadpole non-locally, through a Whitney brane.
- The case of divisors with $h^{0,2}(D) = 1$ is more subtle and model dependent. For these configurations, therefore, we explicitly construct the equation of the Whitney brane and we check whether it factorizes. If no factorization is forced, we add a Whitney brane. In Sec. 7.5.1 we show two interesting explicit examples of this kind.

In Tab. 7.4 we compare the total $D3$-charge contribution (in the absence of fluxes) that can be obtained for a given $h^{1,1}$ when we cancel the $D7$-tadpole either locally or non-locally. More precisely, the local $D3$-charge contribution is obtained by canceling *all* the $D7$-tadpoles with SO(8) stacks, regardless the topology of the corresponding divisor. The non-local contribution is instead obtained by placing a Whitney brane on top of every $O7$-plane wrapping a non-rigid divisor (and, of course, a SO(8) stack on the rigid ones). We perform this computation for each model with a given $h^{1,1}$ and we select the case with the largest $D3$-charge contribution, which is the one reported in the table. It is clear that non-local $D7$-tadpole cancellation significantly enhances (of an average factor of 13) the $D3$-tadpole contribution with respect to local configurations.

We notice in particular that the upper bound for local $D7$-charge cancellation found in Tab. 7.4 (at $h^{1,1} = 11$), precisely matches the estimation done in (7.5). This bound is

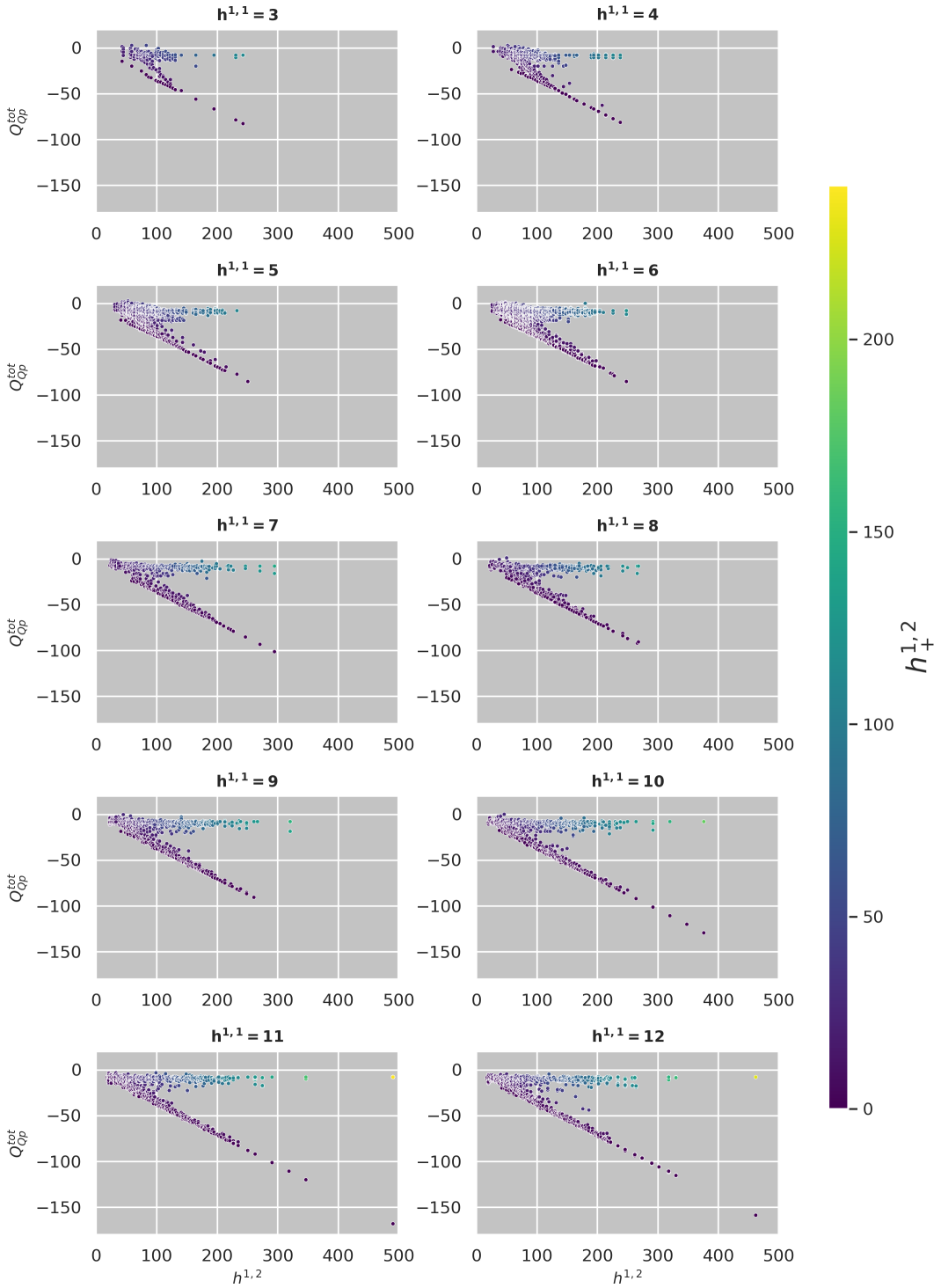

Figure 7.3: Overview of the $D3$-charge contribution from Op-planes. The data are complete for $h^{1,1} \leq 6$ (see Tab. 7.1), while for $h^{1,1} \geq 7$ we refer to the models collected in Tab. 7.2. Different colors indicate different values of $h_+^{1,2}$ and we have omitted models with positive charge.

$h^{1,1}$		2	3	4	5	6
D3-charges $\lvert Q_{\rm D3}\rvert$	local	276	248	244	256	256
	non-local	3678	3272	3212	3280	3280

$h^{1,1}$		7	8	9	10	11	12
D3-charges $\lvert Q_{\rm D3}\rvert$	local	304	276	272	388	504	476
	non-local	4000	3594	3408	5036	6664	6258

Table 7.4: Comparison between local and non-local $D7$-tadpole cancellation for different values of $h^{1,1}$.

enhanced in presence of non-local configurations, where we find:

$$-Q_{D3}^{\rm non-local} \leq 6664\,. \tag{7.10}$$

In general, the models with the minimal $D3$-charge contribution from Op-planes (corresponding to the diagonal line in Fig. 7.3) do not contain $O3$-planes and are therefore not suitable for $\overline{D3}$ uplift (though they admit, e.g., a T-brane background). Given the focus of this thesis on this uplifting mechanism, it is useful to report also the maximal $D3$-charge obtained for an orientifold model with two or more 'collapsable'[8] $O3$-planes. We find:

$$-Q_{D3}^{\overline{\rm D3}\ \rm uplift} \leq 3592\,, \tag{7.11}$$

with the maximal value obtained in the model with $(h^{1,1}, h^{1,2}_{-}) = (12, 274)$. We observe that, though smaller than (7.10), it is still quite a large value compared to previous bounds, based on local tadpole cancellation.

We stress again that this analysis does not take into account any flux contribution. The fluxes can either decrease the (absolute value of the) total $D3$-charge (e.g the flux on the Whitney brane, see (5.63)) or increase it (e.g. fluxes generating a non-vanishing FI-term inducing a T-brane background). When considering an explicit model, these fluxes need to be taken into account. However, as explained before, we do not expect them to change the order of magnitude of our estimations.

Let us conclude our analysis of local and non-local tadpole cancellation by directly comparing the contributions to the $D3$-charge provided by a SO(8) stack and a Whitney brane on a single divisor D, that is (in the absence of fluxes):

$$Q_{\rm SO(8)}(D) = -(4+4)\cdot\frac{\chi(D)}{24}\,; \qquad Q_{\rm W}(D) \simeq -\frac{\chi(4D)}{12} - 9\int_X D^3\,. \tag{7.12}$$

In this case, we consider only the divisors *always* admitting both configurations, that is the ones with Hodge numbers $h^{0,2}(D) > 1$ and $h^{0,1}(D) = 0$. The results of this comparison

[8] See the caption of Fig. 5.2 for the meaning of 'collapsable' $O3$-planes in this context.

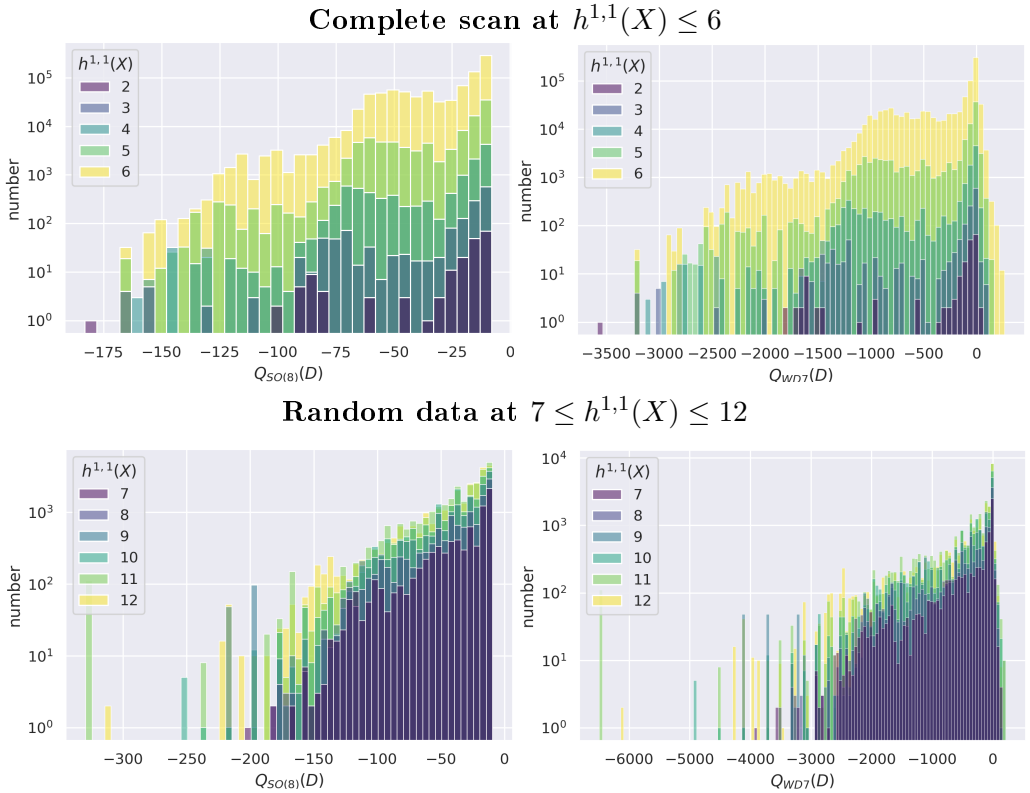

Figure 7.4: Local vs non-local tadpole cancellation. The two histograms on the left show the distribution of $Q_{\mathrm{SO}(8)}(D)$, while the ones on the right present $Q_{\mathrm{W}}(D)$. In both cases we consider only divisors with $h^{0,2}(D) > 1$ and $h^{0,1}(D) = 0$ (therefore admitting both branes configurations). We distinguish the data obtained from the complete scan at $h^{1,1}(X_3) \leq 6$ (top) and the random ones for $7 \leq h^{1,1}(X_3) \leq 12$.

are plotted in Fig. 7.4. The maximal $D3$-charge contribution from $D7$-branes on a single divisor turns out to be:

$$|Q_{\mathrm{SO}(8)}(D)|_{\max} = \begin{cases} 183 \\ 329.3 \end{cases} \quad ; \quad |Q_{\mathrm{W}}(D)|_{\max} = \begin{cases} 3585 & h^{1,1}(X) \leq 6 \\ 6489.3 & 7 \leq h^{1,1}(X) \leq 12 \end{cases} .$$

Finally, the values of the average $D3$-charge obtained for each $h^{1,1}$ with both sources are collected in Tab. 7.5. Also from this analysis we notice a significant enhancement of $Q_{\mathrm{W}}(D)$, in this case by an average factor of 11.

7.5.1 Examples with Whitney branes

In this section we present two simple Calabi-Yau threefolds wth $h^{1,1} = 3$, containing toric divisors with different topologies. For each divisor D_i, we study the locus:

$$\eta_i^2 - z_i^2 \chi_i = 0 \tag{7.13}$$

describing, as we know, a Whitney brane, and we check whether the explicit form of the polynomials η_i and χ_i forces the brane to factorize. As anticipated in the previous

section, this analysis suggests that divisors with $h^{0,2} > 0$ always admit a fully non-local Whitney brane, while divisors with $h^{0,2} = 1$, need to be checked case by case, since the (possible) factorization depends on the weights matrix of the ambient space in which the CY is defined. The two examples below are chosen precisely because they both contain a non-rigid divisor with $h^{0,2} = 1$, but only one of the two admits a proper Whitney brane on such divisor.

Notice, however, that usually we are interested in the divisor with the highest weights (since it maximizes $-Q_{D3}$), which generically have $h^{0,2}, h^{1,1} \gg 1$ (and therefore a Whitney brane).

Example 1: a SO(8) stack for a non-rigid SD_1 divisor

The first example we consider is the CY defined in the variety:

z_1	z_2	z_3	z_4	z_5	z_6	z_7	D_H
0	0	1	1	1	1	4	8
0	1	0	0	1	1	3	6
1	0	1	0	1	2	5	10

$$\text{SR} = \{z_1 z_6, z_2 z_5, z_3 z_4 z_7\}\,. \tag{7.14}$$

This model can be found also in the database [106] (ID#237, triangulation #1). The Hodge numbers (which in this case can be equivalently computed either via `CohomCalg` or with the procedure exposed in Sec. 5.1.1) are:

$$\begin{aligned} &h^\bullet(D_1) = \{1,0,0,9\}, \quad h^\bullet(D_2) = \{1,0,0,8\}, \quad h^\bullet(D_3) = \{1,0,1,21\}\,, \\ &h^\bullet(D_4) = \{1,0,0,12\}, \quad h^\bullet(D_5) = \{1,0,2,29\}, \quad h^\bullet(D_6) = \{1,0,3,38\}\,, \\ &h^\bullet(D_7) = \{1,0,26,177\}\,. \end{aligned} \tag{7.15}$$

Hence we have three rigid divisors (D_1 is a dP_8, D_2 a dP_7 and D_4 a rigid but not del Pezzo NdP_{11}), a special deformation divisor SD_1 (D_3) and three non-rigid deformation divisors D_5, D_6, D_7, with $h^{0,2} > 1$.

As usual, the rigid divisors are such that the locus (7.13) is always forced to factorize as $\eta_i = z_i^4$, $\chi_i = z_i^6$ ($i \in \{1,2,4\}$), corresponding to the standard SO(8) stacks. On the other side, the locus on the divisors D_5, D_6 and D_7 is described by generic polynomials, hence we can cancel the corresponding possible $D7$-charge with Whitney branes.

Let us instead consider the more interesting case of the divisor SD_1, corresponding to $z_3 = 0$. The only ($h^{0,2}(D_3) = 1$) possible deformation of the defining equation of D_3 can be determined by looking at the GLSM weights (7.14). Since the coordinate z_3 has weights $(1,0,1)$, only deformations involving coordinates with weights $(*,0,*)$ can be considered, that is only combinations of z_1 and z_4. In particular, the defining equation for D_3, can be equivalently written as:

$$[D_3] \;:\; z_3 + \alpha z_1 z_4 = 0\,. \tag{7.16}$$

which is indeed the only possible deformation of D_3.

The Whitney brane, if present, must wrap a divisor in the class $8[D_3]$, with degrees $(8,0,8)$. A generic element of this class can be derived by (7.16) and it is described by the

equation:

$$P_8(z_3,\, z_1 z_4) \equiv \sum_{i=0}^{8} \alpha_i\, z_3^i\, (z_1 z_4)^{8-i} = 0\,, \tag{7.17}$$

where P_8 is a homogeneous polynomial of degree 8, in two variables, which clearly admits precisely 8 zeroes. If we impose the invariance under the involution $z_3 \mapsto -z_3$, indeed, all the odd powers of z_3 are ruled out, as well as the odd powers of $z_1 z_4$ (as it is manifest from (7.17)) and the equation can be recast to:

$$\prod_{i=1}^{4} (z_3 - \beta_i(z_1 z_4))(z_3 + \beta_i(z_1 z_4)) = 0\,. \tag{7.18}$$

Being a valid description of *any* invariant representative of the class $8[D_3]$, the above equation is also suitable to define the Whitney brane in this class, which therefore is forced to factorize into 4 pairs of brane/image brane that can in principle intersect each other.

The reason why the case $h^{0,2} = 1$ is somehow special, is that there is the possibility that the GLSM matrix is such that the divisor class $[D]$ has a representative of the form (7.16), but e.g. the class $2[D_3]$ (hence also the class $8[D_3]$) admits additional deformations spoiling the factorization. This would have happened, as an example, if the model under consideration had included an additional coordinate with degrees $(2, 0, 1)$. In this case, a generic representative of the class $2[D_3]$, would have been:

$$z_3^2 + \alpha_1 z_3 z_1 z_4 + \alpha_2 (z_1 z_4)^2 + \beta z_0 z_1 = 0 \tag{7.19}$$

where the presence of $z_0 z_1$ spoils the factorization. Nothing forbids the existence of this kind of coordinates in the KS database: an explicit example is provided in the next section.

Example 2: Whitney brane on a divisor with $h^{0,2} = 1$

We consider the model:

z_1	z_2	z_3	z_4	z_5	z_6	z_7	D_H
0	0	1	1	1	2	1	6
0	1	0	0	1	1	0	3
1	0	2	3	2	4	0	12

$$\text{SR} = \{z_1 z_4, z_2 z_5, z_3 z_6 z_7\}\,. \tag{7.20}$$

corresponding to ID#57 (triangulation #3) in [106] and whose toric divisors have the Hodge numbers:

$$\begin{aligned} &h^\bullet(D_1) = \{1,0,0,10\}, \quad h^\bullet(D_2) = \{1,0,0,8\}, \quad h^\bullet(D_3) = \{1,0,1,20\}\,, \\ &h^\bullet(D_4) = \{1,0,2,30\}, \quad h^\bullet(D_5) = \{1,0,2,28\}, \quad h^\bullet(D_6) = \{1,0,6,56\}\,, \\ &h^\bullet(D_7) = \{1,1,0,2\}\,. \end{aligned} \tag{7.21}$$

Hence, D_1 is a rigid but not del Pezzo NdP_9, D_2 is a dP_7 and D_7 is a Wilson divisor (all of them support the usual SO(8) stacks). Furthermore, D_4 is a special deformation

Complete scan at $h^{1,1} \leq 6$			**Random data at** $h^{1,1} \leq 12$		
$h^{1,1}(X_3)$	$Q_{\mathrm{SO}(8)}(D)$	$Q_{\mathrm{WD7}}(D)$	$h^{1,1}(X_3)$	$Q_{\mathrm{SO}(8)}(D)$	$Q_{\mathrm{WD7}}(D)$
2	−25.82	−269.77	7	−35.21	−391.76
3	−28.31	−316.69	8	−37.82	−428.97
4	−29.78	−342.26	9	−40.12	−458.18
5	−30.27	−344.21	10	−40.27	−457.08
6	−30.53	−339.49	11	−42.90	−497.89
7	−30.16	−321.89	12	−42.23	−480.87

Table 7.5: Average $D3$-charge contribution for local and non-local $D7$-tadpole cancellation.

divisor SD_2, while D_5 and D_6 are other non-rigid deformation divisors (admitting a generic Whitney brane). Finally, D_3 has the Hodge numbers of a K3 (but it is not, see Sec. 5.1.1, because $D_3^2 D_i = 2$ for $i = 2, 5, 6$).

Let us analyze this last divisor similarly to what we did in the previous section. The representative of the class $D_3 : \{z_3 = 3\}$ admits only the deformation

$$z_3 = \alpha z_1^2 z_7 = 0\,, \tag{7.22}$$

hence, again, $h^{0,2} = 1$. In this case, however, the representation of the class $2[D_3]$ may also include the coordinate z_4:

$$z_3^2 + \alpha_1 z_3 z_1^2 z_7 + \alpha_2 (z_1^2 z_7)^2 + \beta z_1 z_4 z_7 = 0\,, \tag{7.23}$$

from which we can deduce the generic expression for a representative of the class $8[D_3]$:

$$\sum_{i=0}^{8} \sum_{j=0}^{4} \alpha_{ij} z_3^{8-i-2j} (z_1^2 z_7)^i \, (z_1 z_4 z_7)^j = 0 \tag{7.24}$$

which is a non-factorisable non-homogeneous polynomial in three coordinates. Hence the equation (7.24) is compatible with the presence of a fully recombined Whitney brane in the class $8[D_3]$.

Notice that for a proper K3 divisor, we expect, to find an analogous situation to (7.18), where, furthermore, the branes do not intersect each other ($U(1)^4$ configuration). The fact that the Whitney brane is not factorisable in this case is therefore an additional signal of the fact that the divisor under consideration is not a K3.

7.5.2 Large $D3$-charge and genus-one fibrations

Looking at the plots in Fig. 7.3, we notice that while the data at small $h^{1,2}$ do not present any particular structure, an interesting trend appears for $h^{1,2} > 100$, where we clearly observe two distinct dominant lines. We believe that this emergent structure in the distribution of $D3$-charges has not yet been observed in the literature.

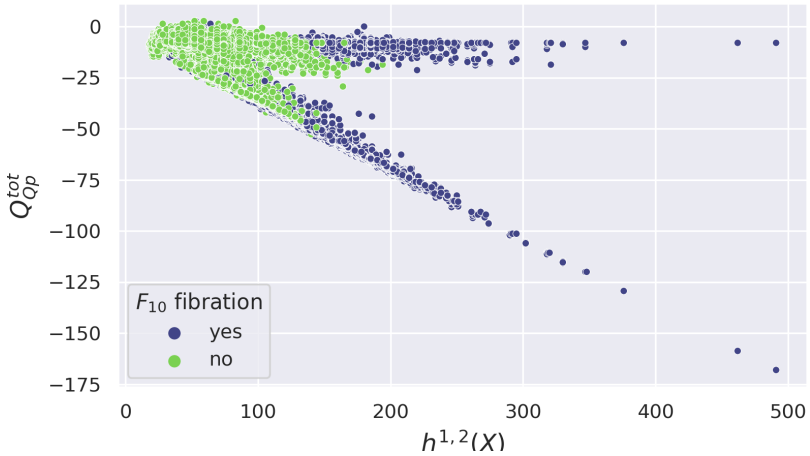

Figure 7.5: $D3$-charge contributions from orientifold planes with $h^{1,1} \leq 12$ as a function of $h^{1,2}(X_3)$. The two different colors distinguish the models associated to a F_{10} fibration (blue) from all the others.

An explanation of this distribution can be found in the fact that it has been observed that a very large fraction of the set of known Calabi-Yau threefolds, especially the ones with large Hodge numbers, is composed by genus-one fibrations (most of which are elliptic fibrations i.e. genus one fibrations with a global section) over complex base surfaces. First, comparing the elliptically fibered toric CY threefolds that can be constructed with F-theory based methods and CY hypersurfaces obtained from reflexive polytopes as described in Sec. 5.1, the authors of [178] found an exact match for all Hodge number pairs with $h^{1,2} \geq 240$ (or $h^{1,1} \geq 240$). This means that all CY manifolds which are hypersurfaces in toric varieties with the above Hodge numbers are reproduced by elliptically fibered Calabi-Yau's over some explicitly determined base surface. Furthermore, in [179] a complementary approach, based on the analysis of *fibered polytopes*[9] led to the observation that all the CY threefolds with $h^{1,2}(h^{1,1}) \geq 150$ admit an explicit genus one fibration and all the ones with $h^{1,1} \geq 195$ or $h^{1,2} \geq 228$ show an elliptic fibration. Finally, in [181] a systematic analysis of all the 473.8 million reflexive polytopes of the Kreuzer Skarke database [105] confirms that the 99.994% of all known CYs constructed as toric hypersurfaces are birationally equivalent to a CY with an elliptic or genus one fibration. In other words, only 29 223 of these polytopes are not fibered[10]. Similar results have been found also for CICY threefolds [182, 183].

The 16 2d reflexive polytopes [184] (see also Appendix A of [185]) correspond to 16 distinct types of genus one fibrations F_i. The Kreuzer-Skarke database, appears to be

[9] A fibered polytope is a (4d) polytope Δ° in the N lattice containing a lower dimensional (2d) sub-polytope which passes through the origin and is itself a reflexive polytope. A fibered polytope is compatible with the presence of a genus one fibration for the associated CY threefold [180] (with the fiber defined on the surface obtained from the sub-polytope), though in [181] it was stressed that there are some subtleties occuring when relating the fibration of the polytopes to the actual toric variety.

[10] In our analysis, we encountered 2 857 of these polytopes in the complete data at $h^{1,1} \leq 7$ and 60 in the random ones at $7 < h^{1,1} \leq 12$.

dominated, at least at large Hodge numbers, by polytopes associated to a standard F_{10} fibration, whose elliptic fiber is defined on the weighted projective space $\mathbb{CP}^2_{[2,3,1]}$ [178]. We checked this feature also for the favorable 4d polytopes of our database, computing the 2d sub-polytopes and the fibration type of each of them (by means of the algorithm of [181]), verifying that the presence of F_{10} is indeed dominant, especially at $h^{1,2} \gtrsim 200$. Not surprisingly, precisely this fibration structure turns out to be responsible for the trend observed in Fig. 7.3, as we checked by computing the charge distribution for the different types of fibres. This is particularly evident in Fig. 7.5, where we show again the charge distribution from Op-planes, distinguishing models corresponding to F_{10} fibrations from all the others: the former clearly dominate at large $h^{1,2}$, regardless the value of $h^{1,1}$. In the regime $h^{1,2} < 200$, similar sub-dominant patterns are found also for elliptic F_6 and F_8 as well as non-elliptic F_4 fibrations, while all the others show an approximately constant distribution of the $D3$-charge, as a function of $h^{1,2}$.

Let us analyze in more detail what happens in the F_{10} case, where the equation of the CY takes the Weierstrass form:

$$y^2 = x^3 + f(w)xz^4 + g(w)z^6 \,. \tag{7.25}$$

Here, w denotes the set of coordinates on the toric 2d base $\mathcal{B}$ and x, y, z are projective coordinates on $\mathbb{CP}^2_{[2,3,1]}$. The CY condition on the total space X_3 requires f and g to be sections of $\mathcal{O}(-4K_{\mathcal{B}})$ and $\mathcal{O}(-6K_{\mathcal{B}})$, where $K_{\mathcal{B}}$ is the canonical class of the base $\mathcal{B}$.

At fixed w, the above equation describes a torus, whose $\mathbb{Z}_2$ involution (with four fixed points) is implemented by taking either $y \mapsto -y$ or $z \mapsto -z$ (notice that the equation written in the Weierstrass form is automatically invariant under these involutions). In particular, the toric coordinate y has clearly a high degree (and it is in fact the coordinate with the highest degree among the ones of the considered threefold). As a consequence, the corresponding divisor D_y has a large Euler characteristic, which is the main reason why we find the largest $D3$-charges for these models.

It is interesting to notice that we may also add to (7.25) a term of the form $a(w)x^2z^2$, which would allow us to consider also the involution $x \mapsto -x$. Given that the degree of x is also large, one would expect a large contribution to the $D3$-charge in this case as well, even if lower than the one coming from $y \mapsto -y$. However, in this case the invariant equation of the CY would read:

$$y^2 = (a(w)x^2 + g(w)z^4)z^2 \,, \tag{7.26}$$

which has a manifest (non crepantly resolvable) singularity at $z = y = 0$. This singularity can not be deduced by the topological invariants of the $D7/O7$'s since they do not touch it ($xyz \in SR$). However, this kind of situation was excluded from our analysis thanks to the check on the polytope Δ_k associated to the invariant equation, which in this case is not reflexive[11]. If we had included such models, we would have obtained a second diagonal line in the plots of Fig. 7.3.

[11] This is due to the fact that the monomial x^3, which we need to rule out in order to get an invariant equation, is associated with a vertex of the full polytope Δ.

A simple example of CY with genus one fibrations: $\mathbb{CP}^2_{[1,1,1,6,9]}$

Let us apply the argument described above to the very simple example of the degree 18 hypersurface $\mathbb{CP}^2_{[1,1,1,6,9]}$[186, 187], which has also an important role in LVS [12].

The corresponding ambient space is described by the weights matrix:

	z_1	z_2	z_3	z_4	z_5	z_6	D_H
$\mathbb{C}^*_1$	1	1	1	6	9	0	18
$\mathbb{C}^*_2$	0	0	0	2	3	1	6

(7.27)

from which it is manifest the presence of an elliptic fibration over the base $\mathcal{B} = \mathbb{CP}^2$ (parametrized by the coordinates z_1, z_2, z_3), with fibre F_{10} (hypersurface in $\mathbb{CP}^2_{[2,3,1]}$), parametrized by z_5, z_6, z_7.

The SR ideal is:

$$I_{\rm SR} = \{z_1 z_2 z_3, z_4 z_5 z_6\} \tag{7.28}$$

and the divisors have topology:

$$\begin{aligned}
&h^\bullet(D_i) = \{1,0,2,30\}, && \chi(D_i) = 36, \quad i = 1,2,3 \quad (SD_2)\,,\\
&h^\bullet(D_4) = \{1,0,28,218\}, && \chi(D_4) = 276\,,\\
&h^\bullet(D_5) = \{1,0,65,417\}, && \chi(D_5) = 549\,,\\
&h^\bullet(D_6) = \{1,0,0,1\}, && \chi(D_6) = 3 \quad (dP_0)\,.
\end{aligned} \tag{7.29}$$

Finally, it has Hodge numbers $(h^{1,1}, h^{1,2}) = (2, 272)$ and Euler characteristic $\chi(X) = -540$.

From the weights matrix (7.27), we can deduce the most general CY equation with degrees D_H, which reads:

$$\begin{aligned}
z_5^2 = z_4^3 &+ h_9(z_1,z_2,z_3)\, z_5 z_6^3 + h_{12}(z_1,z_2,z_3) z_4 z_6^4 + h_{18}(z_1,z_2,z_3) z_6^6\\
&+ h_3(z_1,z_2,z_3) z_4 z_5 z_6 + h_6(z_1,z_2,z_3) z_4^2 z_6^2\,,
\end{aligned} \tag{7.30}$$

where the $h_n(z_1, z_2, z_3)$ are homogeneous polynomials of degree n in the coordinates of the $\mathbb{CP}^2$ base. Notice that the polynomials h_{3n} are sections of $\mathcal{O}(-nK_{\mathcal{B}})$ and that the equation (7.30) can be brought to the Weierstrass form (7.25)

$$z_5^2 = z_4^3 + f(z_1,z_2,z_3) z_4 z_6^4 + g(z_1 z_2, z_3) z_6^6$$

through two subsequent coordinate changes.

Following the notation of [186], we define $D_4 = 2H$, $D_5 = 3H$ and $D_i = L$, $i = 1, 2, 3$, from which it follows $D_6 = H - 3L$. In terms of the basis L, H the intersection polynomial reads:

$$I_3 = L^2 H + 3L\, H^2 + 9H^3\,. \tag{7.31}$$

The orientifolds obtained by inverting each of the six coordinates z_i can be grouped in three classes, which are representative of the three categories that one generically finds for F_{10} fibrations:

1. *Reflection along the base* $\mathcal{B}$: $z_i \mapsto -z_i$, $i = 1, 2, 3$. The orientifold presents an $O7$-plane wrapping D_i, an $O3$-plane at $z_j = z_k = z_6 = 0$ and three $O3$-planes at $z_j = z_k = z_5 = 0$ [12]. The corresponding Hodge numbers are $(h^{1,2}_+, h^{1,2}_-) = (128, 144)$.

[12] $(i,j,k) \in \{(1,2,3),(2,3,1),(3,1,2)\}$.

The $D3$-charge contribution from the Op-planes reads: $Q_{Op}^{\text{tot}} = -\frac{36}{6} - \frac{4}{2} = -8$. This is, as expected, the minimal $D3$-charge contribution.

2. *Reflection* $z_4 \mapsto -z_4$. There is only an $O7$-plane wrapping D_4 and the Hodge numbers are $(h_+^{1,2}, h_-^{1,2}) = (69, 203)$.

   The $D3$-charge contribution from the Op-planes is $Q_{Op} = -\frac{276}{6} = -46$.

   It is important to notice that the fibre $\mathbb{CP}^2_{[2,3,1]}$ is invariant under this involution only when it degenerates to:

   $$z_5^2 = z_6^2(az_4^2 + bz_6^4)\,. \tag{7.32}$$

   This singularity is inherited by the CY, but the $O7$-plane wrapping D_4 does not touch it ($z_4 z_5 z_6 \in SR$).

3. *Reflection along the fibre* $z_i \mapsto -z_i$, $i = 5, 6$. There are two $O7$-planes wrapping D_5 and D_6 respectively. The Hodge numbers are $(h_+^{1,2}, h_-^{1,2}) = (0, 272)$.

   The $D3$-charge contribution from the Op-planes is $Q_{Op} = -\frac{549}{6} - \frac{3}{6} = -92$.

   This is the class providing the largest contribution to the $D3$-charge, corresponding to the $\mathbb{Z}_2$ involution of the torus, with 4 fixed points in the fiber (fibering these points over the base we obtain the divisors D_5 and D_6, which are wrapped by $O7$-planes).

7.6 Example with $(h^{1,1}, h^{1,2}) = (11, 491)$

In this section, we consider the model for which we observe the largest possible contribution to the $D3$-charge (both from local and non-local tadpole cancellation), see Tab. 7.4.

Such large contribution comes from an involution of a CY threefold X_3 with Hodge numbers $(h^{1,1}, h^{1,2}) = (11, 491)$ and Euler characteristic $\chi(X) = -960$. The ambient space in which the hypersurface is embedded is defined by the following weights matrix:

z_1	z_2	z_3	z_4	z_5	z_6	z_7	z_8	z_9	z_{10}	z_{11}	z_{12}	z_{13}	z_{14}	z_{15}	D_H
1	1	12	28	42	0	0	0	0	0	0	0	0	0	0	84
0	0	6	14	21	1	0	0	0	0	0	0	0	0	0	42
0	0	5	12	18	0	1	0	0	0	0	0	0	0	0	36
0	0	4	10	15	0	0	1	0	0	0	0	0	0	0	30
0	0	4	9	14	0	0	0	1	0	0	0	0	0	0	28
0	0	3	8	12	0	0	0	0	1	0	0	0	0	0	24
0	0	3	7	10	0	0	0	0	0	1	0	0	0	0	21
0	0	2	6	9	0	0	0	0	0	0	1	0	0	0	18
0	0	2	4	7	0	0	0	0	0	0	0	1	0	0	14
0	0	1	4	6	0	0	0	0	0	0	0	0	1	0	12
0	0	0	2	3	0	0	0	0	0	0	0	0	0	1	6

with SR-ideal:

$$\begin{aligned} I_{\rm SR} = \{&z_1z_2, z_3z_6, z_3z_7, z_3z_8, z_3z_9, z_3z_{10}, z_3z_{11}, z_3z_{12}, z_3z_{13}, z_3z_{14}, z_4z_6, z_4z_7, z_4z_8, \\ &z_4z_9, z_4z_{10}, z_4z_{11}, z_4z_{12}, z_4z_{14}, z_5z_6, z_5z_7, z_5z_8, z_5z_9, z_5z_{10}, z_5z_{12}, z_6z_8, z_6z_{10}, \\ &z_6z_{12}, z_6z_{13}, z_6z_{14}, z_6z_{15}, z_7z_{10}, z_7z_{12}, z_7z_{13}, z_7z_{14}, z_7z_{15}, z_8z_{12}, z_8z_{13}, z_8z_{14}, \\ &z_8z_{15}, z_9z_{12}, z_9z_{14}, z_9z_{15}, z_{10}z_{14}, z_{10}z_{15}, z_{11}z_{15}, z_{12}z_{15}, z_4z_5z_{15}, z_5z_{13}z_{14}, \\ &z_5z_{13}z_{15}, z_7z_9z_{11}, z_8z_9z_{11}, z_9z_{10}z_{11}, z_{10}z_{11}z_{13}, z_{11}z_{12}z_{13}, z_{11}z_{13}z_{14}\} \end{aligned} \tag{7.33}$$

and second Chern numbers:

$$\Pi_i = \int_{D_i} c_2(X) = \{24, 24, 168, 368, 548, -4, -4, -4, -4, -4, -4, -4, -4, -4\}\,. \tag{7.34}$$

Computing the Hodge numbers of the divisors, we find that D_1 and D_2 are K3 divisors:

$$h^\bullet(D_1) = h^\bullet(D_2) = \{1, 0, 1, 20\}\,, \quad \chi(D_i) = 24\,;$$

all the divisors D_i with $i = 6, ..., 15$ are (non-diagonal) dP_1:

$$h^\bullet(D_i) = \{1, 0, 0, 2\}, \quad i = 6, \ldots, 15\,,$$

and D_3, D_4, D_5 are deformation divisors with Hodge numbers:

$$\begin{aligned} &h^\bullet(D_3) = \{1, 0, 13, 140\}, \quad h^\bullet(D_4) = \{1, 0, 51, 392\}, \quad h^\bullet(D_5) = \{1, 0, 118, 750\} \\ &\chi(D_3) = 168 \qquad\qquad \chi(D_4) = 496 \qquad\qquad \chi(D_5) = 988\,. \end{aligned}$$

As we can see from the last line of weights in the GLSM matrix above, this CY exhibits a F_{10} fibration with coordinates $z_4, z_5, z_{15} = x, y, z$ over the Hirzebruch surface $\mathbb{F}_{12}$ [13](notice that, besides being the largest value that can be found in the Kreuzer-Skarke database, $h^{1,2} = 491$ is the largest possible value for an elliptic CY threefold [189], in agreement with what we said before regarding the correspondence between CY threefolds and elliptic fibrations at large Hodge numbers).

Analyzing the fixed point locus of each involution we observe that none of them presents $O3$-planes. Moreover, the largest contribution to the $D3$-charge comes from the involution of the torus fibre $z_5 \mapsto -z_5$, which is the coordinate with the largest weights. In general we observe that the $D3$-charges coming from the Op-planes take values in the range $8 \leq$

[13]The Hirzebruch surfaces $\mathbb{F}_n$ ($n \geq 0$; $n \in \mathbb{N}$) correspond to different fibrations of a $\mathbb{CP}^1$ fibre over a $\mathbb{CP}^1$ base. In this case, we can recognize it as follows: the base of the elliptic fibration is the submanifold defined by $z \equiv z_{15} = 0$ (which automatically fixes also the other two coordinates on the fibre, that is z_4 and z_5). By carefully analyzing the SR-ideal (7.33) and the intersection numbers we realize that most of the other coordinates (in particular $\{z_i\}$, with $i = 6, ..., 13$) can be fixed to 1, acting on the corresponding $\mathbb{C}_i^*$ rescalings. After this gauge fixing, we are left with the coordinates and the weights:

z_1	z_2	z_3	z_{14}
1	1	12	0
0	0	1	1

corresponding to the weight matrix of an $\mathbb{F}_{12}$ (see App. A of [188]).

$|Q_{Op}^{\text{tot}}| \leq 168$, depending on the inverting coordinate. A large charge might also come from the involution of the coordinate z_4 of the fibre, but, as we explained above, the corresponding orientifold is singular (with a singularity which is not touched by the $O7$-planes) hence we exclude it from our analysis.

Let us then focus on the involution

$$z_5 \mapsto -z_5 \,, \tag{7.35}$$

for which we have $O7$-planes on D_5, D_6, D_8, D_{12}, D_{13} and D_{15}, which do not intersect each other. Recalling that all the divisors $D_{i>5}$ are dP_1, the Euler characteristic of the orientifold locus reads

$$\chi(O_\sigma) = \chi(D_5) + 5 \cdot \chi(dP_1) = 1008 \,, \tag{7.36}$$

from which we derive, as usual, the invariant Hodge numbers: $(h_-^{1,2}, h_+^{1,2}) = (491, 0)$ (cfr. Eq. (5.37)). The total $D3$-charge coming from the $O7$-planes is therefore:

$$Q_{D3}^{\text{tot}} = -\frac{\chi(O_\sigma)}{6} = -168 \,. \tag{7.37}$$

Let us consider the $D7$-brane configuration ensuring the maximum possible contribution to the (absolute value of the) $D3$-charge. Among the divisors wrapped by an $O7$-plane, only D_5 is non-rigid, the others being, as we said, all dP_1's. Thus, we place the usual SO(8) stacks of 4 branes plus 4 image branes on the rigid divisors, while we cancel the $D7$-tadpole from the $O7$ on D_5 with a Whitney brane.

Since the above divisors do not intersect each other, it is easy to define a B-field ensuring a vanishing gauge flux $\mathcal{F}_i = 0$ for each of the SO(8) stacks:

$$B_2 = \frac{1}{2}\left(D_6 + D_8 + D_{12} + D_{13} + D_{15}\right) \,. \tag{7.38}$$

With this choice, indeed, the pull-back of B_2 on each divisor D_i simply reads $\iota_{D_i}^* B_2 = \frac{D_i}{2}$, therefore canceling the non-integral flux introduced for the sake of Freed-Witten anomaly cancellation. The charge contribution coming from the SO(8) stacks is:

$$Q_{\text{SO}(8)}^{\text{tot}} = -\sum_{i=6,8,12,13,15} \frac{\chi(D_i)}{3} = -5 \cdot \frac{4}{3} = -\frac{20}{3} \,. \tag{7.39}$$

As concerns the Whitney brane, we need to check whether it is possible to choose the integer flux F in a way that makes the flux contribution to the $D3$-charge $Q_{D3,\text{flux}}^W$ (5.63) vanish. As explained in Sec 5.3.1, this is possible whenever at least one of the line bundles $\mathcal{O}(3D_5 - 2F + 2B_2)$ and $\mathcal{O}(3D_5 + 2F - 2B_2)$ is trivial on the Whitney brane. Applying the general rule to the case under examination, this can be done if either $\frac{3}{2}D_5 + B_2$ or $\frac{3}{2}D_5 - B_2$ is an integer form (which therefore can be canceled by the integer F). This is true because, as we can see from the weights matrix, $D_5 + B_2$ is an even form (hence $\frac{D_5+B_2}{2}$ is an integer form). The $D3$-charge contribution coming from the Whitney brane is therefore simply given by (5.62):

$$Q_{D3}^W(D_5) = Q_{D3,\text{geom}}^W(D_5) = -\frac{\chi(4D_5)}{12} - 9\int_{X_3} D_5^3 = -\frac{19\,468}{3} \,, \tag{7.40}$$

where we used $\chi(4D_5) = 30\,352$ and $D_5^3 = 440$.

We stress that if we had canceled also the $D7$-tadpole on D_5 with local $D7$ stacks, the corresponding $D3$-charge would have been

$$Q_{D3}^{\mathrm{SO}(8)}(D_5) = -\frac{\chi(D_5)}{3} = -\frac{988}{3}\,, \tag{7.41}$$

hence the introduction of the Whitney brane enhanced the charge contribution of D_5 by a factor of

$$\frac{Q_{D3}^{W}(D_5)}{Q_{D3}^{\mathrm{SO}(8)}(D_5)} \approx 20\,. \tag{7.42}$$

Summarizing, the total $D3$-charge contribution coming from O-planes/D-branes is:

$$Q_{D3} = Q_{O7}^{\mathrm{tot}} + Q_{\mathrm{SO}(8)}^{\mathrm{tot}} + Q_{D3}^{W} = -6664\,, \tag{7.43}$$

as reported in Tab. 7.4.

A complete analysis of this model from the point of view of moduli stabilization and dS uplift is beyond the scope of this work, but we conclude this section with two observations on this topic. First, among the 10 rigid dP_1, only half are wrapped by an $O7$-plane and therefore support gaugino condensation. For the sake of moduli stabilization, it would be favorable to introduce non-perturbative effects also on the others. However it is not possible to choose a B-field such that all the dP_1 (including the ones without the $O7$) have vanishing gauge fluxes, hence, in particular, the choice (7.38) forbids $\mathcal{O}(1)$ instantons on the remaining divisors ($\mathcal{F}_{E3} \neq 0$). On the other side, rank-2 instantons (see Sec. 5.4) might be allowed, provided that one checks that no chiral modes arise at the intersection with the SO(8) stacks. Finally, since it does not have any $O3$-plane, this model is not suitable for $\overline{D3}$ uplift. However, we expect, at least in principle, to be able to engineer a T-brane background (see Sec. 4.5) allowing for dS minima.

7.7 Conclusions

In the previous chapter, we observed that a specific $D7$-brane configuration, including a Whitney brane, can generate a large (negative) $D3$-charge, possibly sufficient to compensate the large tadpole contribution MK coming from the stabilization of the conifold complex structure modulus. In this chapter (and in the corresponding paper [19]) we explore this possibility in a more systematic way, analyzing the $D3$-tadpole contribution coming from O-planes and D-branes at different values of $h^{1,1} \leq 12$. In particular we have considered CY orientifolds constructed as hypersurfaces in toric varieties starting from the reflexive polytopes collected in the Kreuzer-Skarke database [105], equipped with a holomorphic reflection involution. The database generated from our results includes all favorable FRSTs with $h^{1,1} \leq 7$ and a random selection of cases with $h^{1,1}$ up to 12, for which we computed the orientifold configuration (O-planes) and the D-brane configuration allowing for the largest negative $D3$-charge. One of the main purposes of this work was indeed to compare the $D3$-charge coming from local (SO(8) stacks) and non-local (Whitney branes) $D7$-tadpole cancellation, showing that the second case can produce

much larger contributions with respect to the first one. An important result is indeed that the largest (negative) contribution that we find coming from Whitney branes, that is $|Q_{D3}|^{O3/O7/D7} \lesssim 6664$, largely surpasses any previously observed bound (in particular, if we consider only local D7-tadpole cancellation we find $|Q_{D3}|^{O3/O7/D7} \lesssim 504$).

The large number of geometries analyzed allowed also to observe an interesting pattern in the distribution of the models with respect to their Euler characteristic and, consequently, of their $D3$-charge. This distribution appears to be related to the fibration structure of the considered models (we have accompanied our results with explicit examples, aiming to make our statements more concrete). However, it would be interesting to better understand the observed structure from the mathematical point of view.

Chapter 8

K3 fibrations and $\overline{D3}$ de Sitter uplift

From the phenomenological point of view, an interesting extension to the simple model analyzed in Ch. 6, consists in taking into account a slightly more complicated form for the volume of the CY, the so-called *weak Swiss-cheese* form:

$$\mathcal{V} = f_{3/2}(\tau_j) - \sum_{i=1}^{N_{\rm small}} \kappa_i \tau_i^{3/2} , \qquad \text{with } j = 1, ..., N_{\rm large} . \tag{8.1}$$

In other words, among the $h^{1,1}$ Kähler moduli, $N_{\rm small}$ are associated with small rigid cycles, which can be stabilized, at least in principle, by non-perturbative effects. The remaining $N_{\rm large} = h^{1,1} - N_{\rm small}$ 4-cycles are combined in $f_{3/2}$ which is an homogeneous function of degree $\frac{3}{2}$, playing the role of the large cycle in the standard LVS stabilization.

The simplest example of this kind, with $h^{1,1} = 3$, was constructed in [62], by adding a blow-up mode to the CY hypersurface $\mathbb{CP}^4_{[1,1,2,2,6]}$. The volume in this case reads $\mathcal{V} \propto (\tau_b\sqrt{\tau_f} - \alpha\tau_f^{3/2}) - \kappa_s\tau_s^{3/2} \simeq t_f\tau_f - \kappa_s\tau_s^{3/2}$, where τ_s is a blow-up cycle, which can be stabilized by non-perturbative effects, while τ_f and τ_b are both large cycles (only one of which can be stabilized by the LVS mechanism).

The advantage of this setup is that after having stabilized the small cycles and the overall volume, there is still at least one massless modulus, which can be fixed via sub-leading effects and may have an important phenomenological role[1]. The shallowness of this additional direction in the scalar potential makes the corresponding Kähler modulus a promising candidate as, e.g. the inflaton field in the inflationary paradigm known as *fibre inflation* [153, 137, 146]. In addition to this, the structure base $\times$ fibre, which is manifest in writing the volume as $\mathcal{V} \simeq t_f\tau_f$ allows to study the interesting anisotropic limit $\tau_b \gg \tau_f$, which shows promising features as concerns the purpose of making contact with experiments [190, 191].

In this chapter, based on [20], we will consider in particular the case in which the fibration divisor is a K3 surface (see Sec. 5.1.1). Our purpose is to construct an explicit CY orientifold which, similarly to the one of Ch. 6 allows all the moduli to be stabilized in a dS vacuum obtained by means of an $\overline{D3}$ at the tip of a warped throat and, in addition to this, is a K3-fibration. The new requirement turns out to be not so easy to combine with

[1] See [27] and references therein.

the uplift mechanism under consideration, at least for small values of $h^{1,1}$, as we explain in Sec. 8.1. Nonetheless, we select a promising geometry, which we explicitly analyze in Sec. 8.2.

8.1 Search for suitable models

As a first step towards the construction of an explicit example, we have scanned over the CY threefolds constructed as hypersurfaces in toric varieties (see Sec. 5.1), listed in the Ross Altman Database [107], looking for geometries with promising features. Aiming for an explicit model (therefore not too complicated) we have limited our search to models with $h^{1,1} = 3, 4$ [2] and we have imposed the following requirements:

1. It admits moduli stabilization à la LVS, which means in particular that:
   - $h^{1,2} > h^{1,1} > 1$, so that the Euler characteristic is negative;
   - At least one of the toric divisors is rigid and supports non-perturbative effects. In particular we consider only models presenting at least one 'diagonal' dP divisor.
2. One of the toric divisors is a K3. Notice that the presence of such divisor always implies that the CY is a fibration.

   Models satisfying these first two requirements are a priori suitable for Fibre Inflation.
3. It admits a reflection involution with at least 2 $O3$-planes that can coincide by a complex structure deformation and a sufficiently large (negative) $D3$-charge. The second requirement can be fulfilled if the involution shows $O7$-planes wrapping divisors with a large Euler characteristic: as we have seen in detail in Ch 7, indeed, in this case the contributions from both the $O7$-plane and the $D7$-brane(s) canceling the corresponding $D7$-tadpole are expected to be large. On the basis of our experience in Ch. 6, we require $|Q_{\rm D3}^{O3/O7/D7}| \gtrsim 150$.

The combination of these apparently harmless requirements turns out to be very constraining, at least for the small values of $h^{1,1}$ taken into consideration.

First of all, the need for both a diagonal dP and a K3 divisor sets a strong constraint on the intersection numbers. From Sec. 5.1.1, we recall indeed that a K3 divisor can only appear linearly in the intersection polynomial (as it is characterized by $D_{K3}^3 = D_{K3}^2 D = 0$, for any toric divisor D). On the other side, the diagonal dP, by definition, does not intersect any other divisor in the selected basis so that only the term D_{dP}^3 can appear in the intersection polynomial. After having chosen a basis of the form $\mathcal{B} = \{D_{i_1}, ..., D_{i_{h^{1,1}-2}}, D_{\rm dP}, D_{\rm K3}\}$, therefore, the intersection polynomial can only take the form:

$$I_3 = aD_{dP}^3 + \sum_{i,j=1}^{h^{1,1}-2} b_{ij} D_{\rm K3} D_i D_j + \sum_{i,j,k=1}^{h^{1,1}-2} c_{ijk} D_i D_j D_k \,, \tag{8.2}$$

[2] From the requirements themselves it should be obvious that no model of this kind can appear with $h^{1,1} = 2$.

which for the case $h^{1,1}=3$ reduces to:

$$I_3^{(h^{1,1}=3)} = aD_{dP}^3 + bD_{\rm K3}D^2 + cD^3\,. \tag{8.3}$$

Despite this, the database [107] presents 43 geometries with $h^{1,1}=3$ [144] and 171 with $h^{1,1}=4$, satisfying the requirements (1) and (2). To be more precise, using the CY threefolds arising from the reflexive polytopes of the KS database it has been found that [144, 145, 143]:

- For $h^{1,1}=2$, there are 39 distinct CY geometries, 22 of which have a volume form of the strong Swiss-cheese type with a diagonal del-Pezzo divisor, while there are 10 K3-fibred CY geometries. However, as it is obvious, there are no K3-fibred CY threefolds with additional diagonal del-Pezzo divisor. For this reason we have to minimally look for examples with $h^{1,1}=3$.

- For $h^{1,1}=3$, there are 305 distinct favorable CY geometries, 132 of which have at least one diagonal del-Pezzo divisor, and therefore are a priory suitable for realising LVS. In addition, there are 136 K3-fibred CY geometries, but only 43 of those have, in addition, a diagonal del-Pezzo divisor to support LVS.

- For $h^{1,1}=4$, there are 2000 distinct favorable CY geometries, 750 of which have at least one diagonal del-Pezzo divisor for realising LVS. In addition, there are 865 K3-fibred CY geometries, but only 171 of those have, in addition, at least a diagonal del-Pezzo divisor to support LVS.

The third requirement, however, rules out most of these models. As we mentioned above, indeed, a large (negative) $D3$-charge is associated with divisors (wrapped by $O7$-planes and $D7$-branes) with large Euler characteristic. This excludes both the K3 ($\chi(K3)=24$) and the dP ($\chi\in[3,11]$) divisors. Furthermore, at least three of the divisors of a toric CY (including the dP's) are usually rigid surfaces characterized by the weights $\{1,0,0\},\{0,1,0\}$ and $\{0,0,1\}$, therefore having a small Euler characteristic[3]. In addition to this, generically the coordinate with the largest weights (associated to the largest Euler characteristic and therefore to the largest $D3$-charge) does not admit the desired $O3$-planes configuration. We conclude that in general at most one of the seven (eight) toric divisors of the CY with $h^{1,1}=3$ ($h^{1,1}=4$) can produce a large $D3$-charge contribution, being at the same time associated to an involution with at least two 'collapsable'[4] $O3$-planes (while on most of the cases only one of these two features is realized).

To be more concrete, let us consider the geometries with $h^{1,1}=3,4$, satisfying the requirements (1) and (2). The maximal Euler characteristic that we find for a given divisor of one of the 43 CY orientifolds with $h^{1,1}=3$ is $\chi(D)=232$, which we encounter in 5 CY manifolds: none of these admits an involution with an $O7$-plane wrapping the divisor D and at least 2 $O3$-planes in the desired configuration. Restricting our search to

[3] As an exception, it was noticed that a rigid divisor with large χ ($\chi=111$) can appear for $h^{1,1}=3$ [143].

[4] See the caption of Fig. 5.2 for the meaning of 'collapsable' $O3$-planes in this context.

only models with an involution of this kind, the maximal Euler characteristic we get is $\chi(D) = 54$, for which, considering all the O-planes and $D7$-brane contributions (included the flux contribution on the Whitney brane) the maximal (in absolute value) $D3$-charge that we can obtain[5] is $-Q_{D3}^{O3/O7/D7} = 104$.

The situation with the 171 geometries with $h^{1,1} = 4$ is only slightly better. We find again 5 geometries including the divisor with the largest Euler characteristic, which this time is $\chi(D) = 435$, but, again, none of these is associated with a suitable involution. The maximal Euler characteristics for an involution including $O3$-planes turns out to be $\chi(D) = 65, 66$ and the maximal $D3$-charge contribution (which we find to be associated to $\chi(D) = 65$) is[6] $-Q_{D3}^{O3/O7/D7} = 127$.

We can see therefore, that none of the analyzed models really fulfills our third requirement, if we impose the boundary $|Q_{\rm D3}^{O3/O7/D7}| \gtrsim 150$. In the following, however, we take a less ambitious bound on Q_{D3} and we analyze the model with the largest charge that we could find, that is the one with $-Q_{D3}^{O3/O7/D7} = 127$ and $h^{1,1} = 4$. We will see, in particular, that this model still allows to satisfy the requirement $MK < |Q_{D3}^{O3/O7/D7}|$.

8.2 An explicit example

In this section we analyze the CY threefold, selected as described in the previous section, with the largest negative $D3$-charge among the ones considered. It has $h^{1,1} = 4$, a K3-fibration structure and a diagonal del-Pezzo divisor; it corresponds to the polytope ID#1271 (Triangulation# 1) in the Ross Altman Database [107].

8.2.1 Geometric data

The weights matrix describing the toric ambient space in which the CY three-fold is defined is:

x_1	x_2	x_3	x_4	x_5	x_6	x_7	x_8	D_H
0	0	0	0	0	1	2	1	4
0	0	0	1	1	1	3	0	6
1	0	1	2	0	3	7	0	14
1	1	0	0	0	2	4	0	8

with SR-ideal:

$$\text{SR} = \{x_1x_2, x_2x_5, x_5x_8, x_6x_8, x_1x_3x_6, x_3x_4x_7, x_4x_5x_7\} \tag{8.4}$$

and second Chern numbers:

$$\Pi_i = \int_{D_i} c_2(X) = \{26, 12, 14, 24, -4, 58, 126, -4\}\,. \tag{8.5}$$

The Hodge numbers are $(h^{2,1}, h^{1,1}) = (102, 4)$, hence the Euler characteristic is $\chi(X_3) = -196$.

[5] Assuming that all the stacks of branes wrapping rigid divisors are fluxless.
[6] See footnote 5.

Using `CohomCalg` [139, 140], we find that D_4 is a K3 (indeed it also satisfies the requirement $D_{K3}^2 D_i = 0$, $\forall D_i$ toric divisors). Moreover, D_2 and D_3 correspond to rigid-but-not-del-Pezzo divisors (NdP_9 and NdP_{10} respectively), while D_5 and D_8 have the Hodge numbers of a dP_1. In particular, applying the criteria of [145] we find that D_8 is a non-diagonal dP_1 divisor, while D_5 is a diagonal $\mathbb{CP}^1 \times \mathbb{CP}^1$ surface. Finally, D_1 is a special deformation divisor SD_1 (see Sec. 5.1.1), while D_6 and D_7 are deformation divisors with Hodge diamonds:

$$D_6 : \begin{array}{ccccc} & & 1 & & \\ & 0 & & 0 & \\ 5 & & 53 & & 5 \\ & 0 & & 0 & \\ & & 1 & & \end{array} ; \qquad D_7 : \begin{array}{ccccc} & & 1 & & \\ & 0 & & 0 & \\ 24 & & 163 & & 24 \\ & 0 & & 0 & \\ & & 1 & & \end{array} .$$

Let us consider the following basis of toric divisors, containing the K3 and the diagonal $\mathbb{CP}^1 \times \mathbb{CP}^1$ divisor and such that the last actually appears diagonally in the volume form:

$$\mathcal{B} = \{D_2, D_4, D_5, D_8\} . \tag{8.6}$$

Expanding the Kähler form over this basis, $J = t_2 D_2 + t_4 D_4 + t_5 D_5 + t_8 D_8$, we get the intersection polynomial

$$I_3 = 8D_5^3 - D_2^2 D_8 + 2D_2 D_4 D_8 - D_2 D_8^2 - 4D_4 D_8^2 + 8D_8^3 , \tag{8.7}$$

corresponding to the volume of the CY:

$$\mathcal{V} = \frac{1}{6}\int_{X_3} J^3 = -\frac{t_2^2\, t_8}{2} - \frac{t_2 t_8^2}{2} + \frac{4t_8^3}{3} + 2t_2 t_4 t_8 - 2t_4 t_8^2 + \frac{4t_5^3}{3} . \tag{8.8}$$

We notice that the diagonality of the $\mathbb{CP}^1 \times \mathbb{CP}^1$ divisor D_5 and the linearity of the K3 divisor D_4 are manifest in the intersection polynomial (8.7) as well as in the volume form (8.8).

Starting from the CY Mori cone provided by the database [107], we can derive the Kähler cone conditions:

$$2t_5 + t_8 > 0 , \quad -2t_5 > 0 , \quad -t_2 + 2t_4 - t_8 > 0 , \quad t_2 - 2t_8 > 0 , \tag{8.9}$$

while from the volume (8.8) we immediately obtain the four-cycle volumes $\tau_i = \frac{\partial \mathcal{V}}{\partial t_i}$:

$$\begin{aligned} &\tau_2 = -t_2\, t_8 + 2\, t_4\, t_8 - \frac{t_8^2}{2} ; \qquad \tau_4 = 2\, t_2\, t_8 - 2t_8^2 ; \\ &\tau_5 = 4t_5^2; \qquad \tau_8 = -\frac{t_2^2}{2} + 2\, t_2\, t_4 - t_2\, t_8 - 4\, t_4\, t_8 + 4t_8^2 . \end{aligned} \tag{8.10}$$

We notice, as expected, that with the exception of the cycle corresponding to the diagonal divisor D_5, the above expressions cannot be inverted, hence it is not possible to write the volume exclusively in terms of the 4-cycles. However, the Swiss cheese structure for the diagonal divisor is manifest with this choice of the basis: from (8.10), and imposing the

corresponding KCC, we derive: $t_5 = -\frac{1}{2}\sqrt{\tau_5}$, which, once introduced in the volume (8.8), gives

$$\mathcal{V} = \frac{t_2^2\, t_8}{2} - \frac{3t_2 t_8^2}{2} + \frac{4t_8^3}{3} + 2t_2 t_4 t_8 - 2t_4 t_8^2 - \frac{\tau_5^{3/2}}{6}\,, \tag{8.11}$$

hence $\kappa_5 = \frac{1}{6}$.

8.2.2 Involution, O-planes and D-branes

We consider the involution

$$x_6 \to -x_6, \tag{8.12}$$

for which there are 2 $O7$-planes located at D_6 and D_8 respectively, a single $O3$-plane at $x_1 = x_3 = x_7 = 0$ and 2 $O3$-planes at $x_2 = x_3 = x_7 = 0$.

We have therefore $D^3_{O7} \equiv D^3_6 + D^3_8 = 15$, from which we can compute the correction to the Euler characteristic proposed in [166], due to the presence of orientifold planes:

$$\chi(X_3) \to \chi(X_3) + 2\int_{X_3} D^3_{O7} = -166\,.$$

Moreover, after computing $\chi(O_\sigma) = \chi(D_6) + \chi(D_8) + 3\chi(O3) = 65 + 4 + 3 = 72$, we can use the Lefschetz fixed point theorem (5.37) to derive the values of $h^{1,2}_+(X) = 36$; $h^{1,2}_-(X) = 66$.

The $D3$-charge contribution from the O-planes can be computed with the usual formulas as:

$$Q_{Op} = -\frac{1+2}{2} - \frac{65+4}{6} = -13\,, \tag{8.13}$$

where we used $\chi(D_6) = 65$ and $\chi(D_8) = 4$.

In order to cancel the $D7$-charge, we introduce a stack of four $D7$-branes (plus four image branes) on top of the $O7$-plane wrapping D_8 and a Whitney brane on the divisor D_6. In order to stabilize the blow-up mode τ_5, we want to introduce an $E3$-instanton on the corresponding divisor D_5. Hence, we need to choose the B-field as $B = \frac{D_5}{2}$ so that the gauge flux $\mathcal{F}_5$ vanishes. This ensures that there are no chiral intersections between the branes. The $D3$-charge of the $D7$-branes stack, neglecting possible fluxes whose contribution we consider to be negligible, is given by[7]:

$$Q_{D3}^{(4+4)D7} = -\frac{(4+4)}{24}\chi(D_8) = -\frac{4}{3}\,. \tag{8.14}$$

Finally, we compute the $D3$-charge of the Whitney brane using the formulas (5.62) and (5.63) for the geometric and the flux contributions respectively. The geometric $D3$-charge

[7] In Sec. 8.2.4, we will briefly consider the case in which also the non-diagonal dP divisor D_8 supports a non-perturbative effect (gaugino condensation). If this is the case, one needs also to ensure $\mathcal{F}_8 = 0$. This can be done by choosing the B-field as $B = \frac{D_8}{2} + \frac{D_5}{2}$: indeed $x_5\, x_8 \in$ SR. Anyways, the additional term in B will not change the value of the $D3$-charge from the Whitney brane (obviously it will change the flux contribution in $Q_{D3}^{(4+4)D7}$ (8.14), that we are omitting anyways).

is

$$Q^W_{D3,\text{geom}} = -\frac{359}{3}\,, \tag{8.15}$$

where we used $\chi(4D_6) = 680$ and $D_6^3 = 7$. The flux on the brane is determined by the two-form:

$$F = \sum_i a_i D_i; \quad a_i \in \mathbb{Z}\,.$$

Imposing the condition (5.61) that the Whitney brane is not forced to split into the brane-image brane configuration constrains the possible values of the a_i coefficients. Since $Q^W_{D3.\text{flux}} > 0$, we need to minimize it. Thus, among all the solutions, we choose, in the basis (8.6), $F = -3D_2 - 2D_4 + D_5 + 3D_8$. Plugging this result in (5.63), we find $Q^W_{D3,\text{flux}} = 7$, hence:

$$Q^W_{D3} = Q^W_{D3,\text{geom}} + Q^W_{D3,\text{flux}} = -\frac{338}{3}\,.$$

We conclude that the total $D3$-charge arising from the Op-planes and the D-branes is given by

$$Q_{D3} = -13 - \frac{4}{3} - \frac{338}{3} = -127\,,$$

as anticipated at the end of Sec 8.1.

8.2.3 $O3$-planes at the tip of the warped throat

Let us conclude the analysis of the geometric features of our model, by proving that a highly warped throat is generated in a corner of the complex structure moduli space and that there is a pair of $O3$-planes at the tip of this throat. The computation turns out to be completely analogous to the one described in Sec. 6.4.5, hence here we will summarize the argument without analyzing it again in full detail.

The equation defining the CY three-fold, once restricted to its invariant version with respect to the involution (8.12), can be written as:

$$\begin{aligned} x_7^2 = {} & a\,x_5\,x_6^4\,(x_4 + a_1\,x_3^2 x_5) - 2b\,x_6^2\,x_8^2\,\left[x_1^4\,x_4^2\,x_5^2 + x_2\,P_1(x_1,x_2,x_3,x_4,x_5)\right. \\ & \left. + x_3\,P_2(x_1,x_3,x_4,x_5)\right] + x_2\,P_3(x_1,x_2,x_3,x_4,x_5,x_8) + x_3\,P_4(x_1,x_3,x_4,x_5,x_8) \\ & + c\,x_1^8\,x_4^3\,x_5^3\,x_8^4 = 0\,, \end{aligned} \tag{8.16}$$

where the $P_i(x_j)$ are polynomials in the coordinates $\{x_j\}$ and $a, a_1, b, c \in \mathbb{C}$. It is therefore immediate to see that at the locus $x_2 = x_3 = x_7 = 0$ of the 2 $O3$-planes, it becomes:

$$x_4\,x_5\,x_6^4 - 2b\,x_1^4\,x_4^2\,x_5^2\,x_6^2\,x_8^2 + c\,x_1^8\,x_4^3\,x_5^3\,x_8^4 = 0 \tag{8.17}$$

(where we have redefined the constants b, c in order to get rid of a).

Looking at the SR-ideal (8.4), we notice that the coordinates $\{x_1, x_4, x_5\}$ can never vanish at the locus of these O3-planes. Fixing them to 1 (by an appropriate choice of the $\mathbb{C}^*$ parameters λ_i), (8.17) becomes:

$$x_6^4 - 2b\,x_6^2\,x_8^2 + c\,x_8^4 = 0\,. \tag{8.18}$$

Furthermore, x_6 and x_8 cannot vanish simultaneously. We can therefore fix $x_8 = 1$ as well and obtain:

$$x_6^4 - 2b\,x_6^2 + c = 0\,. \tag{8.19}$$

This equation is completely analogous to Eq. (6.53), hence from now on the argument and its conclusions are precisely the same as in Sec. 6.4.5. We can summarize the main points as follows:

- Redefining $c \equiv b^2 - \delta$, Eq. (8.19) becomes: $(x_6^2 - b)^2 = \delta$. Hence, when $\delta = 0$ the two O3-planes, sitting at the two zeroes of (8.19), go on top of each other at the point $x_6^2 - b\,x_8^2 = 0$, while they are very close to each other when δ is small.
- By analyzing the neighborhood of the point $x_2 = x_3 = x_7 = (x_6^2 - b\,x_8^2)^2 + \delta = 0$, we can see that the equation of the CY (8.16) in an ambient space $\mathbb{C}^4/\mathbb{Z}_2$, is precisely the one of a deformed conifold, where δ parametrizes the size of the blown-up S^3. In the limit $\delta \to 0$, the local geometry develops a conifold singularity at the point $x_2 = x_3 = x_7 = (x_6^2 - b)^2 = 0$.
- In the local patch under consideration, the involution reproduces exactly the geometric action required for the retrofitting of a nilpotent Goldstino sector [103], that is $\{x_2 \to -x_2,\ x_3 \to -x_3,\ x_7 \to -x_7\}$.
- Assuming that the complex structure moduli are fixed so that the S^3 has finite size ($\delta \neq 0$), we can add a $D3$-brane at one of the $O3^-$ points of the S^3 and a $\overline{D3}$ at the other $O3^-$ point. This ensures that the $D3/\overline{D3}$-branes do not contribute to the total $D3$-charge and that there is no perturbative decay channel between them, as they are stuck at the $O3$-planes.

8.2.4 Scalar potential for the Kähler moduli

Let us now compute the supergravity scalar potential for this model. As we already mentioned, the presence of a non-diagonal rigid divisor forbids the definition of the overall volume, and hence of the scalar potential, in terms of the volumes of the 4-cycles only. For this reason, following [61], we conclude that it is convenient to work directly with the 2-cycle volumes t^i. Since we also want to include the conifold modulus Z, our result will be different from the master formulas derived in [61]. However, as we see in detail in the App. D, when considering the large volume limit the only difference is a Z-dependent additional term. In principle, we may be able to engineer two different non-perturbative effects both on the diagonal $\mathbb{CP}^1 \times \mathbb{CP}^1$ D_5 (supporting an $E3$-instanton) and on the non-diagonal D_8, which, being wrapped by an $O7$-plane and by a SO(8) stack of $D7$-branes with $\mathcal{F}_8 = 0$, undergoes gaugino condensation[8]. The result for the total scalar potential

[8] Being non-diagonal, the divisor D_8 needs a more careful analysis, as the intersection with other divisors might produce chiral modes canceling the non-perturbative effect (see Sec. 5.4). However, in our setup the only other $D7$-brane is the Whitney brane on D_6 which does not support chiral matter (in any case the two branes do not intersect each other). We conclude that no chiral mode arises and that, assuming that the same is true for non-chiral modes, gaugino condensation produces a non-vanishing term in the superpotential.

is[9]:

$$\begin{aligned} V = & \frac{8a_5^2A_5^2e^{-2a_5\tau_5}\sqrt{\tau_5}}{s\mathcal{V}} + \frac{2a_8^2A_8^2e^{-2a_8\tau_8}(t_2+4t_4-8t_8)}{s\mathcal{V}} \\ & + \frac{2A_5A_8e^{-a_5\tau_5-a_8\tau_8}(a_8\tau_8+a_5\tau_5+2a_5a_8\tau_5\tau_8)\cos(a_5\theta_5-a_8\theta_8)}{s\mathcal{V}^2} \\ & + \frac{2a_5A_5e^{-a_5\tau_5}W_0\tau_5\cos(a_5\theta_5+\varphi)}{s\mathcal{V}^2} + \frac{2a_8A_8e^{-a_8\tau_8}W_0\tau_8\cos(a_8\theta_8+\varphi)}{s\mathcal{V}^2} \\ & + \frac{3W_0^2\xi}{8\sqrt{g_s}\mathcal{V}^3} + \frac{c''\zeta^{4/3}}{2g_sM^2\pi\mathcal{V}^{4/3}} + \frac{\zeta^{4/3}}{2c'M^2\mathcal{V}^{4/3}}\left(\frac{K^2}{g_s^2}+\frac{M^2\sigma^2}{4\pi^2}+\frac{MK}{g_s\pi}\log\zeta+\frac{M^2}{4\pi^2}\log^2\zeta\right) \end{aligned} \tag{8.20}$$

with $a_5 = 2\pi$ and $a_8 = \frac{\pi}{3}$. Notice that, in order to get a more compact expression, we have introduced, whenever possible, the 4-cycle volumes τ_i. However, the presence of t^i-dependent terms makes clear the fact that this potential needs to be analyzed in terms of these cycles.

The moduli θ_i, σ and ζ can be easily stabilized as usual:

$$\theta_{i_0} = \frac{\pi-\phi}{a_i}; \quad \sigma_0 = 0\,;$$

$$\zeta_0 = e^{-\frac{2\pi K}{g_sM}-\frac{3}{4}+\sqrt{\frac{9}{16}-\frac{4\pi}{g_sM^2}c'c''}}\,.$$

Substituting these values in (8.20) we obtain:

$$\begin{aligned} V = & \frac{8a_5^2A_5^2e^{-2a_5\tau_5}\sqrt{\tau_5}}{s\mathcal{V}} + \frac{2a_8^2A_8^2e^{-2a_8\tau_8}(t_2+4t_4-8t_8)}{s\mathcal{V}} \\ & + \frac{2A_5A_8e^{-a_5\tau_5-a_8\tau_8}(a_8\tau_8+a_5\tau_5+2a_5a_8\tau_5\tau_8)}{s\mathcal{V}^2} \\ & - \frac{2a_5A_5e^{-a_5\tau_5}W_0\tau_5}{s\mathcal{V}^2} - \frac{2a_8A_8e^{-a_8\tau_8}W_0\tau_8}{s\mathcal{V}^2} \\ & + \frac{3W_0^2\xi}{8\sqrt{g_s}\mathcal{V}^3} + \frac{q_0\zeta_0^{4/3}}{\mathcal{V}^{4/3}} \end{aligned} \tag{8.21}$$

where $q_0 = \frac{3}{16\pi^2c'}\left(\frac{3}{4}-\sqrt{\frac{9}{16}-\frac{4\pi c'c''}{g_sM^2}}\right)$. Though admissible, this configuration appears very difficult to analyze, even numerically. For this reason, in order to have a better analytic control, we have decided to analyze a different situation.

8.2.5 LVS and string loop corrections

The main difficulty of the configuration described above relies on the presence of a non-perturbative effect on a non-diagonal divisor. In this section, we assume therefore this effect to be absent (this can be easily done, e.g. by introducing a non-vanishing gauge flux on the corresponding $D7$-branes stack that kills the non-perturbative term coming from gaugino condensation). Looking at the KCC (8.9), we can also notice that, unlike t_5, t_8

[9] Notice that we are using a slightly different notation for ξ, with respect to Ch. 6: here indeed $\xi = -\frac{\chi(X)\,\zeta(3)}{2\,(2\pi)^3}$. The Kähler potential for the Kähler moduli, in particular, is now: $K = -2\ln\left(\mathcal{V}+\frac{\xi}{2g_s^{3/2}}\right)$.

is not arbitrarily contractible to a point (as expected from a non-diagonal divisor), hence it is generically stabilized at a large value. Even though it is possible that the two non-perturbative corrections are of the same order (given also that the 'small' cycle τ_5 appears with a factor 2π, while the 'large' τ_8 is multiplied by $\frac{\pi}{3}$), it is also reasonable to assume that we are in a regime in which the correction coming from gaugino condensation is highly suppressed. We will indeed verify that, at least for our explicit choice of parameters, this assumption is justified by the large value to which the 2-cycle t_8 turns out to be stabilised.

We consider, therefore, the case in which the diagonal $\mathbb{CP}^1\times\mathbb{CP}^1$ (with an $E3$-instanton) and the overall volume are stabilized à la LVS (with the inclusion of the $\overline{D3}$ uplift term), leaving two flat directions that are then fixed by sub-leading string loop corrections as the ones introduced in Sec. 5.5.

It is easy to see that the computation of the LVS scalar potential for $\mathcal{V}$ and τ_5 is exactly the same as the one performed in Ch. 6 for a model with $h^{1,1}=2$. Assuming the axion θ_5 as well as the conifold modulus Z to be stabilized at the usual values, we obtain in particular[10]:

$$V_{LVS+up}=\frac{8g_s a_5^2 A_5^2 e^{-2a_5\tau_5}\sqrt{\tau_5}}{\mathcal{V}}-\frac{2a_5A_5g_s e^{-a_5\tau_5}W_0\tau_5}{\mathcal{V}^2}+\frac{3W_0^2\xi}{8\sqrt{g_s}\mathcal{V}^3}+\frac{q_0\zeta_0^{4/3}}{\mathcal{V}^{4/3}}\,. \tag{8.22}$$

The analysis of the derivatives of V_{LVS} leads to the usual equations

$$\partial_{\tau_5}V=0\Leftrightarrow\mathcal{V}=\frac{3e^{a_5\tau_5}W_0\kappa_5\sqrt{\tau_5}}{a_5A_5}\frac{(1-a_5\tau_5)}{(1-4a_5\tau_5)}\,, \tag{8.23a}$$

$$\partial_{\mathcal{V}}V=0\Leftrightarrow\tau_5^{3/2}\frac{16a_5\tau_5(a_5\tau_5-1)}{(1-4a_5\tau_5)^2}=\frac{\xi}{2g_s^{3/2}\kappa_5}+\frac{16\,q_0\zeta^{4/3}\,\mathcal{V}^{5/3}}{27g_s\kappa_5W_0^2}\,, \tag{8.23b}$$

and allows therefore to fix $\mathcal{V}$ and τ_5.

Sub-leading corrections

Let us now compute the string loop corrections, following what was said in Sec. 5.5. First of all we notice that since D_6 and D_8, which are the only divisors wrapped by $O7/D7$, do not intersect each other, no winding correction is expected to arise[11]. On the other side, the presence of $O3$-planes implies that KK loop corrections (5.71) must be considered. The determination of the transverse 2-cycles $t_i^{\perp}$ would require the analysis of the explicit CY metric. However, here we simply consider these divisors as given by a generic linear combination of the basis 2-cycles $\{t_2,t_4,t_5,t_8\}$, reabsorbing the corresponding coefficients

[10] See footnote 9.

[11] In a recent revisit of the string loop corrections in [192], it has been found that the winding type effects can appear more generically with respect to what was expected from the original proposals of [193, 154, 194, 155]. This result is also consistent with an earlier field theoretic analysis performed in [195]. However, since also these new terms woud have an implicit dependence on the complex structure moduli, it is reasonable to assume that our results will not be significantly modified by the introduction of these terms. Hence, for the sake of simplicity, we will not consider them.

in the complex-structure depending constants $\mathcal{C}_i^{KK}$. The tree-level Kähler metric K_{ij}^0 reads therefore

$$K_{\alpha\beta}^0 = \frac{1}{16\,\mathcal{V}^2}\left(2\,t^\alpha\,t^\beta - 4\mathcal{V}\,k^{\alpha\beta}\right)\,, \tag{8.24}$$

where $k^{\alpha\beta} = (k_{\alpha\beta\gamma}t^\gamma)^{-1}$. Hence, we obtain the following contribution to the scalar potential:

$$V_{g_s}^{\rm KK} = \frac{g_s^3}{2}\frac{|W_0|^2}{16\,\mathcal{V}^4}\sum_{\alpha,\beta}\mathcal{C}_\alpha^{\rm KK}\mathcal{C}_\beta^{\rm KK}\left(2\,t^\alpha\,t^\beta - 4\mathcal{V}\,k^{\alpha\beta}\right)\,, \tag{8.25}$$

where $k^{\alpha\beta}$ is the inverse of the matrix:

$$k_{\alpha\beta} = \begin{pmatrix} -t_8 & 2t_8 & 0 & -t_2+2t_4-t_8 \\ 2t_8 & 0 & 0 & 2t_2-4t_8 \\ 0 & 0 & 8t_5 & 0 \\ t_2+2t_4-t_8 & 2t_2-4t_8 & 0 & -t_2-4t_4+8t_8 \end{pmatrix}\,. \tag{8.26}$$

Finally, we consider the higher derivative correction appearing at $\mathcal{O}(F^4)$ in the scalar potential, whose generic form is given by (5.73). Using the Π_i reported in (8.5), we obtain:

$$V_{F^4} = -\frac{g_s^2}{4}\frac{\lambda\,W_0^4}{g_s^{3/2}\mathcal{V}^4}\left(12\,t_2+24\,t_4-4\,t_5-4\,t_8\right)\,. \tag{8.27}$$

As a final observation, we notice that, apart from the KK-type and winding type string loop effects discussed so far, there can be additional one-loop effects appearing as logarithmic corrections in the Kähler potential [196, 197]. Such terms can arise from specific configurations of $D7$-brane stacks and from a four-dimensional Einstein-Hilbert term localised within the six-dimensional internal space, originally being generated from higher derivative terms in the ten-dimensional string effective action. However, given the specific need to have a minimum of 3 stacks of $D7$-branes with appropriate intersection loci, we do not expect such terms to get generically induced. For these reasons we will not consider these terms in the moduli stabilization analysis of the current work.

8.2.6 Moduli stabilization with dS uplift

Let us now stabilize the scalar potential obtained in the previous section:

$$\begin{aligned} V &= V_{LVS+up} + V_{g_s}^{KK} + V_{F^4} \\ &= \frac{8g_s a_5^2 A_5^2 e^{-2a_5\tau_5}\sqrt{\tau_5}}{\mathcal{V}} - \frac{2g_s a_5 A_5 e^{-a_5\tau_5}W_0\tau_5}{\mathcal{V}^2} + \frac{3g_s W_0^2\hat{\xi}}{8\mathcal{V}^3} + \frac{q_0\zeta_0^{4/3}}{\mathcal{V}^{4/3}} \\ &+ \frac{g_s^3}{2}\frac{|W_0|^2}{16\,\mathcal{V}^4}\sum_{\alpha,\beta}C_\alpha^{\rm KK}C_\beta^{\rm KK}\left(2\,t^\alpha\,t^\beta - 4\mathcal{V}\,k^{\alpha\beta}\right) \\ &- \frac{g_s^2}{4}\frac{\lambda\,W_0^4}{g_s^{3/2}\mathcal{V}^4}\left(12\,t_2+24\,t_4-4\,t_5-4\,t_8\right)\,. \end{aligned} \tag{8.28}$$

Our strategy, as anticipated, is the following:

1. Considering only V_{LVS+up}, we stabilize the overall volume and the small cycle τ_5 using the same procedure presented in Ch. 6 and, in particular, imposing the same requirements listed in Sec. 6.3.1. In this way, besides the two moduli, we also fix the parameters W_0 and g_s, as well as the fluxes M, K.

2. After having fixed τ_5 and $\mathcal{V}$, we include also the other perturbative corrections (that we assume, and check a posteriori, to be subleading) and we stabilize the remaining two moduli, also fixing the parameters $\mathcal{C}_i^{KK}$ and λ.

In order to perform each step, we have used simplicial homology global optimization algorithm [198], implemented in the scientific computing tool `SciPy` [199]. The automatic differentiation based package `JAX` [200] was used for computing the gradients and Hessians of the scalar potential. We have indeed used this relatively simple function, for which we still have a certain amount of analytic control, in order to study these algorithms and to test their application to this kind of setups. The final goal is to expand their use to more involved and generic scalar potentials, in the future.

Stabilization of the overall volume and the small cycle (LVS)

Since the non-perturbative effect is generated by an $E3$-instanton on the divisor D_5, we have $a_5 = 2\pi$. Moreover, we consider, as usual, $A_5 = 1$.

In order to stabilize the 'small' cycle and the overall volume, we apply the same strategy we have used in Sec. 6.3.2. Scanning over values of $W_0 \in [1, 30]$ (with step 1)[12] and $g_s \in [0.01, 0.55]$ (with step 0.001), we compute for each couple of values (W_0, g_s) the minimum and maximum warp factors ρ_{low} (6.16) and ρ_{up} (6.17) allowing for a dS minimum[13]. Then, we scan over integer values of M, K such that:

- $MK < |Q_{D3}^{O3/O7/D7}| = 127$
- The requirement $g_s|M| \gtrsim 5$ (see Sec. 6.3.1) is satisfied[14].
- The corresponding warp factor ρ at the minimum, defined in (6.9), is such that $\rho_{\text{low}} < \rho < \rho_{\text{up}}$.

[12] We have also analyzed a small selection of non-integer values $0 < W_0 < 1$.

[13] It should be noticed that, due to the different notation adopted here for the definition of ξ (see footnote 9), the formulas to be used here actually differ for a factor of $1/2$ with respect to (6.16), (6.17). In other words, the expression (6.18) for the warp factor at the dS minimum becomes: $\rho \simeq \alpha \frac{27 g_s W_0^2 \kappa_5 \tau_5^{1/2}}{40\, a_5 \mathcal{V}^{5/3}}$, with the usual requierment $\alpha \in]1, \frac{9}{4}[$.

[14] In the recent paper [112] it was noticed that the constraint $g_s M^2 \gtrsim 46.1$ disappears after a more accurate computation of the scalar potential for the complex structure modulus Z. Here, indeed, it is proven that the scalar potential for Z far from the minimum (in particular in the IR limit $Z \to 0$) is not well described by (3.35). The numerical analysis of the new scalar potential results in a milder constraint, where a possible destabilization due to the presence of the $\overline{D3}$ is expected only if $g_s M^2 \approx 1$. However, this will not change significantly our results, as (3.35) can still be used in order to approximate the exact scalar potential around its minimum, which is the region we are interested in. Moreover, we still have to satisfy the more constraining condition $g_s|M| \gg 1$.

- The remaining consistency conditions of Sec. 6.3.1 are fulfilled. As concerns these constraints, we notice in particular that the requirement of stabilizing all the Kähler moduli inside the Kähler cone, which was automatically satisfied for the simple construction of Ch. 6, must be instead explicitly checked for the present (more involved) configuration.

We find that the flux numbers corresponding to the minimal contribution to the $D3$-charge are $M = K = 10$[15], hence:

$$(MK)_{\rm min} = 100\,.$$

However, a solution with such flux numbers (and in general with flux numbers smaller than 127) requires a relatively large string coupling. We choose, as an example[16]

$$W_0 = 4; \quad g_s = 0.52\,,$$

from which $g_s M = 5.2$ and we obtain $\zeta = 3.44 \times 10^{-6}$. The string coupling g_s is therefore quite large with respect to the values that are commonly taken into consideration for this parameter[17]. Nonetheless, we decide to keep it and to check whether the perturbative corrections will actually turn out to be much smaller than V_{LVS}, in which case we claim that our setup is reliable. Moreover, we notice that the largeness of g_s is strictly connected to the fact that the $D3$-charge contributions coming from D-branes and O-planes is relatively small. This should in turn be due to the fact that, in order to have a simple construction, we have restricted our search to only those CY geometries for which $h^{1,1} < 5$. We expect therefore to be able to improve this result once a larger number of Kähler moduli is taken into consideration. As an aside, we notice that this result is in complete agreement with the estimations performed in Sec. 6.3.2, as we can see by recalling that we are considering the case $a_5 = 2\pi$ with $\chi(X_3) = -166$.

The moduli at the minimum are evaluated as:

$$\tau_5 = 2.29 \ (t_5 = -0.76); \quad \mathcal{V} = 2.05 \times 10^5\,,$$

which, substituted in the scalar potential (8.22) give: $V^{min}_{LVS+up} = 5.12 \times 10^{-18}\, m_p$.

We notice that all the constraints listed in Sec. 6.3.1, with the caveat of the relatively large value of g_s on which we have commented before, are satisfied. In particular, as concerns the usual energy scales, we find:

$$2\pi M_s = 3.3 \times 10^{-3} m_p = 6.5\, M^{bulk}_{KK}\,; \quad M^{bulk}_{KK} = 5.1 \times 10^{-4} m_p = 51.3\, m_{3/2}\,;$$

$$m_{3/2} = 9.9 \times 10^{-6} m_p\,,$$

which respect the correct hierarchy.

[15] We are aware of the fact that this choice leaves not so much room for the fluxes that are needed in order to stabilize the other complex structure moduli. Nonetheless, similar values of the $D3$-charge are usually accepted in the literature due to the fact that some cancellation between the fluxes is expected. Following this idea, we assume $MK = 100$ to be small enough for our purposes.

[16] There are other possibilities, with g_s always around $\frac{1}{2}$.

[17] A safe bound for the string coupling is considered to be $g_s \lesssim \frac{1}{3}$.

In addition, here we have also taken into consideration the new constraints proposed, after our [18] came out, in [116][18]. Here, the author explicitly computes, for the LVS case with $h^{1,1} = 2$, several corrections to the scalar potential claiming that even though they are sub-leading in the off-shell scalar potential, there is the possibility that they cannot be neglected in on-shell quantities such as the values of the stabilized moduli, or the scalar potential at the minimum. The new requirements come in the form of certain combinations of the parameters and of the stabilized moduli, which one should impose to be much smaller than unity, in order to be sure that the corresponding corrections are actually negligible. The author of [116], in particular, claims that it is impossible to make all this corrections negligible at the same time. A crucial point in this argument, however, is that each of these constraints depends also on the complex structure, via an unknown constant[19] factor $\mathcal{C}_\circ^\circ$. In a generic situation, people usually consider these constants to be $\mathcal{O}(1)$, however nothing forbids them to be smaller. Deriving the explicit mechanism to obtain such values is beyond the scope of this thesis, but, as suggested also in [168], it may be similar to the one proposed in [58] in order to get $W_0 \ll 1$.

Here we have chosen the parameters such that half of the requirements are satisfied, at least marginally, even for $\mathcal{C}_\circ^\circ = 1$. Nevertheless, we claim also the remaining ones to be satisfied, *provided that* the corresponding complex structure - depending constants are small enough[20].

String loop corrections

Now that we have the values of $\mathcal{V}$ and τ_5 we can introduce them in the scalar potential (8.28). We decide, in particular, to write the 2-cycle volume t_4 in terms of the others (since it appears linearly in the volume (8.8)):

$$t_4 = -\frac{-8t_5^3 + 3t_2^2 t_8 + 3t_2 t_8^2 - 8t_8^3 + 6\mathcal{V}}{12t_2 t_8 - 12t_8^2} \,. \tag{8.29}$$

Among the possible choices for the complex structure depending parameters $\mathcal{C}_i^{KK}$ and the combinatorial factor λ allowing for a minimum, we select values that ensure the corrections to be sub-leading:

$$\mathcal{C}_2^{KK} = 5.6 \times 10^{-2}; \quad \mathcal{C}_4^{KK} = 4.6 \times 10^{-3}; \quad \mathcal{C}_5^{KK} = 10^{-3};$$
$$\mathcal{C}_8^{KK} = -3.6 \times 10^{-1}; \quad \lambda = -1.6 \times 10^{-3} \,.$$

With these values we find, after having stabilized all the moduli: $\frac{V_{g_s}^{KK} + V_{F^4}}{V_{LVS+up}} = 2.9 \times 10^{-2}$. The remaining two moduli are then stabilized at:

$$t_2 = 93.2; \quad t_8 = 27.5 \,,$$

[18] See also [67, 168] for further developments. We have already mentioned this topic at the end of Ch. 6.

[19] To be precise, $\mathcal{C}_\circ^\circ$ is a function of the complex structure moduli and of the open string sector moduli, which at this stage, we assume to be all stabilized by the fluxes. This is why we consider it as a constant.

[20] For completeness, we report here the values that we find for the constraints: $\frac{\xi^{2/3} a_5^2 |\mathcal{C}_s^{log}|}{(2\kappa_5)^{2/3} g_s} = 86|\mathcal{C}_s^{log}|$; $\frac{2\xi^{1/3} a_5^2 |\mathcal{C}_1^\xi|}{3(2\kappa_5)^{4/3} g_s} = 162|\mathcal{C}_1^\xi|$; $\frac{2a_5|\mathcal{C}_2^\xi|}{3(2\kappa_5)^{2/3}\xi^{1/3}} = 12|\mathcal{C}_2^\xi|$; $\lambda_1 = 0.14$; $\lambda_2 = 3.5\times10^{-2}\mathcal{C}_b^{KK}$; $\lambda_3 = 6.8\,\mathcal{C}^{\text{flux}}$; $\lambda_4 = 0.3\,\mathcal{C}^{\text{con}}$; $\lambda_5 = 0.3\,\mathcal{C}^F$, where we have highlighted the dependence on the complex-structure dependent constants. For the detailed origin and definition of these constraints, see [116].

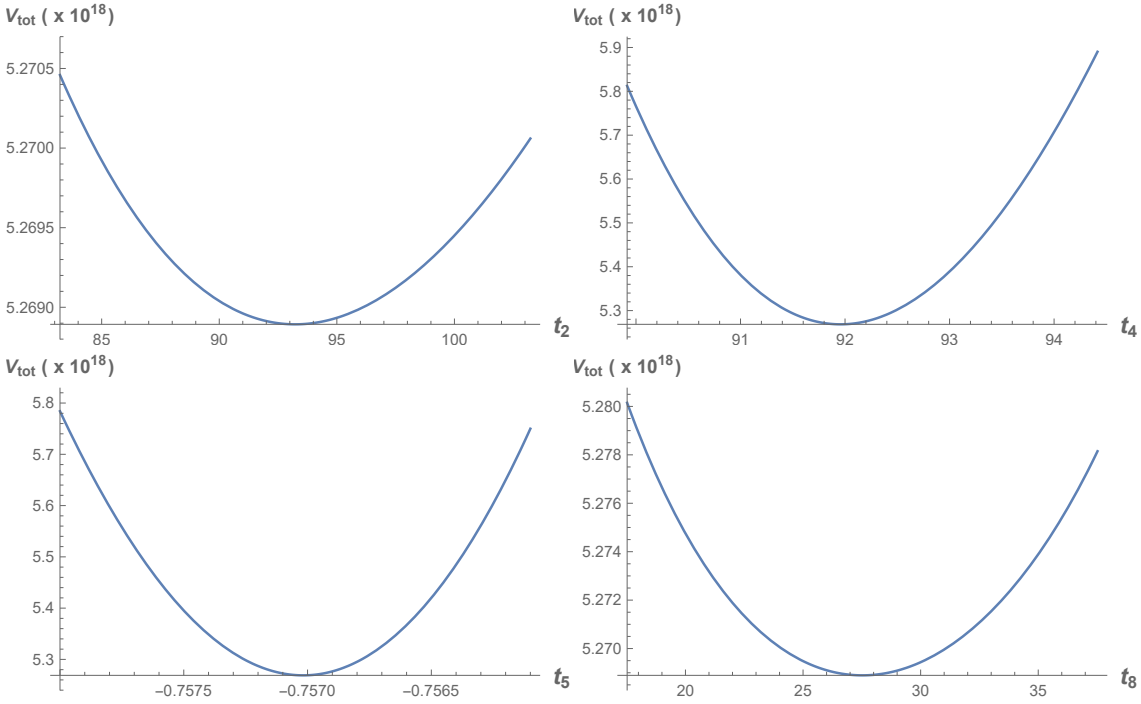

Figure 8.1: Plots of the total scalar potential (8.28) (in units of m_p) along the four directions corresponding to the 4 volume moduli t^i.

from which we derive $t_4 = 91.9$.

In Fig. 8.1, we report the plots of the total scalar potential sliced along the directions corresponding to each of the 4 volume moduli t^i. As an aside, we notice that the stabilized value of the 4-cycle τ_8 is now (8.10): $\tau_8 = 3.1 \times 10^3$; a non-perturbative correction coming from gaugino condensation on the divisor D_8 would be therefore suppressed by a factor $e^{-\frac{\pi}{3}\tau_8}/e^{-2\pi\tau_5} \simeq 10^{-1421}$, confirming the validity of our choice to neglect such effect.

Finally we can compute the masses of the 4 Kähler moduli, considering the full scalar potential (8.28). We obtain:

$$m_1^2 = 3.75 \times 10^{-8} m_p^2 \,; \quad m_2^2 = 3.75 \times 10^{-17} m_p^2 \,;$$

$$m_3^2 = 3.29 \times 10^{-19} m_p^2 \,; \quad m_4^2 = 3.27 \times 10^{-19} m_p^2 \,.$$

Consistently, two of the moduli are much lighter than the others.

To summarise, our numerical model have the following parameters and moduli VEVs corresponding to a dS minimum:

$$W_0 = 4, \quad A_5 = 1, \quad g_s = 0.52, \quad M = 10 = K, \quad \chi_{\text{eff}} = -166, \quad C_2^{KK} = 5.6 \times 10^{-2}$$
$$C_4^{KK} = 4.6 \times 10^{-3}, \quad C_5^{KK} = 10^{-3}, \quad C_8^{KK} = -3.6 \times 10^{-1}, \quad \lambda = -1.6 \times 10^{-3},$$
$$\langle t_2 \rangle = 93.2, \quad \langle t_4 \rangle = 91.9, \quad \langle t_5 \rangle = -0.76, \quad \langle t_8 \rangle = 27.5,$$
$$\langle \tau_2 \rangle = 2.1 \times 10^3, \quad \langle \tau_4 \rangle = 3.6 \times 10^3, \quad \langle \tau_5 \rangle = 2.3, \quad \langle \tau_8 \rangle = 3.1 \times 10^3,$$
$$\langle \mathcal{V} \rangle = 2.05 \times 10^5, \quad V_{min} = 5.2 \times 10^{-18}\, m_p.$$

8.3 Conclusions

In this chapter we have added a small further step towards the construction of phenomenologically interesting dS models in type IIB superstring compactifications, by taking into account a CY orientifold which, besides having all moduli stabilized at a dS vacuum, possesses a K3-fibration structure.

The combination of the new requirement with the ones to be imposed in order to have a setup which is suitable for the uplift mechanism based on $\overline{D3}$-branes, strongly constrains the admissible CY geometries at least for $h^{1,1} = 3, 4$. After having explained the main reasons behind this obstruction, we have selected the best possibility in terms of the $D3$-charge and we have explicitly analyzed it. In particular, after having presented its main geometric features, we have stabilized its four Kähler moduli in two separate steps. First we have fixed à la LVS the overall volume of the CY and the volume of the 4-cycle corresponding to the diagonal $\mathbb{CP}^1 \times \mathbb{CP}^1$ divisor. Then, in order to stabilize the remaining two moduli, we have introduced sub-leading corrections to the scalar potential.

The resulting scalar potential allows for a good amount of analytic control, which we used in order to guide the numerical analysis, performed by means of algorithms that might be used in the future for the study of more generic scalar potentials. This is important, as we know that in order to get phenomenologically interesting constructions several Kähler moduli are needed and the corresponding scalar potentials become increasingly difficult to analyze. Our work therefore adds up to the several efforts that have been recently done in the attempt to analyze in a systematic manner models with an arbitrary number of Kähler moduli.

Our solution satisfies all the constraints reported in Sec. 6.3.1, with the caveat that the string coupling g_s is relatively large. The commonly considered bound for the string coupling is indeed $g_s \lesssim \frac{1}{3}$, while in our case we have $g_s \simeq \frac{1}{2}$. Nonetheless, we have checked that the additional corrections to the scalar potential used for stabilizing the moduli t_2 and t_8 are actually sub-leading for our setup. Therefore we claim our construction to be trustworthy. Moreover, we expect to be able to improve this value of the string coupling by considering models with a larger number of Kähler moduli, which should allow for larger (in absolute value) contributions to the $D3$-charge $|Q_{D3}^{O3/O7/D7}|$.

In our numerical analysis, we have taken into consideration also the constraints recently proposed in [116], but we think that requiring them to be fulfilled for $\mathcal{C}_\circ^\circ = \mathcal{O}(1)$ may be too restrictive. In particular, in our explicit setup we have allowed the constant $\mathcal{C}_i^{KK}$ to be smaller, and we assume other of these constants to be small enough to make some of the corrections considered in [116] numerically suppressed. However, it would be interesting to analyze in more detail these parameters in order to constrain their values on the basis of physical arguments, or at least to derive some mechanism thanks to which they can actually acquire small values.

Finally, we stress that our choice of the values of the many parameters of the model was led by a systematic, but limited scan: more interesting choices might have escaped our analysis. In particular a deeper analysis of the parameter space might be an interesting development for the future.

Chapter 9

Conclusions

The main topic of this thesis was the presence of de Sitter minima in type IIB string compactifications. We focused in particular on the original uplift mechanism, proposed by KKLT [11] and based on the introduction of an $\overline{D3}$-brane at the tip of a highly warped throat. This mechanism, after having survived several challenges over the years, is now confronting additional criticisms related to the problem of canceling the total $D3$-charge within the compact 6d manifold. A model defined in the compact space X_6, indeed, contains several sources of (positive and negative) $D3$-charge: the background fluxes stabilizing the complex structure moduli and the dilaton typically carry positive $D3$-charge, while orientifold planes and D-branes typically carry negative $D3$-charge. The problem is that the presence of a highly warped throat, as well as the need to keep the supergravity approximation under control impose a lower bound on the positive $D3$-charge, which turns out to be generically large ($\mathcal{O}(100)$ in LVS, according to our estimations presented in [18]).

To be more precise, the complex structure modulus parametrizing the highly warped throat is stabilized by turning on M units of flux on the cycle at the tip of the throat and K units of flux on its dual cycle ($M, K \in \mathbb{Z}$). The contribution of these fluxes to the $D3$-charge is $Q_{D3}^{\text{flux}} = MK$. The M units of fluxes are constrained by the condition for the validity of supergravity within the warped throat, approximated to a Klebanov-Strassler throat ($g_s M \gg 1$)[1]. Since the string coupling g_s is required to be small in order to trust the string perturbative expansion, M cannot be taken to be arbitrarily small. On the other side, the need for a de Sitter minimum is already a very strong requirement *per se*, so that once M is fixed, K is essentially fixed as well, resulting in a relatively large product MK.

The negative contribution to the $D3$-charge comes from the geometric features of the compact 6d space and from the choice of the involution. We have considered only favorable Calabi-Yau manifolds constructed as hypersurfaces in toric ambient varieties equipped with a reflection involution whose geometric action changes the sign of one of the toric coordinates z_i. The choice of the involution fixes the $O7$- and $O3$-planes configuration (and the corresponding negative $D3$-charge). Another negative contribution to the $D3$-

[1] In the very recent paper [112], indeed, it was shown that the requirement $g_s M^2 \gtrsim 46.1$ [16] turns out to be significantly relaxed after a more accurate computation of the scalar potential for the complex structure modulus Z, parametrizing the warped throat.

charge, comes from $D7$-branes that we introduce in order to cancel the $D7$-tadpole of the $O7$-planes. There are different possible brane configurations, but, from the point of view of the tadpole cancellation it is convenient, whenever possible, to consider the so-called Whitney brane, which turns out to carry a much larger (in absolute value) $D3$-charge.

In order to analyze these topics, we have followed two main strategies. The first consists in taking advantage of the study of concrete constructions in order to better understand, in a more explicit way, features and issues that are then applicable to more generic configurations. The second strategy, instead, involves the analysis of a single topic (the negative $D3$-charge contribution of a given model) from a statistical point of view, taking into consideration a very large set of different geometries and involutions.

Both strategies led to the conclusion that though complicated, it should still be possible to obtain de Sitter vacua in type IIB string theory, and ruling this possibility out at this stage appears too pessimistic.

The first part of the thesis was devoted to a review of the path that led to the definition of the problem of having dS vacua in string theory. We have started (Ch. 2) from the compactification of the 10d space-time to the 4d one, explaining how this produces a large amount of moduli, corresponding to 4d massless scalar fields. These fields need to be stabilized to large enough masses: in Ch. 3, we have illustrated the main strategies that allow to do this, by generating a scalar potential for the moduli and fixing them to the minimum of this scalar potential. However, the scalar potential constructed with these mechanisms (flux compactification, KKLT and LVS) generically admits only negative-energy (AdS) vacua, while instead only dS vacua would fit the cosmological observation of an accelerating universe. This is the origin of the main topic of the thesis.

In Ch. 4, we have reviewed the most studied uplifting mechanism, by highlighting in particular the new challenges related to the tadpole and mentioning also the existence of several different proposals. Finally, in Ch. 5, we have introduced a few new tools that are particularly useful when one approaches the task of constructing and analyzing concrete realizations of dS vacua in string theory.

Our analysis was limited to type IIB compactifications in LVS. Moreover, we considered only a specific class of CY geometries, allowing only for reflection involutions of a single toric coordinate. In the first part of the thesis we took care of explaining, when needed, the reasons behind these choices and our preference of certain setups rather than others.

In the second part, we have presented the main results of our research work. In Ch. 6, based on [18], we have constructed a simple, but already rich, example of dS minimum in the frame of LVS. We have obtained this minimum by means of an $\overline{D3}$-brane placed on top of an $O3$-plane at the tip of a warped throat, as in the original KKLT proposal. Assuming that all the complex structure moduli but the one parametrizing the throat were fixed by fluxes, we have considered the scalar potential for the remaining complex structure modulus and the two Kähler moduli. Furthermore, before analyzing the concrete model, we have listed a series of requirements that a consistent realization is expected to satisfy (including the ones related to the $D3$-tadpole): we have specified which of them

are automatically realized in constructions of this kind and which ones are, on the other side, particularly constraining. We have translated these constraints into bounds on the $D3$-charge contribution coming from the fluxes, obtaining a lower bound that is typically large (even though not so large as the one obtained in [16]). We enforced our generic considerations, by inspecting different possible geometries, as well as different values of the parameters (even though without aiming for a systematic scan). Finding a CY orientifold satisfying all these constraints turned out to be not easy at all, as many of them are in tension one with the other. Nonetheless, we managed to present a construction in which all the requirements are fulfilled. In particular, the total negative $D3$-charge contribution turns out to be $|Q_{D3}^{O3/O7/D7}| = 149$, which is large enough to compensate the one coming from the fluxes within the throat ($MK = 88$), leaving also room for other fluxes to stabilize the remaining complex structure moduli.

A crucial ingredient in the example of Ch. 6, was the introduction of a Whitney brane. This particular configuration needs to be considered with some additional caution, as its world-volume is singular; nonetheless it appears to generically allow for significantly larger (in absolute value) $D3$-charges, which is promising given our need to cancel a potentially large positive contribution coming from the fluxes. Rendering this statement more concrete was one of the purposes of [19], whose results are reported in Ch. 7, where we took into consideration a very large set of geometries and involutions (all belonging to the class mentioned before), computing the $D3$-charge contribution coming from the orientifold planes and from different D-branes configurations. Here, we have also highlighted the criteria that allow to understand whether a given divisor can support a Whitney brane or need instead to be equipped by different brane configurations. We have found that, when allowing for Whitney branes, the largest $D3$-tadpole in the considered class of models (neglecting the contribution coming from possible worldvolume fluxes) is $|Q_{D3}^{O3/O7/D7}|_{\max} = 6664$, that is, as expected, significantly larger than the bound we can find considering only purely local brane configurations (SO(8) stacks): $|Q_{D3}^{O3/O7/D7}|_{\max} = 504$.

For this analysis we have relaxed the constraint of having dS given by an $\overline{D3}$ at the tip of a warped throat, including in our scan also models which can support different uplift mechanisms, such as T-branes. The largest negative $D3$-charge for models suitable for $\overline{D3}$ uplift is smaller than the one reported before, even though still quite large: $|Q_{D3}^{O3/O7/D7}|_{\max}^{\overline{\text{D3}}\text{ uplift}} = 3592$.

The database obtained in this work contains 71 941 643 orientifolds[2], over 20 millions of which correspond to smooth compactifications. We have analyzed the dependence of the $D3$-charge on several different parameters of the model (such as the number of complex structure moduli or the Euler characteristic of the compact manifold), which might be useful in orienting the choice of promising models to be explicitly taken into consideration in the future. The analysis of this large set of data allowed us to notice a peculiar structure in the distribution of the $D3$-charge as a function of the number of complex structure moduli. We believe it has not been observed in the literature before, and we interpret it as being due to the fibration structure shown by the majority of the geometries with many

[2] We have worked at the level of triangulations, hence the actual number of distinct geometries is smaller, even though we expect it to be still large.

complex structure moduli.

The analysis of explicit models, however, remains a crucial point, as these simple examples might be viewed as small steps towards the construction of a fully realistic description of our universe. The simple analysis of Ch. 6 was useful for the understanding, in a concrete way, of the new tadpole-related challenges as well as of several other obstructions to the realization of dS vacua from $\overline{D3}$ uplift. Nevertheless, having only two Kähler moduli, it did not leave any room for the introduction of other ingredients, more interesting from the phenomenological point of view.

This motivated the analysis of [20], reported in Ch. 8, where we have constructed an example with four Kähler moduli stabilized in a dS minimum, in a set up in which the compact manifold is a K3 fibration. Besides the consistency conditions already analyzed in Ch. 6, we have taken into consideration also the new constraints proposed in [116, 67, 168] (after the publication of our [18]). Moreover, we have highlighted the new challenges deriving from the requirement of having a K3 fibration, which, when considered together to the need for a setup suitable for $\overline{D3}$ uplift, strongly constrains the admissible intersection numbers, and hence the geometries, at least when one limits the search to models with a few Kähler moduli. Our construction satisfies half of the new constraints, which are given as specific combinations of the parameters that are required to be smaller than 1. However, we stress that they all have a dependence on the complex structure and open string sector moduli, usually parametrized in terms of a constant (we assume these moduli to be stabilized) $\mathcal{C}_\circ^\circ$. In order to have the most generic configuration, people usually take these constants to be $\mathcal{O}(1)$, but there is no physical obstruction (at least to our knowledge) towards smaller values. We claim therefore that the remaining constraints can be actually satisfied, under the assumption that the corresponding complex-structure dependent parameters are small enough.

What else can be done? Of course several upgrades and expansions remain open as future research lines. Here we mention the ones we believe to be the most interesting.

First, we stress that while our concrete setups satisfy all the constraints we have imposed (with the caveat mentioned before regarding the new ones), we have been forced to fix some of the parameters of the problem near the boundary of their region of validity (defined by the consistency conditions themselves). This is the case, as an example, of the string coupling g_s which is not so small in [18] and even larger in [20] (even though still smaller than unity). As we explained in Sec. 6.3.2, this limitation is essentially due to the need of having a small tadpole contribution from the fluxes. On the other side, we noticed in Ch. 7 that much larger $D3$-charges are allowed in more generic configurations. It is therefore reasonable to believe that considering these more involved setups might help in the improvement of our control over the approximations.

The analysis of models with several Kähler moduli is certainly much more complicated. Nonetheless it is something one should try to face, sooner or later, especially due to the fact that, as mentioned before, the additional moduli appear to be needed for the inclusion of certain phenomenologically relevant features. We believe our work to be a valid starting point for these constructions for at least two reasons. First, the database constructed

in [19] can be a valuable source for the search of suitable geometries. For this reason it would be useful to extend it to the regime $h^{1,1} \geq 12$ as well as to try to relate it to other existing databases, such as [169] for CICYs and [106] for divisor exchange involutions. The second reason is that our analysis in Ch. 8 allowed us to start developing an algorithm for the numeric analysis of scalar potentials depending on several Kähler moduli. This is usually a difficult task, as the presence of various exponential factors (coming from the non-perturbative corrections to the superpotential) produce directions which are much flatter than the others, rendering the minimization procedure particularly responsive to the choice of initial conditions. Being relatively simple, our model could enjoy a good amount of analytic control, hence we were able to use it to test the validity of this algorithm. In the future we would like to refine it in order to make it suitable for more generic setups, which we expect to be crucial for the analysis of the examples selected from the database [19].

A second interesting topic that is worth a deeper study regards the debate around possible non-negligible corrections to the scalar potential, which has been recently raised by [116, 67, 168]. As mentioned before, the constraints to be imposed in order to ensure that these corrections are actually negligible depend on the (stabilized) complex-structure and open-string moduli in a way that is not explicitly known and is therefore parametrized by an unknown constant. Being able to compute the values of these constants, or at least to constrain them to tighter ranges would be decisive in order to quantify in a more precise way the corresponding constraints as well as to understand whether one should actually worry about these corrections.

Finally, it would be interesting to delve into the complex structure moduli stabilization in order to quantify the amount of fluxes (hence the corresponding $D3$-charge) which is actually needed to stabilize *all* of them. Up to now, a lower bound for the $D3$-charge carried by the fluxes has only been conjectured in [114] (see also Sec. 4.4). A more explicit computation might help to better understand the constraint $|Q_{D3}^{O3/O7/D7}| < MK$, adopted here both in Ch 6 and Ch 8, giving a more concrete idea of how much room one should leave for the remaining background fluxes.

Appendix A

Frames and Energy scales

This appendix is devoted to a collection of some useful formulas regarding the relation between the Einstein frame and the string frame (Sec. A.1) as well as to the presentation of the main energy scales characterizing string compactifications (Sec. A.2).

A.1 Einstein and string frame

The relation between the Einstein frame and the string frame in D dimensions is given by the conformal rescaling [2]:

$$g_{\mu\nu,E} = e^{\frac{-4(\phi-\phi_0)}{D-2}} g_{\mu\nu,s} \tag{A.1}$$

where ϕ_0 is the vacuum expectation value for the dilaton field.

If $D = 10$ as in superstring theory, the above relation reads:

$$G_{MN,E} = e^{-\frac{\phi-\phi_0}{2}} G_{MN,s} \tag{A.2}$$

where for the 10d metric we used the same notation introduced in the main text. The main advantage of this redefinition is that it allows to write the low-energy effective action of the string in a way in which all the fields have canonical kinetic terms.

When converting quantities from the string to the Einstein frame and vice versa, it is useful to keep in mind the following relation, that can be derived from the definition (A.2) (keeping $\phi_0 = 0$ for simplicity):

- Determinant of the metric:

$$\sqrt{-G_s} = e^{\frac{5}{2}\phi}\sqrt{-G_E}\,;$$

- Ricci scalar [23]:

$$R_s = e^{-\frac{\phi}{2}}\left(R_E - \frac{9}{2}\nabla_E^2\phi - \frac{9}{2}\,G_E^{MN}\,\nabla_M^E\phi\nabla_N^E\phi\right)\,;$$

- Laplacians [23]:

$$\nabla_s^2 = e^{-\frac{\phi}{2}}\left(\nabla_E^2 + 2G_E^{MN}\nabla_M^E\phi\,\nabla_N^E\right)\,;$$

- Volume of the CY:

$$\mathcal{V}_E = e^{-\frac{3\phi}{2}}\mathcal{V}_s = g_s^{-3/2}\mathcal{V}_s\,. \tag{A.3}$$

A.2 Energy scales

The only dimensionful parameter in 10d superstring theory is the string mass M_s (or equivalently the string length l_s). Hence all the (dimensionful) quantities can be expressed in units of this scale. Nonetheless, it is useful to present the 4d physical quantities in terms of the 4d Planck mass, which can be related to the string scale via the (dimensionless) string coupling g_s and the volume of the compact space (Sec. A.2.1).

All the other masses of the theory derive from the string mass and they must be taken into account in order to verify that a given model is consistent. While the masses of the several moduli arising in string compactifications are studied in the main text, in Sec. A.2.2 we present the masses of the Kaluza-Klein (KK) modes deriving from string compactification and the mass of the gravitino.

A.2.1 Planck and String mass

In the standard units $\hbar = c = 1$, the string mass is defined as the inverse of the string length:

$$M_s = \frac{1}{l_s} = \frac{1}{2\pi\sqrt{\alpha'}}\,, \tag{A.4}$$

where α' is the so-called Regge slope, which is related to the tension of the fundamental string [1]. Below this scale, only the massless states of the string are excited and the theory reduces to an effective 10d supergravity theory.

The 4d Planck mass is

$$M_p = \sqrt{\frac{1}{G_N}} = 1.22 \times 10^{19} GeV\,, \tag{A.5}$$

from which we define the 4d gravitational coupling as [1]:

$$\kappa_4 = \sqrt{8\pi G_N} = (2.43 \times 10^{18} GeV)^{-1} = \frac{(8\pi)^{1/2}}{M_p}\,. \tag{A.6}$$

Due to the definition of κ_4, it appears convenient to define a *reduced* Planck mass

$$m_p = \kappa_4^{-1} = \frac{M_p}{(8\pi)^{1/2}}\,, \tag{A.7}$$

which allows to avoid annoying 2π factors in several computations.

Let us now come to the relation between the string mass and the Planck mass. Assuming that the string coupling g_s is constant, the 10-dimensional gravitational coupling κ_{10}, whose dimensions are $[\kappa_{10}] = L^4$ is related to the 4-dimensional one by (see also Sec. 2.2.1):

$$\frac{1}{2\kappa_4^2} = \frac{\mathcal{V}_s}{2\kappa_{10}^2 g_s^2}\,, \tag{A.8}$$

where $\mathcal{V}_s$ is the volume of the compact CY space in string frame, in units of l_s. By using the definition of κ_{10} in terms of the string constant α' [5],

$$2\kappa_{10}^2 = (2\pi)^7 \alpha'^4\,,$$

Eq. (A.8) can be recast as a relation between the reduced Planck scale and the string scale:

$$M_s = \frac{g_s}{(4\pi\mathcal{V}_s)^{1/2}} m_p = \frac{g_s^{1/4}}{(4\pi\mathcal{V}_E)^{1/2}} m_p \,, \tag{A.9}$$

where in the last step we converted the result in the Einstein frame, using (A.3). Notice that in the large volume limit, in which we are interested, the string mass is hierarchically smaller than the Planck mass.

A.2.2 Kaluza-Klein and gravitino masses

The compactification of the 10d space produces towers of additional states, which is acceptable from the point of view of the 4d effective field theory, provided that these states are much heavier than any 4d state. An estimation of the mass of the so-called Kaluza-Klein (KK) modes can be obtained from the analysis of the simpler toroidal compactifications, from which we derive that it scales with the inverse of the characteristic length of the compact space $R = R_s l_s$ [13]:

$$M_{KK} \sim \frac{M_s}{R_s}; \quad R_s \gg 1 \,.$$

It is reasonable to assume that, generically, the radius R_s is related to the overall volume of the compact space ($\mathcal{V}_s \sim R_s^6$), therefore we can write

$$M_{KK}^{\text{bulk}} \sim \frac{2\pi M_s}{\mathcal{V}_s^{1/6}} = \frac{\sqrt{\pi}}{\mathcal{V}_E^{2/3}} m_p \,, \tag{A.10}$$

where again we presented the result both in Einstein and string frame. In general, several other KK states are expected to arise associated to open string excitations on D7-branes wrapped around 4-cycles. Their masses can be computed in a similar way as M_{KK}^{bulk} [61]:

$$M_{KK}^{i} = \frac{\sqrt{\pi}}{\sqrt{\mathcal{V}_E}\,\tau_i^{1/4}} m_p \,. \tag{A.11}$$

However, any volume τ_i is smaller than the overall volume of the compact space $\mathcal{V}$, hence all these additional states are heavier than M_{KK}^{bulk}, which therefore is the only one that we need to check in order to test the reliability of the 4d description.

As a consequence of spontaneous supersymmetry breaking, the spin-3/2 gravitino (which is the supersymmetric partner of the graviton) acquires a mass defined as:

$$m_{3/2} = e^{K/2}|W| \simeq \sqrt{\frac{g_s}{2}} \frac{|W_0|}{\mathcal{V}_E} m_p \tag{A.12}$$

due to a super-Higgs mechanism. As it is clear also from the above definition, the gravitino arises in the 4d effective field theory, therefore a consistent theory necessarily has $m_{3/2} \ll M_{KK}^{\text{bulk}}$.

Appendix B

Cohomology and Homology groups

This appendix is mainly based on [22, 201]. Following these references, we start considering real (differential) manifolds and we then explain how the results can be extended to complex manifolds, which are the ones we are interested in.

B.1 Preliminary definitions

Given a (differential) p-form (that is a $[0,p]$-type tensor with completely antisymmetric components) A_p on the real differential manifold X [1], we define:

- A *closed* p-form: A_p such that $dA_p = 0$ [2].
- An *exact* p-form: A_p such that there exists a $(p-1)$ - form B_{p-1}, with $A_p = dB_{p-1}$.

Let us consider instead the set of p-dimensional (differential) submanifolds $\mathcal{C}^p$ of X, endowed with a vector space structure. We define a *p-chain* a_p the formal linear combination of the submanifolds $\mathcal{C}^p$ and:

- A *p-cycle*: $a_p \subset X$ with no boundary, that is such that $\partial a_p = 0$ [3];
- A *trivial* p-chain: a_p such that there exists a $(p+1)$ - chain b_{p+1}, with $a_p = \partial b_{p+1}$.

B.2 Cohomology and Homology groups

Since $d^2 = 0$, we deduce from the definitions of the previous section that any exact p - form is closed. The reverse is generically not true at the global level (unless $X \equiv \mathbb{R}^d$) and the presence of closed non-exact forms can be seen as a measure of the non-triviality of X.

[1] More precisely, on the vector space of p-forms at a point in X.

[2] d indicates the *exterior* derivative, mapping a p-form to a $(p+1)$ - form. A key property of it is $d^2 \equiv 0$ (that is $d(dA_p) = 0,\ \forall A_p$).

[3] Similarly to the exterior derivative, the boundary ∂a_p of a p-chain (with dimensions $p-1$) is such that $\partial^2 \equiv 0$.

In order to quantify this measure, we define the p-th *de Rham cohomology group* of X as the quotient:

$$H^p(X,\mathbb{R}) = \frac{\mathcal{Z}^p}{\mathcal{B}^p}\,, \tag{B.1}$$

where $\mathcal{Z}^p$ is the set of closed p-forms on X and $\mathcal{B}_p$ is the set of exact p-forms. In other words, $H^p(X,\mathbb{R})$ is the set of closed p - forms modulo the equivalence relation

$$A_p \simeq A_p + dB_{p-1}\,.$$

The p-th cohomology group has the structure of a vector space, whose (finite) dimension is given by the Betti number $b^p(X) \equiv \dim H^p(X,\mathbb{R})$.

The same information regarding the topology of X, can be obtained in terms of the submanifolds of X, using therefore, the second set of definitions presented in the previous section. In this case, we define the p-th *homology group* of X as:

$$H_p(X,\mathbb{R}) = \frac{\mathcal{Z}_p}{\mathcal{B}_p}\,, \tag{B.2}$$

where $\mathcal{Z}_p$ is the set of p-cycles in X and $\mathcal{B}_p$ the set of trivial p-cycles. In analogy with the definition of the cohomology group, therefore, $H_p(X,\mathbb{R})$ is the set of p-cycles modulo the equivalence relation

$$a_p \simeq a_p + \partial b_{p+1}\,.$$

The analogy between the two definitions is made formal by the de Rahm theorem, according to which the integration of p-forms over p-dimensional submanifolds of X defines a linear mapping $H^p(X,\mathbb{R}) \times H_p(X,\mathbb{R}) \to \mathbb{R}$. In other words H_p and H^p are *dual* to each other:

$$H^p(X,\mathbb{R}) \simeq H_p(X,\mathbb{R})\,.$$

As a direct consequence, they have the same dimension, indicated by the Betti numbers.

Finally, we recall here also the Poincaré duality (also mentioned in Sec. 5.1), according to which the cohomology groups $H^p(X,\mathbb{R})$ and $H^{D-p}(X,\mathbb{R})$, with $D = \dim X$, are dual to each other. We can therefore summarize the results of this section as:

$$H^{D-p}(X,\mathbb{R}) \simeq H^p(X,\mathbb{R}) \simeq H_p(X,\mathbb{R}) \simeq H_{D-p}(X,\mathbb{R})\,.$$

B.3 Complex manifolds

The definitions and results exposed before can be easily generalized to the case in which X is a complex manifold of complex dimension k.

In particular, we define here a complex (p,q)-form $\gamma_{p,q}$, with $p,q = 0,...,\dim_{\mathbb{C}} X$, as a complex-valued differential form with p holomorphic indices and q anti-holomorphic indices. The exterior derivative d is now given in terms of the *Dolbeault operators* ∂, mapping (p,q)-forms into $(p+1,q)$ - forms, and $\bar{\partial}$, mapping (p,q)-forms into $(p,q+1)$ - forms, as

$$d = \partial + \bar{\partial}\,,$$

with the property $\partial^2 = \bar{\partial}^2 = \partial\bar{\partial} + \bar{\partial}\partial = 0$.

The *Dolbeault cohomology group* is defined as:

$$H^{p,q}_{\bar{\partial}}(X, \mathbb{C}) = \frac{\mathcal{Z}^{p,q}_{\bar{\partial}}}{\mathcal{B}^{p,q}_{\bar{\partial}}} \,, \tag{B.3}$$

where $\mathcal{Z}^{p,q}_{\bar{\partial}}$ is the set of $\bar{\partial}$ - closed (p,q)-forms and $\mathcal{B}^{p,q}_{\bar{\partial}}$ is the set of $\bar{\partial}$ - exact (p,q)-forms. The dimensions of $H^{p,q}_{\bar{\partial}}(X, \mathbb{C})$ are given by the so-called *Hodge numbers* $h^{p,q}$, which are related to the Betti numbers by (considering $\dim_{\mathbb{C}} X = 2 \dim_{\mathbb{R}} X$):

$$b_r = \sum_{p+q=r} h^{p,q} \,. \tag{B.4}$$

Two important relations for the Hodge numbers (extensively used along this thesis) are:

$$h^{p,q} = h^{k-p,k-q} \,, \tag{B.5}$$

which is the consequence of a simple extension of the Poincaré duality to complex manifolds, and

$$h^{p,q} = h^{q,p} \,, \tag{B.6}$$

which is true for any Kähler manifold (hence, in particular, for the CY manifolds we consider in this work).

Appendix C

Canonical Normalization

Often in the text the masses of the stabilized moduli are computed as the eigenvalues of the matrix

$$M^I_J = (K^{I\bar{L}} V_{\bar{L}J})_{\min} \,, \tag{C.1}$$

where $K^{I\bar{L}} = \left(\frac{\partial^2 K}{\partial T_I \partial \overline{T}_L}\right)^{-1}$ is the (transposed) inverse of the Kähler metric $K_{\bar{I}J}$ and $V_{\bar{L}J} = \frac{\partial^2 V}{\partial \overline{T}_L \partial T_J}$ is the matrix of the second derivatives of the scalar potential V. However, $\mathcal{M}^I_J$ is not the mass matrix, but only a matrix with the same eigenvalues. In the following, we review the *canonical normalization* of the Lagrangian, which allows to find the proper mass matrix (useful, for example if one needs to find also the eigenvectors of the matrix, not only the eigenvalues), and we show that it indeed has the same eigenvalues as M. For simplicity, we will only focus on the Kähler moduli T_i, but the argument is easily expansible to the complex structure moduli.

Let us consider the following Lagrangian:

$$\mathcal{L} = K_{\bar{I}J}\, \partial_\mu \overline{T}^I\, \partial^\mu T^J + \partial_{\bar{I}} \partial_J V\, \overline{T}^I\, T^J = (\partial_\mu \overline{T})^t K (\partial^\mu T) + \overline{T}^t\, \partial\partial V\, T \,, \tag{C.2}$$

where the last term is written using the matrix formalism (and t stands for the transpose).

Clearly $\mathcal{L}$ is not written in the canonical form, which would have $K = \mathbb{1}$. The transformation of the fields T_i into their canonically normalized version T_{C_i} can be derived via two simple steps:

1. Diagonalize K, via a unitary transformation U:

$$U : U^\dagger U = \mathbb{1} \text{ such that } U^\dagger K U = \tilde{K}_{(\text{diag})} \,. \tag{C.3}$$

This imposes a redefinition of the fields:

$$(\partial_\mu \overline{T})^t K (\partial^\mu T) = (\partial_\mu \overline{T})^t U (U^\dagger K U)\, U^\dagger (\partial^\mu T) \equiv (\partial_\mu \overline{T}')^t\, \tilde{K}_{(diag)}\, \partial^\mu T' \,, \tag{C.4}$$

where now $T' = U^\dagger T$.

2. Re-scale $K_{(\text{diag})}$ to unity, via the diagonal matrix R:

$$R = \text{diag}(r_1, ..., r_n) : r_I = (\tilde{K}_{\bar{I}I})^{-1/2}\,, \qquad \text{so that } R\tilde{K}R = \mathbb{1} \tag{C.5}$$

where we used the fact that $\tilde{K}_{\bar{I}I} \in \mathbb{R}$, hence $R = R^\dagger$. The corresponding re-scaling of the fields reads:

$$(\partial_\mu \overline{T}')^t\, \tilde{K}\, \partial^\mu T' = [(\partial_\mu \overline{T}')^t R^{-1}](R\tilde{K}R)(R^{-1}\partial^\mu T') \equiv (\partial_\mu \overline{T}_C)^t\, \partial^\mu T_C \tag{C.6}$$

with $T_C = R^{-1}T'$.

We have found out, therefore, that the fields T_i can be converted to the canonically normalized ones through the matrix

$$P \equiv R^{-1}U^\dagger\,. \tag{C.7}$$

Introducing the T_{C_i}'s in (C.2) we find the normalized Lagrangian

$$\mathcal{L} = (\partial_\mu \overline{T}_C)^t\, \partial^\mu T_C + \overline{T}_C^t\, \mathcal{M}\, T_C\,, \tag{C.8}$$

from which we can finally derive the mass matrix $\mathcal{M}$ for the fields T_{C_i}:

$$\overline{T}^t\, \partial\partial V\, T = \overline{T}_C^t\, (P^{-1})^\dagger\, \partial\partial V\, P^{-1}\, T_C \Rightarrow \mathcal{M} = (P^{-1})^\dagger\, \partial\partial V P^{-1}\,. \tag{C.9}$$

Let us finally prove the initial statement according to which the two matrices M (C.1) and $\mathcal{M}$ (C.9) have the same eigenvalues.

First we notice that:

$$K = P^\dagger P\,. \tag{C.10}$$

Indeed

$$(\partial_\mu \overline{T})^t\, K\, (\partial^\mu T) = [(\partial_\mu \overline{T})^t\, U\, R^{-1}]\, [R\, (U^\dagger\, K\, U)\, R]\, [R^{-1}U^\dagger\, (\partial^\mu T) = (\partial_\mu \overline{T})^t\, P^\dagger P\, \partial^\mu T\,,$$

where in the last step we used $R(U^\dagger K U)R = \mathbb{1}$. As a consequence, $K^{-1} = P^{-1}(P^\dagger)^{-1}$.

Our statement is then proven by the following straightforward computation:

$$\begin{aligned}
\det(\mathcal{M} - \lambda\mathbb{1}) &= \det[(P^{-1})^\dagger\, \partial\partial V P^{-1} - \lambda\mathbb{1}] = \\
&= \det[PP^{-1}(P^{-1})^\dagger\, \partial\partial V P^{-1} - \lambda\, P\, \mathbb{1} P^{-1}] = \\
&= \det[P(K^{-1}\, \partial\partial V - \lambda\mathbb{1})\, P^{-1}] = \\
&= \det(P)\det(K^{-1}\, \partial\partial V - \lambda\mathbb{1})\det(P^{-1}) = \det(K^{-1}\, \partial\partial V - \lambda\mathbb{1})\,.
\end{aligned}$$

□

Appendix D

Generic Scalar potential

In this appendix we compute the total LVS scalar potential for a generic number $h^{1,1}$ of Kähler moduli, plus the conifold modulus Z. In order to do so, we follow the strategy of [61], which we also summarized in Sec. 3.3 where the same computation was performed in the absence of Z.

The supergravity low energy theory is described by the usual Kähler potential:

$$K = -\log\left(S+\bar{S}\right) - 2\log\left[\mathcal{V} + \xi\left(\frac{S+\bar{S}}{2}\right)^{3/2}\right] + \frac{9c'M^2|Z|^{2/3}}{\mathcal{V}^{2/3}}\left(\frac{S+\bar{S}}{2}\right)^{-1}, \qquad \text{(D.1)}$$

with $\xi = -\frac{\chi(X_6)\zeta(3)}{4(2\pi)^3}$; $c' \simeq 1.18$.

Since in the end we want to perform the Large Volume limit, we need to assume that there is at least one cycle which is much larger than the others. More generically, we will consider the case in which there are $1 \leq n < h^{1,1}$ small cycles, contributing to the non-perturbative term in the superpotential, which therefore reads:

$$W = W_{cs}e^{i\varphi} - \frac{M}{2\pi i}Z(\log Z - 1) + iKZs + \sum_{i=1}^{n} A_i e^{-a_i T_i}, \qquad \text{(D.2)}$$

where $\left(s = \frac{S+\bar{S}}{2}\right)$ and $W_{cs}e^{i\varphi}$ is, as usual, the VEV of the superpotential for the complex structure moduli (with the exception of the conifold one), which we consider to be stabilized at larger energies.

It is important to notice that, differently from the simple case considered in Ch. 6, here the rigid divisors supporting non-perturbative effects are generically non-diagonal. As a consequence it is impossible (or very difficult) to write the volume:

$$\mathcal{V} = \frac{1}{6}k_{ijk}t^i t^j t^k \qquad \text{(D.3)}$$

in terms of the 4-cycles, that is to solve the set of equations $\tau_i = \frac{\partial \mathcal{V}}{\partial t_i} = \frac{1}{2}k_{ijk}t^j t^k$. The easiest thing to do, following [61], is instead to perform the whole computation in terms of the volumes of the 2-cycles t^i.

D.1 Kähler metric and its inverse

In this section we compute the elements of the Kähler metric (as usual through the derivatives of the Kähler potential). Since the derivatives with respect to the Kähler moduli now require some additional comment, let us start presenting all the elements of the Kähler metric that do *not* involve these derivatives:

$$K_{Z\bar{Z}} = \frac{c' M^2}{s\zeta^{4/3}\mathcal{V}^{2/3}}\,; \quad K_{Z\bar{S}} = -\frac{3c' M^2 \bar{Z}}{2s^2\zeta^{4/3}\mathcal{V}^{2/3}} = \overline{(K_{S\bar{Z}})}\,; \tag{D.4}$$

$$K_{S\bar{S}} = \frac{2\mathcal{V}^2 + \hat{\xi}\mathcal{V} + 8\hat{\xi}^2}{8s^2(\mathcal{V}+\hat{\xi})^2} + \frac{9c' M^2 \zeta^{2/3}}{2s^3\mathcal{V}^{2/3}}\,, \tag{D.5}$$

where $\hat{\xi} = s^{3/2}\xi$.

Let us come to the computation of the derivatives with respect to the Kähler moduli T_i. The difficulty is due to the fact that now we only know how $\mathcal{V}$ depends on the 2-cycles t^i, whose definition in terms of the Kähler moduli T_i is not trivial. Following [61][1], we begin observing that the first derivative of (D.1) with respect to T_i can be written as:

$$K_{T_i} \equiv \frac{\partial K}{\partial T_i} = \frac{\partial K}{\partial \mathcal{V}}\frac{\partial \mathcal{V}}{\partial T_i}\,. \tag{D.6}$$

In order to compute the derivative of the volume we observe that Eq. (D.3) can be written as:

$$\mathcal{V} = \frac{1}{6}t^i(k_{ijk}t^j t^k) = \frac{1}{6}t^i(T_i)\cdot(T_i+\bar{T}_i) \quad \Rightarrow \quad \frac{\partial \mathcal{V}}{\partial T_i} = \frac{1}{6}\left(t^i + (T_i+\bar{T}_i)\cdot\frac{\partial t^j}{\partial T_i}\right) \tag{D.7}$$

where we used $k_{ijk}t^j t^k = 2\tau_i$ and $\tau_i = \frac{T_i+\bar{T}_i}{2}$ ($T_i = \tau_i + i\theta_i$). Finally, the last term can be evaluated by noticing that the following identity holds:

$$t^i = 2(k_{ijk}t^k)^{-1}\tau_j = (k_{ijk}t^k)^{-1}(T_j+\bar{T}_j) \equiv k^{ij}(T_j+\bar{T}_j)\,, \tag{D.8}$$

where we introduced the quantity $k^{ij} = (k_{ijk}t^k)^{-1}$, from which we conclude:

$$\frac{\partial t^i}{\partial T_j} = \frac{1}{2}k^{ij} = \frac{\partial t^i}{\partial \bar{T}_j}\,. \tag{D.9}$$

Introducing this expression into (D.6), we eventually find:

$$\frac{\partial \mathcal{V}}{\partial T_i} = \frac{1}{6}\left(t^i + (T_i+\bar{T}_i)\cdot\frac{(k_{ijk}t^k)^{-1}}{2}\right) = \frac{t^i}{4}\,, \tag{D.10}$$

where in the last term we again used the identity (D.8).

Using the above results, we can now conclude the computation of the Kähler metric:

$$K_{S\bar{T}_i} = \frac{1}{4}\frac{\partial^2 K}{\partial S\partial \mathcal{V}}t^i = \frac{3\sqrt{s}\,t^i\xi}{8(\mathcal{V}+\hat{\xi})^2} + \frac{3c' M^2\, t^i\,\zeta^{2/3}}{4s^2\mathcal{V}^{5/3}} = K_{T_i\bar{S}}\,;$$

$$K_{Z\bar{T}_i} = \frac{1}{4}\frac{\partial^2 K}{\partial Z\partial \mathcal{V}}t^i = -\frac{c' M^2 \bar{Z}\,t^i}{2s\zeta^{4/3}\mathcal{V}^{5/3}} = \overline{(K_{T_i\bar{Z}})}\,;$$

$$K_{T_i\bar{T}_j} = \frac{1}{16}\frac{\partial^2 K}{\partial \mathcal{V}^2}t^i t^j + \frac{1}{8}\frac{\partial K}{\partial \mathcal{V}}k^{ij} = \frac{t^i t^j - 2k^{ij}(\mathcal{V}+\hat{\xi})}{8(\mathcal{V}+\hat{\xi})^2} + \frac{c' M^2\zeta^{2/3}(5t^i t^j - 6k^{ij}\mathcal{V})}{8s\mathcal{V}^{8/3}}\,.$$

[1] See also [202].

The inverse of the Kähler metric is computed as usual. The terms that will be relevant for our computation are:

$$K^{I\bar{J}} = \begin{pmatrix} \kappa_{zz} & \kappa_{zt} Z\, \tau_i \\ \\ \kappa_{zt} \bar{Z}\, \tau_i & \kappa_{tt}^{(1)} k_{ij} + \kappa_{tt}^{(2)} \tau_i \tau_j \end{pmatrix} ; \qquad k_{ij} = k_{ijk} t^k \, , \tag{D.11}$$

where κ_{zz}, κ_{zt}, $\kappa_{tt}^{(1)}$ and $\kappa_{tt}^{(2)}$ are real and do not depend on the individual Kähler moduli; they are defined as:

$$\kappa_{zz} = \frac{s^3 \mathcal{V}^3 \zeta^{4/3}(\mathcal{V} - 2\hat{\xi}) + 3c' M^2 s^2 \zeta^2 \mathcal{V}^{4/3}(8\mathcal{V}^2 - 11\hat{\xi}\mathcal{V} + 8\hat{\xi}^2) + 81 c'^2 M^4 s\, \zeta^{8/3} \mathcal{V}^{2/3} \mathcal{Y}^2}{c' M^2 [s^2 \mathcal{V}^{7/3}(\mathcal{V} - 2\hat{\xi}) + 3c' M^2 s\, \zeta^{2/3} \mathcal{V}^{2/3}(4\mathcal{V}^2 - \mathcal{V}\hat{\xi} + 4\hat{\xi}^2) + 27 c'^2 M^4 \zeta^{4/3} \mathcal{Y}^2]} \, ; \tag{D.12a}$$

$$\kappa_{zt} = \frac{2s\mathcal{V}^{2/3}[s\mathcal{V}^{2/3}(\mathcal{V} - 2\hat{\xi})^2 + 9c' M^2 \zeta^{2/3} \mathcal{Y}^2]}{s^2 \mathcal{V}^{7/3}(\mathcal{V} - 2\hat{\xi}) + 3c' M^2 s\, \zeta^{2/3} \mathcal{V}^{2/3}(4\mathcal{V}^2 - \mathcal{V}\hat{\xi} + 4\hat{\xi}^2) + 27 c'^2 M^4 \zeta^{4/3} \mathcal{Y}^2} \, ; \tag{D.12b}$$

$$\kappa_{tt}^{(1)} = -\frac{4s\mathcal{V}^{5/3}\mathcal{Y}}{s\mathcal{V}^{5/3} + 3c' M^2 \zeta^{2/3} \mathcal{Y}} \, ; \tag{D.12c}$$

$$\kappa_{tt}^{(2)} = \frac{2s\mathcal{V}^{2/3}[s^2\, \mathcal{V}^{10/3}(2\mathcal{V} - \hat{\xi}) + 3c' M^2 s \mathcal{V}^{2/3} \zeta^{2/3} \mathcal{Y}(8\mathcal{V}^2 + \mathcal{V}\hat{\xi} + 8\hat{\xi}^2) + 54 c'^2 M^4 \zeta^{4/3} \mathcal{Y}^3]}{(s\mathcal{V}^{5/3} + 3c' M^2 \zeta^{2/3} \mathcal{Y})[s^2 \mathcal{V}^{7/3}(\mathcal{V} - 2\hat{\xi}) + 3c' M^2 \zeta^{2/3}(s\mathcal{V}^{2/3}(4\mathcal{V}^2 - \mathcal{V}\hat{\xi} + 4\hat{\xi}^2) + 9c' M^2 \zeta^{2/3} \mathcal{Y}^2)]} \, ; \tag{D.12d}$$

where we have used: $\mathcal{Y} = \mathcal{V} + \hat{\xi}$.

D.2 Scalar potential

The scalar potential for the $h^{1,1}$ Kähler moduli and the conifold modulus is given by:

$$V = e^K \left[K^{I\bar{J}} \partial_I W \partial_{\bar{J}} \overline{W} + K^{I\bar{J}} (\partial_I W \partial_{\bar{J}} K \overline{W} + \partial_I K \partial_{\bar{J}} \overline{W} W) + (K^{I\bar{J}} \partial_I K \partial_{\bar{J}} K - 3) |W|^2 \right] .$$

Let us consider each term separately.

$\mathbf{K^{I\bar{J}} \partial_I W \partial_{\bar{J}} \overline{W}}$

This term can be separated in three different contributions, each depending on a different power of the exponential $e^{-a_i \tau_i}$. Recalling that $Z = \zeta e^{i\sigma}$, we find:

$$K^{Z\bar{Z}} \partial_Z W \partial_{\bar{Z}} \overline{W} = \kappa_{zz} \left[\frac{M^2 \sigma^2}{4\pi^2} + \left(sK + \frac{M}{2\pi} \log \zeta \right)^2 \right] ;$$

$$K^{Z\bar{T}_i} \partial_Z W \partial_{\bar{T}_i} \overline{W} + K^{T_i \bar{Z}} \partial_{T_i} W \partial_{\bar{Z}} \overline{W} = \kappa_{zt} \sum_{i=1}^{n} A_i e^{-a_i \tau_i} \left[\frac{M\sigma}{\pi} \cos(a_i \theta_i + \sigma) \right.$$
$$\left. + 2 \left(sK + \frac{M}{2\pi} \log \zeta \right) \sin(a_i \theta_i + \sigma) \right] a_i \tau_i \, \zeta \, ;$$

$$K^{T_i \bar{T}_j} \partial_{T_i} W \partial_{\bar{T}_j} \overline{W} = \sum_{i,j=1}^{n} a_i a_j A_i A_j e^{-a_i \tau_i - a_j \tau_j} \cos(a_i \theta_i - a_j \theta_j) (\kappa_{tt}^{(1)} (k_{ijk} t^k) + \kappa_{tt}^{(2)} \tau_i \tau_j) \, .$$

$\mathbf{K^{I\bar{J}}(\partial_I W \partial_{\bar{J}} K \overline{W} + \partial_I K \partial_{\bar{J}} \overline{W} W)}$

First of all it is convenient to compute the first derivatives of the Kähler potential:

$$\partial_Z K = \overline{(\partial_{\bar{Z}} K)} = \frac{3c' M^2 \bar{Z}}{s\mathcal{V}^{2/3}\zeta^{4/3}} \,; \tag{D.13a}$$

$$\partial_{T_i} K = \partial_{\bar{T}_i} K = \frac{1}{4}\left(-\frac{2}{\mathcal{Y}} - \frac{6c' M^2 \zeta^{2/3}}{s\mathcal{V}^{5/3}}\right) t^i \equiv \kappa_t t^i \,. \tag{D.13b}$$

We can then proceed with the computation of the various terms, starting from the ones depending on $\partial_Z W$ (and its complex conjugate). Using (D.13), as well as (D.11), we find:

$$K^{Z\bar{Z}}(\partial_Z W \partial_{\bar{Z}} K\, \overline{W} + \partial_Z K \partial_{\bar{Z}} \overline{W}\, W) = \kappa_{zz} \frac{3c' M^2}{s\mathcal{V}^{2/3}\zeta^{4/3}} (Z \partial_Z W\, \overline{W} + \bar{Z} \partial_{\bar{Z}} \overline{W}\, W) \,;$$

$$\begin{aligned} K^{Z\bar{T}_i} \partial_Z W \partial_{\bar{T}_i} K\, \overline{W} + K^{T_i \bar{Z}} \partial_{T_i} K \partial_{\bar{Z}} \overline{W} W &= \kappa_{zt}\kappa_t (Z \partial_Z W\, \overline{W} + \bar{Z} \partial_{\bar{Z}} \overline{W}\, W) \sum_{i=1}^{h^{1,1}} \tau_i t^i \\ &= 3\kappa_{zt}\kappa_t \mathcal{V} (Z \partial_Z W\, \overline{W} + \bar{Z} \partial_{\bar{Z}} \overline{W}\, W) \,. \end{aligned}$$

In the last line we used the relation

$$\sum_{i=1}^{h^{1,1}} \tau_i t^i = 3\mathcal{V} \,, \tag{D.14}$$

which can be easily derived from the definitions of $\mathcal{V}$ and τ_i in terms of the volumes t^i of the 2-cycles. The remaining term turns out to be:

$$\begin{aligned} Z \partial_Z W\, \overline{W} + \bar{Z} \partial_{\bar{Z}} \overline{W}\, W = &- \sum_{i=1}^{n} A_i e^{-a_i \tau_i} \zeta \left[\frac{M\sigma}{\pi} \cos(a_i\theta_i + \sigma) + 2\left(sK + \frac{M}{2\pi}\log\zeta\right)\sin(a_i\theta_i + \sigma)\right] \\ &- W_{cs}\zeta \left[\frac{M\sigma}{\pi}\cos(\sigma - \varphi) + 2\left(sK + \frac{M}{2\pi}\log\zeta\right)\sin(\sigma - \varphi)\right] \\ &+ \zeta^2 \left[\frac{M^2\sigma^2}{2\pi^2} + 2\left(sK - \frac{M}{2\pi}(1 - \log\zeta)\right)\left(sK + \frac{M}{2\pi}\log\zeta\right)\right] \,. \end{aligned}$$

As concerns the terms depending on $\partial_{T_i} W = -a_i A_i e^{-a_i T_i}$, we have instead:

$$K^{Z\bar{T}_i} \partial_Z\, K \partial_{\bar{T}_i} \overline{W}\, W + K^{T_i \bar{Z}} \partial_{T_i} W\, \partial_{\bar{Z}} K\, \overline{W} = -\kappa_{zt} \frac{3c' M^2}{s\mathcal{V}^{2/3}\zeta^{4/3}} \sum_{i=1}^{n} A_i a_i \tau_i\, \zeta^2 \left(e^{-a_i T_i}\overline{W} + e^{-a_i \bar{T}_i} W\right) \,;$$

$$K^{T_i \bar{T}_j}(\partial_{T_i} K\, \partial_{\bar{T}_j} \overline{W}\, W + \partial_{T_i} W \partial_{\bar{T}_j} K\, \overline{W}) = -\kappa_t (2\kappa_{tt}^{(1)} + 3\kappa_{tt}^{(2)}\mathcal{V}) \sum_{i=1}^{n} A_i a_i \tau_i \left(e^{-a_i T_i}\overline{W} + e^{-a_i \bar{T}_i} W\right)$$

where in the second line we used again (D.14) and also $k_{ijk} t^j t^k = 2\tau_i$. Moreover:

$$\begin{aligned} e^{-a_i T_i}\overline{W} + e^{-a_i \bar{T}_i} W = \sum_j 2A_j e^{-a_i\tau_i - a_j\tau_j} \cos(a_i\theta_i - a_j\theta_j) + 2e^{-a_i\tau_i} \Big[& W_{cs}\cos(a_i\theta_i + \varphi) \\ & - \frac{M\zeta\sigma}{2\pi}\cos(a_i\theta_i + \sigma) + \zeta\left(\frac{M}{2\pi}(1 - \log\zeta) - sK\right)\sin(a_i\theta_i + \sigma)\Big] \,. \end{aligned}$$

$(\mathbf{K^{I\bar{J}}\partial_I K\partial_{\bar{J}} K - 3})|\mathbf{W}|^\mathbf{2}$

The term depending on the derivative is computed to be:

$$(K^{I\bar{J}}\partial_I K\partial_{\bar{J}} K - 3) = \frac{3s^3\,\mathcal{V}^3\,\hat{\xi}(\mathcal{V}^2 + 14\mathcal{V}\hat{\xi} + 4\hat{\xi}^2) + \zeta^{2/3}\,v_1}{2s\mathcal{V}^{2/3}\mathcal{Y}^2[s^2\mathcal{V}^{7/3}(\mathcal{V} - 2\hat{\xi}) + \zeta^{2/3}\,v_2]} \tag{D.15}$$

where for compactness we introduced $v_{1,2}$, which will turn out to be sub-leading in the usual LVS limit with $\zeta \sim \frac{W_{cs}^{3/2}}{\mathcal{V}^{5/4}}$. More precisely, they are given by:

$$\begin{aligned} v_1 &= 9c'M^2\mathcal{Y}\left[2s^2\mathcal{V}^{4/3}\hat{\xi}(8\mathcal{V}^2 - 5\mathcal{V}\hat{\xi} - 4\hat{\xi}^2) + 3c'\zeta^{2/3}M^2 s\mathcal{V}^{2/3}\mathcal{Y}(\mathcal{V} - 2\hat{\xi})(8\mathcal{V} - \hat{\xi})\right. \\ &\quad \left. + 108c'^2M^4\zeta^{4/3}\mathcal{Y}^3\right]\,; \\ v_2 &= 3c'M^2 s\,\mathcal{V}^{2/3}(4\mathcal{V}^2 - \hat{\xi}\mathcal{V} + 4\hat{\xi}^2) + 27c'^2M^4\zeta^{2/3}\mathcal{Y}^2\,. \end{aligned}$$

Finally, we need to compute $|W|^2$, which turns out to be:

$$\begin{aligned} |W|^2 &= \sum_{i,j=1}^{n} A_i A_j e^{-a_i\tau_i - a_j\tau_j}\cos(a_i\theta_i - a_j\theta_j) \\ &\quad + \sum_{i=1}^{n} A_i e^{-a_i\tau_i}\left[2W_{cs}\cos(a_i\theta_i + \varphi) + \zeta w_1\right] + \left(W_{cs}^2 + \zeta w_2\right) \end{aligned}$$

where again we used the more compact notation $w_{1,2}$ in order to indicate terms that will turn out to be sub-leading:

$$w_1 = -\frac{M\sigma}{\pi}\cos(a_i\theta_i + \sigma) + \left[\frac{M}{\pi}(1 - \log\zeta) - 2Ks\right]\,;$$

$$\begin{aligned} w_2 &= W_{cs}\left[-\frac{M\sigma}{\pi}\cos(\sigma - \varphi) + \left(\frac{M}{\pi}(1 - \log\zeta) - 2Ks\right)\sin(\sigma - \varphi)\right] \\ &\quad + \frac{M^2\sigma^2\zeta}{4\pi^2} + \zeta\left[\frac{M}{2\pi}(1 - \log\zeta) - Ks\right]^2\,. \end{aligned}$$

Total scalar potential

We are finally able to put all the above results together, obtaining

$$e^{-K}V = V_1 + V_2 + V_3\,,$$

where:

$$\begin{aligned} V_1 = \sum_{i,j=1}^{n} e^{-a_i\tau_i - a_j\tau_j} A_i A_j\cos(a_i\theta_i - a_j\theta_j)\left\{\frac{3s^3\,\mathcal{V}^3\,\hat{\xi}(\mathcal{V}^2 + 14\mathcal{V}\hat{\xi} + 4\hat{\xi}^2) + \zeta^{2/3}v_1}{2s\,\mathcal{V}^{2/3}\mathcal{Y}^2[s^2\,\mathcal{V}^{7/3}(\mathcal{V} - 2\hat{\xi}) + \zeta^{2/3}\,v_2]}\right. \\ \left. + a_i a_j[\kappa_{tt}^{(1)}(k_{ijk}t^k) + \kappa_{tt}^{(2)}\tau_i\tau_j] - 2a_i\tau_i\left[\kappa_t(2\kappa_{tt}^{(1)} + 3\kappa_{tt}^{(2)}\mathcal{V}) + \kappa_{zt}\frac{3c'M^2}{s\mathcal{V}^{2/3}}\zeta^{2/3}\right]\right\}\,; \end{aligned}$$

$$
\begin{aligned}
V_2 = \sum_{i=1}^{n} A_i e^{-a_i\tau_i} \Bigg\{ & (2W_{cs}\cos(a_i\theta_i+\varphi)+\zeta\, w_1)\,\frac{3s^3\,\mathcal{V}^3\,\hat{\xi}(\mathcal{V}^2+14\mathcal{V}\hat{\xi}+4\hat{\xi}^2)+\zeta^{2/3}\,v_1}{2s\mathcal{V}^{2/3}\mathcal{Y}^2\,[s^2\mathcal{V}^{7/3}(\mathcal{V}-2\hat{\xi})+\zeta^{2/3}\,v_2]} \\
& + \left[\frac{M\sigma}{\pi}\cos(a_i\theta_i+\sigma)+2\left(sK+\frac{M}{2\pi}\log\zeta\right)\sin(a_i\theta_i+\sigma)\right]\left[\kappa_{zt}\,\zeta(a_i\tau_i-3\kappa_t\mathcal{V})\right. \\
& \left. -\frac{3c'M^2}{s\mathcal{V}^{2/3}\zeta^{1/3}}\kappa_{zz}\right] - 2\left[W_{cs}\cos(a_i\theta_i+\varphi)-\frac{M\zeta\sigma}{2\pi}\cos(a_i\theta_i+\sigma)\right. \\
& \left. +\zeta\left(\frac{M}{2\pi}(1-\log\zeta)-sK\right)\sin(a_i\theta_i+\sigma)\right] a_i\tau_i\left[\kappa_t(2\kappa_{tt}^{(1)}+3\kappa_{tt}^{(2)}\mathcal{V})+\kappa_{zt}\frac{3c'M^2}{s\mathcal{V}^{2/3}}\zeta^{2/3}\right]\Bigg\}\,;
\end{aligned}
$$

$$
\begin{aligned}
V_3 = {} & (W_{cs}^2+\zeta w_2)\,\frac{3s^3\,\mathcal{V}^3\hat{\xi}(\mathcal{V}^2+14\mathcal{V}\hat{\xi}+4\hat{\xi}^2)+\zeta^{2/3}\,v_1}{2s\mathcal{V}^{2/3}\mathcal{Y}^2[s^2\,\mathcal{V}^{7/3}(\mathcal{V}-2\hat{\xi})+\zeta^{2/3}\,v_2]} \\
& + \kappa_{zz}\left[\frac{M^2\sigma^2}{4\pi^2}+\left(sK+\frac{M}{2\pi}\log\zeta\right)^2\right] \\
& + 3\left(\frac{c'M^2}{s\mathcal{V}^{2/3}\zeta^{1/3}}\kappa_{zz}+\kappa_{zt}\kappa_t\mathcal{V}\zeta\right)\left\{-\frac{M\sigma W_{cs}}{\pi}\cos(\sigma-\varphi)+\frac{M^2\sigma^2\zeta}{2\pi^2}\right. \\
& \left. -2\left(sK+\frac{M}{2\pi}\log\zeta\right)\left[W_{cs}\sin(\sigma-\varphi)-\zeta\left(sK-\frac{M}{2\pi}(1-\log\zeta)\right)\right]\right\}\,.
\end{aligned}
$$

As a consistency check we can easily verify that by fixing $\zeta = 0$ we recover the result of [61][2].

D.3 Large Volume Limit

Let us consider the approximation $\zeta \sim \frac{W_{cs}^{3/2}}{\mathcal{V}^{5/4}}$, in the large volume limit. In this regime, the terms appearing in the inverse Kähler metric and in the first derivatives of the Kähler potential can be approximated as:

$$
\kappa_t \simeq -\frac{1}{2\mathcal{Y}}\,;
$$

$$
\kappa_{zz} \simeq \frac{s\mathcal{V}^{2/3}\zeta^{4/3}}{c'M^2}\,; \qquad \kappa_{zt} \simeq \frac{2(\mathcal{V}-2\hat{\xi})}{\mathcal{V}}\,;
$$

$$
\kappa_{tt}^{(1)} \simeq -4\mathcal{Y}\,; \qquad \kappa_{tt}^{(2)} \simeq \frac{2(2\mathcal{V}-3\hat{\xi})}{\mathcal{V}}\,.
$$

Therefore we have:

$$
\begin{aligned}
V_1 \simeq \sum_{i,j=1}^{n} e^{-a_i\tau_i-a_j\tau_j} A_iA_j\cos(a_i\theta_i-a_j\theta_j)\Bigg\{ & \frac{3\hat{\xi}}{2\mathcal{V}}-4\mathcal{Y}(k_{ijk}t^k)a_ia_j \\
& +\frac{2(2\mathcal{V}-3\hat{\xi})}{\mathcal{V}}a_i\tau_ia_j\tau_j+4\frac{(\mathcal{V}-6\hat{\xi})}{\mathcal{V}}a_i\tau_i\Bigg\}\,;
\end{aligned}
\tag{D.16a}
$$

[2] Notice that here we are using a slightly different notation with respect to [61]. In particular, our ξ corresponds to their $\frac{\xi}{2}$.

$$V_2 \simeq \sum_{i=1}^{n} 2e^{-a_i\tau_i} A_i W_{cs} \cos(a_i\theta_i + \varphi) \left[\frac{3\hat{\xi}}{2\mathcal{V}} + 2\frac{(\mathcal{V} - 6\hat{\xi})}{\mathcal{V}} a_i\tau_i \right] ; \tag{D.16b}$$

$$V_3 \simeq W_{cs}^2 \frac{3\hat{\xi}}{2\mathcal{V}} + \frac{s\mathcal{V}^{2/3}\zeta^{4/3}}{c'M^2} \left[\frac{M^2\sigma^2}{4\pi^2} + \left(sK + \frac{M}{2\pi}\log\zeta \right)^2 \right] . \tag{D.16c}$$

To complete this result, finally, we need to consider the term e^K, which in the large volume limit simply reads:

$$e^K \simeq \frac{g_s e^{K_{cs}}}{2\mathcal{V}^2} . \tag{D.17}$$

D.4 An application: $N = h^{1,1} - 1$ blown-up modes

As an application of the formulas derived in the previous section, let us consider the case of a CY three-fold with $h^{1,1} = N + 1$ and a Swiss cheese form of the volume

$$\mathcal{V} = \tau_b^{3/2} - \sum_{i=1}^{N} \kappa_i \tau_i^{3/2} ,$$

where $\kappa_i = \frac{\sqrt{2}}{3\sqrt{9-n}} \in [0.16, 0.47]$ for a dP_n divisor. We assume all the 'small' four-cycles τ_i to be rigid divisors generating some non-perturbative effect to the superpotential: this is the easiest generalization of the case analyzed in Ch. 6.

The scalar potential can be easily derived from Eqs. (D.16), considering for each term only the leading order contributions (with respect to the volume $\mathcal{V}$ of the CY) and noticing that, due to the diagonality of the small divisors,

$$k_{ijk}t^k = k_{iii}t^i = \sqrt{2k_{iii}}\sqrt{\tau_i} , \tag{D.18}$$

where we also used the fact that in this case $\tau_i = \frac{1}{2}k_{iii}(t^i)^2$. We obtain, therefore[3]:

$$\begin{aligned} V_{tot} = &\sum_{i=1}^{N} \left[\frac{8a_i^2 A_i^2 g_s \sqrt{\tau_i} e^{-2a_i\tau_i}}{3\kappa_i\mathcal{V}} + \frac{4a_i A_i g_s \tau_i e^{-a_i\tau_i} W_0}{\mathcal{V}^2} \cos(a_i\theta_i + \varphi) \right] \\ &+ \frac{\zeta^{4/3}}{c'M^2\mathcal{V}^{4/3}} \left[\frac{c'c''}{\pi g_s} + \frac{M^2\sigma^2}{4\pi^2} + \left(\frac{M}{2\pi}\log\zeta + \frac{K}{g_s} \right)^2 \right] + \frac{3\xi}{2\sqrt{g_s}\mathcal{V}^3} W_0^2 , \end{aligned} \tag{D.19}$$

whose minimum, obtained by the analysis of the derivatives, is defined by the following

[3] Notice that in this simple case, terms $\sim e^{-a_i\tau_i - a_j\tau_j}$, $i \neq j$ are generically suppressed, due to the fact that in the case under consideration $k_{ijk} = 0$ $(i \neq j)$. Looking at (D.16a) and considering also (D.17), indeed, we can see that at $i \neq j$ the leading order contribution is $\sim \frac{1}{\mathcal{V}^2}$, therefore negligible with respect to the $\frac{e^{2a_i\tau_i}}{\mathcal{V}}$ terms.

expressions:

$$\sigma = 0\,; \tag{D.20a}$$

$$\theta_i = \frac{\pi - \varphi}{a_i}\,; \tag{D.20b}$$

$$\zeta = e^{-\frac{2\pi K}{g_s M} - \frac{3}{4} + \sqrt{\frac{9}{16} - \frac{4\pi}{g_s M^2} c' c''}}\,; \tag{D.20c}$$

$$\tau_b^{3/2} = \frac{3 e^{a_i \tau_i} W_0 \kappa_i \sqrt{\tau_i}}{a_i A_i} \frac{(1 - a_i \tau_i)}{(1 - 4 a_i \tau_i)}\,; \tag{D.20d}$$

$$e^{a_i \tau_i - a_j \tau_j} = \frac{a_i A_i (4 a_i \tau_i - 1)(a_j \tau_j - 1)}{a_j A_j (4 a_j \tau_j - 1)(a_i \tau_i - 1)} \frac{\kappa_j \sqrt{\tau_j}}{\kappa_i \sqrt{\tau_i}} \qquad \forall i, j\,; \tag{D.20e}$$

$$\frac{\xi}{g_s^{3/2}} = -\frac{8 \rho \tau_b^{5/2}}{27 g_s W_0^2} + \sum_{i=1}^{N} \tau_i^{3/2} \frac{16 a_i \kappa_i \tau_i (a_i \tau_i - 1)}{(1 - 4 a \tau_i)^2}\,, \tag{D.20f}$$

with ρ defined in (6.9).

The main difference with respect to the 2-moduli case (besides the trivial introduction of sums over all the small cycles) is therefore the additional equation (D.20e) which comes from the fact that the volume (D.20d) can be obtained in terms of any of the small cycles, but obviously the result must be independent of the choice of τ_i. The vacuum energy at the minimum is a simple generalization of (6.10):

$$V_{min} = \frac{5\rho}{9\mathcal{V}^{4/3}} - \frac{12 W_0^2 g_s}{\mathcal{V}^3} \sum_{i=1}^{N} \frac{\kappa_i \tau_i^{3/2} (a_i \tau_i - 1)}{(1 - 4 a_i \tau_i)^2}\,. \tag{D.21}$$

Imposing $V_{min} = 0$ we can obtain the $\mathcal{V}$ at a Minkowski minimum:

$$\begin{aligned} \mathcal{V}_{\text{Mink}} &= \left(\frac{108 g_s}{5 q_0}\right)^{3/5} \frac{W_0^{6/5}}{\zeta^{4/5}} \left(\sum_{i=1}^{N} \frac{\kappa_i \tau_i^{3/2} (a_i \tau_i - 1)}{(4 a_i \tau_i - 1)^2}\right)^{3/5} \\ &\simeq \left(\frac{27 g_s}{20 q_0}\right)^{3/5} \frac{W_0^{6/5}}{\zeta^{4/5}} \left(\sum_{i=1}^{N} \frac{\kappa_i \sqrt{\tau_i}}{a_i}\right)^{3/5}\,, \end{aligned} \tag{D.22}$$

where in the last step we considered $a_i \tau_i \gg 1$. This result, depending on a sum of N positive elements, might lead us to conclude that the volume (slowly) increases with N. However, as we show in the rest of this section, this is not the case: keeping fixed all the parameters, $\mathcal{V}_{\text{Mink}}$ generically decreases with N.

Let us see this in more detail. As an immediate generalization of (6.18), we find that on a dS minimum the warp factor ρ is given by

$$\rho \simeq \alpha \frac{27 g_s W_0^2}{20 \tau_b^{5/2}} \sum_{i=1}^{N} \frac{\kappa_i}{a_i} \tau_i^{1/2}\,, \tag{D.23}$$

with $\alpha \in]1, \frac{9}{4}[$. Plugging this result in Eq. (D.20f), we can conclude that in a LVS dS minimum we have:

$$\sum_{i=1}^{N} \kappa_i \tau_i^{3/2} \left(1 - \frac{2\alpha}{5 a_i \tau_i}\right) = \frac{\xi}{g_s^{3/2}} \qquad \text{with} \qquad \alpha \in \left]1, \frac{9}{4}\right[\,. \tag{D.24}$$

Considering again that $a_i \tau_i \gg 1$, this means in particular that $\sum_i \kappa_i \tau_i^{3/2}$ is approximately fixed by the parameters (g_s, χ) of the model, while it does not depend on N:

$$\sum_i \kappa_i \tau_i^{3/2} \simeq \hat{\xi}; \qquad \hat{\xi} \equiv \frac{\xi}{g_s^{3/2}}$$

i.e. the value of the single small 4-cycle τ_i decreases with N. On the other side, the value of the modulus τ_b at the minimum is given by the relation (D.20d), which depends exponentially on only one of the moduli τ_i, therefore we expect it (as well as the volume $\mathcal{V} \simeq \tau_b^{3/2} - \hat{\xi}$) to decrease with N.

From the arguments of Sec. 6.3.2, we expect a decreasing volume to increase the lower bound on the flux charge MK. The end of this section is devoted to better understanding this behavior.

A simple configuration

The simplest possibility consists in considering $a_i = a$; $A_i = A$; $\kappa_i = \kappa$, $\forall i$. In this case, indeed, all the small cycles turn out to be stabilized at the same value (see Eq. (D.20e))

$$\tau_i = \frac{\xi^{2/3}}{N^{2/3} g_s \kappa^{2/3}} \,, \tag{D.25}$$

where χ (hence ξ) and κ are fixed by the geometry, while g_s is chosen, as explained in Sec. 6.3.2, as the maximum possible (in the perturbative regime) which is consistent with a large enough volume ($\mathcal{V} \gg \mathcal{V}_{min}$).

A more precise estimation of the decreasing behavior of the volume $\mathcal{V} \simeq \tau_b^{3/2}$ is obtained by the ratio

$$\frac{\mathcal{V}^{(N)}}{\mathcal{V}^{(N=1)}} = \frac{e^{-a \frac{\hat{\xi}^{2/3}}{\kappa^{2/3}} \left(1 - \frac{1}{N^{2/3}}\right)}}{N^{1/3}} \,, \tag{D.26}$$

where we used (D.20d) for $\mathcal{V}^{(N)}$ and (6.6b) for the standard $N = 1$ ($h^{1,1} = 2$) volume.

As a consequence, the maximum value of g_s allowing for a large enough volume decreases with N. To be more specific, since $g_s^{\max}$ is estimated as the value such as the volume is approximately equal to its minimum allowed value $\mathcal{V}_{\min}$, when N increases we need to change g_s so that the ratio (D.26) is $\simeq 1$, that is:

$$g_s^{(N)} = \frac{g_s^{(1)}}{N^{2/3}} \,. \tag{D.27}$$

This in turns influences the tadpole due to the bound $g_s M \gtrsim (g_s M)_{\min}$, so that, in order to have $g_s^{(N)} M^{(N)} \simeq (g_s M)_{\min}$, we expect $M^{(N)}$ to increase by a factor of $N^{2/3}$ with respect to the case $N = 1$.

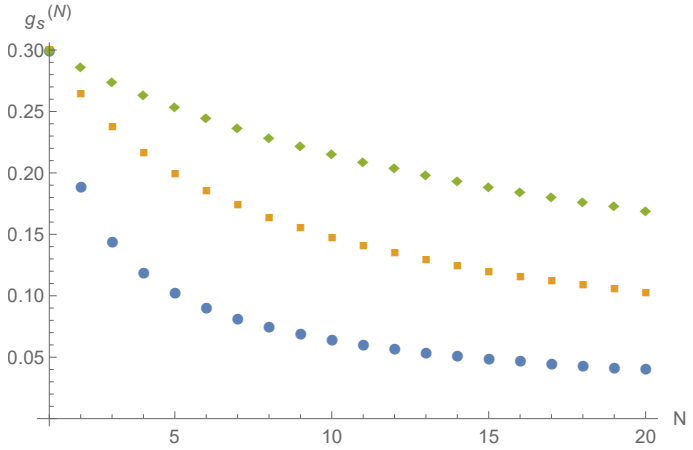

Figure D.1: $g_s^{(N)}$ as a function of N for $g_s^{(1)} = 0.3$. The blue points represent Eq. (D.27) which we can see to be the worst case in terms of the tadpole. The other two curves refers instead to (D.29) (they show therefore an upper bound) for $\chi(X_3) = -100$ (yellow squares), and for $\chi(X_3) = -300$ (green diamonds).

A more generic estimate

Let us consider the generic case in which all 4-cycles are stabilized at (potentially) different values, even though related by (D.20e). Here we can set an upper limit on our estimation, considering that the moduli have to be all stabilized at $\tau_i > 1$ and that $\kappa_i \gtrsim 0.16 = \kappa_0$:

$$\kappa_1 \tau_1 \lesssim \frac{\xi}{g_s^{3/2}} - (N-1)\kappa_0 \,. \tag{D.28}$$

Following the same steps as before, we can write also in this case a relation between $g_s^{(N)}$ and $g_s \equiv g_s^{(1)}$, such that the volume is fixed as $h^{1,1}$ increases:

$$g_s^{(N)} \lesssim \left(\frac{\xi\, g_s^{3/2}}{\xi + (N-1) g_s^{3/2} \kappa_0} \right)^{2/3} . \tag{D.29}$$

Hence, in this more generic case the situation appears more promising (at the price of a more involved analysis), see also Fig. D.1.

Finally we stress that all this argument holds in a situation in which, as in the case analyzed in Ch. 6, we are forced to take a volume $\mathcal{V}$ large, but not-so-large, that is near to the lower bound imposed by the need to keep under control all the approximations. If this is not the case (as one might expect, e.g., when the O-planes/D-branes configuration is such that the upper bound on the fluxes MK is not so strong, especially in presence of E3-instantons, where we observed that very large volumes may appear), the fact that the volume decreases with N might actually have no direct influence on the value of MK.

Bibliography

[1] J. Polchinski, *String Theory, Vol. 1: An introduction to the Bosonic String*. Cambridge Monographs on Mathematical Physics. Cambridge University Press, 1998, 10.1017/CBO9780511816079.

[2] D. Tong, *String Theory*, 0908.0333.

[3] A. Addazi et al., *Quantum gravity phenomenology at the dawn of the multi-messenger era. A review*, *Prog. Part. Nucl. Phys.* **125** (2022) 103948, [2111.05659].

[4] M. Bertolini, "Lectures on supersymmetry." https://people.sissa.it/~bertmat/susycourse.pdf, 2018.

[5] J. Polchinski, *String Theory, Vol. 2: Superstring theory and beyond*. Cambridge Monographs on Mathematical Physics. Cambridge University Press, 1998, 10.1017/CBO9780511618123.

[6] M. B. Green, J. H. Schwarz and E. Witten, *Superstring Theory Vol. 2: 25th Anniversary Edition*. Cambridge Monographs on Mathematical Physics. Cambridge University Press, 11, 2012, 10.1017/CBO9781139248570.

[7] M. B. Green, J. H. Schwarz and E. Witten, *Superstring Theory Vol. 1: 25th Anniversary Edition*, vol. 1 of *Cambridge Monographs on Mathematical Physics*. Cambridge University Press, 2012, 10.1017/CBO9781139248563.

[8] G. Aldazabal, L. E. Ibanez, F. Quevedo and A. M. Uranga, *D-branes at singularities: A Bottom up approach to the string embedding of the standard model*, *JHEP* **08** (2000) 002, [hep-th/0005067].

[9] S. B. Giddings, S. Kachru and J. Polchinski, *Hierarchies from fluxes in string compactifications*, *Phys. Rev. D* **66** (2002) 106006, [hep-th/0105097].

[10] M. R. Douglas and S. Kachru, *Flux compactification*, *Rev. Mod. Phys.* **79** (2007) 733–796, [hep-th/0610102].

[11] S. Kachru, R. Kallosh, A. D. Linde and S. P. Trivedi, *De Sitter vacua in string theory*, *Phys. Rev. D* **68** (2003) 046005, [hep-th/0301240].

[12] V. Balasubramanian, P. Berglund, J. P. Conlon and F. Quevedo, *Systematics of moduli stabilisation in Calabi-Yau flux compactifications*, *JHEP* **03** (2005) 007, [hep-th/0502058].

[13] J. P. Conlon, F. Quevedo and K. Suruliz, *Large-volume flux compactifications: Moduli spectrum and D3/D7 soft supersymmetry breaking*, *JHEP* **08** (2005) 007, [hep-th/0505076].

[14] G. Obied, H. Ooguri, L. Spodyneiko and C. Vafa, *De Sitter Space and the Swampland*, 1806.08362.

[15] H. Ooguri, E. Palti, G. Shiu and C. Vafa, *Distance and de Sitter Conjectures on the Swampland*, *Phys. Lett. B* **788** (2019) 180–184, [1810.05506].

[16] I. Bena, E. Dudas, M. Graña and S. Lüst, *Uplifting Runaways*, *Fortsch. Phys.* **67** (2019) 1800100, [1809.06861].

[17] R. Blumenhagen, D. Kläwer and L. Schlechter, *Swampland Variations on a Theme by KKLT*, *JHEP* **05** (2019) 152, [1902.07724].

[18] C. Crinò, F. Quevedo and R. Valandro, *On de Sitter String Vacua from Anti-D3-Branes in the Large Volume Scenario*, *JHEP* **03** (2021) 258, [2010.15903].

[19] C. Crinò, F. Quevedo, A. Schachner and R. Valandro, *A Database of Calabi-Yau Orientifolds and the Size of D3-Tadpoles*, 2204.13115.

[20] S. AbdusSalam, C. Crinò and P. Shukla, *On K3-fibred LARGE Volume Scenario with de Sitter vacua from anti-D3-branes*, 2206.12889.

[21] T. W. Grimm and J. Louis, *The effective action of Calabi–Yau orientifolds*, *Nuclear Physics B* **699** (Nov, 2004) 387–426, [hep-th/0403067].

[22] L. E. Ibáñez and A. M. Uranga, *String Theory and Particle Physics: An Introduction to String Phenomenology*. Cambridge University Press, 2012, 10.1017/CBO9781139018951.

[23] D. Baumann and L. McAllister, *Inflation and String Theory*, 1404.2601.

[24] D. G. Cerdeno and C. MUNOZ, *Introduction to SUGRA*, *PoS* **corfu98** (1999) 011.

[25] R. Valandro, *Phenomenology from the Landscape of String Vacua*, Ph.D. thesis, Heidelberg U., 2007. 0801.0584.

[26] M. Cicoli, C. Mayrhofer and R. Valandro, *Moduli Stabilisation for Chiral Global Models*, *JHEP* **02** (2012) 062, [1110.3333].

[27] M. Cicoli, M. Kreuzer and C. Mayrhofer, *Toric K3-Fibred Calabi-Yau Manifolds with del Pezzo Divisors for String Compactifications*, *JHEP* **02** (2012) 002, [1107.0383].

[28] M. Cicoli, S. Krippendorf, C. Mayrhofer, F. Quevedo and R. Valandro, *D-Branes at del Pezzo Singularities: Global Embedding and Moduli Stabilisation*, *JHEP* **09** (2012) 019, [1206.5237].

[29] M. Cicoli, S. Krippendorf, C. Mayrhofer, F. Quevedo and R. Valandro, *D3/D7 Branes at Singularities: Constraints from Global Embedding and Moduli Stabilisation*, *JHEP* **07** (2013) 150, [1304.0022].

[30] R. Blumenhagen, V. Braun, T. W. Grimm and T. Weigand, *GUTs in Type IIB Orientifold Compactifications*, *Nucl. Phys. B* **815** (2009) 1–94, [0811.2936].

[31] S. Kachru, R. Kallosh, A. D. Linde, J. M. Maldacena, L. P. McAllister and S. P. Trivedi, *Towards inflation in string theory*, *JCAP* **10** (2003) 013, [hep-th/0308055].

[32] M. Dine and N. Seiberg, *Is the Superstring Weakly Coupled?*, *Phys. Lett. B* **162** (1985) 299–302.

[33] F. Denef, *Les Houches Lectures on Constructing String Vacua*, *Les Houches* **87** (2008) 483–610, [0803.1194].

[34] I. R. Klebanov and M. J. Strassler, *Supergravity and a confining gauge theory: Duality cascades and chi SB resolution of naked singularities*, *JHEP* **08** (2000) 052, [hep-th/0007191].

[35] R. I. Nepomechie, *Magnetic monopoles from antisymmetric tensor gauge fields*, *Phys. Rev. D* **31** (Apr, 1985) 1921–1924.

[36] C. Teitelboim, *Monopoles of Higher Rank*, *Phys. Lett. B* **167** (1986) 69–72.

[37] S. Gukov, C. Vafa and E. Witten, *CFT's from Calabi-Yau four folds*, *Nucl. Phys. B* **584** (2000) 69–108, [hep-th/9906070].

[38] E. Cremmer, S. Ferrara, C. Kounnas and D. V. Nanopoulos, *Naturally Vanishing Cosmological Constant in N=1 Supergravity*, *Phys. Lett. B* **133** (1983) 61.

[39] J. R. Ellis, A. B. Lahanas, D. V. Nanopoulos and K. Tamvakis, *No-Scale Supersymmetric Standard Model*, *Phys. Lett. B* **134** (1984) 429.

[40] A. Giryavets, S. Kachru, P. K. Tripathy and S. P. Trivedi, *Flux compactifications on Calabi-Yau threefolds*, *JHEP* **04** (2004) 003, [hep-th/0312104].

[41] M. Cicoli, D. Klevers, S. Krippendorf, C. Mayrhofer, F. Quevedo and R. Valandro, *Explicit de Sitter Flux Vacua for Global String Models with Chiral Matter*, *JHEP* **05** (2014) 001, [1312.0014].

[42] J. J. Blanco-Pillado, K. Sousa, M. A. Urkiola and J. M. Wachter, *Towards a complete mass spectrum of type-IIB flux vacua at large complex structure*, *JHEP* **04** (2021) 149, [2007.10381].

[43] I. R. Klebanov and A. A. Tseytlin, *Gravity duals of supersymmetric SU(N) x SU(N+M) gauge theories*, *Nucl. Phys. B* **578** (2000) 123–138, [hep-th/0002159].

[44] R. Minasian and D. Tsimpis, *On the geometry of nontrivially embedded branes*, *Nucl. Phys. B* **572** (2000) 499–513, [hep-th/9911042].

[45] L. Aparicio, F. Quevedo and R. Valandro, *Moduli Stabilisation with Nilpotent Goldstino: Vacuum Structure and SUSY Breaking*, *JHEP* **03** (2016) 036, [1511.08105].

[46] S. B. Giddings and A. Maharana, *Dynamics of warped compactifications and the shape of the warped landscape*, *Phys. Rev. D* **73** (2006) 126003, [hep-th/0507158].

[47] M. R. Douglas and G. Torroba, *Kinetic terms in warped compactifications*, *JHEP* **05** (2009) 013, [0805.3700].

[48] E. Dudas and S. Lüst, *An update on moduli stabilization with antibrane uplift*, *JHEP* **03** (2021) 107, [1912.09948].

[49] F. Denef and M. R. Douglas, *Distributions of flux vacua*, *JHEP* **05** (2004) 072, [hep-th/0404116].

[50] S. Ashok and M. R. Douglas, *Counting flux vacua*, *JHEP* **01** (2004) 060, [hep-th/0307049].

[51] M. R. Douglas, *The Statistics of string / M theory vacua*, *JHEP* **05** (2003) 046, [hep-th/0303194].

[52] M. R. Douglas, J. Shelton and G. Torroba, *Warping and supersymmetry breaking*, 0704.4001.

[53] K. Becker, M. Becker, M. Haack and J. Louis, *Supersymmetry breaking and alpha-prime corrections to flux induced potentials*, *JHEP* **06** (2002) 060, [hep-th/0204254].

[54] E. Witten, *Nonperturbative superpotentials in string theory*, *Nucl. Phys. B* **474** (1996) 343–360, [hep-th/9604030].

[55] C. P. Burgess, J. P. Derendinger, F. Quevedo and M. Quiros, *On gaugino condensation with field dependent gauge couplings*, *Annals Phys.* **250** (1996) 193–233, [hep-th/9505171].

[56] P. Berglund and I. Garcia-Etxebarria, *D-brane instantons on non-Spin cycles*, *JHEP* **01** (2013) 056, [1210.1221].

[57] S. de Alwis, R. K. Gupta, F. Quevedo and R. Valandro, *On KKLT/CFT and LVS/CFT Dualities*, *JHEP* **07** (2015) 036, [1412.6999].

[58] M. Demirtas, M. Kim, L. Mcallister and J. Moritz, *Vacua with Small Flux Superpotential*, *Phys. Rev. Lett.* **124** (2020) 211603, [1912.10047].

[59] M. Demirtas, M. Kim, L. McAllister and J. Moritz, *Conifold Vacua with Small Flux Superpotential*, *Fortsch. Phys.* **68** (2020) 2000085, [2009.03312].

[60] R. Álvarez-García, R. Blumenhagen, M. Brinkmann and L. Schlechter, *Small Flux Superpotentials for Type IIB Flux Vacua Close to a Conifold*, *Fortsch. Phys.* **68** (2020) 2000088, [2009.03325].

[61] S. AbdusSalam, S. Abel, M. Cicoli, F. Quevedo and P. Shukla, *A systematic approach to Kähler moduli stabilisation*, *JHEP* **08** (2020) 047, [2005.11329].

[62] M. Cicoli, J. P. Conlon and F. Quevedo, *General Analysis of LARGE Volume Scenarios with String Loop Moduli Stabilisation*, *JHEP* **10** (2008) 105, [0805.1029].

[63] S. de Alwis, R. Gupta, E. Hatefi and F. Quevedo, *Stability, Tunneling and Flux Changing de Sitter Transitions in the Large Volume String Scenario*, *JHEP* **11** (2013) 179, [1308.1222].

[64] J. Gray, Y.-H. He, V. Jejjala, B. Jurke, B. D. Nelson and J. Simon, *Calabi-Yau Manifolds with Large Volume Vacua*, *Phys. Rev. D* **86** (2012) 101901, [1207.5801].

[65] R. Altman, Y.-H. He, V. Jejjala and B. D. Nelson, *New large volume Calabi-Yau threefolds*, *Phys. Rev. D* **97** (2018) 046003, [1706.09070].

[66] K. Choi, A. Falkowski, H. P. Nilles, M. Olechowski and S. Pokorski, *Stability of flux compactifications and the pattern of supersymmetry breaking*, *JHEP* **11** (2004) 076, [hep-th/0411066].

[67] X. Gao, A. Hebecker, S. Schreyer and G. Venken, *The LVS Parametric Tadpole Constraint*, 2202.04087.

[68] B. De Wit, D. Smit and N. Hari Dass, *Residual supersymmetry of compactified $d = 10$ supergravity*, *Nuclear Physics B* **283** (1987) 165–191.

[69] J. M. Maldacena and C. Nunez, *Supergravity description of field theories on curved manifolds and a no go theorem*, *Int. J. Mod. Phys. A* **16** (2001) 822–855, [hep-th/0007018].

[70] W. Boucher, G. W. Gibbons and G. T. Horowitz, *A Uniqueness Theorem for Anti-de Sitter Space-time*, *Phys. Rev. D* **30** (1984) 2447.

[71] D. H. Wesley, *New no-go theorems for cosmic acceleration with extra dimensions*, 0802.2106.

[72] Supernova Cosmology Project collaboration, S. Perlmutter et al., *Measurements of Ω and Λ from 42 high redshift supernovae*, *Astrophys. J.* **517** (1999) 565–586, [astro-ph/9812133].

[73] Supernova Search Team collaboration, A. G. Riess et al., *Observational evidence from supernovae for an accelerating universe and a cosmological constant*, *Astron. J.* **116** (1998) 1009–1038, [astro-ph/9805201].

[74] WMAP collaboration, D. N. Spergel et al., *Wilkinson Microwave Anisotropy Probe (WMAP) three year results: implications for cosmology*, *Astrophys. J. Suppl.* **170** (2007) 377, [astro-ph/0603449].

[75] Planck collaboration, N. Aghanim et al., *Planck 2018 results. VI. Cosmological parameters*, *Astron. Astrophys.* **641** (2020) A6, [1807.06209].

[76] E. J. Copeland, M. Sami and S. Tsujikawa, *Dynamics of dark energy*, *Int. J. Mod. Phys. D* **15** (2006) 1753–1936, [hep-th/0603057].

[77] T. Banks, *Cosmological breaking of supersymmetry?*, *Int. J. Mod. Phys. A* **16** (2001) 910–921, [hep-th/0007146].

[78] W. Taylor and Y.-N. Wang, *The F-theory geometry with most flux vacua*, *JHEP* **12** (2015) 164, [1511.03209].

[79] C. Vafa, *The String landscape and the swampland*, hep-th/0509212.

[80] E. Palti, *The Swampland: Introduction and Review*, *Fortsch. Phys.* **67** (2019) 1900037, [1903.06239].

[81] P. Agrawal, G. Obied, P. J. Steinhardt and C. Vafa, *On the Cosmological Implications of the String Swampland*, *Phys. Lett. B* **784** (2018) 271–276, [1806.09718].

[82] A. Achúcarro and G. A. Palma, *The string swampland constraints require multi-field inflation*, *JCAP* **02** (2019) 041, [1807.04390].

[83] F. Denef, A. Hebecker and T. Wrase, *de Sitter swampland conjecture and the Higgs potential*, *Phys. Rev. D* **98** (2018) 086004, [1807.06581].

[84] J. P. Conlon, *The de Sitter swampland conjecture and supersymmetric AdS vacua*, *Int. J. Mod. Phys. A* **33** (2018) 1850178, [1808.05040].

[85] H. Murayama, M. Yamazaki and T. T. Yanagida, *Do We Live in the Swampland?*, *JHEP* **12** (2018) 032, [1809.00478].

[86] D. Andriot, *On the de Sitter swampland criterion*, *Phys. Lett. B* **785** (2018) 570–573, [1806.10999].

[87] S. K. Garg and C. Krishnan, *Bounds on Slow Roll and the de Sitter Swampland*, *JHEP* **11** (2019) 075, [1807.05193].

[88] H. Ooguri and C. Vafa, *On the Geometry of the String Landscape and the Swampland*, *Nucl. Phys. B* **766** (2007) 21–33, [hep-th/0605264].

[89] A. Bedroya and C. Vafa, *Trans-Planckian Censorship and the Swampland*, *JHEP* **09** (2020) 123, [1909.11063].

[90] S. Kachru, J. Pearson and H. L. Verlinde, *Brane / flux annihilation and the string dual of a nonsupersymmetric field theory*, *JHEP* **06** (2002) 021, [hep-th/0112197].

[91] B. Michel, E. Mintun, J. Polchinski, A. Puhm and P. Saad, *Remarks on brane and antibrane dynamics*, *JHEP* **09** (2015) 021, [1412.5702].

[92] I. Bena, M. Grana and N. Halmagyi, *On the Existence of Meta-stable Vacua in Klebanov-Strassler*, *JHEP* **09** (2010) 087, [0912.3519].

[93] F. F. Gautason, D. Junghans and M. Zagermann, *Cosmological Constant, Near Brane Behavior and Singularities*, *JHEP* **09** (2013) 123, [1301.5647].

[94] E. A. Bergshoeff, K. Dasgupta, R. Kallosh, A. Van Proeyen and T. Wrase, $\overline{\text{D3}}$ *and dS*, *JHEP* **05** (2015) 058, [1502.07627].

[95] R. Kallosh and T. Wrase, *Emergence of Spontaneously Broken Supersymmetry on an Anti-D3-Brane in KKLT dS Vacua*, *JHEP* **12** (2014) 117, [1411.1121].

[96] N. Goheer, M. Kleban and L. Susskind, *The Trouble with de Sitter space*, *JHEP* **07** (2003) 056, [hep-th/0212209].

[97] S. Ferrara, R. Kallosh and A. Linde, *Cosmology with Nilpotent Superfields*, *JHEP* **10** (2014) 143, [1408.4096].

[98] R. Kallosh and A. D. Linde, *O'KKLT*, *JHEP* **02** (2007) 002, [hep-th/0611183].

[99] D. V. Volkov and V. P. Akulov, *On the possible universal neutrino interaction*, *JETP Lett.* **16** (1972) 438.

[100] D. V. Volkov and V. P. Akulov, *Is the neutrino a goldstone particle?*, *Phys. Lett., B, v. 46B, no. 1, pp. 109-110* **46** (1973) 109–110.

[101] M. Rocek and A. A. Tseytlin, *Partial breaking of global $D = 4$ supersymmetry, constrained superfields, and three-brane actions*, *Phys. Rev. D* **59** (1999) 106001, [hep-th/9811232].

[102] R. Kallosh, F. Quevedo and A. M. Uranga, *String Theory Realizations of the Nilpotent Goldstino*, *JHEP* **12** (2015) 039, [1507.07556].

[103] I. n. García-Etxebarria, F. Quevedo and R. Valandro, *Global String Embeddings for the Nilpotent Goldstino*, *JHEP* **02** (2016) 148, [1512.06926].

[104] A. Collinucci, F. Denef and M. Esole, *D-brane Deconstructions in IIB Orientifolds*, *JHEP* **02** (2009) 005, [0805.1573].

[105] M. Kreuzer and H. Skarke, *Complete classification of reflexive polyhedra in four-dimensions*, *Adv. Theor. Math. Phys.* **4** (2000) 1209–1230, [hep-th/0002240].

[106] R. Altman, "Toric calabi-yau database." http://www.rossealtman.com/toriccy/, 2014.

[107] R. Altman, J. Gray, Y.-H. He, V. Jejjala and B. D. Nelson, *A Calabi-Yau Database: Threefolds Constructed from the Kreuzer-Skarke List*, *JHEP* **02** (2015) 158, [1411.1418].

[108] R. Altman, J. Carifio, X. Gao and B. D. Nelson, *Orientifold Calabi-Yau threefolds with divisor involutions and string landscape*, *JHEP* **03** (2022) 087, [2111.03078].

[109] I. Bena, M. Grana, S. Kuperstein and S. Massai, *Anti-D3 Branes: Singular to the bitter end*, *Phys. Rev. D* **87** (2013) 106010, [1206.6369].

[110] I. Bena, M. Graña, S. Kuperstein and S. Massai, *Giant Tachyons in the Landscape*, *JHEP* **02** (2015) 146, [1410.7776].

[111] I. Bena, J. Blåbäck and D. Turton, *Loop corrections to the antibrane potential*, *JHEP* **07** (2016) 132, [1602.05959].

[112] S. Lüst and L. Randall, *Effective Theory of Warped Compactifications and the Implications for KKLT*, 2206.04708.

[113] X. Gao, A. Hebecker and D. Junghans, *Control issues of KKLT*, *Fortsch. Phys.* **68** (2020) 2000089, [2009.03914].

[114] I. Bena, J. Blåbäck, M. Graña and S. Lüst, *The Tadpole Problem*, 2010.10519.

[115] I. Bena, J. Blåbäck, M. Graña and S. Lüst, *Algorithmically solving the Tadpole Problem*, 2103.03250.

[116] D. Junghans, *LVS de Sitter Vacua are probably in the Swampland*, 2201.03572.

[117] U. H. Danielsson and T. Van Riet, *What if string theory has no de Sitter vacua?*, *Int. J. Mod. Phys. D* **27** (2018) 1830007, [1804.01120].

[118] A. Maloney, E. Silverstein and A. Strominger, *De Sitter space in noncritical string theory*, in *Workshop on Conference on the Future of Theoretical Physics and Cosmology in Honor of Steven Hawking's 60th Birthday*, pp. 570–591, 5, 2002, hep-th/0205316.

[119] O. Lebedev, H. P. Nilles and M. Ratz, *De Sitter vacua from matter superpotentials*, *Phys. Lett. B* **636** (2006) 126–131, [hep-th/0603047].

[120] X. Dong, B. Horn, E. Silverstein and G. Torroba, *Micromanaging de Sitter holography*, *Class. Quant. Grav.* **27** (2010) 245020, [1005.5403].

[121] M. Cicoli, A. Maharana, F. Quevedo and C. P. Burgess, *De Sitter String Vacua from Dilaton-dependent Non-perturbative Effects*, *JHEP* **06** (2012) 011, [1203.1750].

[122] A. Retolaza and A. Uranga, *De Sitter Uplift with Dynamical Susy Breaking*, *JHEP* **04** (2016) 137, [1512.06363].

[123] A. Saltman and E. Silverstein, *The Scaling of the no scale potential and de Sitter model building*, *JHEP* **11** (2004) 066, [hep-th/0402135].

[124] D. Gallego, M. C. D. Marsh, B. Vercnocke and T. Wrase, *A New Class of de Sitter Vacua in Type IIB Large Volume Compactifications*, *JHEP* **10** (2017) 193, [1707.01095].

[125] C. P. Burgess, R. Kallosh and F. Quevedo, *De Sitter string vacua from supersymmetric D terms*, *JHEP* **10** (2003) 056, [hep-th/0309187].

[126] M. Rummel and Y. Sumitomo, *De Sitter Vacua from a D-term Generated Racetrack Uplift*, *JHEP* **01** (2015) 015, [1407.7580].

[127] A. P. Braun, M. Rummel, Y. Sumitomo and R. Valandro, *De Sitter vacua from a D-term generated racetrack potential in hypersurface Calabi-Yau compactifications*, *JHEP* **12** (2015) 033, [1509.06918].

[128] M. Cicoli, F. Quevedo and R. Valandro, *De Sitter from T-branes*, *JHEP* **03** (2016) 141, [1512.04558].

[129] M. Haack, D. Krefl, D. Lust, A. Van Proeyen and M. Zagermann, *Gaugino Condensates and D-terms from D7-branes*, *JHEP* **01** (2007) 078, [hep-th/0609211].

[130] S. Cecotti, C. Cordova, J. J. Heckman and C. Vafa, *T-Branes and Monodromy*, *JHEP* **07** (2011) 030, [1010.5780].

[131] M. Kreuzer, *Toric geometry and Calabi-Yau compactifications*, *Ukr. J. Phys.* **55** (2010) 613–625, [hep-th/0612307].

[132] M. Kreuzer and H. Skarke, "Calabi yau data." http://vvv.hep.itp.tuwien.ac.at/~kreuzer/CY/.

[133] M. Kreuzer and H. Skarke, *PALP: A Package for analyzing lattice polytopes with applications to toric geometry*, *Comput. Phys. Commun.* **157** (2004) 87–106, [math/0204356].

[134] V. V. Batyrev, *Dual polyhedra and mirror symmetry for calabi-yau hypersurfaces in toric varieties*, alg-geom/9310003.

[135] J. Louis, M. Rummel, R. Valandro and A. Westphal, *Building an explicit de Sitter*, *JHEP* **10** (2012) 163, [1208.3208].

[136] E. Witten, *Phases of N=2 theories in two-dimensions*, *Nucl. Phys. B* **403** (1993) 159–222, [hep-th/9301042].

[137] M. Cicoli, F. Muia and P. Shukla, *Global Embedding of Fibre Inflation Models*, *JHEP* **11** (2016) 182, [1611.04612].

[138] C. T. C. Wall, *Classification problems in differential topology. v*, *Inventiones mathematicae* **1** (1966) 355–374.

[139] R. Blumenhagen, B. Jurke, T. Rahn and H. Roschy, *Cohomology of Line Bundles: A Computational Algorithm*, *J. Math. Phys.* **51** (2010) 103525, [1003.5217].

[140] R. Blumenhagen, B. Jurke and T. Rahn, *Computational Tools for Cohomology of Toric Varieties*, *Adv. High Energy Phys.* **2011** (2011) 152749, [1104.1187].

[141] V. I. Danilov and A. Khovanskii, *Newton polyhedra and an algorithm for computing hodge-deligne numbers*, *Mathematics of The Ussr-izvestiya* **29** (1987) 279–298.

[142] X. Gao and P. Shukla, *On Classifying the Divisor Involutions in Calabi-Yau Threefolds*, *JHEP* **11** (2013) 170, [1307.1139].

[143] P. Shukla, *Classifying divisor topologies for string phenomenology*, 2205.05215.

[144] M. Cicoli, D. Ciupke, C. Mayrhofer and P. Shukla, *A Geometrical Upper Bound on the Inflaton Range*, *JHEP* **05** (2018) 001, [1801.05434].

[145] M. Cicoli, I. n. G. Etxebarria, F. Quevedo, A. Schachner, P. Shukla and R. Valandro, *The Standard Model quiver in de Sitter string compactifications*, *JHEP* **08** (2021) 109, [2106.11964].

[146] M. Cicoli, D. Ciupke, V. A. Diaz, V. Guidetti, F. Muia and P. Shukla, *Chiral Global Embedding of Fibre Inflation Models*, *JHEP* **11** (2017) 207, [1709.01518].

[147] A. Collinucci, M. Kreuzer, C. Mayrhofer and N.-O. Walliser, *Four-modulus 'Swiss Cheese' chiral models*, *JHEP* **07** (2009) 074, [0811.4599].

[148] D. S. Freed and E. Witten, *Anomalies in string theory with D-branes*, *Asian J. Math.* **3** (1999) 819, [hep-th/9907189].

[149] J. P. Conlon, A. Maharana and F. Quevedo, *Towards Realistic String Vacua*, *JHEP* **05** (2009) 109, [0810.5660].

[150] S. Krippendorf, M. J. Dolan, A. Maharana and F. Quevedo, *D-branes at Toric Singularities: Model Building, Yukawa Couplings and Flavour Physics*, *JHEP* **06** (2010) 092, [1002.1790].

[151] R. Blumenhagen, S. Moster and E. Plauschinn, *Moduli Stabilisation versus Chirality for MSSM like Type IIB Orientifolds*, *JHEP* **01** (2008) 058, [0711.3389].

[152] R. Blumenhagen, M. Cvetic, R. Richter and T. Weigand, *Lifting D-Instanton Zero Modes by Recombination and Background Fluxes*, *JHEP* **10** (2007) 098, [0708.0403].

[153] M. Cicoli, C. P. Burgess and F. Quevedo, *Fibre Inflation: Observable Gravity Waves from IIB String Compactifications*, *JCAP* **03** (2009) 013, [0808.0691].

[154] M. Berg, M. Haack and B. Kors, *String loop corrections to Kahler potentials in orientifolds*, *JHEP* **11** (2005) 030, [hep-th/0508043].

[155] M. Berg, M. Haack and E. Pajer, *Jumping Through Loops: On Soft Terms from Large Volume Compactifications*, *JHEP* **09** (2007) 031, [0704.0737].

[156] M. Cicoli, J. P. Conlon and F. Quevedo, *Systematics of String Loop Corrections in Type IIB Calabi-Yau Flux Compactifications*, *JHEP* **01** (2008) 052, [0708.1873].

[157] D. Ciupke, J. Louis and A. Westphal, *Higher-Derivative Supergravity and Moduli Stabilization*, *JHEP* **10** (2015) 094, [1505.03092].

[158] M. Cicoli, I. n. Garcìa-Etxebarria, C. Mayrhofer, F. Quevedo, P. Shukla and R. Valandro, *Global Orientifolded Quivers with Inflation*, *JHEP* **11** (2017) 134, [1706.06128].

[159] E. Silverstein, *(A)dS backgrounds from asymmetric orientifolds*, *Clay Mat. Proc.* **1** (2002) 179, [hep-th/0106209].

[160] E. Silverstein, *TASI / PiTP / ISS lectures on moduli and microphysics*, in *Theoretical Advanced Study Institute in Elementary Particle Physics (TASI 2003): Recent Trends in String Theory*, pp. 381–415, 5, 2004, hep-th/0405068, DOI.

[161] E. Silverstein, *Simple de Sitter Solutions*, *Phys. Rev. D* **77** (2008) 106006, [0712.1196].

[162] D. Andriot, P. Marconnet and T. Wrase, *Intricacies of classical de Sitter string backgrounds*, *Phys. Lett. B* **812** (2021) 136015, [2006.01848].

[163] F. Quevedo, *Local String Models and Moduli Stabilisation*, *Mod. Phys. Lett. A* **30** (2015) 1530004, [1404.5151].

[164] C. P. Burgess, P. G. Camara, S. P. de Alwis, S. B. Giddings, A. Maharana, F. Quevedo et al., *Warped Supersymmetry Breaking*, *JHEP* **04** (2008) 053, [hep-th/0610255].

[165] M. Cicoli, J. P. Conlon, A. Maharana and F. Quevedo, *A Note on the Magnitude of the Flux Superpotential*, *JHEP* **01** (2014) 027, [1310.6694].

[166] R. Minasian, T. G. Pugh and R. Savelli, *F-theory at order α'^3*, *JHEP* **10** (2015) 050, [1506.06756].

[167] B. V. Bento, D. Chakraborty, S. L. Parameswaran and I. Zavala, *A new de Sitter solution with a weakly warped deformed conifold*, *JHEP* **12** (2021) 124, [2105.03370].

[168] D. Junghans, *Topological Constraints in the LARGE-Volume Scenario*, 2205.02856.

[169] F. Carta, J. Moritz and A. Westphal, *A landscape of orientifold vacua*, *JHEP* **05** (2020) 107, [2003.04902].

[170] C. Vafa, *Evidence for F theory*, *Nucl. Phys. B* **469** (1996) 403–418, [hep-th/9602022].

[171] Y.-H. He and A. Lukas, *Machine Learning Calabi-Yau Four-folds*, *Phys. Lett. B* **815** (2021) 136139, [2009.02544].

[172] S. Sethi, C. Vafa and E. Witten, *Constraints on low dimensional string compactifications*, *Nucl. Phys. B* **480** (1996) 213–224, [hep-th/9606122].

[173] D. R. Morrison and W. Taylor, *Classifying bases for 6D F-theory models*, *Central Eur. J. Phys.* **10** (2012) 1072–1088, [1201.1943].

[174] D. R. Morrison and W. Taylor, *Non-Higgsable clusters for 4D F-theory models*, *JHEP* **05** (2015) 080, [1412.6112].

[175] T. W. Grimm and T. Weigand, *On Abelian Gauge Symmetries and Proton Decay in Global F-theory GUTs*, *Phys. Rev. D* **82** (2010) 086009, [1006.0226].

[176] A. P. Braun, A. Collinucci and R. Valandro, *G-flux in F-theory and algebraic cycles*, *Nucl. Phys. B* **856** (2012) 129–179, [1107.5337].

[177] M. Demirtas and A. Rios-Tascon, "Cytools." https://cytools.liammcallistergroup.com/, 2021.

[178] Y.-C. Huang and W. Taylor, *Comparing elliptic and toric hypersurface Calabi-Yau threefolds at large Hodge numbers*, *JHEP* **02** (2019) 087, [1805.05907].

[179] Y.-C. Huang and W. Taylor, *On the prevalence of elliptic and genus one fibrations among toric hypersurface Calabi-Yau threefolds*, *JHEP* **03** (2019) 014, [1809.05160].

[180] M. Kreuzer and H. Skarke, *Calabi-Yau four folds and toric fibrations*, *J. Geom. Phys.* **26** (1998) 272–290, [hep-th/9701175].

[181] Y.-C. Huang and W. Taylor, *Fibration structure in toric hypersurface Calabi-Yau threefolds*, *JHEP* **03** (2020) 172, [1907.09482].

[182] J. Gray, A. S. Haupt and A. Lukas, *Topological Invariants and Fibration Structure of Complete Intersection Calabi-Yau Four-Folds*, *JHEP* **09** (2014) 093, [1405.2073].

[183] L. B. Anderson, X. Gao, J. Gray and S.-J. Lee, *Fibrations in CICY Threefolds*, *JHEP* **10** (2017) 077, [1708.07907].

[184] V. Bouchard and H. Skarke, *Affine Kac-Moody algebras, CHL strings and the classification of tops*, *Adv. Theor. Math. Phys.* **7** (2003) 205–232, [hep-th/0303218].

[185] Y.-C. Huang and W. Taylor, *Mirror symmetry and elliptic Calabi-Yau manifolds*, *JHEP* **04** (2019) 083, [1811.04947].

[186] P. Candelas, A. Font, S. H. Katz and D. R. Morrison, *Mirror symmetry for two parameter models. 2.*, *Nucl. Phys. B* **429** (1994) 626–674, [hep-th/9403187].

[187] D.-E. Diaconescu and C. Romelsberger, *D-branes and bundles on elliptic fibrations*, *Nucl. Phys. B* **574** (2000) 245–262, [hep-th/9910172].

[188] C. R. Brodie, A. Constantin, R. Deen and A. Lukas, *Index Formulae for Line Bundle Cohomology on Complex Surfaces*, *Fortsch. Phys.* **68** (2020) 1900086, [1906.08769].

[189] W. Taylor, *On the Hodge structure of elliptically fibered Calabi-Yau threefolds*, *JHEP* **08** (2012) 032, [1205.0952].

[190] M. Cicoli, M. Goodsell, J. Jaeckel and A. Ringwald, *Testing String Vacua in the Lab: From a Hidden CMB to Dark Forces in Flux Compactifications*, *JHEP* **07** (2011) 114, [1103.3705].

[191] M. Cicoli, C. P. Burgess and F. Quevedo, *Anisotropic Modulus Stabilisation: Strings at LHC Scales with Micron-sized Extra Dimensions*, *JHEP* **10** (2011) 119, [1105.2107].

[192] X. Gao, A. Hebecker, S. Schreyer and G. Venken, *Loops, Local Corrections and Warping in the LVS and other Type IIB Models*, 2204.06009.

[193] M. Berg, M. Haack and B. Kors, *Loop corrections to volume moduli and inflation in string theory*, *Phys. Rev. D* **71** (2005) 026005, [hep-th/0404087].

[194] M. Berg, M. Haack and B. Kors, *On volume stabilization by quantum corrections*, *Phys. Rev. Lett.* **96** (2006) 021601, [hep-th/0508171].

[195] G. von Gersdorff and A. Hebecker, *Kahler corrections for the volume modulus of flux compactifications*, *Phys. Lett. B* **624** (2005) 270–274, [hep-th/0507131].

[196] I. Antoniadis, Y. Chen and G. K. Leontaris, *Perturbative moduli stabilisation in type IIB/F-theory framework*, *Eur. Phys. J. C* **78** (2018) 766, [1803.08941].

[197] I. Antoniadis, Y. Chen and G. K. Leontaris, *Logarithmic loop corrections, moduli stabilisation and de Sitter vacua in string theory*, *JHEP* **01** (2020) 149, [1909.10525].

[198] S. Endres, C. Sandrock and W. Focke, *A simplicial homology algorithm for lipschitz optimisation*, *Journal of Global Optimization* **72** (10, 2018) .

[199] P. Virtanen, R. Gommers, T. E. Oliphant, M. Haberland, T. Reddy, D. Cournapeau et al., *Scipy 1.0-fundamental algorithms for scientific computing in python*, *CoRR* **abs/1907.10121** (2019) , [1907.10121].

[200] J. Bradbury, R. Frostig, P. Hawkins, M. J. Johnson, C. Leary, D. Maclaurin et al., *JAX: composable transformations of Python+NumPy programs*, 2018.

[201] D. Baumann and L. McAllister, *Inflation and String Theory*. Cambridge Monographs on Mathematical Physics. Cambridge University Press, 2015, 10.1017/CBO9781316105733.

[202] M. Cicoli, A. Schachner and P. Shukla, *Systematics of type IIB moduli stabilisation with odd axions*, *JHEP* **04** (2022) 003, [2109.14624].